RDCK FLOODPLAIN AND STEEP CREEK STUDY

Salmo River

Final
March 31, 2020

BGC Project No.:
0268007

BGC Document No.:
RDCK2-CW-005F

Prepared by BGC Engineering Inc. for:
Regional District of Central Kootenay

TABLE OF REVISIONS

ISSUE	DATE	REV	REMARKS
DRAFT	March 17, 2020		Issued for client review. Note: Flood Hazard Map and Flood Construction Level Map not included. Will be provided in final version.
FINAL	March 31, 2020		Final issue.

LIMITATIONS

BGC Engineering Inc. (BGC) prepared this document for the account of Regional District of Central Kootenay. The material in it reflects the judgment of BGC staff in light of the information available to BGC at the time of document preparation. Any use which a third party makes of this document or any reliance on decisions to be based on it is the responsibility of such third parties. BGC accepts no responsibility for damages, if any, suffered by any third party as a result of decisions made or actions based on this document.

As a mutual protection to our client, the public, and ourselves, all documents and drawings are submitted for the confidential information of our client for a specific project. Authorization for any use and/or publication of this document or any data, statements, conclusions or abstracts from or regarding our documents and drawings, through any form of print or electronic media, including without limitation, posting or reproduction of same on any website, is reserved pending BGC's written approval. A record copy of this document is on file at BGC. That copy takes precedence over any other copy or reproduction of this document.

EXECUTIVE SUMMARY

This report and its appendices provide a detailed flood hazard assessment of the Salmo River and Erie Creek near the Village of Salmo and the unincorporated community of Ymir, British Columbia. These watercourses were chosen as a high priority clear-water hazard amongst hundreds in the Regional District of Central Kootenay (RDCK) from a risk perspective because of their comparatively high hazards and consequences from flooding. This report describes hydrological conditions and details the methods applied to create scenario and hazard maps for the Salmo River and Erie Creek. This work is the foundation for possible future quantitative risk assessments or conceptualization of mitigation measures such as upgrades to existing dikes.

Flood mapping is used for estimating the extent and depth of different magnitude floods for application in community planning, policy development, and emergency response planning in areas subject to flood hazards. Results from a two-dimensional (2-D) hydraulic model developed for about a 32-km length of the Salmo River and about a 7-km length of Erie Creek provide potential flood inundation extents and establish flood construction levels (FCLs) based on both the 20- and 200-year return period flood event or annual exceedance probability (AEP) of 0.05 and 0.005 and include a freeboard allowance for planning purposes.

The following types of maps were produced for the Salmo River and Erie Creek:

- Flood depth, velocity and intensity maps for the 20-, 50-, 200- and 500-year return period flood events
- Designated floodplain maps depicting the 20- and 200-year FCLs including a freeboard allowance of 0.6 m
- Aerial photograph interpretation and channel change mapping.

Flood mapping developed by BGC Engineering Inc. (BGC) provides an update to historical floodplain mapping previously conducted for the Salmo River and Erie Creek (Acres International Ltd., 1990). Implementation of the Salmo River and Erie Creek FCLs, and community planning for development outside of high hazard areas will lead to greater flood resiliency within the Village of Salmo and the unincorporated community of Ymir. Flood mapping results are also provided digitally through a BGC web application called Cambio™.

Channel change mapping conducted by BGC indicates that the Salmo River channel is highly dynamic, suggesting that the flood hazard assessment and modelling should be updated over time. The channel of Erie Creek has remained relatively stable, likely due to the presence of dikes along the lower reach of the creek. Furthermore, the assumptions made on changes in runoff due to climate change will likely need to be updated periodically as scientific understanding evolves.

Table E-1 provides key observations derived from the hazard assessment.

Table E-1 Summary of key hazard assessment results.

Process	Key Observations
Clear-water inundation	Village of Salmo north of the confluence • The regulated dike on Erie Creek is overtopped by a 200-year peak discharge and greater, causing flooding in the Village of Salmo limited to the vicinity of the dike. • The 500-year peak discharge on both Erie Creek and the Salmo River increases flooding in the Village of Salmo Village of Salmo south of the confluence • The 200-year peak discharge on the Salmo River causes flooding of a residential subdivision approximately 550 m southeast of the confluence. The 500-year peak discharge causes a marginal increase in flooding extent. Unincorporated community of Ymir • The 50-year peak discharge causes minor flooding of the southern part of Ymir. The 200-year and 500-year peak discharges cause a marginal increase in flooding extent. Remainder of study area • The 20-year peak discharge causes overland flooding south of the Village of Salmo. The flooding extent increases to reach the entire width of the valley floor when consider high return period peak discharges. Of note, the wastewater treatment plan located south of the Village of Salmo is not subject to flood for peak discharges up to the 500-year event.
Hydraulic Structures (Bridges)	• The water surface elevations for the 200-year flood do not reach the low chord of 11 out of 13 bridges (Table E-2). • The low chord of the Boulder Pit Road and Shambhala Grounds bridges are submerged during the 200-year flood event. Because this flood event also causes inundation in the floodplain at these two crossings, current modelling indicates that the incremental effects of the bridges on the extents of the inundated areas are minimal.
Flood Protection Structures (Dikes)	• Current modelling indicates that the 200-year flood event overtops the crest of the regulated dike along the north (left) bank of Erie Creek near the crossing between Handson Avenue and Ninth Street. Freeboard elsewhere along the dike ranges between 0.3 and 2 m. • The orphaned dikes located long the Salmo River south of the Village of Salmo are overtopped by the 20-year and higher return period floods.

Table E-2 Bridge crossings along the Salmo River and Erie Creek within the study area.

Bridge Crossing	Latitude (°)	Longitude (°)	Low chord elevation (m)	2-D hydraulic model 200-year flood water surface elevation (m)	Freeboard (m)
Erie Creek					
Highway 3 Bridge #1	49.1922	-117.3326	717.1	716.1	1.0
Pedestrian Bridge	49.1885	-117.3278	708.9	707.6	1.3
Highway 3 Bridge #2	49.1898	-117.2847	669.06	666.7	2.4
Carney Bridge Road Davies Avenue Bridge	49.1895	-117.2829	667.4	665.8	1.6
6th Street Bridge	49.1905	-117.2772	663.9	662.7	1.2
Glendale Avenue/Main Street Bridge	49.1913	-117.2751	663.3	661.6	1.7
Salmo River					
Porto Rico Road Bridge	49.2913	-117.2227	737.1	736.6	0.5
Wildhorse Creek Road Bridge	49.2818	-117.2125	728.4	727.5	0.9
Porcupine Road Bridge	49.2606	-117.2108	708.6	707.3	1.3
Boulder Pit Road Bridge	49.2390	-117.2386	691.35	691.4	-0.05
Airport Road Bridge	49.1907	-117.2659	660.1	658.2	1.9
Highway 6 Bridge	49.1411	-117.2640	644	641.9	2.1
Shambahla Grounds Bridge[1]	49.1094	-117.2609	623.1	623.5	-0.4

Notes:
Bridge crossings are listed in a downstream direction.
1. The bridge owner is Shambhala Music Festival. The name of the bridge is unknown.

TABLE OF CONTENTS

LIST OF TABLES

LIST OF FIGURES

LIST OF APPENDICES

LIST OF DRAWINGS

1. INTRODUCTION

The Regional District of Central Kootenay (RDCK, the District) is located in a mountainous region in southeastern British Columbia (BC) that is subject to damaging floods that have resulted in impacts to communities and infrastructure. In 2018, RDCK retained BGC Engineering Inc. (BGC) to carry out a regional geohazard risk prioritization study for the District (BGC, March 31, 2019). Supported by National Disaster Mitigation Program (NDMP) Stream 1 funding, the objective of the study was to characterize and prioritize clear-water flood and steep creek (debris-flood and debris-flow) geohazards. Through the regional study, BGC identified and prioritized 427 clearwater flood and steep creek hazard areas within the RDCK, of which, six floodplains and ten fans in the District were selected for further detailed assessment (Table 1-1, Figure 1-1).

Table 1-1. List of study areas.

Site Classification	Geohazard Process	Hazard Code	Jurisdiction	Name
Floodplain	Clear-water Flood	340	Village of Salmo and RDCK Electoral Area G	Salmo River
		372	Village of Slocan and RDCK Electoral Area H	Slocan River
		393	Town of Creston	Goat River
		408	RDCK Electoral Area A	Crawford Creek
		375	RDCK Electoral Area K	Burton Creek
		423	Village of Kaslo	Kaslo River
Steep Creek	Debris Flood	212	RDCK Electoral Area F	Duhamel Creek
		252	RDCK Electoral Area F	Kokanee Creek
		248	RDCK Electoral Area D	Cooper Creek
		137	RDCK Electoral Area H	Wilson Creek
		242	RDCK Electoral Area E	Harrop Creek
		95	RDCK Electoral Area K	Eagle Creek
		238	RDCK Electoral Area F	Sitkum Creek
	Hybrid Debris Flood/Debris Flow	116	RDCK Electoral Area E	Procter Creek
		251	RDCK Electoral Area E	Redfish Creek
	Debris Flow	36	RDCK Electoral Area A	Kuskonook Creek

The six clear-water flood hazard areas were prioritized either for development of new flood maps or modernization of existing historical flood maps. Flood maps provide information on the hazards associated with defined flood events, such as water depth, velocity of flooding, and the probability of occurrence. These maps are critical decision-making tools for local and regional governments to inform flood mitigation, land use planning, emergency management, and public awareness. In general, the historical flood maps the District are about thirty years out-of-date and lack consideration of additional hydrological data, changes in land use such as urban development, or the impacts of climate change. In response, updated floodplain mapping was conducted by BGC for each of the six prioritized clear-water hazard areas and provided under separate cover along with digital deliverables through a BGC web application called Cambio™ [1].

This report details the approach used by BGC to conduct detailed floodplain mapping for the Salmo River and Erie Creek located near the Village of Salmo and the unincorporated community of Ymir, BC (Drawing 01). Erie Creek is a major tributary to the Salmo River. The Salmo River exits into the Pend d'Oreille River, itself a tributary to the Columbia River. Erie Creek has an approximate watershed area of 240 km^2 at its mouth, while the watershed area along the Salmo River ranges from approximately 300 to 1,061 km^2 between the upstream and downstream ends of the study area. The Salmo River and Erie Creek pose a flood hazard to properties and infrastructure constructed on the floodplain and low-gradient alluvial fan of the creek. These watercourses have a long history of past damaging flood events and are diked, as described in Section 3.

Flood mapping developed by BGC provides an update to historical floodplain mapping conducted previously for the Salmo River and Erie Creek by Acres International Ltd (1990). The BGC update is based on a two-dimensional (2-D) hydraulic model which was developed for about a 32-km length of the Salmo River and 7-km length of Erie Creek using methods described in Section 4. Modelling results described in Section 5 provide estimated flood inundation extents and establishes flood construction levels (FCLs) based on the 200-year return period event or annual exceedance probability (AEP) of 0.5% and includes a freeboard allowance of 0.6 m for planning purposes.

An outcome of this update is an improved basis for community planning, bylaw development, and emergency response planning in developed areas subject to flood hazards, with consideration of climate change. Recommendations are provided in Section 6 and include considerations for next steps from the study such as possible future quantitative risk assessments, or conceptualization of mitigation measures such as upgrades to existing dikes.

BGC is providing a summary report for the entire assessment, *RDCK Floodplain and Steep Creek Study Summary Report* (referred to herein as the "Summary Report"). Readers are encouraged to read the Summary Report to obtain context about the objectives, scope of work, deliverables, and recommendations of the larger study.

---

[1] *www.cambiocommunities.ca.*

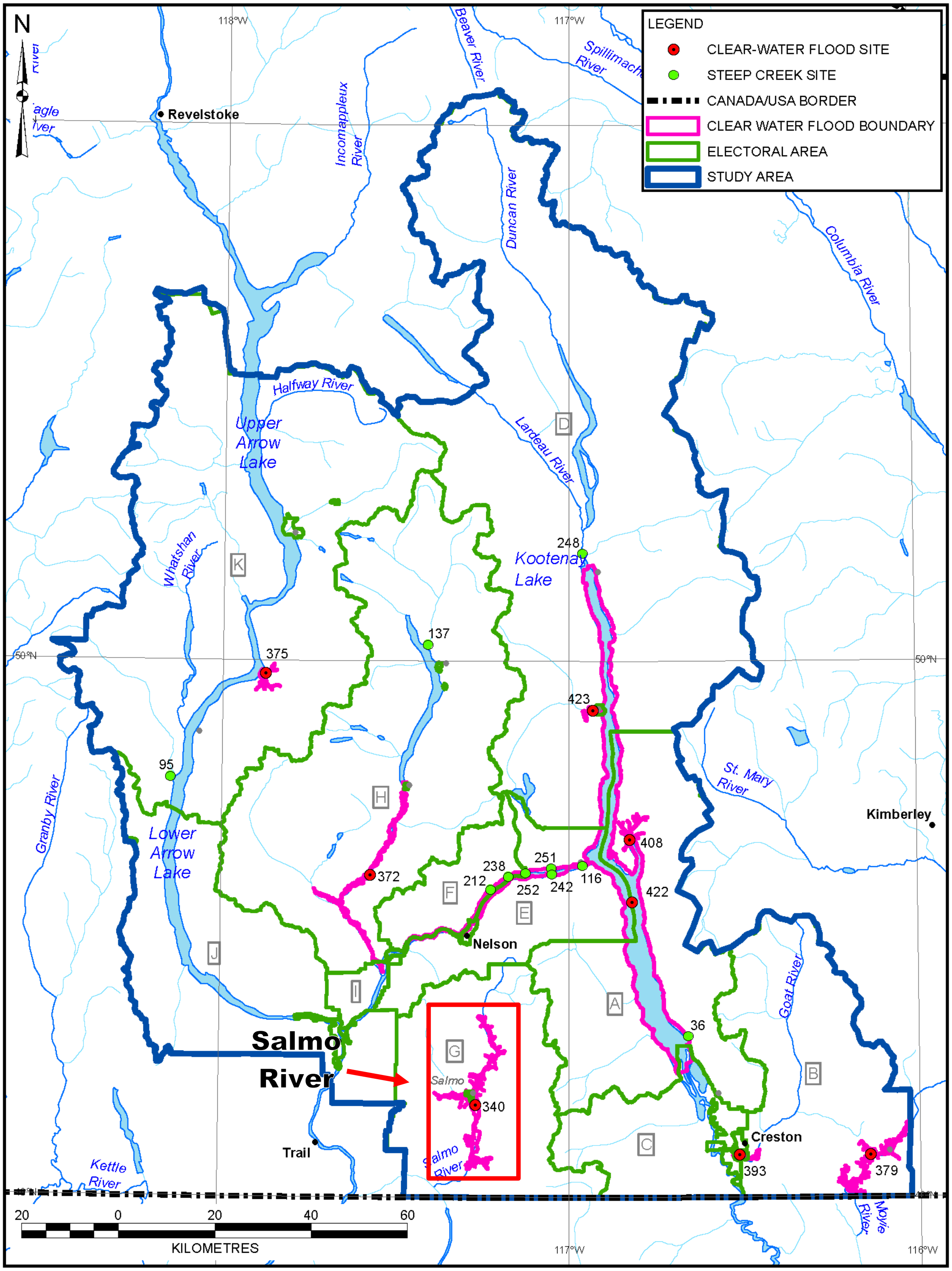

X:\Projects\0268007_RDCK_NDMP_Stream_2_Support\GIS\Production\Report\20190429_Detailed_Hazard_Assessment\Fig01.mxd Date: April 9, 2020 Time: 11:02 AM

Figure 1-1. Hazard areas prioritized for detailed clear-water flood and steep creek mapping. Site labels correspond to hazard identification numbers in Cambio. The Salmo River study area (No. 340) is labelled on the figure (red arrow).

1.1. Scope of Work

BGC's scope of work is outlined in the proposed work plan (BGC, May 24, 2019), which was refined to best meet RDCK's needs as the project developed (BGC, November 15, 2019). The work was carried out under the terms of contract between RDCK and BGC (June 20, 2019). The work scope was funded by Emergency Management BC (EMBC) and Public Safety Canada under Stream 2 of the Natural Disaster Mitigation Program (NDMP). In addition to the scope of services described, detailed floodplain mapping for the Village of Salmo (Salmo) is conducted under a separate contract between Salmo and BGC dated July 19, 2019.

For the Salmo River study area, the scope of work includes:

- Characterization of the study area including regional physiography and hydroclimate, geology, and local watershed and creek characteristics.
- Development of a comprehensive site history of floods and mitigation activity.
- Compilation of data and baseline analyses required as inputs for clear-water flood geohazards assessment. This includes topographic and river bathymetry data collection, hydrologic, hydraulic, and fluvial geomorphologic analyses, and consideration of climate change impacts.
- Complete hazard mapping and assessment according to provincial and national standards including mapping of inundation areas, flow velocity, and flow depth for a range of return periods.
- Integrate flood mapping results with the regional study and disseminate flood hazard mapping and data in web-accessible formats amenable to incorporation into policy and risk-informed decision making.

The scope of work for the study was informed by Engineers and Geoscientists British Columbia (EGBC, 2018) professional practice guidelines, *Legislated Flood Assessments in a Changing Climate in BC,* and EGBC (2017) guidelines for flood map preparation. The hazard assessment was conducted at a Class 2 to 3 level of effort as defined by EBGC (2018) and is consistent with the *Federal Floodplain Mapping Framework* (Natural Resources Canada [NRCan], 2017). Within the NRCan framework, this study provides the foundation to flood risk assessment and mitigations (Figure 1-2).

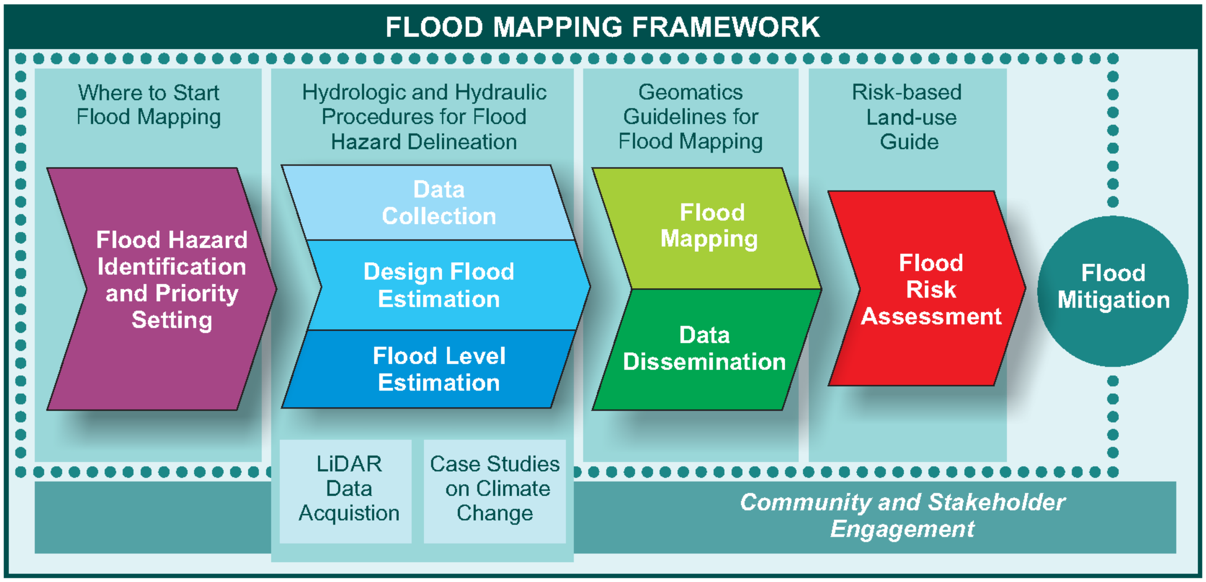

Figure 1-2. Federal flood mapping framework (NRCan, 2017).

1.2. Terminology

This assessment uses specific hazard terminology provided in Appendix A.

1.3. Deliverables

The deliverables of this study include this assessment report and digital deliverables (hazard maps) provided via the Cambio web application and as geospatial data provided to the RDCK.

This report is best read with access to Cambio. Cambio displays the results of both the NDMP Stream 1 and Stream 2 studies. The application can be accessed at www.cambiocommunities.ca, using either Chrome or Firefox web browsers. The Summary Report provides a Cambio user guide.

1.4. Study Team

This study was multidisciplinary. Contributors are listed below, and primary authors and reviewers are listed in Table 1-2.

- Kris Holm, M.Sc., P.Geo., Principal Geoscientist
- Sarah Kimball, M.A.Sc., P.Eng., P.Geo., Senior Geological Engineer
- Rob Millar, Ph.D., P.Eng., P.Geo., Principal Hydrotechnical Engineer
- Hamish Weatherly, M.Sc., P.Geo., Principal Hydrologist
- Betsy Waddington, M.Sc., P.Geo., Senior Geoscientist
- Patrick Grover, M.A.Sc., P.Eng., Senior Hydrotechnical Engineer
- Elisa Scordo, M.Sc., P.Geo., P.Ag., Senior Hydrologist
- Pascal Szeftel, Ph.D., P.Eng., Senior Hydrotechnical Engineer
- Marc Oliver Trottier, M.A.Sc., P.Eng., Intermediate Hydrotechnical Engineer
- Melissa Hairabedian, M.Sc., P.Geo., Senior Hydrologist
- Hilary Shirra, B.A.Sc., EIT, Junior Hydrotechnical Engineer
- Toby Perkins, M.A.Sc., P.Eng., Senior Hydrotechnical Engineer
- Kenneth Lockwood, Ph.D., EIT, Junior Civil Engineer
- Beatrice Collier-Pandya, B.A.Sc., EIT, Geological Engineer
- Matthias Busslinger, M.A.Sc., P.Eng., Senior Geotechnical Engineer
- Carie-Ann Lau, M.Sc., P.Geo., Intermediate Geoscientist
- Vanessa Cuervo, M.Sc., Geohazard Specialist
- Phil LeSueur, M.Sc., P.Geo., Geological Engineer
- Lauren Hutchinson, M.Sc., P.Eng., Intermediate Geotechnical Engineer
- Anna Akkerman, B.A.Sc., P.Eng., Senior Hydrotechnical Engineer
- Matthew Buchanan, B.Sc., GISP, A.D.P., GIS Analyst
- Sophol Tran, B.A., A.D.P., GIS Analyst
- Lucy Lee, B.A., A.D.P., GISP, GIS Analyst/ Developer
- Matthew Williams, B.Sc., A.D.P., GIS Analyst.
- Alistair Beck, B.S.F., Dip CST, Database / Web Application Developer
- Michael Porter, M.Eng., P.Eng., Director, Principal Geological Engineer

Table 1-2. Study team.

Project Director	Kris Holm	
Project Manager	Sarah Kimball	
Overall Technical Reviewer(s)	Rob Millar Hamish Weatherly	
Section	**Primary Author(s)**	**Peer Reviewer(s)**
1	Elisa Scordo	Kris Holm
2	Melissa Hairabedian Vanessa Cuervo	Elisa Scordo
3	Pascal Szeftel	Elisa Scordo
4.1	Pascal Szeftel	Patrick Grover
4.2	Vanessa Cuervo	Pascal Szeftel
4.3	Pascal Szeftel	Elisa Scordo
4.4	Pascal Szeftel	Elisa Scordo
4.5	Pascal Szeftel	Toby Perkins
5.1	Vanessa Cuervo	Betsy Waddington
5.2	Pascal Szeftel Melissa Hairabedian	Elisa Scordo
5.3 – 5.5	Pascal Szeftel	Marc Oliver Trottier Toby Perkins
6.0	Pascal Szeftel Vanessa Cuervo	Elisa Scordo
Appendix A	Hilary Shira	Elisa Scordo
Appendix B	Hilary Shira	Pascal Szeftel
Appendix C	Melissa Hairabedian Patrick Grover	Pascal Szeftel
Appendix D	Melissa Hairabedian Patrick Grover	Pascal Szeftel
Appendix E	Pascal Szeftel	Marc Olivier Trottier

2. STUDY AREA CHARACTERIZATION

The following section provides a characterization of the study area including physiography, hydroclimatic conditions and projected impacts of climate change, glacial history and surficial geology, and a description of the Salmo River and Erie Creek channels and floodplains.

2.1. Physiography

The Salmo River watershed is located in the Montane Cordillera Ecozone which lies in the Northern Columbia Mountains Ecoregion. This ecoregion is a mountainous area bounded by the Southern Rocky Mountain Trench to the east, and the Columbia Highlands to the west. (Demarchi, 2011).

The Salmo River originates approximately 10 km south of Nelson, BC. The river flows generally in a southerly direction, flowing by the unincorporated community of Ymir and Village of Salmo. The Salmo River drains a 1,300 km^2 watershed, where it debouches into the Pend d'Oreille River. A small portion of the watershed extends into the States of Washington and Idaho. The watershed of the Salmo River is densely vegetated with forest cover dominated by western hemlock and western redcedar at lower elevations, and subalpine fir and Engelmann spruce in the sub-alpine (Demarchi, 2011).

The study area covers a 32 km section of the Salmo River. The upstream boundary on the Salmo River is located 1.4 km above of the unincorporated community of Ymir. The downstream boundary on the Salmo River is 700 m below the confluence with the South Salmo River. The study area also includes a 7 km section of Erie Creek, a major tributary that originates in the Bonnington Range and discharges into the Salmo River near the Village of Salmo. The upstream boundary on Erie Creek is located approximately 1.5 km north of Erie Lake (Drawing 01). Notable tributaries, listed from upstream to downstream, include Hidden Creek, Erie Creek, Sheep Creek, and the South Salmo River. The Salmo River watershed boundary is presented in Drawing 02 and the physiographic parameters of the watershed are listed in Table 2-1.

Table 2-1. Watershed characteristics of the Salmo River.

Characteristic	Value
Watershed area (km^2)	1,061
Maximum watershed elevation (m)	2,398
Minimum watershed elevation (m)	607
Watershed relief (m)	1,791
Watershed centroid elevation (m)	1,385
Average channel gradient along the Salmo River (%)	0.4
Average channel gradient along Erie Creek (%)	0.9

2.2. Alluvial Fan and Floodplain Morphology

Downstream of the unincorporated community of Ymir, the Salmo River flows south in a gentle slope valley. The geometry of the Salmo River channel changes gradually from the upstream end to the downstream end of the study area. The width of the valley floor generally increases from approximately 200 m to 1,100 m (Drawing 01). The bankfull width of the Salmo River ranges from 40 to 150 m (Figure 2-1). The active floodplain width ranges from 50 to 300 m and is locally confined by the development of alluvial fans at the mouth of tributaries. The channel gradient decreases from 0.6 to 0.3% in a downstream direction. Throughout the study area, the river channel exhibits a single-thread channel morphology with alternating wandering and straight reaches. Historically, the channel has migrated and avulsed to occupy relict flood channels. The active channel appears to be actively aggrading and depositing large gravel bars.

Figure 2-1. Salmo River. Looking upstream (north) from the Airport Road bridge crossing. Photo: BGC July 31, 2019.

Upstream of Erie Lake, Erie Creek flows south and is confined in a narrow valley before reaching the apex of an alluvial fan[2]. Upon reaching the toe of the opposite (south) valley slope, the channel veers left (east) and debouches in the Salmo River 6.5 km further downstream in a wide area. The bankfull width of Erie Creek ranges from 12 m near the apex of the fan to 80 m near its mouth. The creek has a single-thread meandering channel morphology. Large woody debris jams are influencing channel pattern in the upper section of the channel approximately 1km upstream of

---

[2] A low-gradient cone-shaped depositional feature formed where the river becomes unconfined within a wide valley.

the mouth (Figure 2-2). Aggradation in the lower reach of Erie Creek is evidenced by past dredging efforts to restore flow conveyance.

Figure 2-2. Erie Creek, approximately 150 m upstream from the mouth. Looking upstream (west). Photo: Measurement Sciences Inc. August 7, 2019.

2.3. Hydroclimatic Conditions

Large-scale airflows moving in from the Pacific bring moist, marine air to the BC Interior. The Columbia Mountains, lying perpendicular to the prevailing winds, influence the distribution of precipitation and temperatures within the Columbia River watershed. Air masses rising over the Columbia Mountains produce an area of increased precipitation. Precipitation takes the form of rain in the summer and deep snow in the winter. Cold air from the arctic infrequently enters this area because it is protected by mountain ranges from all sides (Demarchi, 2011).

The upper watershed of the Salmo River at an elevation of 2,400 m receives a mean annual precipitation (MAP) of approximately 2,100 mm (based on the 1961-1990 historical climate normals), whereas the Village of Salmo at an elevation of 660 m receives a MAP of approximately 720 mm (Wang et al., 2016). Averaged across the watershed, the MAP is 1,400 mm, of which approximately 730 mm falls as snow. The mean annual temperature (MAT) in the watershed is 3.4ºC. The spatial distribution of MAP, MAT, and precipitation as snow (PAS) is depicted in Figure 2-2, based on climate data from Wang et al. (2016).

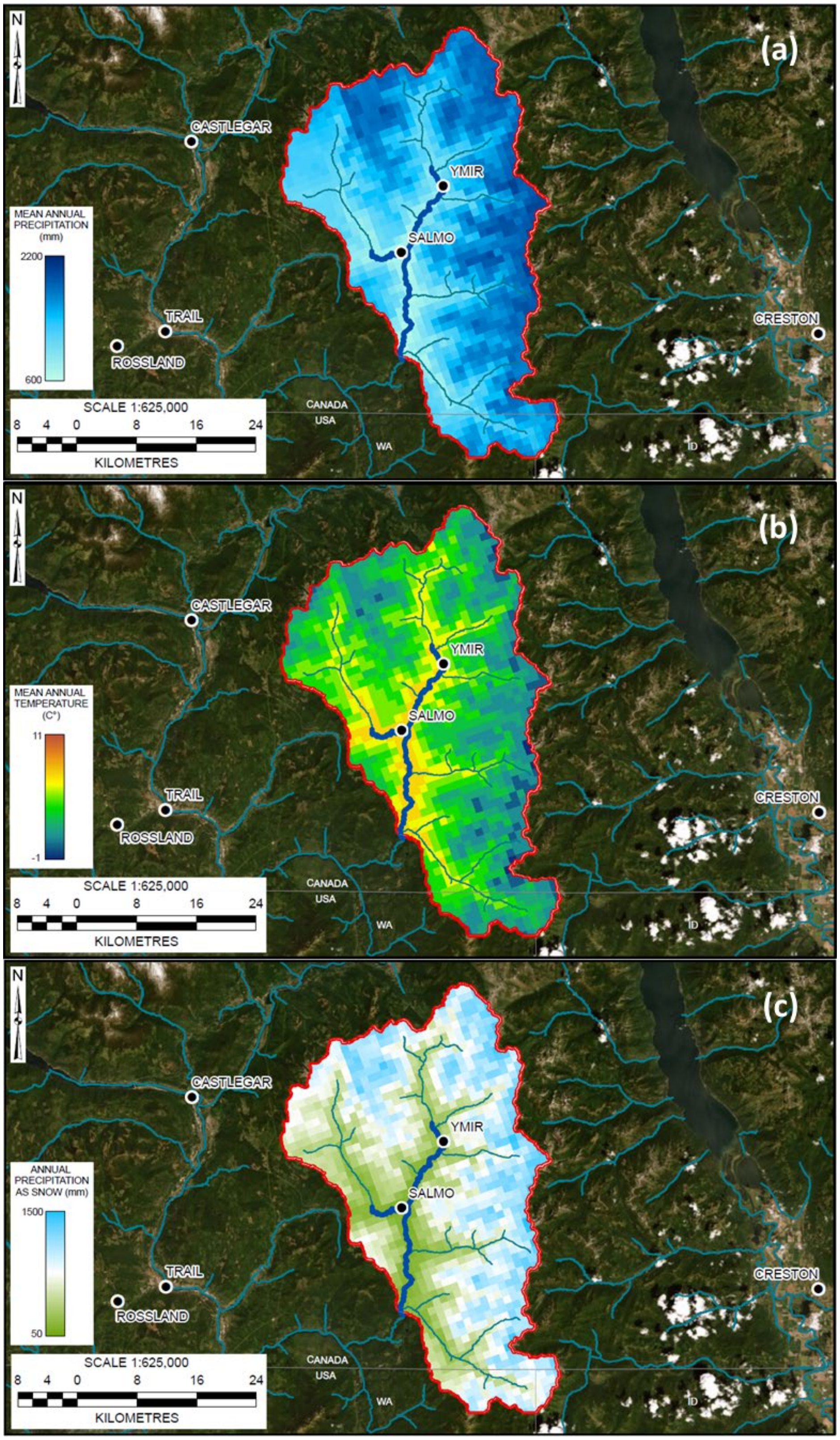

Figure 2-3. **Historical (1961 to 1990) mean annual precipitation (MAP) (a), mean annual temperature (MAT) (b), and precipitation as snow (PAS) (c) averaged over the Salmo River watershed.**

The Salmo River is currently gauged at Water Survey of Canada's (WSC) S*almo River near Salmo* (08NE074) hydrometric station located 4 km downstream from the confluence with the South Salmo River (Drawing 02). Annual maximum peak instantaneous flow records illustrated in Figure 2-4 are caused by snowmelt or rain-on-snow events and generally occur between late April and early June. The flood quantiles (Q2-Q500) plotted in Figure 2-4 were used in the determination of the design flows, as detailed in Section 4.3.

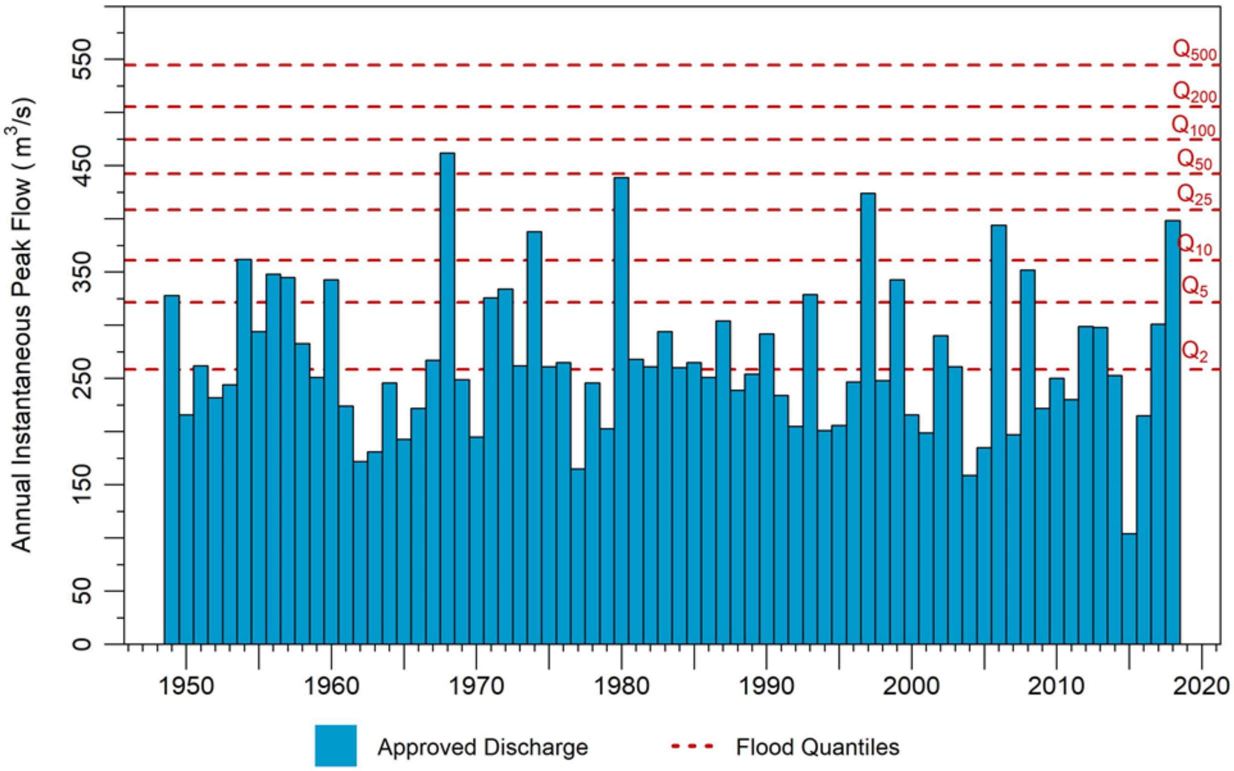

Figure 2-4. Annual maximum peak instantaneous discharge at *Salmo River near Salmo* (08NE074).

Hidden Creek drains a watershed area of 56 km^2 and debouches into the Salmo River approximately 6.5 km upstream from the Village of Salmo (Drawing 02). It is currently gauged at WSC's *Hidden Creek near the Mouth* (08NE114) hydrometric station located immediately upstream from its confluence with the Salmo River. The annual maximum peak instantaneous flows on Hidden Creek are illustrated in Figure 2-5.

The timing of peak flows on Hidden Creek coincides with that on the Salmo River a majority of the time: in 84% of the years on record, flows on Hidden Creek peaked the day before, or on the same day as the flows on the Salmo River. Flows on Erie Creek are not gauged.

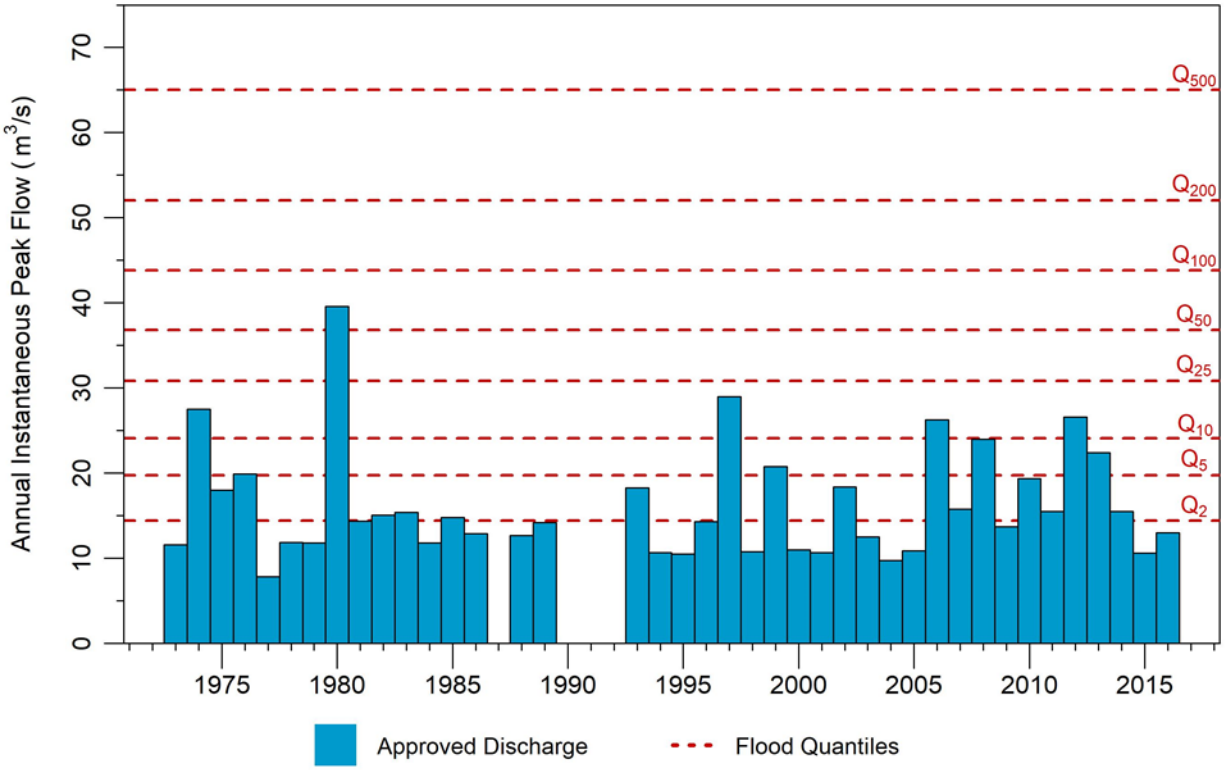

Figure 2-5. Annual maximum peak instantaneous discharge at *Hidden Creek near the Mouth* (08NE114).

2.4. Climate Change Impacts

The MAT averaged over the Salmo River watershed is projected to increase from 3.4ºC (based on historical period 1961 to 1990) to 7.0ºC by 2050 (based on period 2041 to 2070) assuming the representative carbon pathway 8.5 (RCP 8.5). The MAP is projected to increase to 1,480 mm, while PAS is projected to decrease to 460 mm by 2050 (Wang et al, 2016). Projected changes by 2050 (2041 to 2070) in climate variables from historical (1961 to 1990) conditions for the Salmo River watershed are presented in Table 2-3.

Table 2-2. Projected change (RCP 8.5, 2050) from historical (1961 to 1990) conditions for the Salmo River watershed.

Climate Variable	Projected Change
MAT	+3.6 ºC
MAP	+80 mm
PAS	-260 mm

Extreme flood events in the Montane Cordillera are often associated with rain-on-snow events in the spring (Harder et al., 2015). Although the effects of climate change on precipitation are not clear, projected increases in temperature are expected to have the largest impact on annual minimum temperatures occurring in the winter months (Harder et al., 2015). The effects of temperature change differ throughout the region. High elevation regions throughout parts of the Montane Cordillera (e.g., Upper Columbia watershed) are projected to experience increases in snowpack due to increased precipitation, and although temperatures are projected to increase, these areas remain above the freezing level. At lower elevations, increased precipitation and temperature will result in increased winter runoff and smaller snowpack (Loukas & Quick, 1999; Schnorbus et al., 2011).

Changes in streamflow vary spatially and seasonally based on snowfall and rainfall changes and topography-based temperature gradients. Current research suggests that streamflow will increase in the winter and spring in this region due to earlier snowmelt and more frequent rain-on-snow events, while earlier peak flow timing is expected in many rivers (Schnorbus et al., 2014; Farjad et al., 2016). Peak flows may increase or decrease depending on the watershed characteristics and the balance of temperature and precipitation changes described above.

2.5. Glacial History and Surficial Geology

Between 2 million and 10,000 years ago ice sheets advanced and retreated into the Kootenay region (Turner et al., 2009). The final glaciation which ended approximately 10,000 years ago is responsible for many of the surficial materials in the area. South-flowing glaciers carved deep troughs which now hold Kootenay, Arrow and Slocan lakes. Ice dammed the lakes during deglaciation. This resulted in lake levels approximately 150 m higher than present, and the deposition of silts and clays in isolated terraces near the lake shore. Processes of erosion and deposition have continued since deglaciation, creating the younger deposits such as the fluvial materials found along the streams. Slopes around Salmo are bedrock with a thin discontinuous cover of till and colluvium. Thicker fluvial sediments are deposited along the Salmo River valley (Fulton et al., 1984).

3. SITE HISTORY

3.1. Area Development

Prior to European arrival, the Sinixt Nation would travel upriver from the mouth of the Salmo River to hunt and harvest salmon and berries. The Salmo River was also used a route to access the Kootenay River (Nellestijn & Ells, 2008). Mining provided the impetus for European settlements in the Salmo River valley. Salmon Siding (later Village of Salmo) and Quartz Creek Settlement (later the unincorporated community of Ymir) grew rapidly, supported by the mining boom that originated in the late 1800s. Gold mining was predominantly centered around the unincorporated community of Ymir between 1896 and 1904 and shifted south to the Village of Salmo with the discovery of orebodies in the Sheep Creek watershed and rapid expansion of the Hudson Bay Queen and Motherlode mines (Salmo Watershed Streamkeepers Society (SWSS), 2000). Production of gold in the Salmo River watershed slowly declined over the next decades due to increasing recovery costs and unfavorable market conditions and came to a halt in 1951. The discovery of tungsten and lead-zinc orebodies at the Hudson Bay mine sustained economic development in the valley until closure of the mine in 1978. Today, agriculture, forestry, manufacturing, and tourism remain the dominant economic drivers in the Salmo River valley and support a population of 1,140 in the Village of Salmo, and 245 in the unincorporated community of Ymir (Statistics Canada, 2016). The estimated total improvement value of parcels intersecting the Salmo River hazard area based on the 2018 BC Assessment Data is $185,426,500 (BGC, March 31, 2019).

3.2. Historical Flood Events

The Salmo River and Erie Creek have overtopped their banks on numerous occasions since the start of records. The first major flood recorded occurred in 1933, and impacted infrastructure along the Salmo River and Sheep Creek. In the mid-1960s the Ministry of Transportation and Highways constructed approximately 3,650 m (12,000 feet) of diking along the left (east) bank of the Salmo River downstream of the confluence with Erie Creek (BC MOE, 1981). Since the major flood event of 1933, several notable events have occurred in 1968, 1980, and more recently in 2006 and 2018 (see Figure 3-1). The 1968 flood event is the largest recorded to date at the *Salmo River near Salmo* hydrometric station with an instantaneous peak flow of 462 m^3/s and estimated return period of 80 years (Section 4.3.1). The flood occurred on June 2, 1968 as a result of nearly 50 mm of rain falling on a rapidly melting snowpack (Acres International Ltd., 1990). The event caused extensive flooding in the Village of Salmo. Significant reconstruction of the diking system and dredging of streambed sediments from the channel to increase flow conveyance occurred following the 1968 flood event and ongoing annual maintenance has been required since then, including local placement of a riprap armour to mitigate erosion.

The provincial floodplain mapping program began in BC in 1974 aimed at identifying flood risk areas. This was in part due to the large Fraser River flood of 1972, which resulted in damage in the BC Interior. From 1975 to 2003, the province managed development in designated floodplain areas under the Floodplain Development Control Program. In 2003, the Program ended resulting in a significant change in how MFLNRO participated in land use regulation in flood-prone areas.

The responsibility for developing and applying floodplain mapping tools was transferred to local governments, with the requirement that provincial guidelines be taken into consideration (EGBC 2017).The historical event inventory is based upon a variety of sources including newspaper articles, government records and consulting reports. Some sources may not be completely accurate or only provide partial records of flood events but are provided to present an overview of historical events.

Flood History

Salmo River flooding threats, May 2018 (Province of BC)

Car body and rip rap channelization on the Salmo River (Courtesy of Salmo Watershed Streamkeepers Society)

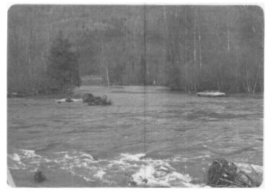

Robertson Farm flooding at bridge crossing, April 1980 (Environment Canada)

Old Highway 3 south of Salmo, May 1975 (Environment Canada)

Fishing on Salmo River, ca. 1900 (Trail City Archives)

May 2018 - Flooding threats on the Salmo River caused evacuation alerts to residences along waterways

May 23, 2013 - Salmo River reached 5-year flood levels

May 19, 2011 - River levels peaked below 2-year flood levels

May 15-23, 2006 - Salmo River reached 20-year flood levels

April 30, 1993 - Landslide into Salmo River

February 5, 1986 - Flooding and dyke breach caused overland flow, location uncertain

January 17, 1986 - Flooding of Salmo River - flood history sent to Minister

January 14, 1985 - Dyke breaches and erosion observed, location uncertain

April 29, 1980 - Flooding - peak flow 439 m^3/s (50-year flood) at WSC hydrometric station 08NE074 downstream of Salmo caused by unseasonal weather and thunderstorms; dike and four erosion washouts, and one log jam were observed, location uncertain

June 14, 1976 - Dike breached in flood event, location uncertain

May 21, 1975 - Shallow flooding on highway just south of Salmo, peak flow 261 m^3/s at WSC hydrometric station 08NE074 downstream of Salmo

June 1974 - Flooding occurred due to above-average snowpack.; high flows (388 m^3/s) caused some dyke breaching

August 18, 1972 - Flooding of CanEx tailings ponds

May 13, 1971 - Salmo Elementary School evacuated when the Salmo River washed out the approach to Glendale Avenue Bridge, peak flow 326 m^3/s at WSC hydrometric station 08NE074 downstream of Salmo

June 2, 1968 - Flood of Record - Peak flow 462 m^3/s (80-year flood) at WSC hydrometric station 08NE074 downstream of Salmo resulted from 50 mm of rain and rapid snowmelt. Great Northern Railway bridge washed out (21 km N of Salmo). Highway South of Salmo under 0.8 m of water. Erosion of dikes built by Ministry of Transport & Highways, locations uncertain

May 21-29, 1954 - Waters reached the pavement near the airport, but subsided a short time later

June 11, 1948 - Flooding caused extensive damage along the Columbia River from Trail to Oregon. Flooding presumed along the Salmo River

June 1933 - Regional flood, unusually warm period during spring freshet, between Nelson and Nelway, Great Northern Railway line washed out at Porto Rico for 30-40 m and Bridge No. 25

May 22, 1928 - Heavy rainstorm caused flooding at Porto Rico and Hall communities, northern end of the watershed

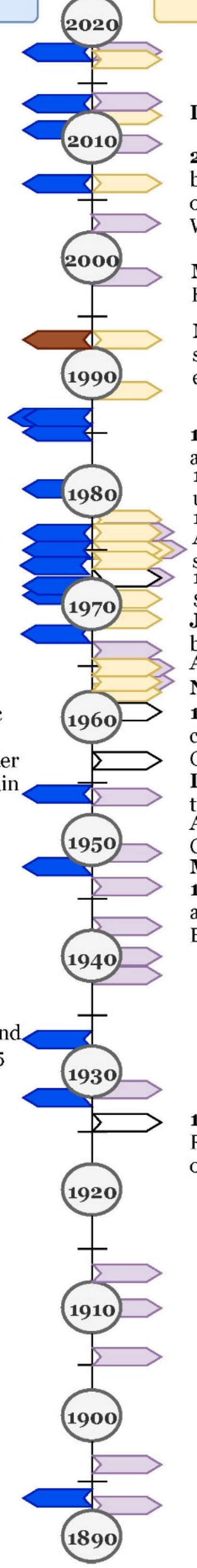

Mitigation

December 13, 2012 - Berm dredging

2006 - Works on channelized sections of Salmo River include boulder clusters, rock groyne improvement, j-hook vane, opposing rock deflectors, and revegetation of banks by Salmo Watershed Streamkeepers Society (SWSS)

May/June 1997 - Heavy rain washed out a section of Highway 3 between Salmo and Creston, location uncertain

May 29, 1993 - Highway department used a stockpile of surplus rock from improvements on Wildhorse Creek Road to erect a dike

1977 - Bank damaged by erosion armoured with rock riprap and low dike added, location uncertain

1976 - Log jam in channel removed, dike repaired, location uncertain

1975 - Emergency stream clearing initiated to reduce erosion

April 18, 1975 - Poor riprap works done, channel cut in stream, location uncertain

1974 - Ministry of Infrastructure and Transport spent $20,000 to rebuild dikes and clear channels

June 19, 1973 - Unauthorized change to channel alignment by sawmill

August 24, 1971 - Riprap placement, location uncertain

November 6, 1969 - New dike built, location uncertain

1965 - Highways channelized 3km of the river, excavating a channel to straighten the alignment and cut off meanders. Gravel from the channel pushed to riversides to form a berm

December 15, 1964 - Railway removed unauthorized dike that was causing erosion, location uncertain

April/May 1963 - Car body bank revetment to stabilize CanEx tailings

May 5, 1961 - Channel excavation near Ymir

1955-1958 - Ministry of Transport and Highways dredged and straightened river downstream of the confluence with Erie Creek

1926 - Significant channelization and alteration of the Salmo River using a D9 dozer and other equipment instream by owner of mill at Sheep Creek

Development

July 2018 - Salmo River Bridge completed at Salmo (SNT Engineering)

2014 - Margaux Resources acquired the Jersey-Emerald project

2010 - Expansion of Whitewater Ski Resort

2003 - Ministry of Agriculture and Lands Contaminated Sites Branch to "stabilize tailing and prevent deleterious substances from entering the Salmo River at Yankee Girl tailings site." Work to proceed in 2006–2008 to complete containment and partial treatment of this site

1998 - The Salmo Watershed Streamkeepers Society (SWSS) incorporated

1976 - Whitewater Ski Resort opened in Ymir bowl

1975 - A 27 m double-single chord reinforced Bailey Bridge was erected over the Salmo River at Ymir

1973 - CanEx closes the Jersey-Emerald Mine due to low commodity prices and high taxes

1966 - Salmo River Bridge north of Ymir on Highway 6 reconstructed

1965 - Erie Creek Provincial Park established

1964 - The bridge across the Salmo River at Porcupine Creek was reconstructed

1954 - Emerald Mine capacity 2,200 tons/day

1949 - CanEx ceased milling tungsten at Emerald Mine and converted to concentrate on lead and zinc

1946 - Salmo incorporated as a village

1940 - Yankee Girl Mine amalgamated with Dundee Mine

1939 - Emerald Mine produced 200 tons/day of tungsten ore during WWII

1929 - Production stopped at Yankee Girl Mine

1913 - Yankee Girl Mine started production

June 5, 1910 - New bridge constructed at Salmo

1906 - J. Waldbesen developed lead ore Emerald Mine/Jersey property (evolved to CanEx Mine) 11 km southeast of Salmo

December 1896 - Dundee Gold Company started mining at what would later become Ymir

1893 - Salmo founded as "Salmon Siding", and later officially trimmed to Salmo

🟦 Flood (major flood)
🟫 Landslide
▷ Channel location
🟨 Mitigation
🟪 Development event

Figure 3-1. Summary of recorded flood history, mitigation, and development history at the Salmo River and Erie Creek.

3.3. Flood Protection and Hydraulic Structures

3.3.1. Bridges

A total of 13 bridge crossings of the Salmo River and Erie Creek were identified within the study area (Figure 3-2). Table 3-1 summarizes key bridge dimensions and characteristics. Bridge descriptions and photographs are provided in Appendix E.

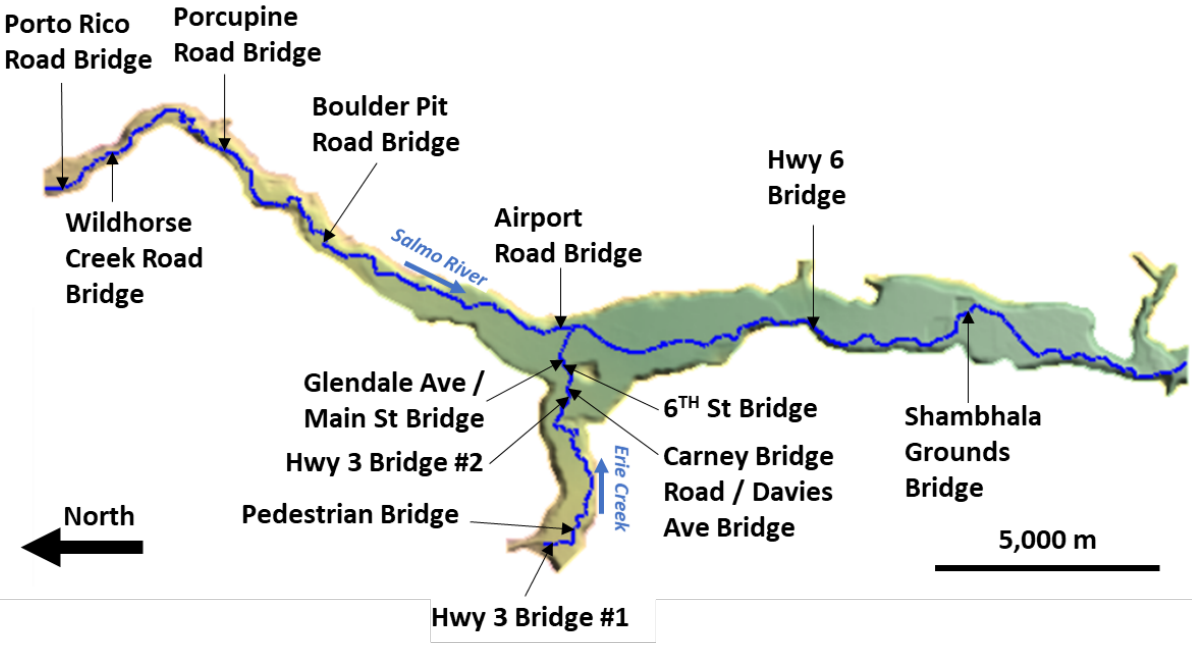

Figure 3-2. Bridge crossings along the Salmo River and Erie Creek within the study area.

Table 3-1. Bridge crossings along the Salmo River and Erie Creek within the study area

Bridge Crossing	Latitude (°)	Longitude (°)	Construction Date (year)	Length (m)	Width (m)	Deck orientation to flow direction (°)	Low chord elevation (m)	Number of in-channel piers
Erie Creek								
Highway 3 Bridge #1	49.1922	-117.3326	1952	19	9	90	717.1	0
Pedestrian Bridge	49.1885	-117.3278	N/A	46	6	30	708.9	0
Highway 3 Bridge #2	49.1898	-117.2847	1980	49	11	90	669.1	0
Carney Bridge Road / Davies Avenue Bridge	49.1895	-117.2829	2010	22	6	90	667.4	0
6th Street Bridge	49.1905	-117.2772	2017	33	3	90	663.9	0
Glendale Avenue / Main Street Bridge	49.1913	-117.2751	N/A	30	11	90	663.3	2
Salmo River								
Porto Rico Road Bridge	49.2913	-117.2227	1965	31	8	60	737.1	1
Wildhorse Creek Road Bridge	49.2818	-117.2125	1975	28	7	65	728.4	0
Porcupine Road Bridge	49.2606	-117.2108	1990	45	5	90	708.6	1
Boulder Pit Road Bridge	49.2390	-117.2386	N/A	32	5	90	691.4	0
Airport Road Bridge	49.1907	-117.2659	1956	40	10	50	660.1	0
Highway 6 Bridge	49.1411	-117.2640	1980	78	12	45	644.0	2
Shambhala Grounds Bridge[1]	49.1094	-117.2609	2018	46	5	90	623.1	0

Notes:

Bridge crossings are listed in a downstream direction.

[1] The bridge owner is Shambhala Music Festival. The name of the bridge/bridge crossing is unknown.

3.3.2. Dikes

Approximately 1,000 m of dike have been constructed on the left (north) bank of Erie Creek, which are managed by the Village of Salmo and regulated under the Dike Maintenance Act (Figure 3-3). Historical records indicate that in the mid-1960s the Ministry of Transportation and Highways constructed approximately 12,000 feet (3,650 m) of diking along the left (east) bank of the Salmo River downstream of the confluence with Erie Creek (BC MoE,1981). Dike construction initially used streambed sediments dredged from the channel to increase flow conveyance (Figure 3-4). The dikes were upgraded in the following decades, typically following flood events in response to bank erosion that threatened dike integrity. Currently the dikes south of the confluence with Erie Creek are considered an orphan flood protection structure that is not being maintained by an owner or diking authority (Boyer, 2009).

Figure 3-3. Regulated dikes along the left (north) bank of Erie Creek. Satellite imagery from Bing.

Figure 3-4. Dike on the right bank of the Salmo River, looking upstream towards the Village of Salmo. Photo: BGC, July 31, 2019.

3.4. Previous Mitigations

Historically, a considerable amount of gravel was excavated from the channel of the Salmo River. Starting in the mid-1950s, the Ministry of Transportation and Highways channelized and straightened approximately 3,650 m (12,000 feet) of the Salmo River channel downstream from the Erie Creek confluence in an attempt to increase flow conveyance and minimize flooding. Gravel removals ceased in the mid-1980s due to concerns from Fisheries and Oceans Canada (DFO) that the removals were adversely affecting fish habitat (BC MoE, 1981). Diking along the Canadian Exploration Ltd. (CanEx) tailings disposal area, about 10 km south of the Village of Salmo, was armoured with junk car bodies in 1963 (CanEx, Figure 3-5). Additional dike sections were armoured with riprap in subsequent decades (BC MoE, 1981).

Figure 3-5. “Junk” car bodies placed along the CanEx tailings disposal area. Looking downstream. Photo: CanEx (1963).

Root wads placed to provide fish habitat and lessen flow velocities against the dike were observed by BGC approximately 1,200 m downstream from the Erie Creek confluence (Figure 3-6).

Figure 3-6. Looking downstream at fish habitat restoration structures. Photo: BGC, July 31, 2019.

3.5. Bank Erosion and Avulsion History

Lateral channel migration resulting from bank erosion and sediment deposition is a natural process in alluvial rivers. Channel migration may occur as gradual erosion at the outside of river bends, or as sudden widening of the river during floods. Gradual channel migration generally results from sediments being eroded along the outer bank of a meander bend and deposited as a point bar along the inside of the meander bend (Charlton, 2007). Changes in the geometry of a channel may impact flooding by decreasing its capacity of conveying flows or adding uncertainty to channel path during high-flow conditions.

There are no historical studies addressing avulsion[3], bank erosion, and resulting channel changes within the entire study area; however, some relevant information can be obtained from the review of the historical documentation (Table 3-2).

Table 3-2. Relevant historical bank erosion and avulsion information.

Year	Reported Observations	Reference
1963	Bank erosion south of Sheep Creek, noted to be undermining dikes and threatening tailings ponds adjacent to Salmo River	CanEx (1963)
1976	Erosion of both banks of Salmo River occurs downstream of the Sheep Creek confluence due to the formation of two gravel bars in the main channel, one upstream and one downstream of the confluence. Erosion at this location has been an ongoing issue due to accumulation of gravel bars in the Salmo River.	BC Department of Environment, Water Resources Services (1976)
1990	Bank erosion noted as a concern to residents along lower Erie Creek.	Acres International Ltd. (1990)

---

[3] Lateral displacement of a stream from its main channel into a new course across its fan or floodplain (Oxford University Press, 2008).

4. METHODS

This section summarizes the assessment methodology applied to the Salmo River and Erie Creek. Additional details on the methodology applied are summarized in Appendices C, D and E.

4.1. Field Data, Topographic Data, and River Bathymetric Surveys

4.1.1. Field work and Site Investigations

Fieldwork on the Salmo River and Erie Creek was conducted on July 5, 2019 and July 31, 2019 by BGC personnel (Elisa Scordo, P.Geo., Marc Oliver Trottier, P.Eng., and Rob Millar, P.Geo., P.Eng.). Fieldwork included observations at bridge and other infrastructure crossing locations and flood protection structures (e.g., dikes). The fieldwork was also conducted to coordinate the survey extent and data collection/location of cross sections with the survey crews.

4.1.2. Topographic Mapping

Detailed topographic data of the floodplain were available from a high-resolution lidar dataset obtained from RDCK and flown in July 2018. BGC was provided with tiles containing the classified point cloud and 1 m bare-earth Digital Elevation Model (DEM). Lidar coverage provided by RDCK for the entire study area is shown in Figure 4-1.

The lidar data were provided with the following coordinate system:

- Horizontal Datum: NAD83 CSRS
- Projection: UTM Zone 11 North
- Vertical Datum: CGVD 2013
- Geoid Model: CGG2013.

As part of the lidar acquisition, orthophotos were not collected. As a result, the classification of the raw lidar point cloud contained inaccuracies particularly around gravel bars and the location of the river shoreline. Lidar acquisition was also limited to above the waterline and channel changes occurred after the lidar was flown. In order to account for this, BGC collected additional ground and bathymetric survey data to capture in-channel features that were not classified in the lidar survey.

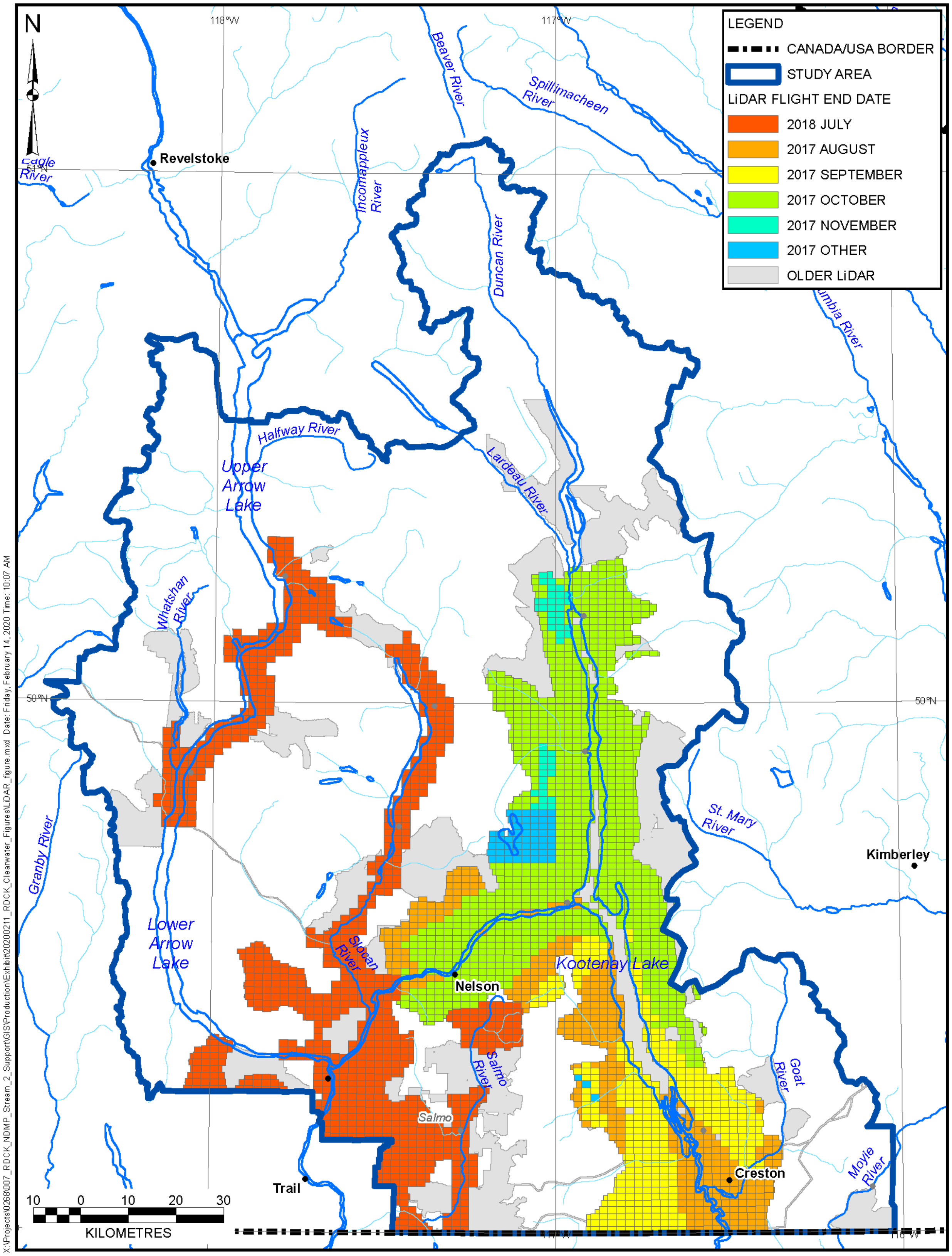

Figure 4-1. Lidar coverage for clear-water flood study sites.

4.1.3. Ground and Bathymetric Surveying

BGC contracted Midwest Surveys Inc. (MSI) to conduct a detailed survey of the Salmo River and Erie Creek (Drawing 03). The scope of work included surveying of the channel bed, bridges, and dikes. A combination of Static Global Navigation Satellite System (GNSS) techniques, real-time kinematic (RTK) and real-time network (RTN) techniques were used to establish a precise, reliable Survey Control Network (SCN) for the length of the project. The SCN was integrated with existing BC Survey Control and/or the Canadian Base Network. The survey data were provided in the 3TM NAD 83 (CSRS) UTM 11 North coordinate system with elevation in the CGVD2013 Vertical Datum.

The survey was conducted from July 28 to August 8, 2019. The survey covered approximately 32 km of the Salmo River and 7 km of Erie Creek. Surveying of the channels was completed using GNSS RTK GPS and in locations where the water depth was too deep to be waded safely, hydrographic surveying (sonar) from a boat was used. A summary of locations collected using survey and sonar techniques is presented in Drawing 03. Channel cross sections, extending from bank to bank and approximately perpendicular to the channel, were collected at a typical spacing of 200 to 300 m. Cross-section spacing was reduced to 50 to 100 m in areas of rapid channel changes.

Bridges were surveyed to collect details such as the length of the span, width of the bridge, top of curb elevation, low chord elevation and width of piers. A total of 1,000 m of dikes along the left (north) bank of Erie Creek were also surveyed, including crest elevation and length (Figure 3-3).

4.1.4. Survey Equipment, Accuracy and Processing Software

Table 4-1 provides a list of survey equipment and the reported accuracy. Hypack 2018 Hydrographic Software was used to correlate global position system (GPS) and hydrographic data together.

Table 4-1. Summary of MSI survey equipment.

Equipment Type	Reported Accuracy
GPS	
Trimble R10 GNSS	• Single Baseline: <30 km • Horizontal (RTK): 8 mm + 1 ppm RMS • Vertical (RTK): 15 mm + 1 ppm RMS • Horizontal (Static GNSS): 3 mm + 0.1 ppm RMS • Vertical (Static GNSS): 3.5 mm + 0.4 ppm RMS
Total Station	
Leica TCR 403 Trimble SX3 Robotic Scanning Total Station	• Angular Accuracy: +/- 3" • EDM Range: 1 m – 2,500 m to single prism • Reflectorless EDM Range: 1 m – 100 m • Distance Accuracy: 2 mm + 2 ppm • Distance Accuracy Scanning: 2 mm + 1.5 ppm
Hydrographic Equipment	
Odom Echotrac CV-100	• Depth Range: <0.30 m to 600 m • Accuracy (Corrected for Sound Velocity): 0.01 m +/-0.1 % depth

4.1.5. Terrain Creation

Following completion of the survey, BGC integrated the bathymetry data with the lidar bare-earth DEM to generate a 1.0 m resolution continuous terrain model for use in 2-D hydraulic modelling (HEC-RAS). A DEM for the channel was generated by creating a boundary around the survey points with a 1 m buffer zone on either side using lidar data. The lidar and survey data were then meshed together using an iterative finite difference interpolation method similar to the discretized thin plate spline technique (Wahba, 1990).

Hydraulic structures were not included in the terrain. Bridge decks were removed from the DEM to not artificially dam the flows. The flow hydraulics at bridge crossings are detailed in Appendix E.

4.2. Channel Change and Bank Erosion Analysis

Floods induce high shear stresses on channel banks, which can promote bank erosion. Non-cohesive materials such as sands and gravels are more susceptible to this process than cohesive banks. Standard hydraulic models to simulate floods do not consider bank erosion and assume the channel geometry is static. BGC conducted a separate analysis to assess changes in the floodplain and channel, and their potential influence on flooding.

Channel change mapping and bank erosion approaches using remote sensing have been widely used to detect variations in the position of channel geomorphology features (e.g., channels, banks, and bars) (Trimble & Cook, 1991; Marcus, 2012). These methods have been reviewed and considered suitable to quantify the rate of change over a study period (Lawler, 2006).

This section briefly describes the study area, data and methods used to document planform channel changes within the floodplain and analyze the bank erosion processes observed between 1990 and 2019. It also outlines the limitations and uncertainties of the methodology.

4.2.1. Channel Change and Bank Erosion Study Area

The analysis focused on two areas where historical channel changes and bank erosion was evident within the reviewed timeframe, and where channel changes were expected to impact flood hazards (Table 3-2, Figure 4-2A). The first section includes an 8 km long segment of Erie Creek (Figure 4-2B). The second section extends for 8 km along the Salmo River (south section) (Figure 4-2C). These areas were divided into reaches to facilitate the analysis of the channel changes. The main characteristics of the identified reaches are described in Section 5.1.

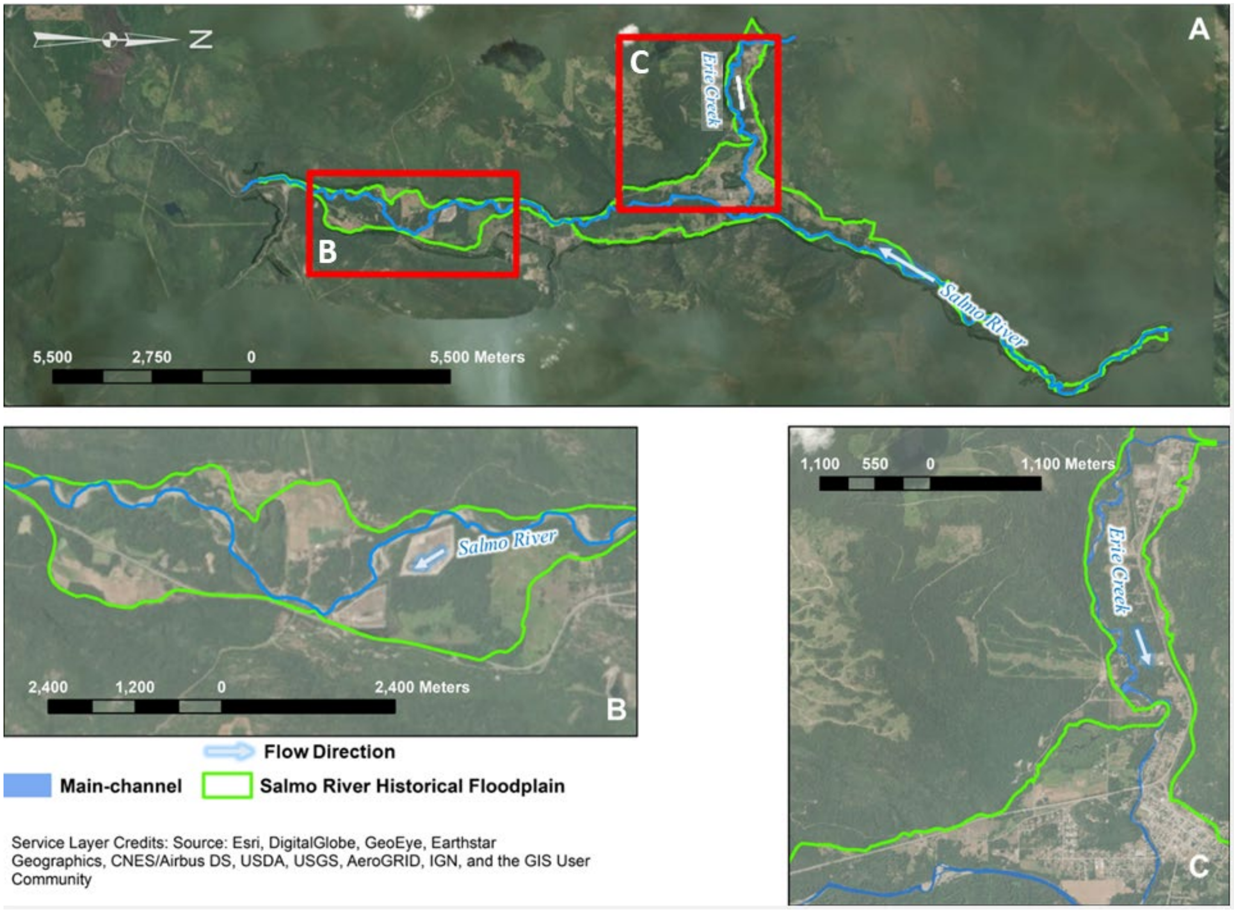

Service Layer Credits: Source: Esri, DigitalGlobe, GeoEye, Earthstar Geographics, CNES/Airbus DS, USDA, USGS, AeroGRID, IGN, and the GIS User Community

Figure 4-2. Channel change and bank erosion study areas. (A) Salmo River study area overview. (B) Salmo River (south section). (C) Erie Creek.

4.2.2. Data Sources

The data sources for this analysis consisted of aerial photographs and high-resolution satellite imagery supported with lidar. The characteristics of these data are described in Table 4-2. The channel mapping was also informed by the river bathymetric survey described in Section 4.1.

Table 4-2. Aerial photographs and high-resolution satellite imagery used in the analysis.

Imagery	Year	Roll / Frame	Photo Number	Nominal Scale	Source
Aerial photograph	1990	BCB9003	83-82,80-78	1:15000	BC Government
High-resolution imagery	2003	N/A	N/A	1:10,000	Google Earth Pro (v 7.3.2.5776)
Aerial photograph	2004	BCC04031	75-78	1:30000	BC Government
High-resolution imagery	2009	N/A	N/A	1:10,000	Google Earth Pro (v 7.3.2.5776)
High-resolution imagery	2012	N/A	N/A	1:10,000	Google Earth Pro (v 7.3.2.5776)
High-resolution imagery	2018	N/A	N/A	0.8 m resolution	Digital Globe from ESRI World Imagery

4.2.3. Methods

In this analysis, the following tasks were completed:

Data preparation:

This task involved the acquisition of historical aerial photographs and imagery for georeferencing and mosaics creation. All the imagery and photographs were georeferenced to the same coordinate systems (NAD 1983 CSRS UTM, Zone 11N).

Geomorphic analysis:

The geomorphic analysis involved three steps. First, distinct channel reaches were delineated (i.e., length of the channel with similar physical characteristics). These reaches were then used to quantify the average net erosion recorded in the analyzed period.

Second, the channel thalweg and planform were delineated. The channel planform refers to the form of a river as viewed from above (Charlton, 2007). The 2019 thalweg was generated from the river bathymetric survey data. The historical channel thalwegs were interpreted from the historical photographs and manually digitized on-screen.

Third, geomorphic features were mapped using defined geomorphic criteria developed by BGC based on Wheaton et al. (2015); Howes and Kenk (1997) and Church (2006) (Table 4-3 and Table 4-4).

Table 4-3. Geomorphic features used for geomorphic floodplain and channel mapping.

Feature	Type	Map Symbol	Description
Channel	Main-channel	Fmc	Flowing channel with distinct banks that carries most of the river discharge. This feature is always active.
	Side-channel	Fsc	Flowing channel with distinct banks that carries a portion of the river discharge less than the main-channel. This feature is active.
	Back-channel	Fbc	Abandoned channel with distinct banks whose downstream end is connected to the river but whose upstream end is plugged. This feature is always active.
	Flood-channel	Ffc	Channel with distinct banks connected to a main or side channel only in overbank flood conditions.
Bars	Abandoned-channel	Fac	Inactive channel remnant(s). No longer directly connected to active flow (e.g., oxbow lake). It can become active during high-flow events.
	Lateral and point bars	Flb	Deposition and accumulation of sediments against the bank (lateral or side bars) and on the inside of a meander bend (point bars).
	Mid-channel bar	Fmb	Feature characterized by the accumulation of sediments within the main channel. When the position of the bar become stable and vegetated during decades, they are commonly called islands.
Plain	Floodplain	Fp	Includes the level-ground area susceptible to overbank flow or flooding during high-flow events.
Fan	Alluvial fan/delta	Ff	A fan is a relatively smooth sector of a cone with a slope gradient from apex to toe up to and including 15°, and a longitudinal profile that is either straight, or slightly concave or convex (Howes and Kenk, 1997).
Terrace	Terrace	Ft, FGt LGt	Flat or gently sloping areas bounded by an adjacent scarp. Fluvial terrace (Ft) deposits consist of channel deposits that may include some overbank materials.

Table 4-4. Levels of activity assigned to the geomorphic features.

Activity Class	Map Symbol	Description
Active	A	This indicates that the fluvial processes were active on the identified geomorphic feature at the time when the remote sensing data were collected. The floodplain and lateral, point or mid-channel bars are considered active until vegetation cover is established. Less than 75% of vegetation coverage or isolated patches of vegetation were classified as active.
Dormant/ Inactive	D	This indicates that there is no observable evidence of fluvial processes being active on the identified feature at the time when the remote sensing data was collected. The floodplain and lateral, point or mid-channel bars are considered dormant when at least 75% of the mapped feature is covered by vegetation.

Channel Change and Bank Erosion Analysis

The channel banks and geomorphic features delineated in the previous stage were used to quantify net bank erosion between the analyzed periods. A spatial analysis using ArcGIS software by ESRI (version 10.6.1) was applied to estimate the net change in riverbank positions between each set of imagery. The following steps were completed:

- A numerical value of 1 (active) or 2 (dormant/inactive) was assigned to each mapped feature in the shapefile attribute table. The values were determined as per the activity criteria described in Table 4-4. The general assumption was that unvegetated bars are active and would be submerged during bankfull conditions and, therefore, part of the active channel. A raster layer consisting of 1 and 2 values was created for each year of analysis.
- Then, the map algebra tool was used to subtract any two raster layers and estimate net change within the period. Negative values indicate bank erosion or channel migration, zero values indicate no change within the period, and positive values indicate either bar stabilization or deposition (Table 4-5).

Table 4-5. Channel change classes.

Map Algebra Results	Class	Definition
-1	Bank Erosion, Channel Migration	Lateral migration of the channel due to the removal of bank material has occurred at the raster cell.
0	No Change	The channel features remained the same at the raster cell between the reviewed periods.
1	Stabilization, Bank Accretion	Two conditions are possible for this result. First, pre-existing channel bars have remained stable during the period, allowing for vegetation to grow (stabilization). Second, the fluvial processes acting during the reviewed timeframe have promoted the sideway deposition along channel meanders (lateral accretion).

4.2.4. Limitations and Uncertainties

Some limitations of the interpretation of remote sensing data to the quantification of channel change include:

- The scale and resolution of available aerial photographs, which affects the level of detail that can be identified for a given year.
- The geometric distortion that results from terrain and imagery acquisition method (e.g., camera tilt in aerial photographs). These factors may result in a displacement of the geomorphic features from its true position.
- The degree to which the historical photographs represent relevant channel changes within the investigated timeframe to within tolerable levels of accuracy.
- Challenges related to the quantification of the error during the process. Possible sources of error in this analysis include scanning, georeferencing error and on-screen digitizing errors.

- The discharge at the time of image capture. At higher discharges, most gravel bars would be inundated.

These errors were reduced in this study by applying common procedures including:

- Focusing on the central part of each aerial photograph
- Scanning the paper photographs at a high resolution
- Conducting geometric corrections on ArcGIS 10.6.1 software using the spline transformation tool which is commonly used when local accuracy is required.

4.3. Hydrological Analysis

4.3.1. Flood Frequency Analysis

4.3.1.1. Salmo River

Peak discharge estimates along the Salmo River were calculated using a pro-rated flood frequency analysis (FFA) based on the Annual Maximum Series approach. In this approach, the maximum peak instantaneous discharge is considered for each year on record. The Generalized Extreme Value (GEV) probability distribution function was fit to peak discharge records. The parameters of the distribution were calculated using the L-moments method of inference.

Historical streamflow data recorded at the *Salmo River near Salmo* (08NE074) and *Hidden Creek neat the Mouth* (08NE114) hydrometric stations were used in the pro-rated FFA (Section 2.3). Hydrometric station information is listed in Table 4-6.

Table 4-6. Hydrometric station information.

Station Name	Salmo River near Salmo	Hidden Creek near the Mouth
Station ID	08NE074	08NE114
Real-time recording	Yes	Yes
Latitude	49°02'49" N	49°14'04" N
Longitude	117°17'39" W	117°14'21" W
Drainage Area (km^2)	1,240	57
Record Period	1949 to current	1973 to current
Record Length (Complete years of data)	70	40
# Years of published peak instantaneous flows	66	40
Approximate Elevation (m)	593	737
Hydrologic Regime	Natural	Natural
Location with Respect to the Village of Salmo	17 km south	5.5 km north

The pro-rated FFA transfers peak discharge information from hydrometric stations to ungauged locations by relating peak discharge to watershed area. The equation used for this relationship is as follows (Eq. 4-1):

$$Q = a \cdot A^b \qquad \text{[Eq. 4-1]}$$

where *Q* is the annual maximum peak instantaneous discharge (m^3/s) and *A* is the watershed area (km^2) and *a* and *b* are a site-specific exponents whose values are calibrated on peak discharge estimates from the Salmo River near Salmo and Hidden Creek near the Mouth hydrometric stations. This procedure is identical to that presented by Acres International Ltd. (1990).

Discharge was increased incrementally along the Salmo River using Eq. 4-1 applied to several locations with increasing watershed area. The discrete discharge increments were assigned to tributaries to the Salmo River in a procedure described in Section 4.4.2.3.

4.3.1.2. Erie Creek

A regional FFA was performed to estimate peak discharge for Erie Creek. The use of the regional FFA was necessary as there is no hydrometric station on Erie Creek. The regionalization of floods procedure was completed using the index-flood method based on the delineation of homogeneous hydrologic regions. As part of the regional FFA, the Erie Creek watershed was assigned to the "*4 East hydrologic region for watersheds less than 500 km^2*" based on its characteristics. Hydrologic regions are made up of hydrometric stations that share similar watershed characteristics. The hydrologic regions that cover the RDCK include region 1 West, 4 East, and 7. The methodology for the regional FFA as well as the estimation of peak discharge at the hydrometric stations are described in Appendix C.

For this project, the mean annual flood was selected as the index flood. A dimensionless regional growth curve was developed from peak discharge data to scale the mean annual flood to peak discharge estimates. The index flood for each creek is determined from watershed characteristics. The index flood value was estimated for the Erie Creek watershed using an ensemble of multiple regression models developed at the provincial scale.

4.3.2. Climate Change Considerations

The Engineers and Geoscientists British Columbia (EGBC) offer guidelines that include procedures to account for climate change when flood magnitudes for protective works or mitigation procedures are required (EGBC, 2018). The impacts of climate change on peak discharge estimates in Salmo River and Erie Creek were assessed using statistical and process-based methods (Appendix D). The statistical methods included a trend assessment on historical flood events using the Mann-Kendall test as well as the application of climate-adjusted variables (mean annual precipitation, mean annual temperature, and precipitation as snow) to the Regional FFA model. The process-based methods included the trend analysis for climate-adjusted flood data offered by the Pacific Climate Impacts Consortium (PCIC).

4.4. Hydraulic Modelling

4.4.1. General Approach

The preparation of flood hazard maps requires the development of a hydraulic model. The two-dimensional (2-D) hydraulic model HEC-RAS 2-D (Version 5.0.7) was used to simulate the flood scenarios summarized in Table 4-7. HEC-RAS is a public domain hydraulic modelling program developed and supported by the United States Army Corps of Engineers (Brunner & CEIWR-HEC, 2016). Each scenario was modelled with climate-change adjusted peak discharges to represent projected future conditions in the period 2050 to 2100 as described in Section 5.2.1.1.

Table 4-7. Return period classes.

Return Period (years)	Annual Exceedance Probability
20	0.05
50	0.02
200	0.005
500	0.002

Further details on modelling methods are presented in Appendix E and summarized in the sections below. The numerical modelling and mapping conducted for the Salmo River study area were based on existing conditions captured in the terrain model. Regulated dikes along Erie Creek and orphaned dikes along the Salmo River were incorporated as part of the DEM and assumed to function as intended up to the peak discharges at which they are being overtopped. Therefore, dike breach scenarios were excluded from the flood hazard assessment.

4.4.2. Model Inputs

Key model inputs include: (1) the topographic model to represent the floodplain and in-channel bathymetry, and (2) the boundary conditions at the upstream and downstream ends of the study area. Table 4-8 summarizes the key numerical modelling inputs selected for the HEC-RAS 2-D model.

Table 4-8. Summary of numerical modelling inputs.

Variable	HEC-RAS
Topographic Input	Lidar (2018); bathymetry (2019)
Mesh Resolution	Variable (3 - 30 m)
Manning’s n	0.035 (in-channel); varied based on landcover data (NALCMS, 2015, (out of channel), Manning’s n values from Chow (1959).
Upstream boundary condition	Steady flow (Q_{20}, Q_{50}, Q_{200}, and Q_{500})
Downstream boundary condition	Normal depth, with a friction slope of 0.007m/m (0.7%)

4.4.2.1. Terrain Model

Following completion of the survey, BGC integrated the bathymetry data and surveyed cross sections with the lidar to generate a DEM for use in hydraulic modelling following the approach described in 4.1.2.

4.4.2.2. Hydraulic Structures

Bridges

There are 13 bridges across the Salmo River and Erie Creek within the study area. The 2-D model terrain was initially developed with the bridge decks and piers removed. HEC-RAS 2-D cannot model high-flow conditions (e.g., when the water surface elevation is greater than the low chord of the bridge). Incorporation of bridge piers can be accomplished within the 2-D model but at significant computational cost. To address this, one-dimensional (1-D) models of the bridge crossings were developed. The water surface elevations resulting from the 1-D bridge models were checked against the water surface elevations resulting from the 2-D model.

Culverts

Erie Creek discharges into Erie Creek through two 1.2 m diameter concrete culverts (Figure 4-3). Highway 6 crosses Boulder Creek atop a 2.4 m diameter culvert. These culverts were incorporated into the 2-D model. A number of additional culverts pass flow through the Highway 3 and Highway 6 embankments. These culverts were not considered in the modelling because they are small (<1,200 mm diameter) and were assumed to be blocked by debris during flood events.

Figure 4-3. Outlet of Erie Lake, looking downstream. Photo: BGC July 31, 2019.

Breaklines

Breaklines are linear features created to locally orient the computational mesh and improve the representation of terrain features. Breaklines were introduced in the computational mesh to capture dike crests, road embankments, ditches and channels, and local high-ground features (e.g., terraces). An illustration of how breaklines capture terrain feature and influence mesh orientation is provided in Appendix E.

4.4.2.3. Model Domain

The model domain covers a 32 km section of the Salmo River and a 7 km section of Erie Creek (Figure 4-4). The upstream boundary on the Salmo River is located 1.4 km above of the unincorporated community of Ymir. The downstream boundary on the Salmo River is 700 m below the confluence with the South Salmo River. The upstream boundary on Erie Creek is located approximately 1.5 km north of Erie Lake. The downstream boundary of the model domain was set approximately 500 m downstream of the downstream end of the study area so that the uncertainty of the downstream boundary condition would not affect modelling results within the study area (Section 4.4.2.4).

Figure 4-4. Salmo River study area. Satellite imagery from Bing.

4.4.2.4. Boundary Conditions

The upstream boundaries on the Salmo River and Erie Creek were modelled as inflow boundaries. The upstream boundaries were defined as steady-state inflow hydrographs for the peak discharges of interest. Discharge along Erie Creek and the Salmo River was increased incrementally by accounting for discrete contributions from tributaries. Seven tributaries along the Salmo River, including Erie Creek and one tributary along Erie Creek (Erie Lake), were included as inflow boundaries (Figure 4-4). The upstream boundaries at the tributaries were also defined as steady-state inflow hydrographs for the peak discharges of interest.

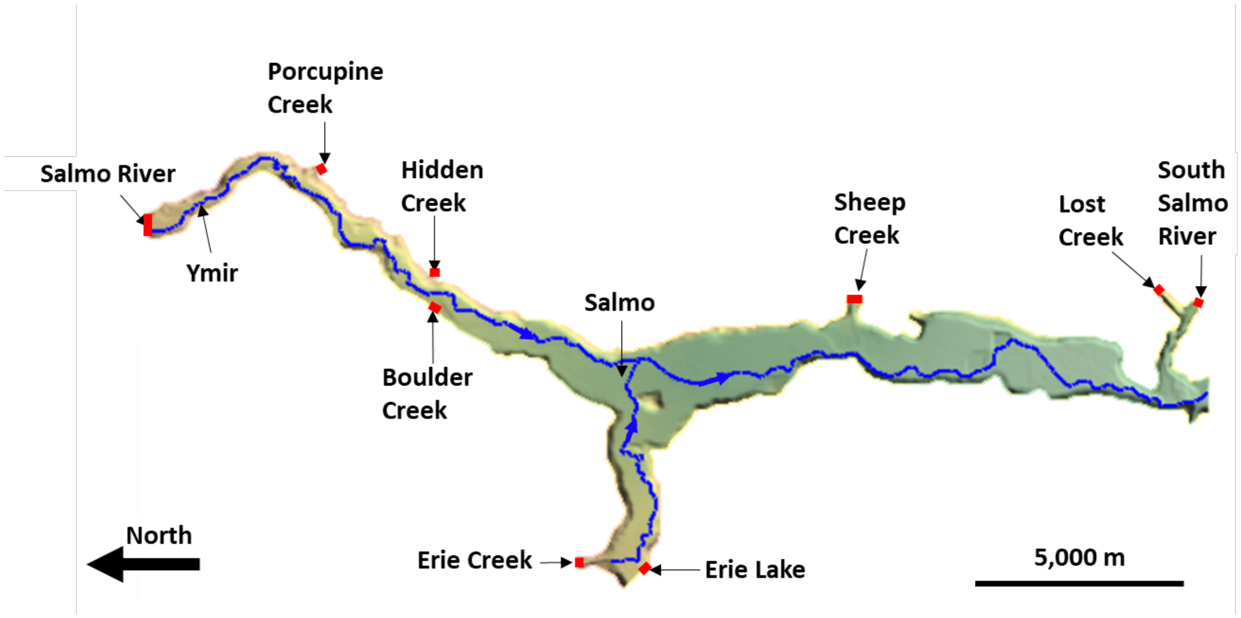

Figure 4-5. Salmo River study area modelling domain and location of upstream boundaries (red), including tributaries.

The normal depth boundary condition was used at the downstream end of the model domain. This assumes that the friction slope (approximately equal to the water slope) is equal to the channel slope. The normal depth assumption can cause errors in model results at the downstream boundary. Therefore, the downstream boundary of the model domain was set approximately 500 m downstream of the downstream end of the study area so that the uncertainty of the friction slope propagating upstream would not affect modelling results within the study area.

4.4.2.5. Development of Flooding Scenarios

To develop complete flood hazard maps for the Salmo River study area, two separate flooding scenarios were modelled; flooding on the Salmo River, and flooding on Erie Creek. The results of these two scenarios were then combined to determine the final flood hazards.

4.5. Hazard Mapping

BGC prepared hazard maps based on the results from the numerical flood modelling. Specifically, BGC prepared two types of maps for the Salmo River study are: hazard scenario maps and an FCL map. The scenario maps support emergency planning and risk analyses, and the FCL map supports communication and policy implementation, as described further below.

4.5.1. Hazard Scenario Maps

Hazard scenario maps display the hazard intensity (destructive potential) and extent of inundated areas for each scenario assessed. Two versions of the hazard scenario maps for each return period are provided: i) maps showing flood depth, and ii) maps showing flow impact force (IF) defined as the combination of fluid bulk density (ρ), area of impact (A) and velocity (v) shown in Equation 4-2:

$$IF = \rho \, A \, v^2 \qquad \text{[Eq. 4-2]}$$

For clearwater flooding, 1000 kg/m^3 was assumed for ρ as shown Equation 4-2. The area of impact represents the area of the object that is impacted or the portion thereof. For this level of study, depth of flow from modelling results is used as a proxy for the height of the area and the impact force is then represented as an impact force per unit width, in this case 1 m.

Maps displaying flow depth support assessments where inundation is the primary mechanism of damage. Flow impact force maps highlight locations where a combination of higher flow velocity and depth may warrant additional assessment (i.e., analyses of bank stability, erosion, or life safety). Table 4-9 provides a description of the flow impact force ranges and their impacts on life safety and impacts on the built environment. A flow depth map for the 200-year peak discharge is provided in this report in Drawing 06. Flow depth and flow impact force maps for all return periods are displayed on Cambio.

Table 4-9. Flow intensity values shown on the flood hazard scenario maps (Cambio)

Impact Force (kN/m)	Description
≤ 1	Slow flowing shallow and deep water with little or no debris. High likelihood of water damage. Potentially dangerous to people in buildings, in areas with higher water depths.
1 to 10	Mostly slow but potentially fast flowing shallow or deep flow with some debris. High likelihood of sedimentation and water damage. Potentially dangerous to people in the basement or first floor of buildings without elevated concrete foundations.
10-100	Fast flowing water and debris. High likelihood of structural building damage and severe sediment and water damage. Dangerous to people on the first floor or in the basement of buildings. Replacement of unreinforced buildings likely required.
>100[1]	Fast flowing debris. High likelihood of building destruction. Very dangerous to people in buildings irrespective of floor.

Note:

1. Flow intensities greater than 100 kN/m in clear water creeks are generally confined to the main channel.

4.5.2. Flood Construction Level Mapping

FCLs are required for areas adjacent to river floodplains for consideration during planning. An FCL can be incorporated into regulation by authorities to provide guidance for new constructions on the extent and elevation of possible flooding in the area. In BC, FCLs are calculated as the higher of the following scenarios:

- Water surface profile for the design peak instantaneous flow plus 0.3 m of freeboard
- Water surface profile for the design daily flow plus 0.6 m of freeboard.

A freeboard is applied to the estimated water surface profile to account for uncertainties in the calculation of the water surface elevations. As noted in EGBC (2017, 2018), freeboard has been set higher than these minimum values for many rivers in BC to account for sediment deposition, debris jams, and other factors. Recently, several studies have recommended using 0.6 m of freeboard above the design peak instantaneous flow (Kerr Wood Leidal [KWL] 2014, 2017; Northwest Hydraulic Consultants [NHC], 2009, 2014, 2018). As such, we have selected to use this approach as well for the Salmo River study area. This approach is used even for communities that are protected from flooding by a diking system due to the potential for a dike to fail during a major flood due to factors such as channel scour, material deposition or toe erosion (Water Management Consultants, March 19, 2004).

Depending on the situation, the presence of a dike may lead to a local rise in the flood levels as the dike constrains the flow within the channel. Should a dike fail through overtopping or geotechnical failure, the resulting flooding depth and extent of flooding may be greater than if the dike was not present due to the elevated flood level (e.g., Figure 4-6).

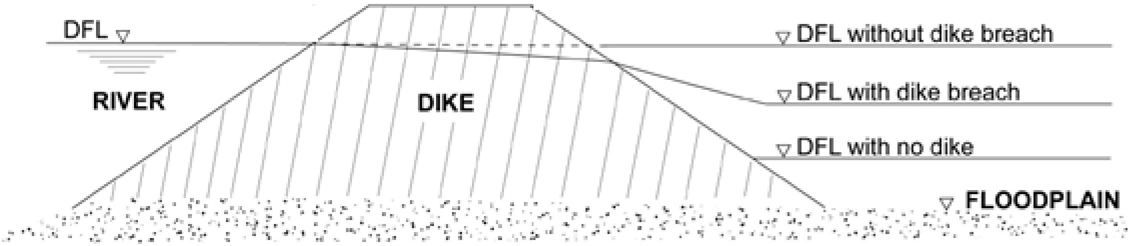

Figure 4-6. **Definition of design flood levels (DFL) in the presence of a dike. DFL refers to the estimated water levels from a design flood event such as the 200-year return period flood (Modified from Water Management Consultants March 19, 2004).**

Because dike breach scenarios were excluded from the flood hazard assessment, FCLs developed from the modelling results are conservative. In large floodplains or areas with complex diking systems, a more detailed approach to estimating FCLs may be warranted. This could include carrying out dike breach scenarios to model flood wave propagation through the floodplain, which may affect resulting FCLs.

For the Salmo River study area, the FCLs were generated by creating isolines from the predicted 200-year water surface plus a 0.6 m freeboard and extending the isolines across the limits of the floodplain generally perpendicular to the flow direction. The FCL maps are presented in Drawing 07

5. RESULTS

5.1. Channel Change Mapping and Bank Erosion

The objective of the geomorphic and bank erosion analysis was to document historical changes in channel width, fluvial landforms, and related geomorphic processes using aerial photographs, and high-resolution imagery. The geomorphic units were mapped for the successive years and were considered in the channel change analysis. The changes estimated over the reviewed timeframe are shown in Drawings 04 for Erie Creek, and Drawing 05 for the Salmo River South Section. The channel reaches identified within each area are shown in Figure 5-1 for Erie Creek and Figure 5-2 for the Salmo River (South Section). The main characteristics of these reaches, including average bank retreat based on the planimetric review, are provided in Table 5-1 and Table 5-2. A description of the observed channel changes as it relates to flood hazard follows.

5.1.1. Erie Creek Alluvial Fan

At the Erie Creek alluvial fan, the channel displays an irregular pattern characterized by straight and wandering segments that exhibit different channel dynamic and lateral stability. Six channel reaches were identified along this creek (ER-1, ER-2, ER-3, ER-4, ER-5, and ER-6) (Figure 5-1). The average bankfull width within these reaches ranges from approximately 12 m (ER-1) to 80 m wide (ER-6). The average channel gradient decreases from around 2% at ER-1 to 0.3% near the confluence with the Salmo River (distal zone of the fan at ER-6). Reaches ER-1 and ER-4 are generally confined and have remained relatively constant through the 1990 – 2019 record (Drawing 04). The other reaches have undergone noticeable changes throughout the reviewed timeframe. The main observations are summarized as follows:

<u>Progressive erosion of the outer bank of meander bends</u>:

Channel meanders typically develop when the channel is unconfined. Gradual erosion was identified at channel meander bends, promoting an increase of the meander curvature. Such processes were observed along Reaches ER-3 and ER-5 (Drawing 04). Although the average bank retreat varied, there were areas in which the maximum bank retreat reached several meters throughout the reviewed timeframe. For example, up to 20 m of bank retreat was recorded at a meander bend on ER-3 between 2004 and 2009 (approximately 1.5 km downstream of the Highway 3 Bridge #1). This retreat caused the migration of the channel centreline towards the right (south) bank to its current location. Within the 2009 – 2018 period, the channel centreline migrated south by more than 50 m at ER-5. For comparison, the average bankfull width for this reach is 40 m. The presence of the regulated dikes along Erie Creek affected the lateral stability of the channel within reach ER-5. The diked downstream segment of ER-5, up to approximately 950 m upstream of Highway 3 bridge #2, appeared generally stable, although signs of localized bank erosion were observed within the reviewed timeframe. In contrast, the channel in the upstream segment of reach ER-5 has been noticeably unstable, especially 300 m upstream from the upstream end of the dike. Measurable geomorphic changes within this reach may affect flow dynamics and flood hazards.

Reoccupation of former flood channels and avulsions:

Although the channel is confined at specific locations (e.g., ER-1 and ER-4), there is evidence in the high-resolution imagery and aerial photographs of past channel avulsion within the alluvial fan. Drawing 04 illustrates locations where the estimated channel thalweg has moved to new locations during the reviewed timeframe. Recent observations of aggradation confirm past efforts to dredge the mouth of Erie Creek and the Salmo River below the confluence.

Channel aggradation:

A gradual change in channel morphology from single-thread meandering to braided was observed with the most downstream 350 m of ER-6 in the reviewed imagery (Figure 2-2). This suggests that aggradation is an active process within the reach, and especially immediately upstream of the confluence with the Salmo River. Aggradation is a distinctive process on the distal section of alluvial fans, and often requires management to restore channel flow capacity (Section 3.4).

Table 5-1. Channel reaches characterization and average bank retreat for Erie Creek.

Reach	Length[1] (m)	Bankfull Width Variation[2] (m)	Channel Pattern	Average Slope (%)	Average Bank Retreat (m)		
					1990-2004	2004-2009	2009 - 2018
ER-1	1160	5 - 28	Single thread-straight	2	-	-	4
ER-2	765	14-30	Single thread-meandering	0.8	-	-	7
ER-3	1310	28-53	Wandering[3]	1.3	2	7	11
ER-4	655	12-21	Single thread-straight	0.6	-	-	2
ER-5	2445	20- 30	Wandering[3]	0.9	7	5	7
ER-6	1745	12-80	Multiple thread-braided	0.6	2	-	6

Notes:
1. Based on 2018 lidar and 2019 bathymetry data.
2. Accuracy is +/- 2 m
3. Wandering implies the watercourse is transitional between meandering (single-thread) and braided (multiple-thread).

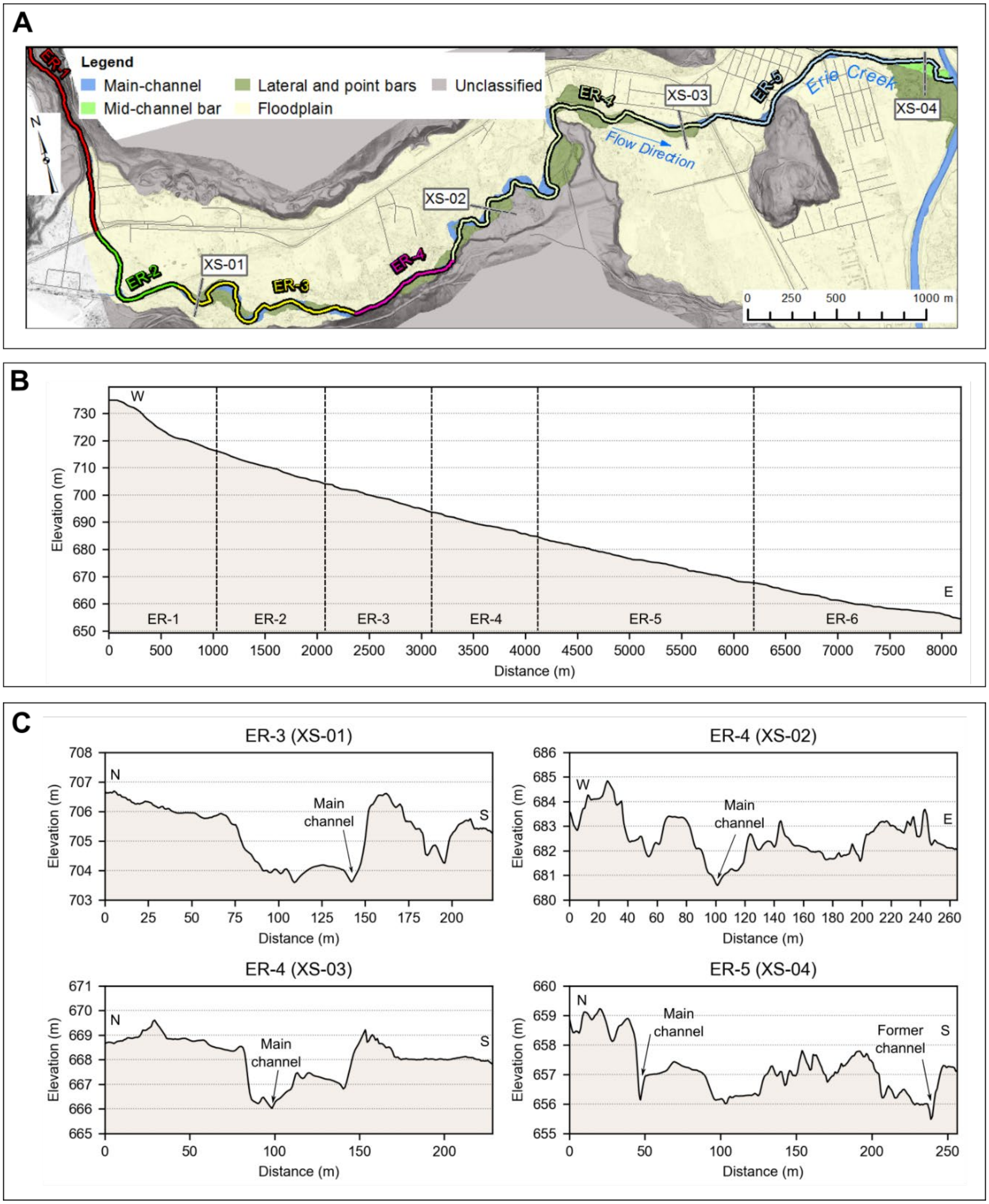

Figure 5-1. Channel reaches within the Erie Creek floodplain. (A) Plan view of the creek and floodplain. (B) Channel longitudinal profile. (C) Examples of cross sections within the reaches. Section lines are from left to right bank. Cross section XS-04 illustrates a case of past channel avulsion.

5.1.2. Salmo River (South Section)

The overall morphology of the Salmo River (South Section) displays characteristics of a wandering gravel-bed channel (Drawing 05). Three channel reaches were classified within this section of the Salmo River. The average bankfull width of the main channel within these reaches is approximately 40 m to 170 m wide. The average channel gradient is about 0.2%. Throughout the reviewed timeframe, the channel changes observed within the Salmo River (south section) were similar to the changes observed at Erie Creek for the wandering reaches. For instance: (1) channel widening is occurring at low channel slope and unconfined locations; and, (2) the maximum bank retreat values were comparable with the values measured at Erie Creek (Table 5-2). Despite these similarities, and unlike Erie Creek, the channel of the Salmo River (south section) appeared to be stabilizing over time. Flood channels and bars that were identified as active during the first reviewed period (2003 - 2012) revegetated or became abandoned channels since. Notable departures from this general trend included a channel segment south of the Sheep Creek (SR-2) confluence, where the retreat of the left (east) bank is on-going. During the 2004 - 2012 timeframe, the channel bank retreated up to 20 m from its previous location along a 500 m long section immediately downstream of the CanEx tailings disposal areas. Then, between 2012 and 2019, the channel migrated several meters further east, along an approximately 1 km section adjacent to the tailings disposal areas. Despite past mitigation efforts, bank erosion appears to be an active on-going process since it was initially reported on by CanEx (1963).

Table 5-2. Channel reaches characterization and average bank retreat Salmo River (South Section).

Reach	Length[1] (m)	Bankfull Width Variation[2] (m)	Channel Pattern	Average Slope (%)	Average Bank Retreat 2003-2012 (m)	Average Bank Retreat 2012-2018 (m)
SR-1	1740	40-70	Single thread-meandering[3]	0.2	9	5
SR-2	2960	55-170	Single thread-meandering[3]	0.3	8	5
SR-3	3110	40-70	Wandering[3]	0.2	5	3

Notes:

1. Based on 2018 lidar and 2019 bathymetry data.
2. Accuracy is +/- 2 m
3. Wandering implies the watercourse is transitional between meandering (single-thread) and braided (multiple-thread).

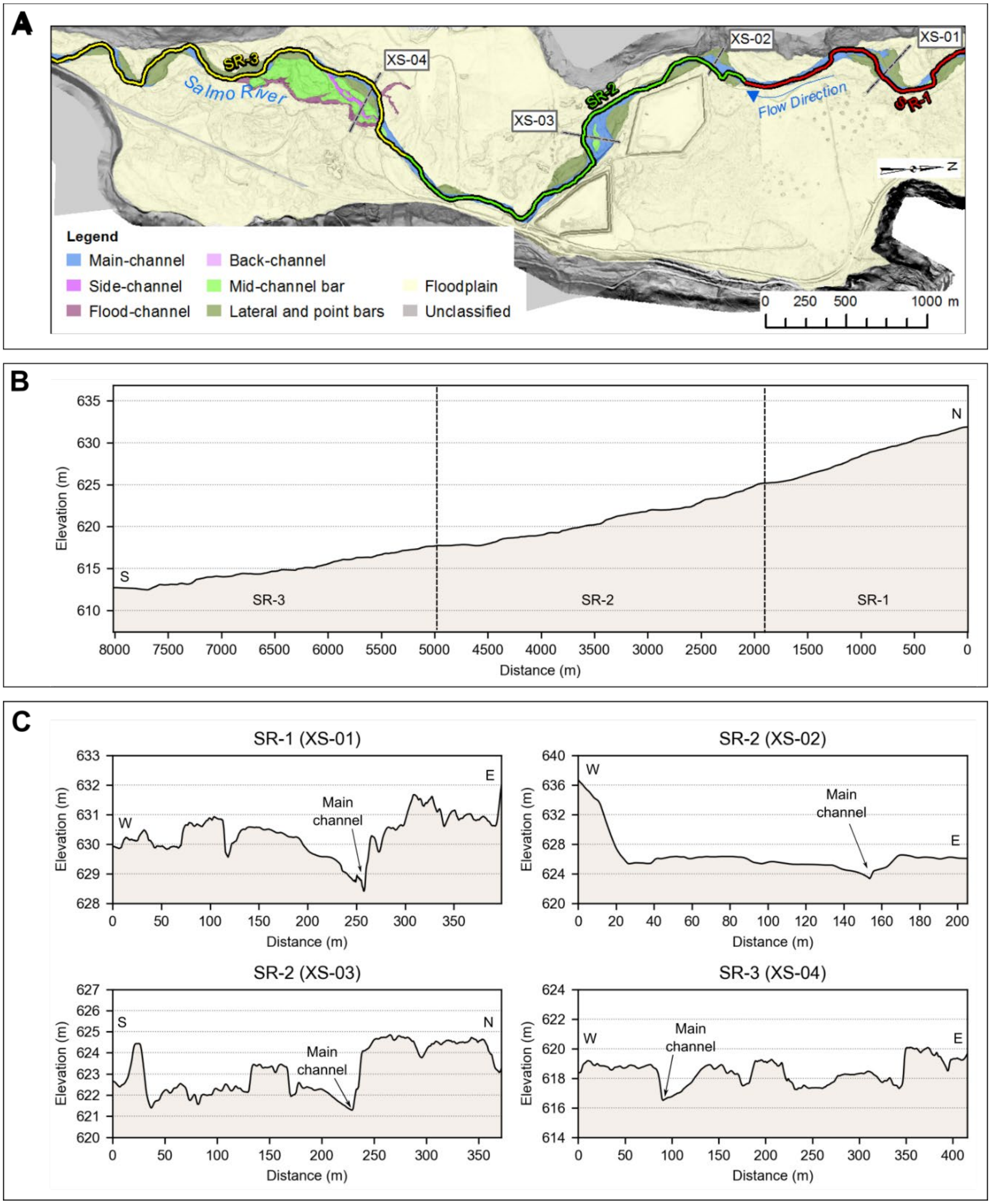

Figure 5-2. Channel reaches within the South Section Salmo River floodplain. (A) Plan view of the river and floodplain. (B) Channel longitudinal profile. (C) Examples of cross sections within the reaches. Cross section lines are from left to right bank.

5.2. Hydrological Analysis

5.2.1. Flood Frequency Analysis

Historical flood quantiles estimated at the *Salmo River near Salmo* and *Hidden Creek near the Mouth* hydrometric stations using historical peak instantaneous discharge records are presented in Table 5-3.

Table 5-3. Historical flood quantiles.

Return Period (years)	AEP	Salmo River near Salmo (m^3/s)	Hidden Creek near the Mouth (m^3/s)
2	0.5	260	14
20	0.05	400	29
50	0.02	440	37
200	0.005	505	52
500	0.002	545	65

Note: Salmo River flood quantiles were rounded to the nearest 5 m^3/s.

5.2.2. Accounting for Climate Change

Statistical trend analysis results show that there is no significant trend in the historical peak flow time series for both *Salmo River near Salmo* (08NE074) and *Hidden Creek near the Mouth* (08NE114) (Table 5-5). Trend analysis results for the PCIC climate-adjusted 200-year flood event (process-based prediction) show that the mean of the for the *Salmo River near Salmo* (08NE074) shows a small increase for the 2009 to 2038 period (+8%) followed by small decrease for the 2039 to 2068 period (-97%).

Table 5-4. Trend analysis results.

Hydrometric Station	Name	Start Year	End Year	p-value[1]	Trend Direction	Sen's Slope[2]
08NE074	Salmo River Near Salmo	1949	2018	0.47	-	-0.29
08NE114	Hidden Creek Near the Mouth	1973	2016	0.73	-	0.02

Notes:

1. A p-value of less than 0.05 is considered significant.
2. A positive Sen's slope indicates an increasing trend in the flow.

The results of the statistical and process-based methods were found to be inconsistent across the RDCK by 2050 (2041 to 2070). The climate change impact assessment results were difficult to synthesise in order to select climate-adjusted peak discharges on a site-specific basis. The assessment of the trends in the discharge records was inconclusive. The results of the statistical flood frequency modelling generally show a small decrease in the flood magnitude, while the results of the process-based discharge modelling generally show an increase with a wide range in magnitude. As a result, peak discharge estimates were adjusted upwards by 20% to account for the uncertainty in the impacts of climate change in the RDCK as per Appendix D.

5.2.3. Climate-Adjusted Peak Instantaneous Discharge

5.2.3.1. Salmo River

Eq. 4-1 (Section 4.3.1) fit to historical flood quantiles listed in Table 5-3 resulted in pro-ration relationships presented in Table 5-4.

Table 5-5. Pro-ration relationships.

Return Period (years)	AEP	$Q = a \cdot A^b$	
		a	b
2	0.5	0.300	0.966
20	0.05	0.872	0.875
50	0.02	1.314	0.832
200	0.005	2.464	0.761
500	0.002	3.756	0.711

These relationships were applied to the Salmo River to derive historical and climate-change adjusted peak instantaneous discharge at six locations within the Salmo River study area (Table 5-5).

Table 5-6. Historical and climate change adjusted peak instantaneous discharge estimates along the Salmo River.

Salmo River	Catchment Area (km^2)	Peak Discharge (m^3/s)							
		AEP=0.05		AEP=0.02		AEP=0.005		AEP=0.002	
		Historical	Climate-Adjusted	Historical	Climate-Adjusted	Historical	Climate-Adjusted	Historical	Climate-Adjusted
Salmo River upstream boundary	301	130	155	150	180	190	230	220	260
Salmo River below Porcupine Creek	389	160	195	190	225	230	275	260	315
Salmo River below Hidden and Boulder Creeks	470	190	230	220	265	265	320	300	360
Salmo River below Erie Creek	691	270	320	300	365	355	430	395	470
Salmo River below Sheep Creek	852	320	385	360	430	420	500	455	550
Salmo River below South Salmo River (downstream boundary)	1061	390	465	430	520	495	595	535	640

Notes:

1. Climate-change adjusted peak discharges are 20% higher than historical peak discharges (Section 4.3.2)
2. Peak instantaneous discharge estimates were rounded to the nearest 5 m^3/s.

For comparison, Acres International Ltd. (1990) estimated the 200-year (AEP=0.005) peak instantaneous discharge to be 185 m^3/s at the upstream boundary, and 502 m^3/s at the downstream boundary of the model domain.

Discharge contributions from the tributaries were then inferred from the peak discharges along the Salmo River, as listed in Table 5-6.

Table 5-7. Climate change adjusted peak instantaneous discharge estimates along the Salmo River, and discharge contribution from tributaries.

	Peak Discharge (m^3/s)							
	AEP=0.05		AEP=0.02		AEP=0.005		AEP=0.002	
	Salmo River	Tributary	Salmo River	Tributary	Salmo River	Tributary	Salmo River	Tributary
Salmo River upstream boundary	155		180		230		260	
Porcupine Creek		40		45		45		55
Salmo River below Porcupine Creek	195		225		275		315	
Hidden Creek		25		30		35		35
Boulder Creek		10		10		10		10
Salmo River below Hidden and Boulder Creeks	230		265		320		360	
Erie Lake		5		5		5		5
Erie Creek		85		95		105		105
Salmo River below Erie Creek	320		365		430		470	
Sheep Creek		65		65		70		80
Salmo River below Sheep Creek	385		430		500		550	
South Salmo River		55		60		65		60
Lost Creek		25		30		30		30
Salmo River below South Salmo River (downstream boundary)	465		520		595		640	

Note: Peak instantaneous discharge estimates were rounded to the nearest 5 m^3/s.

5.2.3.2. Erie Creek

The historical and climate-adjusted peak instantaneous discharges estimated at the mouth of Erie Creek based on the regional FFA are listed in Table 5-7. For comparison, Acres International Ltd (1990) estimated the 200-year (AEP=0.005) peak instantaneous discharge to be 136 m^3/s at the mouth of Erie Creek.

Table 5-8. Historical and climate-adjusted peak instantaneous discharge estimates for Erie Creek based on the regional FFA study.

Return Period (Years)	AEP	Historical Discharges (m^3/s)	Climate-adjusted Peak Discharges (m^3/s)
20	0.05	65	85
50	0.02	80	100
200	0.005	100	130
500	0.002	120	150

Note: Peak instantaneous discharge estimates were rounded to the nearest 5 m^3/s.

5.2.3.3. Peak Discharge Reconciliation for Erie Creek

A comparison of Table 5-6 and Table 5-7 indicates that peak discharge increments assigned to Erie Creek differ from the peak discharges estimated from the regional FFA. As indicated in Section 4.4.2.5, this led to the development of two separate flooding scenarios, one along the Salmo River, and the other along Erie Creek. The results of these two scenarios were then combined to determine the final flood hazards.

5.3. Hydraulic Modelling

The simulated flood profiles for the 200-year flood event are shown in Figure 5-2 and Figure 5-3. Figure 5-4 illustrates freeboard along the regulated dike and at bridge crossings for Erie Creek for the 200-year flood event. A summary of the key observations from the hydraulic modelling is included in Table 5-8.

Table 5-9. Summary of modelling results.

Process	Key Observations
Clear-water inundation	Village of Salmo north of the confluence • The regulated dike on Erie Creek is overtopped by a 200-year peak discharge and greater, causing flooding in the Village of Salmo limited to the vicinity of the dike. • The 500-year peak discharge on both Erie Creek and the Salmo River increases flooding in the Village of Salmo Village of Salmo south of the confluence • The 200-year peak discharge on the Salmo River causes flooding of a residential subdivision approximately 550 m southeast of the confluence. The 500-year peak discharge causes a marginal increase in flooding extent. Unincorporated community of Ymir • The 50-year peak discharge causes minor flooding of the southern part of Ymir. The 200-year and 500-year peak discharges cause a marginal increase in flooding extent. Remainder of study area • The 20-year peak discharge causes overland flooding south of the Village of Salmo. The flooding extent increases to reach the entire width of the valley floor when consider high return period peak discharges. Of note, the wastewater treatment plan located south of the Village of Salmo is not subject to flood for peak discharges up to the 500-year event.
Hydraulic Structures (Bridges)	• The water surface elevations for the 200-year flood do not reach the low chord of 11 out of 13 bridges (Table 5-9). • The low chord of the Boulder Pit Road and Shambhala Grounds bridges are submerged during the 200-year flood event. Because this flood event also causes inundation in the floodplain at these two crossings, current modelling indicates that the incremental effects of the bridges on the extents of the inundated areas are minimal.
Flood Protection Structures (Dikes)	• Current modelling indicates that the 200-year flood event overtops the crest of the regulated dike along the north (left) bank of Erie Creek near the crossing between Handson Avenue and Ninth Street. Freeboard elsewhere along the dike ranges between 0.3 and 2 m. • The orphaned dikes located long the Salmo River south of the Village of Salmo are overtopped by the 20-year and higher return period floods.

Table 5-10. Bridge crossings along the Salmo River and Erie Creek within the study area.

Bridge Crossing	Latitude (°)	Longitude (°)	Low chord elevation (m)	2-D hydraulic model 200-year flood water surface elevation (m)	Freeboard (m)
Erie Creek					
Highway 3 Bridge #1	49.1922	-117.3326	717.1	716.1	1.0
Pedestrian Bridge	49.1885	-117.3278	708.9	707.6	1.3
Highway 3 Bridge #2	49.1898	-117.2847	669.06	666.7	2.4
Carney Bridge Road / Davies Avenue Bridge	49.1895	-117.2829	667.4	665.8	1.6
6th Street Bridge	49.1905	-117.2772	663.9	662.7	1.2
Glendale Avenue / Main Street Bridge	49.1913	-117.2751	663.3	661.6	1.7
Salmo River					
Porto Rico Road Bridge	49.2913	-117.2227	737.1	736.6	0.5
Wildhorse Creek Road Bridge	49.2818	-117.2125	728.4	727.5	0.9
Porcupine Road Bridge	49.2606	-117.2108	708.6	707.3	1.3
Boulder Pit Road Bridge	49.2390	-117.2386	691.35	691.4	-0.05
Airport Road Bridge	49.1907	-117.2659	660.1	658.2	1.9
Highway 6 Bridge	49.1411	-117.2640	644	641.9	2.1
Shambahla Grounds Bridge[1]	49.1094	-117.2609	623.1	623.5	-0.4

Notes:
Bridge crossings are listed in a downstream direction.
[1] The bridge owner is Shambhala Music Festival. The name of the bridge is unknown.

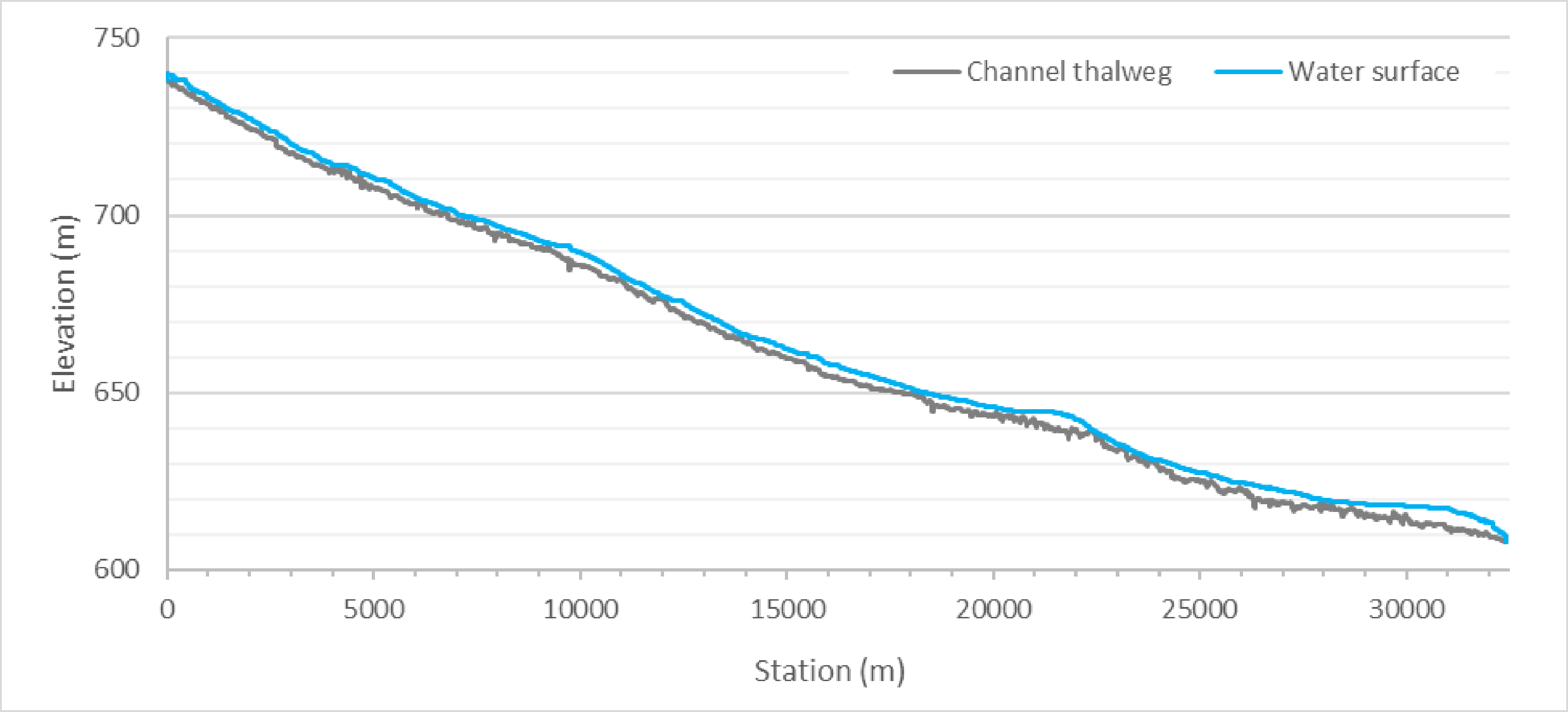

Figure 5-3. 200-year water surface profile along the Salmo River within the extent of the study area. Water surface profile extends from north (upstream) of Ymir to south (downstream) of the confluence with the South Salmo River.

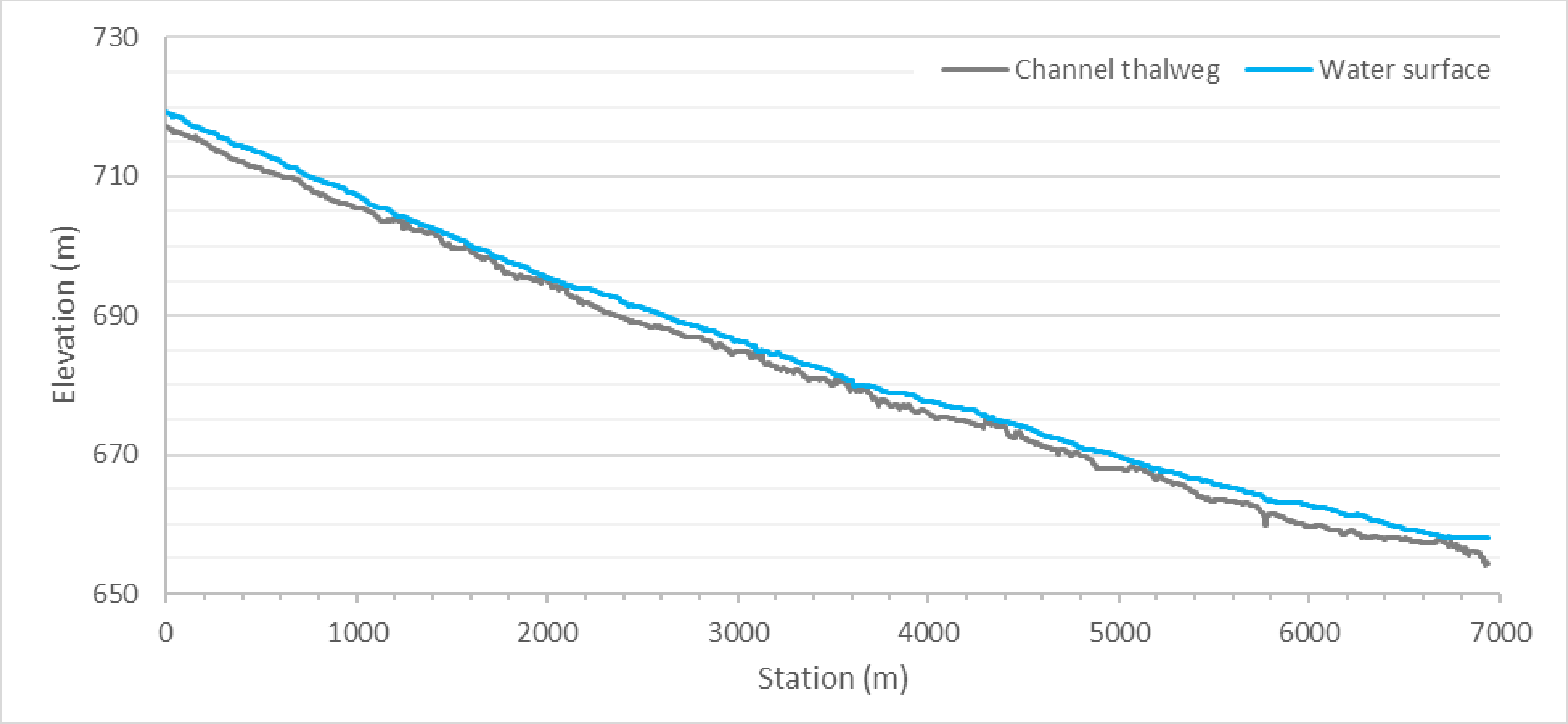

Figure 5-4. **200-year water surface profile along Erie Creek within the extent of the study area. Water surface profile extends from north (upstream) of Erie Lake to the confluence with the Salmo River.**

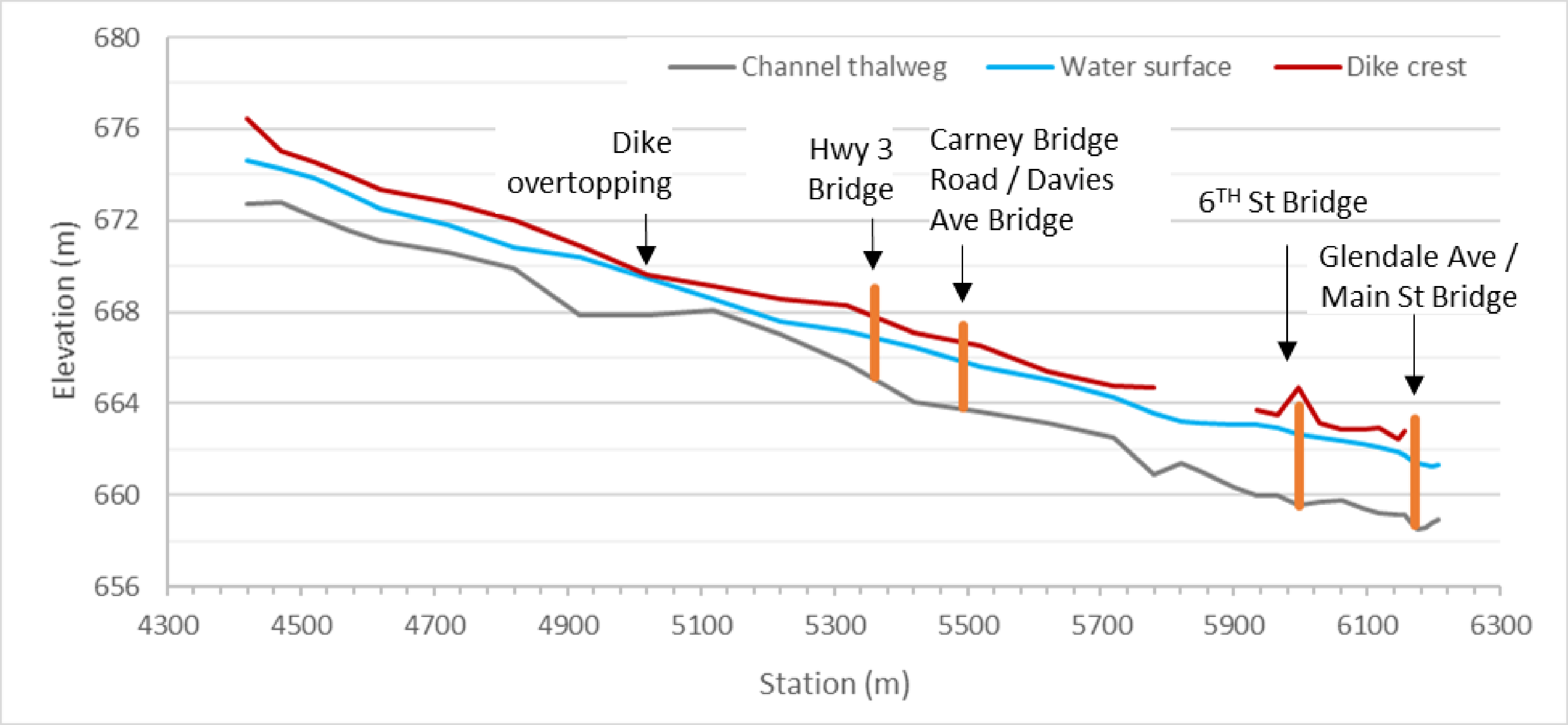

Figure 5-5. **Model profile showing the 200-year water surface elevation, dike crest elevation, and bridge openings to low chord elevation (orange bars) along the lower reach of Erie Creek.**

5.4. Flood Hazard Mapping

Hazard scenario results from the range of return periods modelled are presented in Cambio. Drawing 06 provides modelled water depths for the 200-year return period event.

5.5. Flood Construction Level Mapping

FCL results for the 200-year water surface elevation plus 0.6 m freeboard are presented on Drawing 07. Note that elevations from the FCLs have not been surveyed in the field and should not be relied upon for accuracy of ground levels at the building lot scale

Further note that updated FCLs depart from the historical FCLs, notably in the Village of Salmo south of Erie Creek. While the FCL maps prepared by BGC for the Salmo River study area represent a snapshot in time, the historical study (Acres International Ltd., 1990) accounted for the activity of the Erie Creek alluvial fan in the FCL maps by considering avulsion of the channel on the fan.

6. SUMMARY AND CONSIDERATIONS

This report provides a detailed flood hazard assessment of the Salmo River study area, which includes the Salmo River and Erie Creek floodplains. This area was chosen as a high priority site amongst hundreds in the RDCK due to its comparatively high risk. This report has resulted in digital hazard maps that provide a basis for quantitative risk assessment, if required. It also provides the basis to inform the conceptualization and potential design and construction of mitigation measures should those be found to be required for the Salmo River study area. A variety of analytical desktop and field-based tools and techniques were combined to understand the geomorphological and hazard history, hydrology, and hydraulics of the Salmo River study area.

6.1. Flood Hazard Assessment

6.1.1. Channel Change Mapping and Bank Erosion

Channel change mapping and bank erosion analyses were completed to assess historical geomorphic changes in the study area and how these changes influence channel migration and flood hazards. In summary:

- Fluvial landforms were identified and delineated in the different sets of photographs and high-resolution imagery. This analysis is useful to understand the geomorphic evolution of the channel and how these processes may influence flooding. For instance, bed aggradation and mid-bar formation can divert water overbank or form new paths. The data for Erie Creek and Salmo River (south section) indicate that avulsion has occurred within the assessed areas. Avulsion predominantly led to the reoccupation of previous flood channels.
- The channel change maps (Drawings 04 and 05) illustrate the areas of recorded change between the reviewed photographs and high-resolution imagery (e.g., bank erosion, channel shifting, and stabilization or deposition). These changes were quantified to determine average bank retreat rates within the reviewed timeframe (Table 5-1 and Table 5-2). In general, it was found that both Erie Creek and Salmo River (south section) are laterally unstable. The most significant changes within the studied reaches are characterized by sudden lateral displacement of the channel thalweg and progressive bank retreat on the outside of meander bends. The critical areas for future bank erosion hazard assessment include the following channel reaches ER-3, ER-5 and ER-6, including the regulated dikes in Erie Creek, and the SR-2 and SR-3 reaches along Salmo River (south section).

The resulting maps depict channel geomorphology dynamics within the study area and their possible influence on flood hazards. Further efforts to assess bank erosion should focus on estimating the erosion hazard for the different return periods.

6.1.2. Adjustments for Projected Climate Change

Historical peak discharges estimated for the Salmo River and Erie Creek were adjusted to account for future climate change. Key findings applied to flood mapping are:

- The climate change impact assessment results were difficult to synthesize to select climate-adjusted peak discharges on a site-specific basis. Consequently, a 20% increase in peak discharge was adopted (Appendix D).
- The climate-change adjusted 200-year peak discharges for the Salmo River ranged from 230 m^3/s at the upstream end of the study area, to 595 m^3/s at the downstream end of the study area.
- The climate-change adjusted 200-year peak discharges for Erie Creek was 130 m^3/s at the confluence with the Salmo River.

6.1.3. Hydraulic Modelling

A 2-D hydraulic model developed using HEC-RAS was used to simulate selected hazard scenarios. Table 5-8 provides key observations derived from the numerical modelling. The water surface profiles for the 200-year flood event are presented in Figure 5-2 and Figure 5-3 for the Salmo River and Erie Creek. The hydraulic modelling demonstrates that the key hazards and associated risks stem from potential dike overtopping and breaches along Erie Creek (Figure 5-4).

6.1.4. Flood Hazard Mapping

Model results are cartographically expressed in two ways:

1. The individual hazard scenarios are captured through hazard maps that display estimated flow velocity, flow depth and flood intensity. These maps can support assessment of development proposals and can be used for emergency planning.
2. An FCL map that combines the estimated water surface elevation for the 200-year return period event plus a 0.6 m freeboard. The FCL map can support development proposals in designated hazard zones.

Both the individual scenario hazard and FCL maps serve as decision-making tools to guide subdivision and other development permit approvals.

6.2. Limitations and Uncertainties

While systematic scientific methods were applied in this study, a number of uncertainties remain. As with all hazard assessment and concordant maps, the hazard maps prepared for the Salmo River study area represent a snapshot in time. Future changes to the Salmo River study area including the following may warrant re-assessment and/or re-modelling:

- Substantial flood events
- Major changes in the channel planform
- Effects of future climate change
- Alteration to the existing dikes or construction of additional flood control structures
- Future development in the floodplain
- Bridge re-design.

The assumptions made on changes in runoff due to climate change reflect the current state of knowledge and will likely need to be updated occasionally as scientific understanding of such processes evolves. Despite these limitations and uncertainties, BGC believes that a credible hazard assessment has been achieved on which land use decisions can be made.

6.3. Considerations for Hazard Management

This section notes issues specific to the Salmo River study area that could be considered in the short term given the findings of this study.

Key considerations are:

- The results of the channel change and bank erosion analysis show key areas that warrant further bank erosion hazard assessment. Additional steps to understand bank erosion and hazard in the study area should include a characterisation of: 1) bank susceptibility (erodibility); and 2) critical shear stresses required to erode the banks at areas susceptible to erosion for the different discharge events. These areas include the regulated dikes along Erie Creek.
- The flood mapping conducted for a range of return periods provides an improved hazard basis and update to historical floodplain mapping with consideration of climate change.
- Data from high flow events were not available for model calibration. Collection of evidence for historical high flow events along the Salmo River and Erie Creek would support calibration of the hydraulic model. This could be accomplished through installation of streamflow gauge(s) within the study area, or the recording and survey of highwater marks after flood events.
- The regulated dike on Erie Creek is susceptible to overtopping by a 200-year peak discharge or greater, which would cause flooding in the Village of Salmo. Sections of the orphaned dikes along the Salmo River south of the Village of Salmo are susceptible overtopping by a 20-year peak discharge or greater; however, the waster water treatment plant offset from the west (right) bank of the river is not susceptible to flooding by peak discharges up to the 500-year event. An assessment of the geotechnical stability of the dikes was excluded from the scope of this study. A hydrotechnical and geotechnical assessment of the dikes could be completed in the future as part of a separate scope of work to recommend adjustments to the dike elevations to ensure adequate freeboard and to assess the stability of the dikes.
- Hydraulic modelling (1-D and 2-D) of bridge crossings indicates that there is no freeboard allowance for the 200-year flood event at the Boulder Pit Road bridge and Shambhala Grounds bridge crossings.
- The FCLs presented in Drawing 07 for the 200-year return period flood event plus 0.6 cm freeboard provides an improved basis for community planning, bylaw development, and emergency response planning in areas subject to flood hazards, with consideration of climate change. The application of the FCL map requires discussions and regulatory decisions for both existing and proposed development. Building and floodproofing elevations should be established from legal survey and benchmarks. Setback distances from the natural boundaries of watercourses are not shown on maps. FCLs provide a standards-based approach which are simple to apply and interpret. In some cases, the FCL may be impossible or impractical to implement for several reasons. Allowances should be permitted for stakeholders to apply for a site-specific reduction in the FCLs

contingent on a report by a suitably qualified Professional Engineer, preferably using a risk-based approach.

6.4. Recommendations

Recommendations are provided in the Summary Report (BGC, 2020) as they pertain to all studied RDCK creeks.

7. CLOSURE

We trust the above satisfies your requirements at this time. Should you have any questions or comments, please do not hesitate to contact us.

Yours sincerely,

BGC ENGINEERING INC.
per:

Pascal Szeftel, Ph.D., P.Eng.
Senior Hydrotechnical Engineer

Elisa Scordo, M.Sc., P.Geo.
Senior Hydrologist

Melissa Hairabedian, M.Sc., P.Geo
Senior Hydrologist

Patrick Grover, M.A.Sc., P.Eng.
Senior Hydrotechnical Engineer

Reviewed by:

Rob Millar, Ph.D., P.Eng., P.Geo.
Principal Hydrotechnical Engineer

Hamish Weatherly, M.Sc., P.Geo.
Principal Hydrologist

PS/RM/HW/mp/syt

Final stamp and signature version to follow once COVID-19 restrictions are lifted

REFERENCES

Acres International Ltd. (1990, December). Floodplain Mapping Salmo River Design Brief.

BGC Engineering Inc. (2020). *RDCK Floodplain and Steep Creek Study, Summary Report (*Draft). Prepared for Regional District of Central Kootenay

BGC Engineering Inc. (2019, March 31). *Flood and Steep Creek Geohazard Risk Prioritization* [Report]. Prepared for Regional District of Central Kootenay.

BGC Engineering Inc. (2019, May 24) *NDMP Stream 2 Application: Flood Mapping* [Work Plan (Revised)]. Prepared for Regional District of Central Kootenay.

BGC Engineering Inc. (2019, November 15) *NDMP Stream 2 Project Deliverables* (Revised)]. Prepared for Regional District of Central Kootenay.

Boyer, D. (2009, March 24). *Orphan Flood Protection Works*. Letter addressed to Ramona Mattix, Manager of Development Services RDCK.

British Columbia Department of Environment Water Resources Service. (1976, February). *Salmo River flood and erosion control report*.

British Columbia Ministry of Environment (BC MOE), Water Management Branch (1981, May). *Salmo River - Flood Protection*.

Brunner, G.W. & CEIWR-HEC. (2016). HEC-RAS River Analysis System 2D Modeling User's Manual. Retrieved from www.hec.usace.army.mil

Canadian Exploration Limited. (1963, June 27). A report on the use of "junk" car bodies for river protection as carried out by Canadian Exploration Limited on the Salmo River below the lead zinc tailing disposal area.

Charlton, R. (2007). *Fundamentals of fluvial geomorphology*. Routledge.

Chow, V.T. (1959). *Open-channel hydraulics*. New York, McGraw-Hill, 680 p.

Church, M. (2006). Bed material transport and the morphology of alluvial river channels. *Annual Review of Earth and Planetary Sciences, 34*, 325-354. https://doi.org/10.1146/annurev.earth.33.092203.122721

Demarchi, D.A. (2011, March). *An introduction to the ecoregions of British Columbia (3rd ed.)*. Victoria, BC: British Columbia Ministry of Environment, Ecosystem Information Section. Retrieved from https://www2.gov.bc.ca/assets/gov/environment/plants-animals-and-ecosystems/ecosystems/broad-ecosystem/an_introduction_to_the_ecoregions_of_british_columbia.pdf

Engineers and Geoscientists BC. (2017, January). *Professional practice guidelines: Flood mapping in BC*. Retrieved from https://www.egbc.ca/getmedia/8748e1cf-3a80-458d-8f73-94d6460f310f/APEGBC-Guidelines-for-Flood-Mapping-in-BC.pdf.aspx

Engineers and Geoscientists BC. (2018, July). *Professional practice guidelines: Legislated flood assessments in a changing climate in BC*. Retrieved from https://www.egbc.ca/getmedia/f5c2d7e9-26ad-4cb3-b528-940b3aaa9069/Legislated-Flood-Assessments-in-BC.pdf.aspx

Farjad, B., Gupta, A., & Marceau, D.J. (2016). Annual and seasonal variations of hydrological processes under climate change scenarios in two sub-catchments of a complex watershed. *Water Resources Management, 30*(8). 2851-2865. https://doi.org/10.1007/s11269-016-1329-3

Fulton, R.J., Shetsen, I., Rutter, N.W. (1984). *Surficial Geology, Kootenay Lake, British Columbia-Alberta*. Geological Survey of Canada, Open File 1084, 2 sheets.

Harder, P., Pomeroy, J.W., and Westbrook, C.J. (2015). Hydrological resilience of a Canadian Rockies headwaters basin subject to changing climate, extreme weather, and forest management. *Hydrological Processes, 29*, 3905-3924. https://doi.org/10.1002/hyp.10596

Howes, D.E., & Kenk, E. (1997). *Terrain classification system for British Columbia (version 2)*. BC Ministry of Environment and BC Ministry of Crown Lands, Victoria, BC.

Kerr Wood Leidal. (KWL, 2014). *Creek Hydrology, Floodplain Mapping and Bridge Hydraulic Assessment – Floodplain Development Permit Area, Flood Construction Level Development and Use* [Report]. Prepared for the City of North Vancouver and the District of North Vancouver.

Kerr Wood Leidal. (KWL, 2017). *Wildlife Enhancement Program at Burton Flats Design Feasibility Final Report*. Prepared for BC Hydro. Ref: CLBWORKS-30B.

Lawler, D.M. (2006). The measurement of river bank erosion and lateral channel change: a review. *Earth Surface Processes and Landforms, 18*(9), 777-821. https://doi.org/10.1002/esp.3290180905

Loukas, A. & Quick, M.C. (1999). The effect of climate change on floods in British Columbia. *Nordic Hydrology, 30*(3), 231-256. https://doi.org/10.2166/nh.1999.0013.

Marcus, W.A. (2012). Remote sensing of the hydraulic environment in gravel-bed rivers. In M. Church, P. Biron, and A. Roy (Eds.), *Gravel-bed rivers: Processes, tools, environments* (pp. 259-285). Wiley-Blackwell.

Natural Resources Canada (NRCan). (2017). Federal Floodplain Mapping Framework. Version 1.0, General Information Product 112e. 20 pp.

Nellestijn, G. & Ells, B. (2008). *A History of the Salmo River Watershed*.

Northwest Hydraulic Consultants (NHC). (2009, May). *Flood Risk Evaluation and Flood Control Solutions, Phase 1. (34920)* [Report]. Prepared for the City of Prince George.

Northwest Hydraulic Consultants (NHC). (2014, May). *Simulating the Effects of Sea Level Rise and Climate Change on Fraser River Flood Scenarios (GS14LMN-035)* [Report]. Prepared for BC Ministry of Forests Lands and Natural Resource Operations.

Northwest Hydraulic Consultants (NHC). (2018, November 22). *Lillooet River Floodplain Mapping, Phase 1. (3002903*) [Report]. Prepared for the Pemberton Valley Dyking District Office.

North American Land Change Monitoring System (NALCMS). (n.d.). Land Cover, 2015 (Landsat, 30m). [Data]. Extracted November 21 2019, From Commission for Environmental Cooperation website: http://www.cec.org/tools-and-resources/map-files/land-cover-2010-landsat-30m

Oxford University Press. (2008). In M. Allaby (Ed.), *A dictionary of Earth Sciences*, Third Edition (pp. 654). Oxford, England.

Salmo Watershed Streamkeepers Society (SWSS). (2000). Inventory of Mine Tailings and Ponds in the Salmo Watershed. November 2000.

Schnorbus, M., Bennett, K., Werner, A., & Berland, A. (2011). *Hydrologic Impacts of Climate Change in the Peace, Campbell and Columbia Watersheds, British Columbia, Canada. Hydrologic Modelling Project* Final Report (Part II). Victoria: Pacific Climate Impacts Consortium.

Schnorbus, M., Werner, A., & Bennett, K. (2014). Impacts of climate change in three hydrologic regimes in British Columbia, Canada. *Hydrological Processes, 28*, 1170-1189. https://doi.org/10.1002/hyp.9661

Statistics Canada. (2016). Census Profile, 2016 Census [Webpage]. Retrieved from https://www12.statcan.gc.ca/census-recensement/2016/dp-pd/prof/index.cfm?Lang=E

Trimble, S.W. & Cooke, R.U. (1991). Historical sources for geomorphological research in the United States. *The Professional Geographer, 43*(2), 212-228. https://doi.org/10.1111/j.0033-0124.1991.00212.x

Turner, R.J.W., Anderson, R.G., Franklin, R., & Fowler, F. (2009). *Geotour guide for the West Kootenay, British Columbia. Geology, landscapes, mines ghost towns, caves and hot springs*. Geological Survey of Canada Open file 6135, British Columbia Geological Survey Geofile 2009-06.

Wahba, G. (1990). Spline models for Observational data. Paper presented at CBMS-NSF Regional Conference Series in Applied Mathematics. Philadelphia: Soc. Ind. Appl. Maths.

Wang, T., Hamann, A. Spittlehouse, D.L., & Carroll, C. (2016). Locally downscaled and spatially customizable climate data for historical and future periods for North America. PLoS One 11: e0156720. https://doi.org/10.1371/journal.pone.0156720

Water Management Consultants Inc. (2004, March 19). *Floodplain Mapping: Guidelines and Specifications* [Report]. Prepared for Fraser Basin Council.

Wheaton, J. M., Fryirs, K. A., Brierley, G., Bangen, S. G., Bouwes, N., & O'Brien, G. (2015). Geomorphic mapping and taxonomy of fluvial landforms. *Geomorphology, 248*, 273-295. https://doi.org/10.1016/j.geomorph.2015.07.010

APPENDIX A
TERMINOLOGY

Table A-1 defines terms that are commonly used in geohazard assessments. BGC notes that the definitions provided are commonly used, but international consensus on geohazard terminology does not fully exist. **Bolded terms** within a definition are defined in other rows of Table A-1.

Table A-1. Geohazard terminology.

Term	Definition	Source
Active Alluvial Fan	The portion of the fan surface which may be exposed to contemporary hydrogeomorphic or avulsion hazards.	BGC
Aggradation	Deposition of sediment by a (river or stream).	BGC
Alluvial fan	A low, outspread, relatively flat to gently sloping mass of loose rock material, shaped like an open fan or a segment of a cone, deposited by a stream at the place where it issues from a narrow mountain valley upon a plain or broad valley, or where a tributary stream is near or at its junction with the main stream, or wherever a constriction in a valley abruptly ceases or the gradient of stream suddenly decreases	Bates and Jackson (1995)
Annual Exceedance Probability (P_H) (AEP)	The Annual Exceedance Probability (AEP) is the estimated **probability** that an event will occur exceeding a specified magnitude in any year. For example, a flood with a 0.5% AEP has a one in two hundred chance of being reached or exceeded in any year. AEP is increasingly replacing the use of the term **'return period'** to describe flood recurrence intervals.	Fell et al. (2005)
Avulsion	Lateral displacement of a stream from its main channel into a new course across its fan or floodplain. An "avulsion channel" is a channel that is being activated during channel avulsions. An avulsion channel is not the same as a paleochannel.	Oxford University Press (2008)
Bank Erosion	Erosion and removal of material along the banks of a river resulting in either a shift in the river position, or an increase in the river width.	BGC
Clear–water flood	Riverine and lake flooding resulting from inundation due to an excess of clear-water discharge in a watercourse or body of water such that land outside the natural or artificial banks which is not normally under water is submerged.	BGC
Climate normal	Long term (typically 30 years) averages used to summarize average climate conditions at a particular location.	BGC
Consequence (C)	In relation to risk analysis, the outcome or result of a **geohazard** being realised. Consequence is a product of **vulnerability** (V) and a measure of the **elements at risk** (E)	Fell et al. (2005); Fell et al. (2007), BGC

Term	Definition	Source
Consultation Zone	The Consultation Zone (CZ) includes all proposed and existing development in a geographic zone defined by the approving authority that contains the largest credible area affected by specified **geohazards**, and where damage or loss arising from one or more simultaneously occurring specific **geohazards** would be viewed as a single catastrophic loss.	Adapted from Porter et al. (2009)
Debris Flow	Very rapid to extremely rapid surging flow of saturated, non-plastic debris in a steep channel (Hungr, Leroueil & Picarelli, 2014). Debris generally consists of a mixture of poorly sorted sediments, organic material and water (see Appendix B of this report for detailed definition).	BGC
Debris Flood	A very rapid flow of water with a sediment concentration of 3-10% in a steep channel. It can be pictured as a flood that also transports a large volume of sediment that rapidly fills in the channel during an event (see Appendix B of this report for detailed definition).	BGC
Design Peak Daily Flow	The design flow (e.g. 200-year flood) based on the analysis of annual maximum daily average discharge records.	BGC
Design Peak Instantaneous Flow	The design flow (e.g. 200-year flood) based on the analysis of annual maximum instantaneous discharge records.	BGC
Elements at Risk (E)	This term is used in two ways: a) To describe things of value (e.g., people, infrastructure, environment) that could potentially suffer damage or loss due to a **geohazard**. b) For risk analysis, as a measure of the value of the elements that could potentially suffer damage or loss (e.g., number of persons, value of infrastructure, value of loss of function, or level of environmental loss).	BGC

Term	Definition	Source
Encounter Probability	This term is used in two ways: a) **Probability** that an event will occur and impact an element at risk when the element at risk is present in the **geohazard** zone. It is sometimes termed **"partial risk"** b) For quantitative analyses, the **probability** of facilities or vehicles being hit at least once when exposed for a finite time period L, with events having a **return period** T at a location. In this usage, it is assumed that the events are rare, independent, and discrete, with arrival according to a statistical distribution (e.g., binomial or Bernoulli distribution or a Poisson process).	BGC
Erosion	The part of the overall process of denudation that includes the physical breaking down, chemical solution and transportation of material.	Oxford University Press (2008)
Flood	A rising body of water that overtops its confines and covers land not normally under water.	American Geosciences Institute (2011)
Flood Construction Level (FCL)	A designated flood level plus freeboard, or where a designated flood level cannot be determined, a specified height above a natural boundary, natural ground elevation, or any obstruction that could cause flooding.	BGC
Flood mapping	Delineation of flood lines and elevations on a base map, typically taking the form of flood lines on a map that show the area that will be covered by water, or the elevation that water would reach during a flood event. The data shown on the maps, for more complex scenarios, may also include flow velocities, depth, or other hazard parameters.	BGC
Floodplain	The part of the river valley that is made of unconsolidated river-borne sediment, and periodically flooded.	Oxford University Press (2008)
Flood setback	The required minimum distance from the natural boundary of a watercourse or waterbody to maintain a floodway and allow for potential bank erosion.	BGC

Term	Definition	Source
Freeboard	Freeboard is a depth allowance that is commonly applied on top of modelled flood depths. There is no consistent definition, either within Canada or around the world, for freeboard. Overall, freeboard is used to account for uncertainties in the calculation of a base flood elevation, and to compensate for quantifiable physical effects (e.g., local wave conditions or dike settlement). Freeboard in BC is commonly applied as defined in the BC Dike Design and Construction manual (BC Ministry of Water, Land and Air Protection [BC MWLAP], 2004): a fixed amount of 0.6 m (2 feet) where mean daily flow records are used to develop the design discharge or 0.3 m (1 foot) for instantaneous flow records.	BC Ministry of Water, Land and Air Protection [BC MWLAP] (2004)
Frequency (f)	Estimate of the number of events per time interval (e.g., a year) or in a given number of trials. Inverse of the **recurrence interval** (**return period**) of the **geohazard** per unit time. Recurring **geohazards** typically follow a **frequency**-magnitude (F-M) relationship, which describes a spectrum of possible **geohazard magnitudes** where larger (more severe) events are less likely. For example, annual **frequency** is an estimate of the number of events per year, for a given **geohazard event magnitude**. In contrast, annual **probability** of exceedance is an estimate of the **likelihood** of one or more events in a specified time interval (e.g., a year). When the expected **frequency** of an event is much lower than the interval used to measure **probability** (e.g., **frequency** much less than annual), **frequency** and **probability** take on similar numerical values and can be used interchangeably. When **frequency** approaches or exceeds 1, defining a relationship between **probability** and **frequency** is needed to convert between the two. The main document provides a longer discussion on **frequency** versus **probability**.	Adapted from Fell et al. (2005)
Hazard	Process with the potential to result in some type of undesirable outcome. Hazards are described in terms of scenarios, which are specific events of a particular frequency and magnitude.	BGC
Hazardous flood	A flood that is a source of potential harm.	BGC

Term	Definition	Source
Geohazard	Geophysical process that is the source of potential harm, or that represents a situation with a potential for causing harm. Note that this definition is equivalent to Fell et al. (2005)'s definition of Danger (threat), defined as an existing or potential natural phenomenon that could lead to damage, described in terms of its geometry, mechanical and other characteristics. Fell et al. (2005)'s definition of danger or threat does not include forecasting, and they differentiate Danger from Hazard. The latter is defined as the **probability** that a particular danger (threat) occurs within a given period of time.	Adapted from CSA (1997), Fell et al. (2005).
Geohazard Assessment	Combination of **geohazard analysis** and evaluation of results against a **hazard tolerance standard** (if existing). Geohazard assessment includes the following steps: a. **Geohazard analysis**: identify the **geohazard** process, characterize the geohazard in terms of factors such as mechanism, causal factors, and trigger factors; estimate **frequency** and magnitude; develop **geohazard scenarios**; and estimate extent and intensity of **geohazard scenarios**. b. Comparison of estimated hazards with a hazard tolerance standard (if existing)	Adapted from Fell et al. (2007)
Geohazard Event	Occurrence of a **geohazard**. May also be defined in reverse as a non- occurrence of a **geohazard** (when something doesn't happen that could have happened).	Adapted from ISO (2018)
Geohazard Intensity	A set of parameters related to the destructive power of a **geohazard** (e.g., depth, velocity, discharge, impact pressure, etc.)	BGC
Geohazard Inventory	Recognition of existing **geohazards.** These may be identified in geospatial (GIS) format, in a list or table of attributes, and/or listed in a **risk register**.	Adapted from CSA (1997)
Geohazard Magnitude	Size-related characteristics of a **geohazard**. May be described quantitatively or qualitatively. Parameters may include volume, discharge, distance (e.g., displacement, encroachment, scour depth), or acceleration. In general, it is recommended to use specific terms describing various size-related characteristics rather than the general term magnitude. Snow avalanche magnitude is defined differently, in classes that define destructive potential.	Adapted from CAA (2016)

Term	Definition	Source
Geohazard Risk	Measure of the **probability** and severity of an adverse effect to health, property the environment, or other things of value, resulting from a geophysical process. Estimated by the product of **geohazard probability** and **consequence**.	Adapted from CSA (1997)
Geohazard Scenario	Defined sequences of events describing a **geohazard** occurrence. Geohazard scenarios characterize parameters required to estimate risk such **geohazard extent** or **runout exceedance probability,** and **intensity.** Geohazard scenarios (as opposed to **geohazard risk scenarios**) typically consider the chain of events up to the point of impact with an element at risk, but do not include the chain of events following impact (the **consequences**).	Adapted from Fell et al. (2005)
Hazard	Process with the potential to result in some type of undesirable outcome. Hazards are described in terms of scenarios, which are specific events of a particular frequency and magnitude.	BGC
Inactive Alluvial Fan	Portions of the fan that are removed from active hydrogeomorphic or avulsion processes by severe fan erosion, also termed fan entrenchment.	BGC
LiDAR	Stands for Light Detection and Ranging, is a remote sensing method that uses light in the form of a pulsed laser to measure ranges (variable distances) to the Earth. These light pulses - combined with other data recorded by the airborne system - generate precise, three-dimensional information about the shape of the Earth and its surface characteristics.	National Oceanic and Atmospheric Administration, (n.d.).
Likelihood	Conditional **probability** of an outcome given a set of data, assumptions and information. Also used as a qualitative description of **probability** and **frequency**.	Fell et al. (2005)
Melton Ratio	Watershed relief divided by square root of watershed area. A parameter to assist in the determination of whether a creek is susceptible to flood, debris flood, or debris flow processes.	BGC
Nival	Hydrologic regime driven by melting snow.	Whitfield, Cannon and Reynolds (2002)
Orphaned	Without a party that is legally responsible for the maintenance and integrity of the structure.	BGC
Paleofan	Portion of a fan that developed during a different climate, base level or sediment transport regime and which will not be affected by contemporary geomorphic processes (debris flows, debris floods, floods) affecting the active fan surface	BGC

Term	Definition	Source
Paleochannel	An inactive channel that has partially been infilled with sediment. It was presumably formed at a time with different climate, base level or sediment transport regime.	BGC
Pluvial – hybrid	Hydrologic regime driven by rain in combination with something else.	BGC
Probability	A measure of the degree of certainty. This measure has a value between zero (impossibility) and 1.0 (certainty) and must refer to a set like occurrence of an event in a certain period of time, or the outcome of a specific event. It is an estimate of the **likelihood** of the magnitude of the uncertain quantity, or the **likelihood** of the occurrence of the uncertain future event. There are two main interpretations: i) Statistical – **frequency** or fraction – The outcome of a repetitive experiment of some kind like flipping coins. It includes also the idea of population variability. Such a number is called an “objective” or relative frequentist probability because it exists in the real world and is in principle measurable by doing the experiment. ii) Subjective (or Bayesian) probability (degree of belief) – Quantified measure of belief, judgement, or confidence in the **likelihood** of an outcome, obtained by considering all available information honestly, fairly, and with a minimum of bias. Subjective probability is affected by the state of understanding of a process, judgement regarding an evaluation, or the quality and quantity of information. It may change over time as the state of knowledge changes.	Fell et al. (2005)
Return Period (Recurrence Interval)	Estimated time interval between events of a similar size or **intensity**. Return period and **recurrence interval** are equivalent terms. Inverse of **frequency**.	BGC
Risk	Likelihood of a geohazard scenario occurring and resulting in a particular severity of consequence. In this report, risk is defined in terms of safety or damage level.	BGC
Rock (and debris) Slides	Sliding of a mass of rock (and debris).	BGC
Rock Fall	Detachment, fall, rolling, and bouncing of rock fragments.	BGC

Term	Definition	Source
Scour	The powerful and concentrated clearing and digging action of flowing air or water, especially the downward erosion by stream water in sweeping away mud and silt on the outside curve of a bend, or during a time of flood.	American Geological Institute (1972)
Steep-creek flood	Rapid flow of water and debris in a steep channel, often associated with avulsions and bank erosion and referred to as debris floods and debris flows.	BGC
Steep Creek Hazard	Earth-surface process involving water and varying concentrations of sediment or large woody debris. (see Appendix B of this report for detailed definition).	BGC
Uncertainty	Indeterminacy of possible outcomes. Two types of uncertainty are commonly defined: a) Aleatory uncertainty includes natural variability and is the result of the variability observed in known populations. It can be measured by statistical methods, and reflects uncertainties in the data resulting from factors such as random nature in space and time, small sample size, inconsistency, low representativeness (in samples), or poor data management. b) Epistemic uncertainty is model or parameter uncertainty reflecting a lack of knowledge or a subjective or internal uncertainty. It includes uncertainty regarding the veracity of a used scientific theory, or a belief about the occurrence of an event. It is subjective and may vary from one person to another.	BGC
Waterbody	Ponds, lakes and reservoirs	BGC
Watercourse	Creeks, streams and rivers	BGC

REFERENCES

American Geological Institute. (1972). *Glossary of Geology*. Washington, DC.: Author.

American Geosciences Institute. (2011). *Glossary of Geology* (5th ed.). Virginia: Author.

Bates, R.L. & Jackson, J.A. (1995). *Glossary of Geology* (2nd ed.). Virginia: American Geological Institute.

Canadian Avalanche Association (CAA). (2016). Technical Aspects of Snow Avalanche Risk Management – Resources and Guidelines for Avalanche Practitioners in Canada (C. Campbell, S. Conger, B. Gould, P. Haegeli, B. Jamieson, & G. Statham Eds.). Revelstoke, BC, Canada: Canadian Avalanche Association.

Canadian Standards Association (CSA). (1997). *CAN/CSA – Q859-97 Risk Management: Guideline for Decision Makers*. CSA Group, Toronto, ON, pp. 55.

Fell, R., Ho., K.K.S., LaCasse, S., & Leroi, E. (2005). A framework for landslide risk assessment and management. In Hungr, O., Fell, R., Couture, R. (Eds.) *Landslide Risk Management:* Proceedings *of the International Conference on Landslide Risk Management.* Vancouver, BC.

Fell, R., Whitt, G. Miner, A., & Flentje, P.N. (2007). Guideline for Landslide Susceptibility, Hazard and Risk Zoning for Land Use Planning. *Australian Geomechanics Journal* 42: 13-36.

Hungr, O., Leroueil, S. and Picarelli, L. (2014) The Varnes Classification of Landslide Types, an Update. Landslides, 11, 167-194. https://doi.org/10.1007/s10346-013-0436-y

International Organization for Standardization (ISO). (2018). *ISO 31000:2018 Risk Management – Guidelines*. Retrieved from https://www.iso.org/standard/65694.html

BC Ministry of Water, Land and Air Protection. (MWLAP) (2004). *Flood Hazard Area Land Use Management Guidelines*.

National Oceanic and Atmospheric Administration. (n.d.) What is LIDAR? [Web page]. Retrieved from https://oceanservice.noaa.gov/facts/lidar.html

Oxford University Press. (2008). *A dictionary of Earth Sciences* (3rd ed.). Oxford, England: Author.

Porter, M., Jakob, M., & Holm, K. (2009, September). Proposed Landslide Risk Tolerance Criteria. *GeoHalifax 2009*. Paper presented at the meeting of the Canadian Geotechnical Society, Halifax, Canada.

Whitfield, P.H., Cannon, A.J., & Reynolds, C.J. (2002). Modelling Streamflow in Present and Future Climates: Examples from the Georgia Basin, British Columbia. *Canadian Water Resources Journal, 27*(4), 427 – 456. https://doi.org/10.4296/cwrj2704427.

APPENDIX B
SITE PHOTOGRAPHS

Photo 1.

Looking downstream (south) from the right bank of the Salmo River, approximately 800 m downstream from the confluence of Erie Creek. Photo: BGC, July 5, 2019.

Photo 2.

Dike steepened by erosion along the west bank of the Salmo River, approximately 800 m downstream of the confluence of Erie Creek. Photo: BGC, July 5, 2019.

Photo 3.

Standing on a dike along the west bank of the Salmo River, looking downstream, approximately 1 km downstream of the confluence of Erie Creek. Photo: BGC, July 31, 2019.

Photo 4.

Bedrock visible along right bank of the Salmo River, at FSR bridge, approximately 750 m upstream of Boulder Mill Creek Road Bridge. Photo: BGC, July 31, 2019.

Photo 5.

Standing on the left bank of the Salmo River looking downstream (south) to the east of Ymir. Photo: BGC, July 31, 2019.

Photo 6.

Culverts from Erie Lake emptying into Erie Creek. Photo: BGC, July 31, 2019.

Photo 7.

Culverts emptying into the Salmo River, approximately 2.5 km downstream of Porcupine Bridge. Photo: MSI, August 2, 2019.

Photo 8.

Woody Debris deposited along Erie Creek, approximately 200 m upstream of the confluence with the Salmo River. Photo: MSI, August 7, 2019.

Photo 9.

Woody debris deposited along the Salmo River, approximately 1.5 km upstream of Porcupine Bridge. Photo: MSI, July 31, 2019.

Photo 10.

Woody debris deposited along the Salmo River, approximately 1.5 km upstream of Porcupine Bridge. Photo: MSI, July 31, 2019.

APPENDIX C
HYDROLOGICAL ANALYSIS METHODS

C.1. INTRODUCTION

Estimating flood magnitude is of fundamental importance to reliable floodplain mapping. As most watercourses are not gauged, flood magnitude is commonly estimated for an ungauged catchment using a Regional Flood Frequency Analysis (Regional FFA). There are several methods to complete a Regional FFA. This appendix documents the methodology followed by BGC Engineering Inc. (BGC) for the regionalization of floods in British Columbia using the index-flood method (Dalrymple 1960).

This appendix begins with a description of Regional FFA and the index-flood method (Section C1.0). The study area over which the index-flood is developed is discussed in Section C2.0. The data acquisition and compilation to support the analysis is described in Section C3.0. A description of the methods and assumptions for the regionalization of floods is included in Section C4.0. Results for the different hydrologic regions that cover the Regional District of Central Kootenay (RDCK) are presented in Section C5.0, while the application of the index-flood method to ungauged catchments in the RDCK is presented in Section C6.0. Finally, the limitations of the study are discussed in Section C7.0.

C.1.1. Regional FFA

Extreme events are rare by definition and record lengths at hydrometric stations are often short. Regional FFA accounts for short record lengths by trading space for time where flood events at several hydrometric stations are pooled to estimate flood magnitude in a homogeneous region. Homogeneous regions can be defined as geographically contiguous regions, geographically non-contiguous regions, or as hydrological neighbourhoods. Grouping catchment areas of similar catchment characteristics into homogeneous regions is a critical part of Regional FFA because hydrologic information can be transferred accurately only within a region that is homogeneous. The more homogeneous a region is, the more reliable the flood quantile estimates. Some heterogeneity may be deemed acceptable in some cases. Studies show that even moderately heterogeneous regions can yield more accurate flood quantile estimates than a single-station FFA (Hosking & Wallis, 1997).

C.1.2. Index-flood Method

Several methods have been developed to conduct a Regional FFA in homogeneous regions. Among the quantile estimation methods, the index-flood is considered superior to other models (Ouarda et al., 2008). The index-flood is a method of regionalization with a long history in FFA (Dalrymple, 1960). The index-flood method involves the development of a dimensionless regional growth curve assumed to be constant within a homogenous region. The index-flood method also requires the selection of an index-flood which can be the mean annual flood, the median annual flood, or another quantile of choice calculated at each hydrometric station in the region.

The probability distribution of flood events at hydrometric stations in a homogeneous region are identical apart from a site-specific scaling factor, the index-flood. The parameters of the probability distribution are estimated at each hydrometric station. These at-site estimates are combined using a weighted average to generate a regional estimate. The regional growth curve is thus a dimensionless quantile function common to every hydrometric station in the region and takes on the following form (Eq. C-1):

$$X_T = Q_T \,/\, Q_m \qquad \text{[Eq. C-1]}$$

where X_T is the growth factor for return period $_T$, Q_T is the flood magnitude at return period $_T$, and Q_m is the index-flood magnitude. The flood magnitude at any return period is calculated using this relationship given the index-flood estimate.

C.1.3. Application to Ungauged Catchments

The index-flood method can be applied to an ungauged catchment by developing a regional relationship between the index-flood and catchment characteristics at hydrometric stations in the region. The relationship can be expressed in many forms including a multivariate linear regression. Flood events can be assumed to depend on the characteristics of individual catchments such as area, elevation, percent lake, forest coverage, mean annual precipitation, mean annual temperature, etc. Once the catchment characteristics are extracted at the ungauged site, the index-flood can be estimated. The flood magnitude of any annual exceedance probability (AEP) can be estimated for an ungauged catchment using the index-flood estimate and the regional growth curve by re-organizing equation Eq. C1-1.

C.2. STUDY AREA

A Regional FFA for British Columbia represents a considerable challenge given its regional variations in precipitation caused by sharp changes in topography as well as diverse geology. The proportion of annual precipitation that falls as snow as opposed to rain increases with latitude, elevation, and distance from the Pacific Ocean. Significant regional variations in precipitation are observed in British Columbia, influenced by the various mountain ranges. Storms approaching the West Coast are lifted rapidly along the windward mountain slopes, resulting in widespread precipitation. A rain shadow is created on the lee side of the mountains. For example, Tofino receives an average of 3,160 mm of annual precipitation while Nanaimo, on the east coast of Vancouver Island, receives 1,060 mm.

This climate pattern is repeated several times from east to west. As the weather systems approach the Coast Mountains, orographic effects result in twice as much precipitation in North Vancouver compared to Vancouver proper. Moving to the east, the Okanagan Valley is located on the lee side of the Coast Mountains resulting in an arid to semi-arid climate with annual precipitation on the order of 350 mm. The cycle is repeated over the Monashees, the Columbia Trench, and the Rocky Mountains. These orographic effects impact flood events and complicate regionalization efforts due to significant areal variations in precipitation, even for small catchments. These significant variations in precipitation suggest that a multivariate approach to regionalization is practical for British Columbia.

Similar to precipitation, surficial geology in the province demonstrates significant spatial variability. This variability is important in that while two catchments may be located in a similar precipitation zone, the hydrologic response can be significantly different. Catchments dominated by colluvial veneers and bedrock will tend to have larger unit peak flows, than those mantled by coarse morainal sediment, with the latter tending to attenuate peak flows through available soil moisture storage. To avoid introducing boundary effects at the border with the Unites States and Alberta, the study area was extended to include the northern portion of Washington, Idaho, and Montana as well as the eastern Slopes of the Rocky Mountains. A map of the study area is presented in Figure C-1.

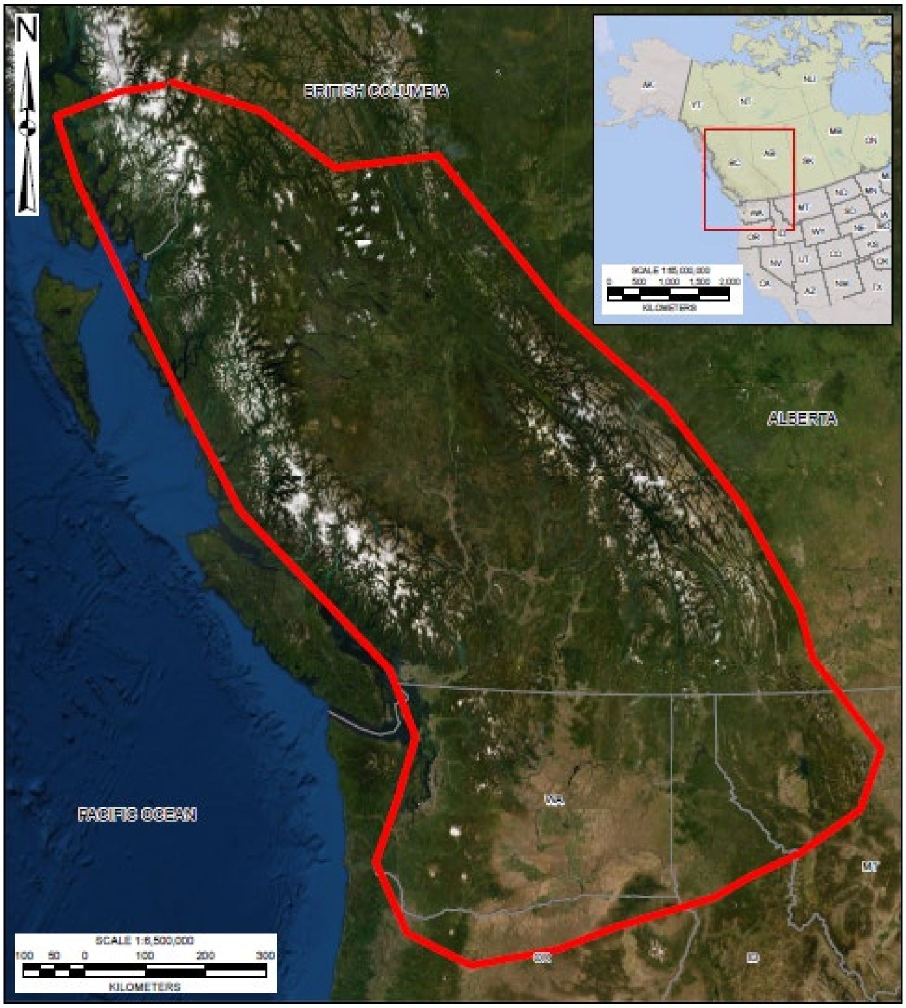

Figure C-1. Study area where the red outline defines the boundary.

C.3. DATA ACQUISITION AND COMPILATION

A large component of this study consisted of acquiring the data and compiling it in a format that was usable for analysis. Suitable hydrometric stations in the study area were identified and the flood records were acquired from the appropriate monitoring agency. The catchment polygons upstream from the hydrometric stations were then delineated and the area calculated using methods specific to the scale of the catchment. Lastly, a suite of catchment characteristics was selected based on potential to influence flood events. These catchment characteristics were extracted for each polygon. The acquisition and the compilation of this rich dataset was the most time-consuming portion of the procedure. The following sections include a detailed description of how the data were acquired and how the dataset was compiled for analysis.

C.3.1. Hydrometric Stations

A total of 3,309 hydrometric stations are located within the study area. Of these, 2115 are managed by the Water Survey of Canada (WSC) and the remaining 1194 are managed by the United States Geological Survey (USGS).

C.3.2. Flood Records

As an initial step, all flood events recorded at the hydrometric stations were extracted. This extraction was challenging as records are stored differently by the WSC and USGS. In Canada, flood events are stored in the HYDAT database, which includes the annual maximum peak instantaneous streamflow, the maximum average daily streamflow, as well as the date and time of each event. The catchment area and the number of years on record are also available in the HYDAT database. The flood records were acquired directly from the HYDAT database for hydrometric stations in Canada. In the US, flood events are stored online on websites specific to each hydrometric station. The annual maximum peak instantaneous streamflow, the catchment area, and the number of years on record are also stored in this way. This information was extracted from the online storage space using a programming script for each USGS hydrometric station.

C.3.3. Maximum Peak Instantaneous Streamflow

The preferred metric for analysis is the annual maximum peak instantaneous streamflow. However, it is not uncommon for flood records to have more annual maximum average daily streamflow records than peak instantaneous values, which are greater in magnitude. The ratio (I/D) between maximum peak instantaneous and maximum average daily streamflow is typically greater for small catchments than for very large catchments. Therefore, where only a maximum daily streamflow is reported for some years, maximum peak instantaneous streamflow values can be estimated from available maximum average daily streamflow records using regression analysis.

The reliability of the regression analysis was judged based on the coefficient of determination (R^2) in combination with the Cook distance (D). The R^2 is the proportion of the variance in the peak instantaneous streamflow that is predictable from the average daily streamflow. The D value is computed for every record within a sample and is used to assess the influence of each record on the regression (e.g., outliers). The regression analysis was deemed acceptable by BGC if the R^2 was greater than 0.95 and the maximum D value was less than 25. In this case, the maximum peak instantaneous streamflow record was extended using the regression analysis for a longer record length. Alternatively, maximum peak instantaneous streamflow record remained as-is where the regression analysis was deemed unacceptable.

C.3.4. Catchment Polygons

The catchment polygons at hydrometric stations within the study area were estimated using two different approaches.

1. River Networks Tools™[1] (RNT).
2. Using an Environmental Systems Research Institute (ESRI) process (i.e., GIS-based).

The RNT-based approach is dependent on the delineation of a stream network, while the ESRI-based process is dependent on topographic data. Catchment polygons were defined for all hydrometric stations located within the study area. Catchment delineation based on a stream network was observed to be more reliable for small catchments, especially where topographic relief is low. The catchment polygons defined by the ESRI process were selected for larger catchments (>1,000 km^2), while the RNT-based approaches were selected for smaller catchment areas (<1,000 km^2). The selection of the best catchment polygon for analysis could not be checked directly as the monitoring agencies (WSC and USGS) do not publish polygon shape information.

C.3.5. Catchment Areas

The catchment area was estimated for each catchment polygon (RNT, modification based on RNT, and ESRI) at each hydrometric station. The catchment area for each polygon was then compared with the value published by the respective monitoring agency. The catchment area published by monitoring agencies is generally considered most reliable (although recognizing many of the catchment areas for the WSC stations were calculated with 1:50,000 scale mapping and may not reflect more recent topographic mapping) and was used to quality check the calculated areas.

The estimated value of the catchment area was deemed acceptable if it was within ±15% of the published value. If more than 1 catchment area estimate (of the 3) was within ±15% of the published value, the catchment area with the smallest difference relative to the published value was selected as the best estimate for analysis. Approximately 90% of catchment polygons were within ±15% of the published value.

Published values are not available for all hydrometric stations. In those cases, the catchment area was deemed acceptable if the 3 estimates were within ±15% of each other. Catchment areas that did not meet the ± 15% criteria were not included in the analysis. A total of 2269 hydrometric stations were removed from the analysis because either the catchment area was deemed

---

[1] The RNT is a proprietary software developed by BGC. RNT is based on publicly available 1:24,000-scale or better topographic and hydrographic datasets throughout North America that BGC has compiled and systematically developed to support a wide range of hydrotechnical calculations (e.g., catchment area) and site-specific precipitation and flood monitoring.

unreliable or water level data only was recorded at the station. Manual quality checks were not completed for these catchments due to the time-consuming nature of this effort. The number of hydrometric stations lost that could have been considered useful is considered negligible. The number of hydrometric stations in the study area is summarized in Table C-1. The ESRI catchment polygons were used for the hydrometric stations at the border between Canada and the United States because the polygons based on the two RNT approaches are observed to be poorly delineated due to differences in data resolution available between both countries.

Table C-1. Number of hydrometric stations in the study area.

Criteria	Number
Hydrometric Stations in Study Area	3284
Station with Unacceptable Catchment Area Estimates	2269
Stations with Acceptable Catchment Area Estimates	1015

C.3.6. Catchment Characteristics

Catchment characteristics were selected based on potential to influence flood events. A suite of 18 catchment characteristics was ultimately selected and estimated for each hydrometric station, as summarized in Table C-2. Several data sources were used to compile the catchment characteristics which are described in the following sections.

C.3.6.1. Catchment Statistics

The Shuttle Radar Topography Mission (STRM) dataset (Farr et al. 2007) was used to extract the catchment elevation statistics. The catchment elevation statistics were averaged over the catchment area. This dataset was used to calculate the catchment area (just for catchments over 1000 km^2), relief, length, and slope. The centroid statistics were also extracted from this dataset.

C.3.6.2. Climate Variables

The Climate North America (ClimateNA) dataset was used to estimate the climate variables for each catchment polygon (Wang et al., 2016). The climate variables were averaged over the catchment area and were based on the average for the period 1961 to 1990.

Table C-2. List of selected catchment characteristics.

Type	No.	Acronym	Characteristic	Units	Dataset
Catchment	1	Centroid_Lat	Latitude at the centroid location in the catchment polygon	degrees	STRM
	2	Centroid_Long	Longitude at the centroid location in the catchment polygon	degrees	
	3	Centroid_Elev	Elevation at the centroid location in the catchment polygon	m	
	4	Area	Area of the catchment polygon	km^2	
	5	Relief	Maximum minus minimum catchment elevation	m	
	6	Length	Area divided by perimeter	km	
	7	Slope	Catchment length divided by relief times 100	%	
Climate	8	MAP	Mean annual precipitation	mm	Climate NA
	9	MAT	Mean annual temperature	°C	
	10	PAS	Precipitation as snow	mm	
	11	PPT_wt	Winter precipitation (Dec, Jan, Feb)	mm	
	12	PPT_sp	Spring precipitation (Mar, Apr, May)	mm	
	13	PPT_sm	Summer precipitation (Jun, Jul, Aug)	mm	
	14	PPT_fl	Fall precipitation (Sep, Oct, Nov)	mm	
Physiographic	15	Forest	Forest cover in the catchment	%	NALCMS
	16	Water_Wetland	Wetland and open water cover in the catchment	%	
	17	Urban	Urban cover in the catchment	%	
	18	CN	Inferred based on integrating land cover and soils cover	unitless	NALCMS and HYSOGs250m

C.3.6.3. Land cover

The North American Land Change Monitoring System (NALCMS) land cover products include the 2005 land cover map of North America. This dataset includes 19 land cover classes derived from 250 m Moderate Resolution Spectroradiometer (MODIS) image composites (Latifovic et al., 2012). This dataset was used to calculate the percent forest, percent wetland and lake, and the urban portion of the catchment.

C.3.6.4. Curve Number

The curve number (CN) is an empirical parameter used for predicting runoff from rainfall. BGC integrated the land cover (NALCMS) and the hydrologic soils group (HYSOGs250m) datasets to infer the average CN over each catchment. The NALCMS dataset is described in Section C.3.6.3. The HYSOGs250m dataset represents typical soil runoff potential at a 250 m spatial resolution (Ross et al., 2018). Hydrologic soils groups are defined based on soil texture, depth to bedrock or depth to groundwater. There are four basic groups: A, B, C, D. Four additional groups are included where the depth to bedrock is considered to be less than 60 cm: AD, BD, CD, and DD. The area covered by each hydrologic soils group is summed for a total area over the catchment for each hydrologic soils group.

The CN was assigned following guidance from the USGS (1986). The CN values for soils where the depth to bedrock or depth to groundwater.is expected to be less than 0.6 m from the surface (i.e., D soils) were assumed to be the same as the case where it is not expected to be close to the ground surface. The CN value assignment for the combinations of land cover and hydrologic soils groups identified in the catchments is presented in Table C-3. The CN values were averaged over the catchment area using a weighted mean. The weight reflects the percentage of the area covered by a given CN value.

Table C-3. CN values based on the integration between the land cover and soils datasets.

Land Cover (NALCMS, 2005)	Cover Type (USGS, 1986)	Soils			
		HSG-A	HSG-B	HSG-C	HSG-D
Temperate or sub-polar needleleaf forest	Woods - Good	30	55	70	77
Temperate or sub-polar broadleaf deciduous forest	Woods - Good	30	55	70	77
Mixed forest	Woods - Good	30	55	70	77
Temperate or sub-polar shrubland	Brush - brush-weed-grass mixture with brush the major element - Fair	35	56	70	77
Temperate or sub-polar grassland	Pasture, grassland, or range—continuous for grazing - Good	39	61	74	80
Sub-polar or polar grassland-lichen-moss	Pasture, grassland, or range—continuous for grazing - Good	39	61	74	80
Sub-polar or polar barren-lichen-moss	Desert shrub - major plants include saltbrush. Greasewood, creosotebush, blackbrish, bursage, palo verde, mesquite, and cactus - good	49	68	79	84
Sub-polar taiga needleleaf forest	Woods - Good	30	55	70	77
Cropland	Row crops - straight row (SR)	63	74	81	85
Barren land	Desert shrub - major plants include saltbrush. Greasewood, creosotebush, blackbrish, bursage, palo verde, mesquite, and cactus - good	49	68	79	84
Urban and built-up	Urban districts - commercial and business	89	92	94	95
Snow and ice	NA	0	0	0	0
Wetland	NA	0	0	0	0
Water	NA	0	0	0	0

C.4. METHODS AND ASSUMPTIONS

Once the dataset is compiled for analysis, the regionalization of floods procedure can begin. A description of the methods and assumptions for the index-flood method is included in this section.

C.4.1. Flood Statistics Calculations

Flood statistics were calculated using the flood record at each of the selected hydrometric stations (2101) in the study area. Flood statistics include L-moments and flood quantile estimates.

C.4.1.1. L-moments

The L-moment approach in the index-flood procedure was used by BGC for the regionalization of floods in British Columbia. The shape of a probability distribution has traditionally been described by the moments of the distribution including the mean, standard deviation, skewness, and kurtosis. However, moment estimators have some undesirable properties where the skewness and kurtosis can be severely biased. Both have algebraic bounds that depend on the sample size (Hosking & Wallis 1997).

L-moments are an alternative system for describing the shape of probability distributions. Studies have shown that L-moments are unbiased, less sensitive to outliers, and are better estimators of distribution parameters especially for short to moderate record length (Hosking, 1990). Furthermore, L-moments allow for the efficient computation of parameter estimates and flood quantile estimates.

L-moments evolved as modifications to the probability weighted moments (Greenwood et al., 1979). In terms of probability weighted moments, L-moments are defined as λ_1, λ_2, λ_3, and λ_4 with their mathematical expressions published for a range of probability distributions in Hosking and Wallis (1997, Appendix).

Dimensionless versions of L-moments are defined as L-moment ratios by dividing the higher order L-moments by λ_2. L-moment ratios are defined by Eq. C-2:

$$\tau_r = \lambda_r / \lambda_2 \qquad \text{[Eq. C-2]}$$

L-moment ratios depict the shape of a distribution independently of its scale measurement. Refer to Table C-4 for L-moment terminology.

Table C-4. L-moment terminology.

Symbol (population)	Symbol (sample)	Definition
λ_1	ι_1	L-location or the mean of the distribution
λ_2	ι_2	L-scale
τ	t	L-CV
τ_3	t_3	L-skewness
τ_4	t_4	L-kurtosis

C.4.1.2. At-site Flood Quantile Estimates

The flood quantile estimates at hydrometric stations are referred to as 'at-site' estimates and are used to compare with the modeled quantile estimates to assess the validity of the model. Flood quantile estimates were calculated using the flood data by means of a single-station FFA. A popular approach in FFA is the Annual Maximum Series (AMS) where the maximum peak instantaneous streamflow for each year on record is used for analysis. The basic assumption is that the flood events are independent and identically distributed from a single population of flood events.

A probability distribution is selected to describe the flood events in the record. The true form of the underlying probability distribution is not known and there is no standard distribution appropriate in all cases. The goal is to select a probability distribution that fits the observed data well but also generates robust quantile estimates that are not sensitive to physical deviations of the true probability distribution (Hosking & Wallis, 1997). In extreme value statistics, data follow one of three extremal types of distributions: Gumbel, Fréchet, or Weibull (Coles, 2001). These three distributions can be expressed as a single formula and are considered a family of distributions known as the Generalized Extreme Value (GEV) distribution. The GEV distribution is shown to arise as an asymptotic model for maximum values in a sample and hence can be viewed as a natural model for observed flood events. For these reasons, the GEV distribution was used to describe the recorded flood events. No statistical tests were used to assess this choice because the GEV distribution is considered flexible to account for the variability captured at a single hydrometric station.

The parameters of the GEV distribution were estimated using the L-moments. The flood quantiles were calculated for a range of return periods (Table C-5). The reliability of the quantile estimates depends on a range of factors including the record length and the range of flood event magnitudes captured in the record. The longer the record length, the more reliable the quantile estimates.

Table C-5. Return period and associated AEP.

Return Period (Years)	AEP
2	0.5
5	0.2
10	0.1
20	0.05
50	0.02
100	0.001
200	0.005
500	0.002

C.4.2. Formation of Hydrological Regions

The catchment characteristics extracted over the catchment polygons were used to group the hydrometric stations into hydrological regions using a cluster analysis. Cluster analysis is an objective method for creating regions (Tasker, 1982) which historically were based subjectively using geographical, political, administrative or physiographic boundaries. The essence of cluster analysis is to identify clusters (groups) of hydrometric stations such that the stations within a cluster are similar while there is dissimilarity between the clusters. Hosking and Wallis (1997) suggest that cluster analysis is the most practical method of forming regions for large datasets and provides several opportunities for subjective adjustments to the regions. The algorithm used by BGC to group hydrometric stations is Agglomerative Hierarchal Clustering.

C.4.2.1. Data Preparation

The catchment characteristics at each hydrometric station were normalized so that the average is zero and the standard deviation is approximately 1. The distance metric used is the Euclidian distance between the catchment characteristics. The suite of catchment characteristics at all hydrometric stations were compared to one another and organised using Ward's Distance measure (d) (Ward, 1963).

C.4.2.2. Number of Hydrological Regions

Several statistical measures were used to guide the number of clusters to partition the hydrometric stations. The statistical measures include the Elbow Method, the Silhouette Score, and review of the dendrogram. The selection of the number of clusters was also subjectively assessed by reviewing the physical basis of the cluster distribution (e.g., is there a physical meaning behind the number and distribution of the clusters?).

The Elbow Method accounts for the percentage of variance explained as a function of the number of clusters. The percentage of the variance explained decreases with increasing number of clusters. The minimum number of clusters that provides the most gain in the variance explained was selected for analysis.

The Silhouette Score is a measure of how similar the catchment of a hydrometric station is to its own cluster compared to other clusters. The Silhouette Score was calculated for each hydrometric gauge station and averaged over each cluster. The Silhouette Score ranges from -1 to +1 where a high value indicates that the hydrometric stations are well matched to their own clusters and poorly matched to neighboring clusters.

The dendrogram represents how the clustering algorithm (i.e., agglomerative hierarchal clustering) groups the catchments and depicts a road map of the merging procedure showing which catchments were merged and when in order of increasing cluster distance.

The spatial distribution of the clusters was then reviewed to verify that they are physically plausible. This review was done by superimposing the clusters on a map of British Columbia to see whether there is a physical meaning supporting the cluster distributions.

C.4.2.3. Manual Adjustments of Hydrologic Regions

The clusters identified using the clustering algorithm were adjusted manually to increase homogeneity. The manual adjustments were completed by considering the topography, spatial patterns in hydrological processes, and ecozones in Canada. The clusters were further separated based on the scale of catchment area to respect the statistical requirement for constancy in the coefficient of variation (CV) for homogeneous regions.

C.4.2.4. Refinement of the Hydrometric Station Selection

The hydrometric station selection was refined to increase the homogeneity of the clusters by reducing the variability introduced by many hydrometric stations. The refinement process was guided by the following 5 criteria.

1. Catchments upstream of hydrometric stations with a regulation level greater than 25% were not included for analysis. The level of regulation is inferred by proportion of the catchment area upstream of the dams to the total catchment area upstream of the hydrometric station.
2. The catchment area range considered in the regionalization extends up to 5,000 km^2. Catchments with a greater catchment area size are most likely well gauged and studied that a regionalization of flood is not required.
3. Nested hydrometric stations along the same watercourse were also removed from the region to reduce cross-correlation.
4. A minimum of 6 years of maximum peak instantaneous streamflow data was set as a minimum for analysis. While this threshold is low, it is considered adequate since the influence of each hydrometric stations on the model reflects the record length.
5. Hydrometric stations recording water level only were excluded from the analysis at the onset. Hydrometric stations recording water level and streamflow measurements but located within or immediately at the outlet of lakes were also removed from the analysis.

The flow regime at these locations is considered heavily regulated precluding the use of frequency analysis to estimate peak flows.

In addition to these criteria, discordancy (*Di*) was considered to refine the selection. The discordancy is measured in term of the L-moments of the data at the hydrometric stations within a cluster. The formal definition for *Di* is found in Hosking and Wallis (1997, equation 3.3, page 46). A hydrometric station is considered discordant if *Di* is “large”. The definition of “large” depends on the number of hydrometric stations in the cluster. If the cluster includes more than 15 hydrometric stations, the critical value for the discordancy statistic is 3. Discordancy was calculated for each hydrometric station within each hydrologic region. Hydrometric stations with *Di* values greater than 3 were removed from the cluster. This process was re-iterated until no more hydrometric stations showed *Di* values greater than 3.

C.4.2.5. Testing for Homogeneity

The hypothesis for homogeneity is that the probability distribution of the flood events at the hydrometric stations within a cluster is the same except for a site-specific scale factor. The goal is to have clusters that are sufficiently homogenous that the regionalization of floods is advantageous to a single station FFA. Testing for homogeneity is done using the H-Test. The H-Test result helps assess whether the hydrometric stations in a cluster may reasonably be considered homogeneous. The formal definition for the H-Test is found in Hosking and Wallis (1997, equation 4.5, page 63). Of note, some level of heterogeneity is expected in these clusters due to the natural variability of hydrological processes that control flood events. The H-Test is not intended to be used as a significance test but rather as a guideline to inform whether the re-definition of a region could lead to a meaningful increase in the accuracy of the flood quantile estimates (Hosking and Wallis 1993).

C.4.3. Regionalization

Once the clusters were considered sufficiently homogeneous, they were considered “hydrologic regions”. The regionalization of floods was then completed for each region. The L-moment approach in the index-flood procedure was used by BGC for the regionalization exercise. The procedure for each hydrologic region included: averaging the L-moments, selecting a distribution, estimating the parameters, developing the growth curve, and estimating the index-flood. The mean annual flood (MAF) was selected as the index-flood for this study. The following sections describe the methods and assumptions for the regionalization of floods for a given hydrologic region.

C.4.3.1. Regional L-moments

The L-moment ratios were averaged over each hydrologic region. A weighted average was used where the weight reflected the number of observations at each hydrometric station. The weighted average was used to put more weight on hydrometric stations with a longer record length. The weighted average helps take advantage of all available data as it is often limited in many areas of the province. The regional average L-moment ratios are defined in Table C-6. The L-moment ratios are used rather than the L-moments because they yield slightly more accurate quantile estimates.

Table C-6. Definition for regional average L-moment ratios.

Symbol (sample)	Definition
ι_1^R	L-location or the mean of the distribution
ι_2^R	L-scale
t^R	L-CV
t_3^R	L-skewness
t_4^R	L-kurtosis

C.4.3.2. Distribution Selection for Growth Curves

The selection of an appropriate probability distribution for the growth curves was done using a goodness-of-fit test and review of L-moment ratio diagrams. These tests were completed to assess the variability imposed compiling the results of many hydrometric stations into a single growth curve. The goodness-of-fit test was based on 1,000 simulations and looked at a suite of candidate distributions. The candidate probability distributions included Generalised Logistic (GLO), Generalised Extreme Value (GEV), Generalised Pareto (GPA), Generalised Normal (GNO), and Pearson Type III (PE3). Probability distributions with Z statistics $\leq$1.64 were deemed acceptable (Hosking & Wallis, 1997). The regional L-moments were also plotted with the L-skewness and L-kurtosis relationships for two (Exponential (E), Gumbel (G), Logistic (L), Normal (N), and Uniform (U)) and three-parameter (GLO, GEV, GPA, GNP, PE3) candidate distributions in L-moment ratio diagrams. The plotting position of the regional L-moments was reviewed for the distribution selection that provided an acceptably close visual fit.

C.4.3.3. Parameter Estimation

The regional L-moments were used to estimate the parameters of the selected probability distribution. The equations used to estimate the parameters for the GEV distribution are found in Hosking and Wallis (1997, A.52, A.55, and A.56, page 196) in addition to other select probability distributions.

C.4.3.4. Growth Curves and Error Bounds

The index-flood was selected to be the MAF. As a result, the regional mean was set to 1 ($\iota_1^R = 1$). The probability distribution was fit by equating the L-moment ratios of the population (λ_1, τ, τ_3, τ_4) to the regional average L-moment ratios (ι_1^R, t^R, t_3^R, t_4^R).

One of the strengths of the Regional FFA completed using the regional L-moments is that the procedure is useful even when the assumptions are not all satisfied (e.g., possibility of heterogeneity, misspecification of the probability distribution, and statistical dependence between observations at different sites). An approach to estimate the accuracy of the estimated flood quantiles is by Monte Carlo simulation. A Monte Carlo simulation was therefore run to estimate the variability in the quantile estimates from the regional GEV distribution. This variability was used to set the error bounds on the regional growth curve.

C.4.3.5. Index-flood Estimation

The index-flood was estimated using a multiple linear regression. Regression is a classic statistical method to describe the relationship between a dependent variable (index-flood) and independent variables (catchment characteristics). The multiple linear regression model is expressed as follows:

$$Q_T = aA^b B^c \dots N^n \quad \text{[Eq. C-3]}$$

where Q_T is the flood magnitude at return period $_T$, A, B, …, N are the catchment characteristics, a is the regression constant, and b, c, …, n are the regression coefficients. Base 10 logarithms are used to convert this equation to a linear form by transforming the variables to the following:

$$\log Q_T \ = \log a + b(\log A) + c\,(\log B) + \cdots + n\,(\log N) \quad \text{[Eq. C-4]}$$

These coefficients were estimated using the Weighted Least Squares method introduced by Tasker (1980), which accounts for the sampling error introduced by unequal record lengths. Unequal record lengths mean that the sampling errors of the observations (flood quantiles) are not equal (heteroscedastic) and the assumption of constant variance in Ordinary Least Squares method is not valid.

The top 5 models were selected using consideration for the adjusted R^2 and the Bayesian information criterion (BIC). The 5 models with the lowest BIC were selected and the index-flood estimate was averaged. Select diagnostic plots were reviewed to control the quality of the regressions. The diagnostic plots are listed in Table C-7. The index-flood model was developed over two scales: regional and provincial. These two scales were compared to assess the influence of the distribution of hydrometric stations on the reliability of the MAF estimate.

Table C-7. Diagnostic plots.

Plot	Diagnostic
At-site vs. Modeled	Inspect for a one to one relationship as close to as possible
At-site Quantile vs. Modeled Quantile	Inspect whether the distribution of the fitted values match the distribution of the observed values
At-site Quantiles vs. Modeled Residuals	Inspect for constancy in residuals. Residuals are the differences between the at-site and the modeled estimates

C.4.3.6. Regional Model

The first scale considered is the regional scale where the MAF was modeled over an area consistent with the hydrologic regions defined across the province. This scale is consistent with the scale used to do develop the regional growth curves.

C.4.3.7. Provincial Model

The second scale considered is the provincial scale where all hydrometric stations across the province, that meet the selection criteria, were used to model the MAF. The provincial model was developed to capture the range of hydrological processes that control flood events in British Columbia.

C.4.3.8. Flood Quantile Estimates

Flood quantile were than estimated using the regional growth curve and index-flood estimates (both scales) for all hydrometric stations in a given region. Quantile plots were generated to compare the at-site and modeled results over the range of AEPs.

C.4.3.9. Catchment Characteristic Transformations

The relationship between flood events and catchment characteristics need not be linear. Experience and judgement were used to guide the selection of independent variables and inform the relationship between flood events and catchment characteristics. An exhaustive comparison of correlations between flood magnitude and catchment characteristics showed that catchment area and catchment length are proportional to flood magnitude. For this analysis, the remaining catchment characteristics needed to be log transformed.

C.4.4. Error Statistics

The quality of the flood quantile estimates was assessed using select error statistics including the Root Mean Square Error (SRMSE), the Percent Error (SPE), and the Bias (SBIAS) for the following AEPs: 0.5, 0.1, 0.02, 0.005. The standardized version of the error statistics is used to account for the different scales (Table C-8).

Table C-8. Error statistics, definitions, and diagnostic.

Error Statistic (acronym)	Definition	Diagnostic
SRMSE	Standard deviation of the residuals.	Inspect how concentrated the modeled estimates are around the line of best fit.
SPE	The difference between the modeled and at-site estimate, divided by the at-site estimate, multiplied by 100%.	Inspect how close the modeled estimate is to the at-site estimate/
SBIAS	The tendency to overestimate or underestimate the modeled variable.	Inspect for a consistent over or underestimate of the modeled variable

The mathematical expressions for the SRMSE, SPE, and SBIAS are included below in Eq. C-5, Eq. C-6, and Eq. C-7.

$$SRMSE = \sqrt{\frac{\sum_{i=1}^{Np}\left(\frac{Qm_{mod}^{i}-Qm_{at-site}^{i}}{Qm_{at-site}^{i}}\right)}{Np}} \quad \text{[Eq. C-5]}$$

$$SPE = \frac{\sum_{i=1}^{Np} abs\left(\frac{Qm_{mod}^{i}-Qm_{at-site}^{i}}{Qm_{at-site}^{i}}\right)}{Np} * 100 \quad \text{[Eq. C-6]}$$

$$SBIAS = \frac{\sum_{i=1}^{Np} \left(\frac{Qm_{mod}^{i}-Qm_{at-site}^{i}}{Qm_{at-site}^{i}}\right)}{Np} \quad \text{[Eq. C-7]}$$

C.4.5. Decision Tree

A decision tree model was used to assign hydrologic regions to ungauged catchments. A decision tree was built using the Random Forest classification algorithm. The decision tree model was based on the catchment characteristics at the hydrometric stations in the study area. A total of 500 random samples were pulled from the dataset (with replacement). From each random sample, a decision tree was generated by using 3 variables at each decision point. The hydrologic region assignment was based on majority votes. The out-of-bag (OBB) error rate was 7.2%. The OBB is a method of measuring the prediction error specific to random forest algorithms.

C.4.6. Statistical Software

The statistical software used by BGC for the analysis was R (R Core Team, 2019). R is a free software environment for statistical computing. The analysis is completed with support from several packages. These packages are listed in Table C-9 for reference.

Table C-9. Analysis and associated R package.

Analysis	R Packages	Authors
Flood Statistics	Lmom	J. R. M. Hosking
Clustering	stats	R Core Team
Discordancy, H-Test, Distribution Selection, Parameter Estimation, and Growth Curve Development	lmomRFA	J. R. M. Hosking
Index-flood Estimation	stats and leaps	R Core Team and Alan Miller
Random Forest decision tree	Rpart, randomForest	Andy Liaw and Matthew Wiener

C.5. RESULTS

C.5.1. Hydrometric Station Selection

A total of 1015 hydrometric stations were included in the analysis. The hydrometric stations were distributed across the study area with a greater concentration in the south compared to the north, largely reflecting population density. There is also a greater concentration of hydrometric stations in the United States than Canada (Figure C-2).

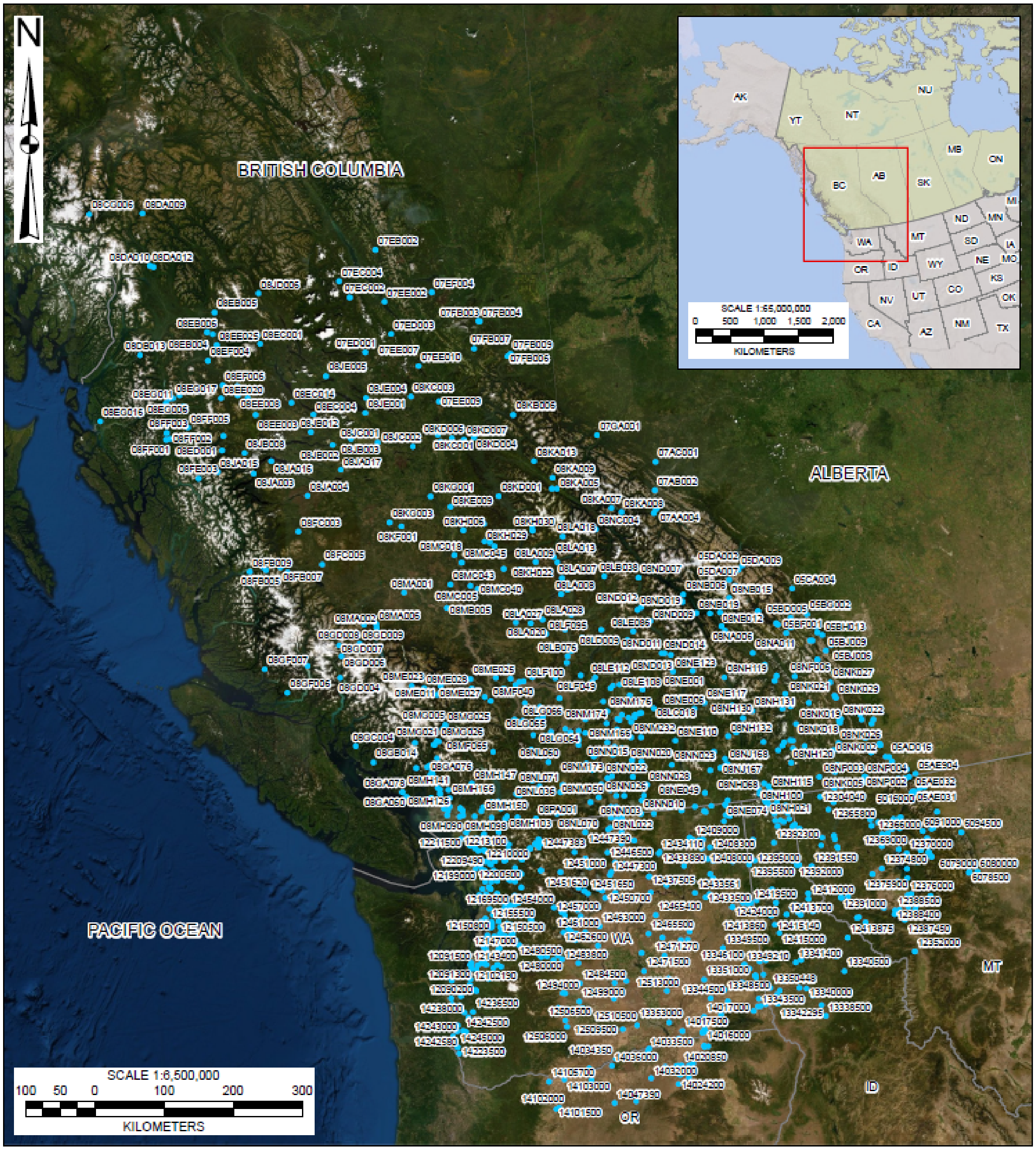

Figure C-2. Distribution of hydrometric stations within the study area.

The 18 catchment characteristics and their range in magnitude are summarized over the 1015 hydrometric stations in Table C-10. The climate catchment characteristics show a wide range in magnitude which is not surprising considering the sharp regional contrast imposed by the topography. The urban catchments are concentrated in coastal Washington.

Table C-10. Summary of catchment characteristics, including the mean, maximum, and minimum values over all hydrometric stations considered for analysis (1,015).

Type	No.	Acronym	Mean	Min	Max	Standard Deviation
Catchment	1	Centroid_Lat	49.3092758	43.75066	57.094597	2.3
	2	Centroid_Long	-119.5562752	-130.965466	-112.917172	3.5
	3	Centroid_Elev	1,133	18	3,046	534
	4	Area	7,572	1.3	601,746	38,417
	5	Relief	1,639	19	4,355	791
	6	Length	5	0.2	71	7
	7	Slope	62	4	350	49
Climate	8	MAP	1,299	218	4,173	787
	9	MAT	4.1	-3.0	10.9	3.0
	10	PAS	499	25	2191	323
	11	PPT_wt	476	71	1,683	328
	12	PPT_sp	283	56	955	173
	13	PPT_sm	185	31	522	77
	14	PPT_fl	355	58	1,329	249
Physiographic	15	Forest	61	0	100	25
	16	Water_Wetland	1	0	18	2
	17	Urban	2	0	100	12
	18	CN	68	55	94	6

C.5.2. Formation of Hydrological Regions

Based on an interative selection process, the 1,015 hydrometric stations were ultimately organized into 10 clusters. The results of the Elbow Method showed that a selection of approximately 10 hydrological regions explained the most variance in the catchment characteristics (Figure C-3).

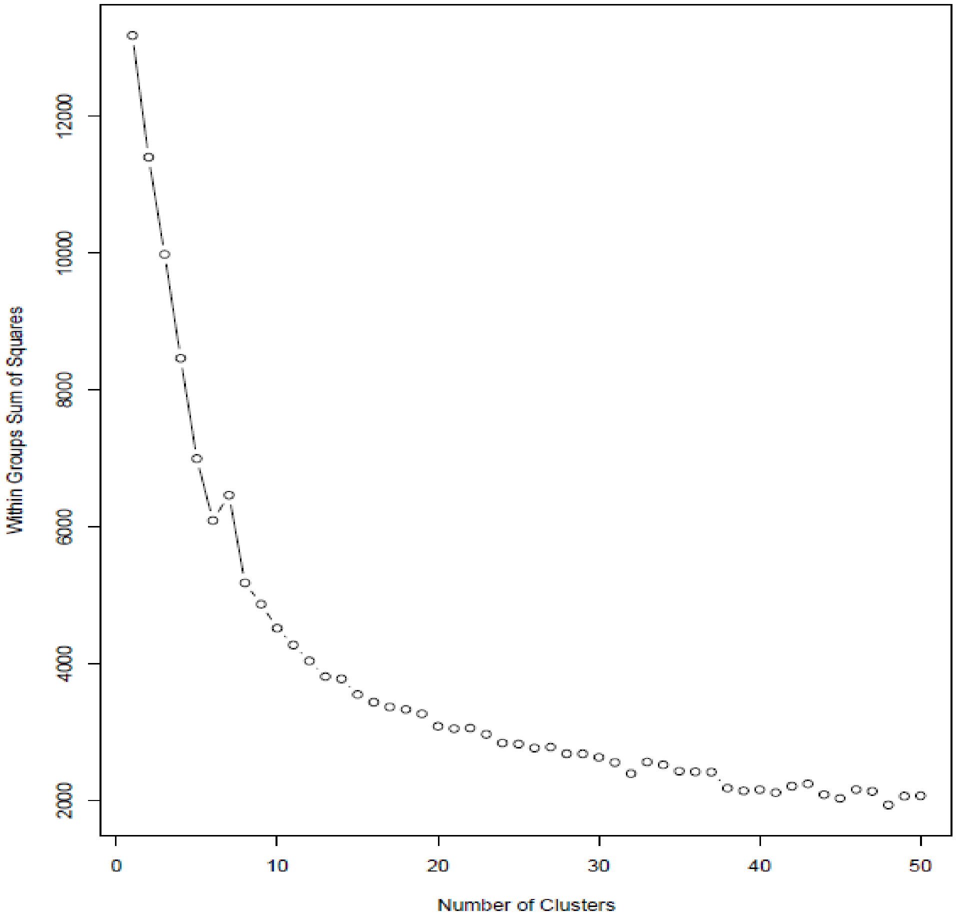

Figure C-3. The Elbow Plot.

The Silhouette Scores for the 10 clusters suggested some difficulty in organising the hydrometric stations based on catchment characteristics (Figure C-4). The average Silhouette Score is 0.2, suggesting that the hydrometric stations are poorly assigned to their hydrological regions. A low Silhouette Score is expected however, as it reflects the physical variability across the study area.

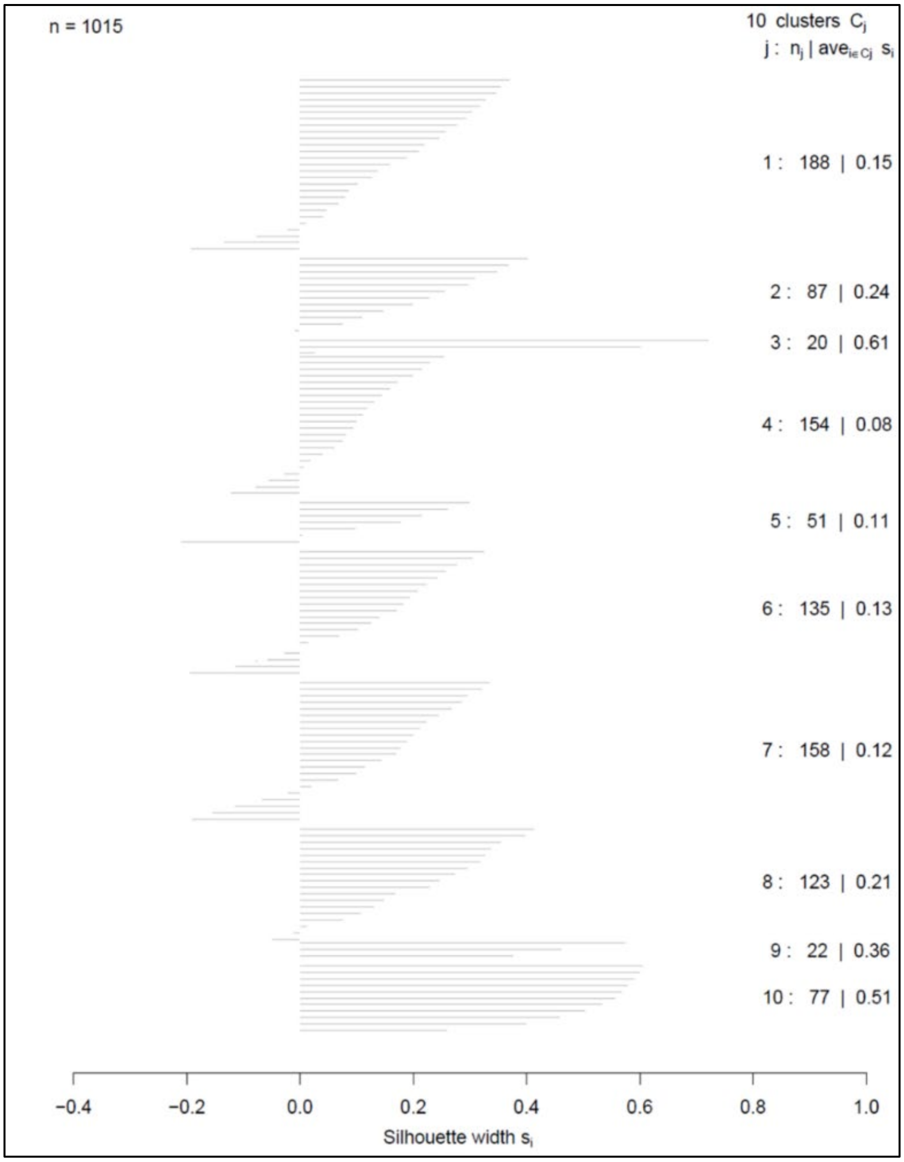

Figure C-4. Silhouette score.

The organization of the hydrometric stations into clusters is compiled in a dendrogram (Figure C-5). The y-axis is the dissimilarity index based on the distance metric. The horizontal axis represents the Ward's Distance (d). The green boxes separate the clusters. The 10 clusters are shown along the bottom of the dendrogram. Because we do not know how many clusters there should be in the landscape, the merging process was stopped once the clusters were more dissimilar than a threshold of approximately 90. The threshold was selected to generate a number of clusters consistent with the Elbow Plot.

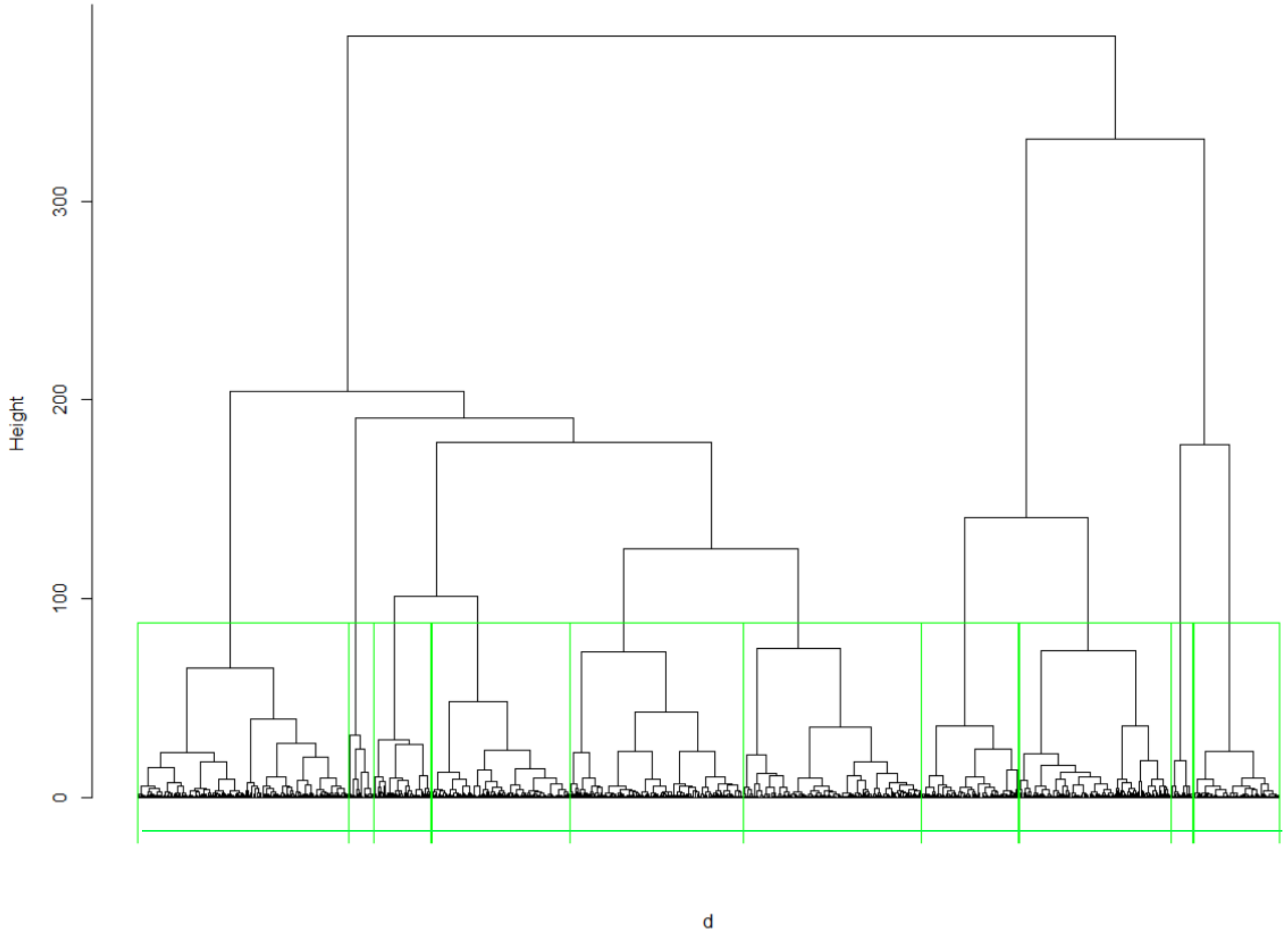

Figure C-5. Dendrogram.

C.5.2.1. Physical Basis of Regions and Flood Characteristics

The spatial distribution of the clusters is considered physically plausible, considering the range in the climate catchment characteristics. Significant regional variations are expected due to the influence of the mountain ranges across the study area (e.g., Coast Mountains, Monashees, the Columbia Trench, and the Rocky Mountains). These orographic effects are expected to control, at least in part, the distribution clusters (Figure C-6).

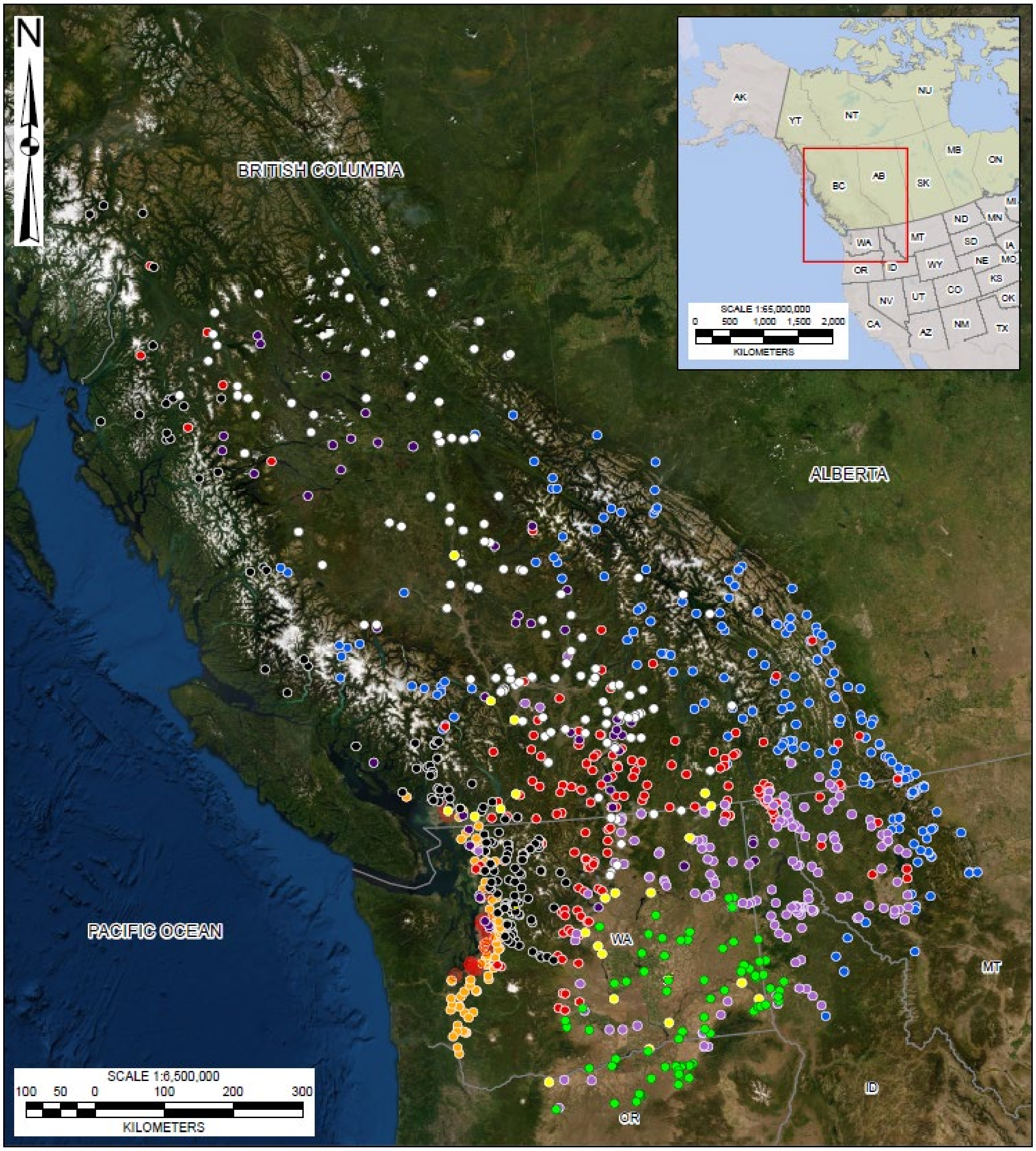

Figure C-6. Spatial distribution of 10 clusters.

The clusters that cover the RDCK region include 1 (blue), 4 (red), and 7 (lilac) with 188, 154, and 158 hydrometric stations, respectively. Cluster 1 is defined by the influence of the Rocky Mountains to the east forming the physiographic boundary with Alberta. Most flood events in this cluster are caused by snowmelt or rain-on-snow events in the spring. The eastern range of the Coastal mountains to the west also includes a small group of hydrometric station assigned to Cluster 1. Cluster 4 is defined generally by a climate characteristic of the semi-arid plateau between major mountain ranges. Most flood events are snowmelt dominated in the spring. In this drier climate, evaporation from water surfaces and from the land as well as transpiration from vegetation make up a large component of the regional water balance. Additional hydrometric stations assigned to Cluster 4 are in the montane cordillera to the east where flood events are often associated with rain-on-snow events during the spring freshet. Cluster 7 is defined by the southern edge of the Rocky Mountains in northwestern Montana. Significant floods in this region are caused by runoff from rain associated with moist air masses from the Gulf of Mexico, although most annual peak streamflow events are from snowmelt or rain-on-snow events in the spring.

C.5.2.2. Manual Adjustments

The clusters were further separated manually due to the large number of hydrometric stations in each cluster. Cluster 1 was separated into the eastern and western ranges of the Rocky Mountains. The small group of hydrometric stations located along the eastern range of the Coastal Mountains were also separated from Cluster 1. Cluster 4 was separated into the eastern portion in the montane cordillera and the western portion in the semi-arid plateau. Cluster 7 was not separated due to the limited geographic spread of the hydrometric stations. Based on these manual adjustments, Cluster 1 West, 4 East, and 7 cover the RDCK region (Figure C-7).

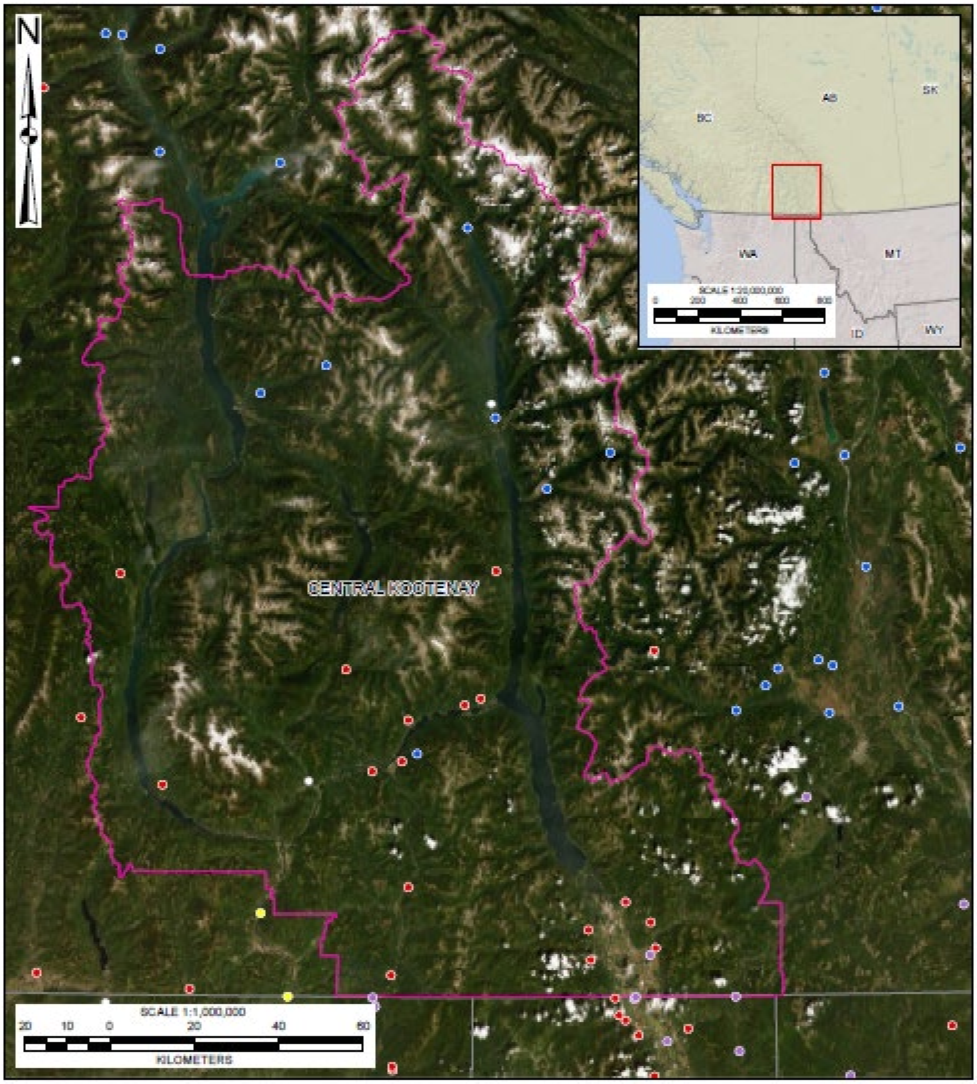

Figure C-7. Clusters that cover the RDCK region.

The clusters were further separated based on the scale of catchment area. The coefficient of variation (CV) is required to be constant for a given homogeneous region. A relationship between the catchment area and L-CV is observed in the clusters that cover the RDCK. However, the strength of the relationship varies considerably (Table C-11). In a flood regionalization study in British Columbia, Wang (2000) observed that in L-moment space, the L-CV varied with catchment area for the defined clusters making them heterogeneous. Wang (2000) demonstrated that the small catchments show an increase and the large catchments show a decrease in the L-CV.

Table C-11. R^2 for regression between catchment area and L-CV

Cluster	Number of Hydrometric Stations	R^2 for regression between catchment area and L-CV
1 West	88	0.01
4 East	45	0.12
7	158	0.15

To account for the lack of constancy in the L-CV reported by Wang (2000) and observed in the clusters, the range in the catchment area considered in the study was modified to include two groups: 1) less than 500 km^2 and 2) more than 500 km^2 up to 5,000 km^2. The clusters that cover the RDCK region thus include the following which will be the focus of the results herein.

- Cluster 1 West < 500 km^2
- Cluster 1 West > 500 km^2
- Cluster 4 West < 500 km^2
- Cluster 4 West > 500 km^2
- Cluster 7 < 500 km^2
- Cluster 7 > 500 km^2.

C.5.2.3. Refinement of the Hydrometric Station Selection

The final number of hydrometric stations, including the range of discordancy (*Di*) values, for each hydrologic region is presented in Table C-12. The number of hydrometric stations removed is based on the criteria presented in Section C.4.2.4.

Table C-12. Final number of hydrometric stations and range in discordancy measure for each hydrologic region.

Cluster	Catchment Area Range	Initial Number of Hydrometric Stations	Number of Hydrometric Stations Removed	Final Number of Hydrometric Stations	Di (Min)	Di (Max)	Di (Mean)
1 West	< 500 km^2	36	10	26	0.13	3.0	1
	> 500 km^2	52	28	24	0.09	3.0	1
4 East	< 500 km^2	43	9	34	0.04	2.8	1
	> 500 km^2	2	Not enough data for regionalisation				
7	< 500 km^2	75	35	40	0.09	2.6	1
	> 500 km^2	83	65	18	0.11	2.9	1

C.5.2.4. Homogeneity

The H-Test results are summarized in Table C-13. A cluster is declared heterogeneous if H is sufficiently “large”. Hosking and Wallis (1997) recommend a cluster be considered “definitely heterogeneous” if H $\geq$ 2. Increasing the threshold implies that more heterogeneous regions are included in the analysis. Guse, Thieken, Castellarin, & Merz (2010) assessed the effect of the H-Test threshold on the performance of probabilistic regional envelope curves in Germany. Increasing the H-Test threshold from 2 to 4 resulted in a larger number of regions considered for analysis. This increase is important as it can include hydrometric stations that would have been excluded otherwise.

The reality is that while removing hydrometric stations may improve the homogeneity of a region, there may be some important reasons why the H-Test score is high. For example, the site may include a hydrometric station where a very large flood occurred. A representative heterogeneous region is better than a region that has been forced to be homogeneous (Robson and Reed 1999).

The physical variability of British Columbia was recognized by Wang (2000) where the average value for the H-Test was 6.85 based on 19 clusters. The physiographic regions in BC may be less distinct than other regions. As a result, the threshold for the H-Test was relaxed to what is practical for British Columbia.

Table C-13. Number of hydrometric stations, Discordancy values, and H-Test results.

Hydrologic Region	Catchment Area Rrange	Number of Hydrometric Stations	H-Test
1 West	< 500 km^2	26	6.8
	> 500 km^2	24	9.0
4 East	< 500 km^2	34	13.1
	> 500 km^2	2	Not enough data
7	< 500 km^2	40	4.5
	> 500 km^2	18	7.7

C.5.3. Regionalization

C.5.3.1. Regional Probability Distributions

The regionally averaged L-moments are presented in Table C-14 for hydrologic region 1 West, 4 East, and 7. For the index-flood procedure, $\iota_1$is set to 1.

Table C-14. Regionally averaged L-moments.

Hydrologic Region	Catchment Area Range	Number of Hydrometric Stations	l_1	l_2	t_3	t_4
1 West	< 500 km^2	26	1	0.1796	0.2519	0.1879
	> 500 km^2	24	1	0.1756	0.2411	0.2012
4 East	< 500 km^2	34	1	0.2364	0.2245	0.1624
7	< 500 km^2	40	1	0.3014	0.2539	0.1904
	> 500 km^2	18	1	0.2601	0.2138	0.1924

The Z-statistics for a range of candidate probability distributions is presented in Table C-15. The candidate probability distributions include GLO, GEV, GPA, GNO, and PE3. Probability distributions with Z statistics ≤1.64 are deemed acceptable (Hosking & Wallis 1997). All candidate distributions are deemed acceptable for the hydrologic regions that cover the RDCK based on the Z-statistic.

Table C-15. Goodness of fit Z statistic for probability distribution selection.

Hydrological Region	Catchment Area Range	GLO	GEV	GNO	PE3	GPA
1 West	< 500 km^2	1.30	-0.34	-1.14	-2.57	-4.47
	> 500 km^2	0.53	-1.59	-2.50	-4.16	-6.85
4 East	< 500 km^2	3.30	0.69	-0.21	-1.92	-5.60
7	< 500 km^2	1.41	-0.59	-1.59	-3.38	-5.66
	> 500 km^2	0.62	-1.79	-2.55	-4.01	-7.54

To help make the decision on the most representative probability distribution, L-moment diagrams were plotted for each hydrologic region. The t_3 and t_4 position of the regional average relative to the relationships for five three-parameter (GLO, GEV, GPA, GNP, PE3) and five two-parameter (E, G, L, N, and U) candidate probability distributions are depicted in Figure C-8. The three-parameter probability distributions are depicted by the coloured lines while the two-parameter distributions are depicted by the black squares. The L-skewness and L-kurtosis ratio for each hydrologic region is depicted by the cross symbol on Figure C-8. The GEV probability distribution gives an acceptably close fit to the regional L-moments for the different hydrologic regions. As a result, the GEV probability distribution was deemed representative for all hydrologic regions.

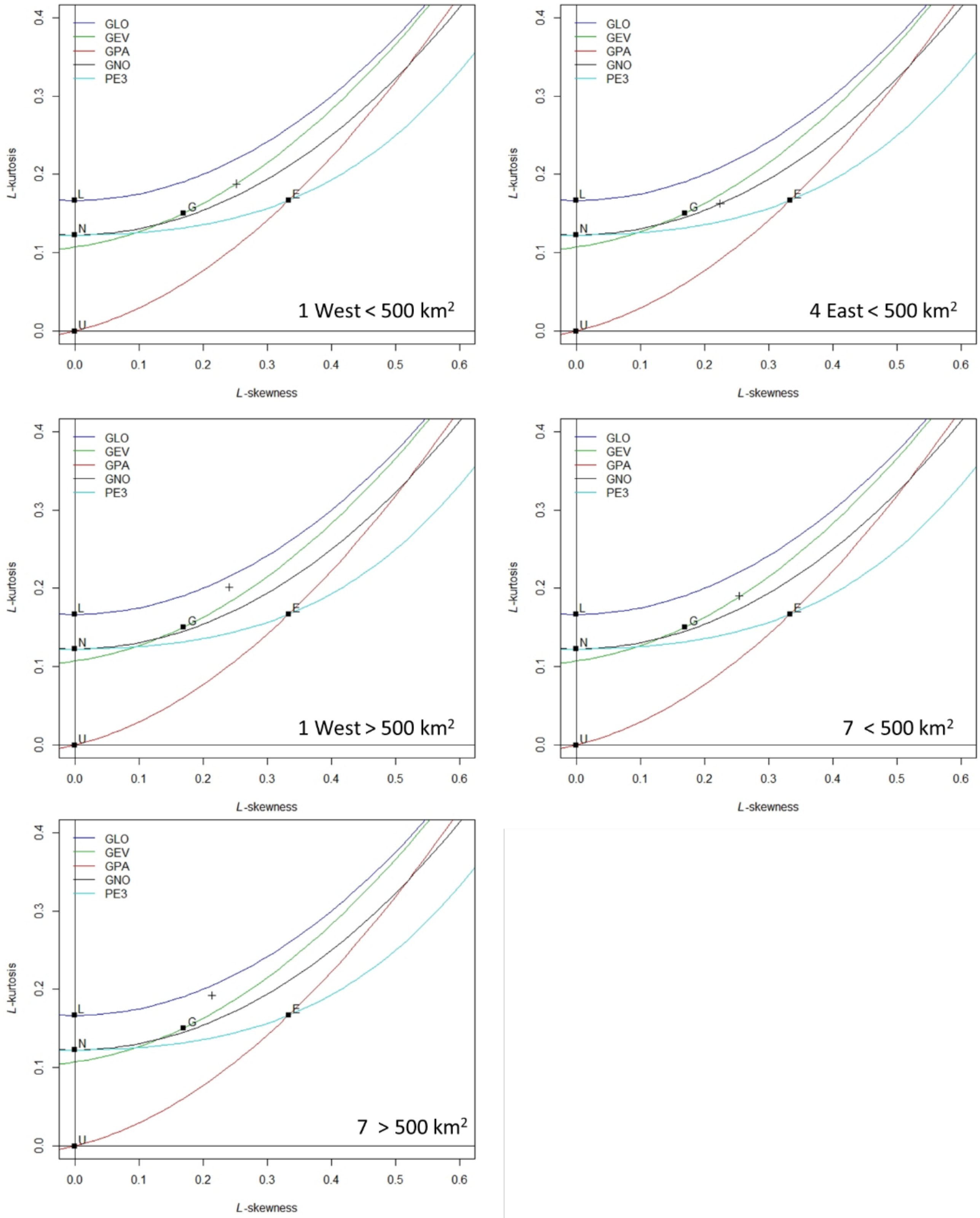

Figure C-8. L-moment ratio diagram for each hydrologic region.

C.5.3.2. Parameter Estimation

The regionally weighted L-moments are used to estimate the parameters of the GEV probability distribution. The parameters for each hydrologic region are presented in Table C-16.

Table C-16. Parameter estimates for the GEV distribution.

Hydrological Region	Catchment Area limit	ξ	α	κ
1 West	< 500 km^2	0.8369	0.2280	-0.1236
	> 500 km^2	0.8421	0.2269	-0.1078
4 East	< 500 km^2	0.7908	0.3139	-0.0832
7	< 500 km^2	0.7257	0.3814	-0.1266
	> 500 km^2	0.7724	0.3513	-0.0671

C.5.3.3. Growth Curves and Error Bounds

The regional growth curves and error bounds are presented for each region in Figure C-9.

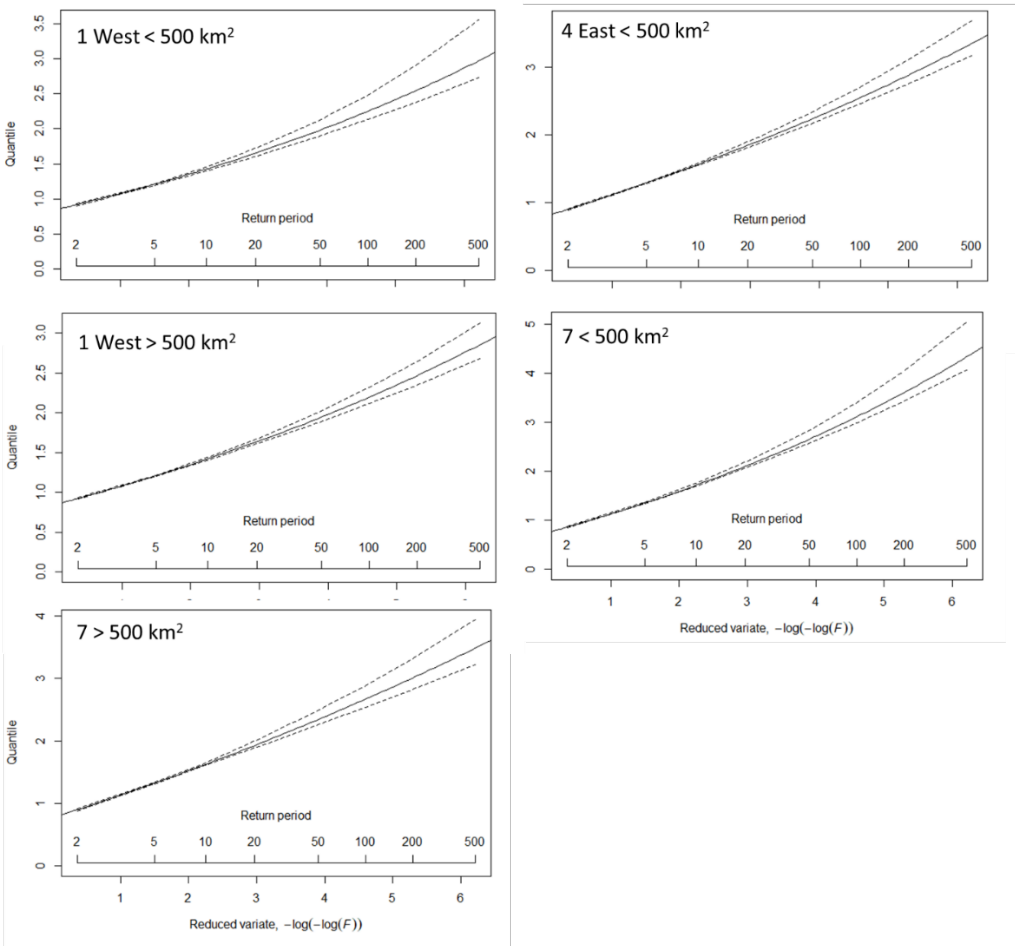

Figure C-9. Growth curves for each hydrologic region.

C.5.3.4. Index Flood

The regional equations for the index-flood for each hydrologic region are presented in Table C-17. The provincial equations are also included at the end of Table C-17. The results are reported to 5 significant figures. However, a total of 5 equations are developed for each hydrologic region and across the province with the intention to average the index-flood estimates. Consequently, the results should be rounded to the nearest unit for flood magnitudes greater than 10 m^3/s. The adjusted R^2 is included for comparison of the models. Models with more catchment characteristics tend to have a lower adjusted R^2 as these models are penalized for increased number of independent variables.

Table C-17. Regional and provincial equations for the index-flood including the adjusted R^2.

Hydrologic Region	Catchment Area Range	Index-flood Equations		Adj. R^2
1 West < 500 km²	42 to 454 km²	1	$\log Q_m = 10.169 + 1.8553(\log Area) - 0.012434(Slope) + 0.098984\ (Cen\_Long) + 0.0055555(PPT_{fl}) + 0.34911(Water\_Wetland)$	0.91
		2	$\log Q_m = 12.127 + 1.9358(\log Area) - 0.013271(Slope) + 0.11264\ (Cen\_Long) - 0.00022260(Cen\_Elev) + 0.0053230(PPT_{fl}) + 0.40695(Water\_Wetland)$	0.92
		3	$\log Q_m = 6.951 + 1.8564(\log Area) - 0.011048(Slope) + 0.071361\ (Cen\_Long) + 0.0053236(PPT_{fl})$	0.90
		4	$\log Q_m = -0.96349 + 1.7509(\log Area) - 0.0095976(Slope) + 0.0043293(PPT_{fl})$	0.89
		5	$\log Q_m = -3.2303 + 2.1932(\log Area) + 0.0015075(MAP)$	0.88
1 West > 500 km²	586 to 4312 km²	1	$\log Q_m = -2.5781 + 2.0480(\log Area) + 0.0012740\ (MAP)$	0.83
		2	$\log Q_m = -2.3716 + 1.8939(\log Area) + 0.41806(\log Catch\_Length) + 0.0012775(MAP)$	0.82
		3	$\log Q_m = 1.3411 + 1.9306(\log Area) + 0.18827(\log Catch\_Length) + 0.0011046\ (MAP) - 0.04866(CN)$	0.82
		4	$\log Q_m = -0.70946 + 1.6015(\log Area) - 0.0081664(Slope) + 0.0013574\ (MAP) + 0.057906\ (MAT) - 0.0036032(Forest)$	0.83
		5	$\log Q_m = 0.40059 + 1.6514(\log Area) - 0.0082135(Slope) + 0.0010135\ (MAP) + 0.15045\ (MAT) - 0.016425(Forest) - 0.19361(Water\_Wetland)$	0.88

Hydrologic Region	Catchment Area Range	Index-flood Equations		Adj. R^2
4 East < 500 km^2	6 to 441 km^2	1	$\log Q_m = -3.5763 + 2.7620(\log Area) - 0.15167(MAT) + 0.0035040(PPT_{wt}) - 0.26513(Water\_Wetland)$	0.96
		2	$\log Q_m = -4.1636 + 2.7871(\log Area) + 0.0037150(PPT_{wt}) - 0.30562(Water\_Wetland)$	0.96
		3	$\log Q_m = -1.8437 + 2.6974(\log Area) + 0.0038(PPT_{wt}) - 0.18063(MAT) + 0.0030438(PPT_{wt}) - 0.28288(Water_{Wetland}) - 0.020392(CN)$	0.96
		4	$\log Q_m = -4.0189 + 2.7063(\log Area) + 0.0047397(PPT_{fl}) - 0.3056(Water\_Wetland)$	0.95
		5	$\log Q_m = -1.3176 + 2.6880(\log Area) - 0.00069570(MAP) - 0.19022(MAT) + 0.0044279(PPT_{wt})$	0.96
7 < 500 km^2	8 to 471 km^2	1	$\log Q_m = -3.8856 + 1.8844(\log Area) + 0.010435(PPT_{fl})$	0.74
		2	$\log Q_m = -3.9002 + 1.9484(\log Area) + 0.10058(PPT_{fl}) - 0.17007(Water\_Wetland)$	0.74
		3	$\log Q_m = -4.4499 + 2.0486(\log Area) + 0.0051660(PPT_{wt}) + 0.0062765(PPT_{sm}) - 0.21014(Water\_Wetland)$	0.74
		4	$\log Q_m = -20.730 + 1.7210(\log Area) + 0.36720(Cen\_Lat) - 0.00093400(Cen_{Elev}) + 0.13920(PPT_{sp}) - 0.30900(Water\_Wetland)$	0.75
		5	$\log Q_m = -1.9967 + 2.9199(\log Area) - 0.44581(\log Catch\ Length) + 0.22219(Cen\_Lat) + 0.11838(Cen\_Long) + 0.007305(PPT_{wt}) - 0.32687(Water\_Wetland)$	0.75

Hydrologic Region	Catchment Area Range	Index-flood Equations		Adj. R^2
7 >500 km²	529 to 4138 km²	1	$\log Q_m = -2.8251 + 2.0765(\log Area) - 0.65058(MAT) - 0.01087(PAS) + 0.15245(PPT_{wt}) + 0.014215(PPT_{sm}) + 0.14232(Forest)$	0.93
		2	$\log Q_m = 0.51542 + 1.4852(\log Area) - 0.024121(Slope) - 0.0078710(MAP) - 0.69867(MAT) - 0.010055(PAS)$	0.93
		3	$\log Q_m = -0.28887 + 2.1311(\log Area) - 0.00048080(Cen_{Elev}) - 0.59076(MAT) - 0.10256(PAS) + 0.14034(PPT_{wt}) + 0.14291(PPT_{sm}) + 0.018084(Forest)$	0.94
		4	$\log Q_m = -12.290 + 4.2860(\log Area) - 4.4640(\log Catch\_Length) + 0.54240(Cen\_Lat) + 0.19690(Cen\_Long) - 0.0066490(PAS) + 0.013790(PPT_{wt}) + 0.38640(Forest)$	0.94
		5	$\log Q_m = -6.0632 + 2.1265(\log Area) + 0.0053923(PPT_{wt}) + 0.030556(Forest)$	0.90
Provincial Model	1 to 4,888 km²	1	$\log Q_m = -10.280 + 2.0840(\log Area) - 0.052950(Cen\_Long) + 0.00078170(PAS) + 0.0045490(PPT_{sp}) - 0.077680(Water\_Wetland) + 0.015770(CN)$	0.88
		2	$\log Q_m = -10.990 + 2.0900(\log Area) - 0.054870(Cen\_Long) + 0.00079820(PAS) + 0.0045680(PPT_{sp}) + 0.0022550(Forest) - 0.079050(Water\_Wetland) + 0.020340(CN)$	0.88
		3	$\log Q_m = -9.7160 + 2.0890(\log Area) - 0.044870(Cen_{Long}) - 0.00015400(Cen\_Elev) + 0.00095000(PAS) + 0.0043910(PPT_{sp}) + 0.0027010(Forest) - 0.081050(Water\_Wetland) + 0.021030(CN)$	0.89
		4	$\log Q_m = -8.3390 + 2.0610(\log Area) - 0.047040(Cen_{Long}) + 0.00070070(PAS) + 0.0043090(PPT_{sp}) + 0.0027010(Forest)$	0.88
		5	$\log Q_m = -2.7860 + 2.0520(\log Area) - 0.0023640(PPT_{wt}) + 0.0028430(PPT_{sm}) - 0.063700(Water\_Wetland)$	0.88

C.5.4. Error Statistics

The weighted standardized error statistics for the regional and provincial model over a range of flood quantiles for the different hydrologic regions are presented in Table C-18. The error statistics are not consistent across all hydrologic regions. The regional model may be selected for the 4 East < 500 km^2 hydrologic region. In the case of the 1 West region, either the regional or provincial model would be considered adequate. Lastly, the regional model is probably the model of choice for the 7 hydrologic region. As expected, the error statistics for the lower flood quantiles are lower than those for higher flood quantiles reflecting the increased uncertainty in higher quantile estimates.

Table C-18. Weighted standardized error statistics for the regional and provincial models over a range of flood quantiles. Green highlighted cells depict a positive bias while the red highlighted cells depict a negative bias.

Error Stats	AEP	1 West < 500 km^2		1 West > 500 km^2		4 East < 500 km^2		7 < 500 km^2		7 > 500 km^2	
		Regional Qm	Provincial Qm	Regional Qm	Provincial Qm	Regional Qm	Provincial Qm	Regional Qm	Provincial Qm	Regional Qm	Provincial Qm
SRMSE	0.5	0.24	0.31	0.27	0.26	0.39	0.92	2.71	3.80	0.19	0.99
	0.1	0.28	0.31	0.26	0.28	0.33	0.69	3.08	4.10	0.21	0.96
	0.02	0.40	0.41	0.31	0.33	0.38	0.64	3.70	4.80	0.27	1.01
	0.005	0.54	0.53	0.38	0.39	0.45	0.66	4.37	5.59	0.36	1.09
SPercent Error	0.5	18	21	20	21	27	59	70	122	15	65
	0.1	22	24	20	24	22	45	74	128	14	65
	0.02	31	32	25	29	27	39	84	144	20	68
	0.005	42	40	30	33	34	38	97	165	29	74
SBIAS	0.5	0.03	-0.08	0.04	-0.09	0.07	0.30	0.39	1.03	0.03	0.39
	0.1	0.06	-0.06	0.04	-0.07	0.07	0.23	0.44	1.08	0.03	0.39
	0.02	0.09	-0.03	0.06	-0.06	0.08	0.20	0.52	1.21	0.04	0.42
	0.005	0.13	0.02	0.08	-0.03	0.10	0.20	0.62	1.37	0.06	0.45

C.6. APPLICATION TO UNGAUGED CATCHMENTS

The goal of the regionalization of floods is to estimate quantiles for ungauged catchments in the RDCK. A total of 12 catchments are modeled for clearwater floods. To begin, a catchment polygon was defined for each ungauged catchment, as shown in Figure C-10. The suite of 18 catchment characteristics were then extracted and averaged over the area for each ungauged catchment. The resulting catchment characteristics are presented in Table C-19.

The ungauged catchments were subsequently assigned to one of the hydrologic regions identified across the study area. The hydrologic region assignment was completed using the Random Forest classification algorithm. Once a hydrologic region was assigned to the ungauged catchment; the index-flood was estimated based on the appropriate model (regional and / or provincial). The flood quantiles were then estimated for a range of AEPs using the index-flood estimate and the appropriate regional growth curve. The hydrologic region assignment, index-flood estimate, and flood quantiles for each ungauged catchment are presented in Table C-20.

The magnitude of the flood quantiles is influenced by the catchment characteristics. This is because the index-flood is calculated using a multiple linear regression that depends on the catchment characteristics that define the best 5 models for a given region. Two catchments of similar area may have significantly different flood quantile estimates because of major differences in catchment characteristics. For example, Lost Creek and Porcupine Creek share comparable catchment areas of 62 km^2 and 68 km^2, respectively. However, flood quantiles for Porcupine Creek are 35% greater than Lost Creek, with the difference in magnitude attributed to difference in climate characteristics.

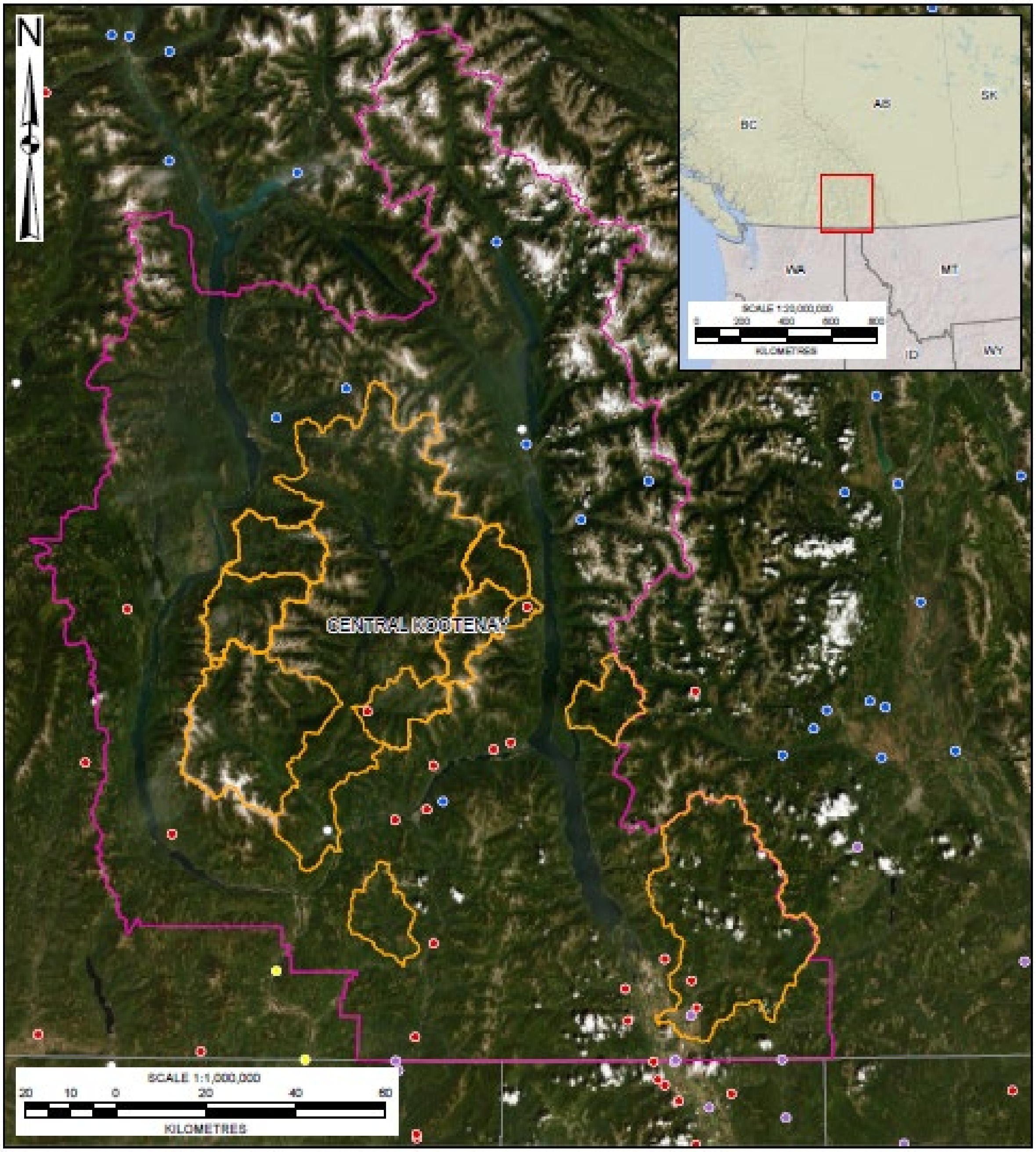

Figure C-10. Catchment polygons for the ungauged catchments.

Table C-19. Catchment characteristics for the clearwater sites located in the RDCK region.

Catchment Name	Area (km^2)	Relief (m)	Catchment Length (km)	Slope (%)	Centroid Latitude (degrees)	Centroid Longitude (degrees)	Centroid Elevation (m)	MAP (mm)	MAT (°C)	PAS (mm)	PPT_wt (mm)	PPT_sp (mm)	PPT_sm (mm)	PPT_fl (mm)	Forest (%)	Water and Wetland (%)	Urban (%)	CN
Crawford Creek	186	2092	2.53	83	49.693818	-116.700089	1181	1116	3.0	590	383	233	198	302	88	0.0	0.2	70
Keen Creek	202	2066	2.37	87	49.861962	-117.119617	1584	1390	1.3	857	460	307	240	384	66	0.2	7.7	67
Upper Kaslo Creek	150	1927	2.35	82	49.990505	-117.046683	1182	1244	2.7	668	416	265	223	340	90	0.0	0.8	70
Kalso Creek at Kootenay Lake	386	2228	3.09	72	49.914818	-117.077853	1280	1312	2.1	756	438	284	230	360	78	0.2	4.3	68
Lemon Creek	206	2046	2.58	79	49.717145	-117.338618	1956	1322	2.7	754	461	284	206	370	90	0.1	0.7	65
Burton at Arrow Lake	530	2323	4.13	56	49.952644	-117.773748	1300	1242	2.4	704	4280	258	220	336	85	0.3	1.2	64
Caribou Creek	238	2235	2.97	75	50.019565	-117.726695	1213	1260	2.4	709	432	261	226	341	92	0.1	0.3	67
Snow Creek	291	2314	3.05	76	49.897831	-117.811685	1742	1227	2.3	700	425	255	216	331	80	0.3	1.8	63
Little Slocan River	818	2281	5.40	42	49.664986	-117.79715	1612	1161	2.8	643	416	245	188	313	82	0.5	1.7	63
Slocan River	3475	2544	8.13	31	49.85497	-117.525816	1196	1224	3.0	666	431	256	206	332	81	2.9	2.1	66
Goat River	1259	2111	6.01	35	49.28428	-116.347233	1050	857	3.2	433	284	194	163	217	88	0.1	0.2	69
Erie Creek Upstream End	201	1575	2.71	58	49.288665	-117.392234	1010	1265	3.8	617	435	286	210	333	95	0.0	0.0	62

Table C-20. Hydrologic region assignment for the ungauged catchments.

Catchment Name	Hydrometric Station	Catchment Area (km²)	Hydrologic Region[1]	Qm (m³/s)	Flood Quantiles		
					0.05 AEP (m³/s)	0.02 AEP (m³/s)	0.005 AEP (m³/s)
Crawford Creek	-	186	7	27	50	61	80
Keen Creek	08NH132	202	pro-rated	-	78	94	125
Upper Kaslo Creek	08NH005	150	pro-rated	-	99	120	160
Kaslo Creek at Kootenay Lake	08NH005	386	pro-rated	-	160	200	260
Lemon Creek	08NJ160	206	pro-rated	-	72	84	105
Burton at Arrow Lake	-	530	4	80	150	180	230
Caribou Creek	-	238	4	42	78	94	120
Snow Creek	-	291	4	45	83	100	130
Little Slocan River		818	4	103	190	230	290
Slocan River	08NJ013	3475	pro-rated	-	685	770	880
Goat River	8NH004	1259	7	-	387	430	500
Erie Upstream End	-	201	4	35	65	79	102

Note:

1. A pro-rated calculation is completed when a representative hydrometric station is located upstream or downstream from the ungauged site and has a record length considered long enough for reliable frequency analysis. Flood quantile estimates calculated at the hydrometric station are transferred to the ungauged site by relating the annual maximum peak instantaneous streamflow at the hydrometric station to the ungauged site using catchment area size.

C.7. UNCERTAINTY

The process of flood regionalization is inherently uncertain because of the several limitations. The probability distribution of flood events is unknown. While there are statistical tools to help reach a 'best estimate', it is not possible to know what the probability distribution is in practice. As a result, the flood quantile estimates are supported by a mathematical model that is considered reliable based on the available flood data.

The regionalisation of floods tends to underestimate peak flows for small catchments and overestimate peak flows for larger catchments. This is in part due to differences in hydrological processes that control peak flows. For example, maximum annual peak instantaneous flows in small catchments within the study area are more likely controlled by rainfall compared to larger catchment that tend to be more snowmelt-dominated in the spring. The rainfall control in small catchments reflects the greater likelihood that a rainfall event, like a convective storm, covers the entire catchment area. In the case for larger catchments, it is more likely for snowmelt to occur across the entire area in the spring.

While hydrometric stations with catchment areas starting from approximately 6 km^2 up to 5,000 km^2 are included in the analysis, it is not likely that the equations apply to catchments if they are either too small or too large. The regional models are only reliable if applied within the range of catchment areas used to build the models in the first place. Extrapolation beyond the limit of the model may yield poor or unreliable results.

The regional models are as reliable as the data that is used to support them. There is inherent measurement error in flood events, especially for larger flood events. Furthermore, the data record may simply be incorrect due to a transcription error. In addition, the measuring device may have been moved to a new location or trends over time may come about from changes in the monitoring device. It is not possible to inspect every record at every hydrometric station to control for these sources of error because so much data are pooled across such a large area.

The same applies to the catchment polygon delineation. Much of the catchment delineation was automated using tools that were developed to speed up this process (RNT and ESRI tools). Manual spot checks were completed in conjunction with quality control of the area by means of comparison with published values. Nevertheless, it was not possible to inspect every catchment polygon to control for delineation errors due to the high number of polygons that were generated for this study. It is expected that these sources of error are negligible next to the quantity of data that is processed across the study area.

Trends in the flood record imposed by climate change, land use change, wildfires, insect infestations, or urban development generally precludes the use of frequency analysis. Trend analyses were completed on the flood record to account for some level of trend. However, the flood record often captureCreate s a small window of the flood history at a given location. The limited record makes it difficult to identify a real trend from an artifact of the data record. Therefore, no hydrometric stations were discarded from the analysis due to the presence of a trend in the flood record.

REFERENCES

Coles, S. (2001). *An Introduction to Statistical Modeling of Extreme Values*. Springer Verlag London Limited. 208 p.

Dalrymple, T. (1960). *Flood Frequency Analysis*. US Geological Survey. Water Supply Paper, 1543 A.

Farr, T.G., et al. (2007), The Shuttle Radar Topography Mission. *Reviews of Geophysics, 45*, RG2004, https://doi.org/10.1029/2005RG000183.

Greenwood, J.A., Lanswehr, J.M., Matalas, N.C., & Wallis, J.R. (1979). Probability weighted moments: Definition and relation to parameters of several distributions expressible in reserve form. *Water Resources Research, 15*, 1049-54.

Guse, B., Thieken, A.H., Castellarin, A., & Merz, B. (2010). Deriving probabilistic regional envelope curves with two pooling methods. *Journal of Hydrology, 380(1-2)*, 14-26. https://doi.org/10.1016/j.jhydrol.2009.10.010

Hosking, J.R.M. (1990). L-moments: Analysis and estimation of distributions using linear combinations of order statistics. *Journal of the Royal Statistical Society, Series B, 52*, 105-24.

Hosking, J.R.M. & Wallis, J.R. (1993). Some statistics useful in regional frequency analysis. *Water Resources Research*, 29, 271-81.

Hosking, J.R.M. & Wallis, J.R. (1997) *Regional Frequency Analysis: An Approach Based on L-moments*. Cambridge University Press, UK. http://dx.doi.org/10.1017/cbo9780511529443.

Latifovic, R., Homer, C., Ressl, R., Pouliot, D. Hossain, S.N., Colditz, R.R., Olthof, I., Giri, C., & Victoria, A. (2012). North American Land Change Monitoring System. In C. Giri (Ed) *Remote Sensing of Land and Land Cover: Principles and Applications* (p. 303-324). CRC Press.

Ouarda, T.B.M.J., St-Hilaire, A., & Bobée, B. (2008). Synthèse des développements récents en analyse régionale des extrêmes hydrologiques. *Journal of Water Sciences, 21*, 219–232. https://doi.org/10.7202/018467ar.

R Core Team. (2019). R: A language and environment for statistical computing. R Foundation for Statistical Computing, Vienna, Austria. https://www.R-project.org/.

Robson, A.J. & Reed, D.J. (1999). Statistical Procedures for Flood Frequency Estimation. Flood Estimation Handbook, vol. 3. Institute of Hydrology, Wallingford, UK.

Ross, C.W., Prihodko, L., Anchang, J., Kumar, S., Ji, W., & Hanan, N.P. (2018). HYSOGs250m, global gridded hydrologic soil groups for curve-number-based runoff modeling. ORNL Distributed Active Archive Center. https://doi.org/10.3334/ORNLDAAC/1566.

Tasker, G.D. (1980). Hydrologic regression and weighted least squares. *Water Resources Research, 16(6)*, 1107–1113.

Tasker, G.D. (1982). Comparing methods of hydrologic regionalization. *Water Resources Bulletin, 18*(6), 965-970.

United States Geological Survey (USGS). (1986). *Urban hydrology for small watersheds*. Technical report 55.

Wang, T., Hamann, A., Spittlehouse, D., & Carroll, C. (2016). Locally Downscaled and Spatially Customizable Climate Data for Historical and Future Periods for North America. *PLoS ONE 11(6)*: e0156720. https://doi.org/10.1371/journal.pone.0156720.

Wang, Y. (2000). Development of methods for regional flood estimates in the province of British Columbia (Doctoral dissertation). Retrieved from University of British Columbia. 200 pp.

Ward, J.H., Jr. (1963). Hierarchical Grouping to Optimize an Objective Function. *Journal of the American Statistical Association, 58*, 236–244.

APPENDIX D
CLIMATE CHANGE CONSIDERATIONS

D.1. INTRODUCTION

The hydroclimate of British Columbia (BC) is complex because of proximity to the Pacific Ocean, mountainous terrain, and extent in latitude. The hydrologic regime is either freshet-dominated (nival regime) or snow-influenced (hybrid nival-pluvial or nival-glacial regimes) throughout most of BC (Eaton & Moore, 2010). Hydrologic trends over recent decades generally include a warming and decreasing snowpack (Kang, Shi, Gao, & Déry, 2014) and earlier onset of spring melt (Déry et al., 2009). The hydrologic response to climate change in BC is expected to be influenced by the regional variability in projected temperature and precipitation changes and by regional variations in physical geography. For example, snow dynamics are strongly influenced by elevation-based temperature gradients resulting in large spatial variations in regions of diverse topography (Schnorbus, Werner, & Bennett, 2014). Also, warmer hybrid nival-pluvial regimes may be more sensitive to changes in regional temperature, precipitation, and rainfall trends (Whitfield, Cannon, & Reynolds, 2002).

Climate change impacts were assessed by BGC for the clear-water flood watersheds using statistically- and process-based methods. This appendix presents a description of these methodologies and their results. This appendix begins with a description of the anticipated climate change impacts on the hydroclimate within the RDCK (Section D.2). The climate change sensitivity of clear-water flood watersheds within the region is examined in Section D.3. Finally, an evaluation of the climate change impacts using statistically- and process-based methods for the clear-water flood watersheds is presented in Section D.4. This appendix ends with a summary of the method that was used to account for the climate change impacts on the hydrology of these watersheds in the RDCK region.

D.2. CLIMATE CHANGE IMPACTS

D.2.1. Hydroclimate

Historical changes to climate have been documented in BC (Barnett et al., 2008). While there is a natural variability component to the changes in climate, such as El Niño Southern Oscillation (ENSO) and the Pacific Decadal Oscillation (PDO), historical trends in western North America have been attributed to climate change in the form of increased regional warming (Barnett et al., 2008).

Climate change is projected to impact the overall mean as well as the extremes for a range of climate variables including temperature, precipitation, snow, and rainfall intensities. Projected change in mean annual precipitation (MAP), temperature (MAT), and precipitation as snow (PAS) from historical conditions (1961 to 1990) for clear-water flood watersheds across the RDCK region for 2050 (average of years 2041 to 2070) are presented in Table D-1.

The climate-adjusted variables are calculated using projections based on the Representative Carbon Pathway (RCP) 8.5 which are averaged across 15 fifth phase Coupled Model Intercomparison project (CMIP5) models (CanESM2, ACCESS1.0, IPSL-CM5A-MR,MIROC5, MPI-ESM-LR, CCSM4, HadGEM2-ES, CNRM-CM5, CSIRO Mk 3.6, GFDL-CM3, INM-CM4, MRI-CGCM3, MIROC-ESM, CESM1-CAM5, GISS-E2R) that were chosen to represent all major clusters of similar atmosphere-ocean general circulation models (AOGCMs) (Knutti, Massin, & Gettleman, 2013), and that had high validation statistics in their CMIP3 equivalents.

Table D-1. Projected change (RCP 8.5, 2050) from 1961 to 1990 historical conditions (Wang et al., 2016).

Watershed	Change in MAP (mm)	Change in MAT (ºC)	Change in PAS (Snow Water Equivalent, mm)
Crawford Creek	59	3.5	-206
Keen Creek	82	3.6	-239
Upper Kaslo Creek	72	3.6	-231
Kalso Creek at Kootenay Lake	76	3.6	-233
Lemon Creek	82	3.5	-252
Burton at Arrow Lake	73	3.5	-221
Caribou Creek	75	3.5	-225
Snow Creek	72	3.6	-217
Little Slocan River	69	3.5	-215
Slocan River	74	3.5	-220
Goat River	40	3.5	-151
Erie Creek Upstream End	69	3.6	-247

Projected changes in average climate variables across the RDCK by 2050 show that there is likely to be:

- A net increase in MAP ranging from 40 mm to 82 mm
- A net increase in MAT ranging from 3.5 ºC to 3.6 ºC
- A net decrease in PAS ranging from 151 mm to 252 mm.

In addition, short-term precipitation extremes (sub-daily) are expected to increase in most of North America with a warming atmosphere. The frequency of extremes increases 5-fold in large parts of Canada in December, January, and February (Figure D-1a). The frequency of extremes decreases to approximately a 2-fold increase in southeast BC in June, July, and August (Figure D-1b). This shift in frequency covers the period January 2001 to September 2013. The increase is due to a shift towards moister and warmer climatic conditions (Prein et al., 2017). Extremes in short-term precipitation contributes to the frequency and magnitude of flood events, especially for small watersheds where soil storage is either low or full (i.e., < 250 km^2).

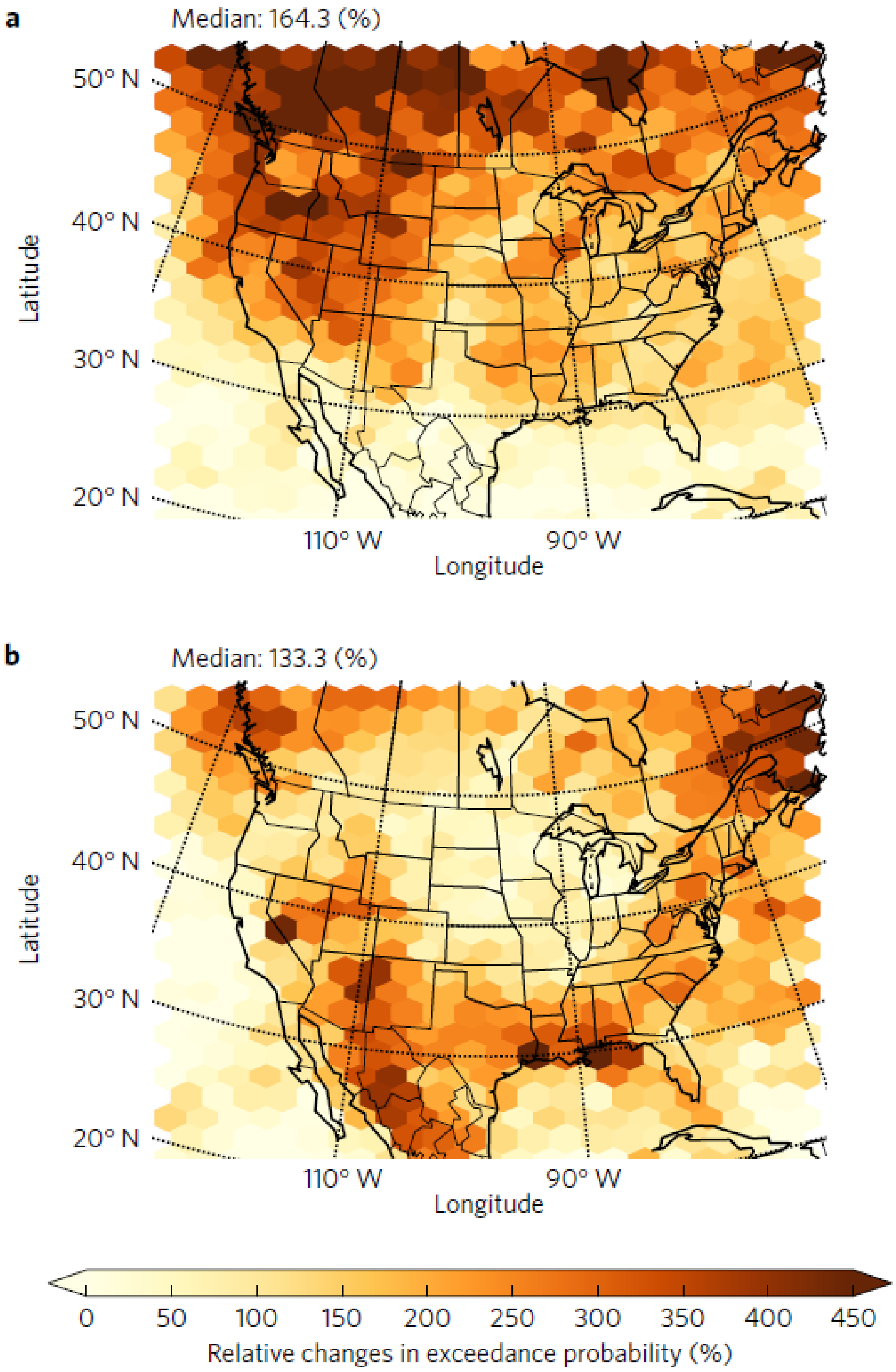

Figure D-1. Change in the exceedance probability of hourly precipitation intensities for (a) December, January, and February, and (b) June, July, and August (Prein et al, 2017).

D.2.2. Peak discharges

The RDCK is situated within the Montane Cordillera ecozone which covers most of southern BC. Extreme flood events in this area are often associated with rain-on-snow events in the spring (Harder et al., 2015). A hydrograph example where the regime is freshet-dominated is shown in Figure D-2. Although the effects of climate change on precipitation are not clear, projected increases in temperature are expected to have the largest impact on annual minimum temperatures occurring in the winter months (Harder et al., 2015).

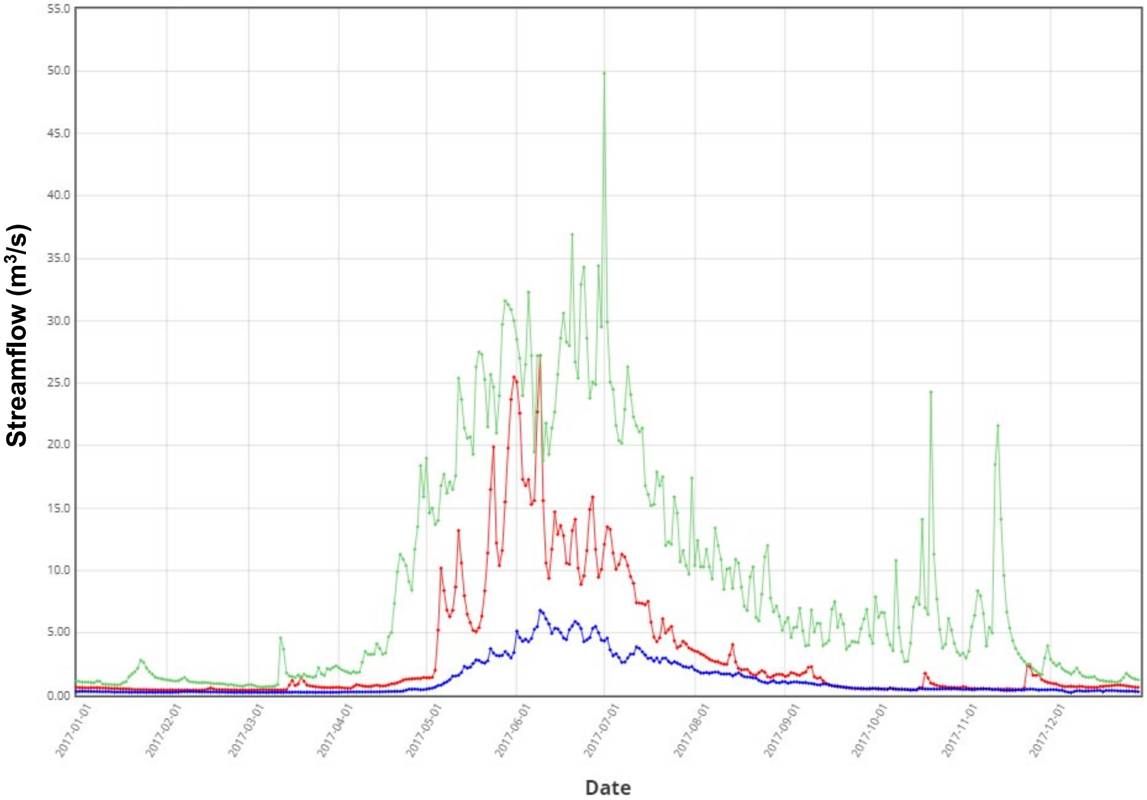

Figure D-2. **Example freshet-driven hydrologic regime for Keen Creek below Kyawats Creek (08NH132). Green line is the maximum streamflow, the blue line is the minimum streamflow, and the red line is the 2017 streamflow.**

The effects of temperature change differ throughout the region. High elevation regions throughout parts of the Montane Cordillera (e.g., Upper Columbia watershed) are projected to experience increases in snowpack, limiting the response in high elevation watersheds while lower elevations are projected to experience a decrease in snow water equivalent (Loukas & Quick, 1999; Schnorbus et al., 2014).

Projected changes in streamflow vary spatially and seasonally based on snow and precipitation changes and topography-based temperature gradients. Researchers anticipate that streamflow will increase in the winter and spring in the RDCK due to earlier snowmelt and more frequent rain-on-snow events, while earlier peak flow timing is expected in many rivers (Schnorbus et al., 2014; Farjad, Gupta, & Marceau, 2016).

D.3. WATERSHED SENSITIVITY

The RDCK includes 6 detailed clear-water flood study areas (Crawford Creek, Kaslo Creek, Slocan River, Burton Creek, Goat River, and Salmo River). Each study area includes one or more clear-water flood watersheds that were assessed to inform the floodplain delineation. All clear-water flood watersheds in the RDCK are characterized by a freshet-dominated regime. Freshet-dominant regimes are characterized by a maximum annual streamflow in the spring

In a warmer climate, hydrologic regime shifts are likely to intensify although regional responses are expected due to each watershed's unique characteristics like elevation range and proximity to the 0^{o}C air temperature threshold during the cold season. The largest changes in the timing of peak floods would be expected for those areas with a hydrologic regime that shifts from a freshet-dominated to rainfall dominated regime. Therefore, those watersheds with the thinnest snowpacks would be the most sensitive.

The RDCK can be sub-divided into five regions, each with a relatively different, typical snowpack depth (Figure D-3). Two of those five regions cover the clear-water flood watersheds. The typical snow depths for the clear-water flood watersheds ranges from moderate snowpack at high elevations for Goat River and Crawford Creek to moderate to deep snowpack for the remaining sites (Table D-2). The elevation range for each clear-water flood watershed is included in Table D-2 for reference. The clear-water flood watershed with largest projected change in precipitation as snow by 2050 is Lemon Creek (decrease of 252 mm) followed by Erie Creek Upstream End (decrease of 247 mm) and Keen Creek (decrease of 239 mm) as listed in Table D-1. Hydrographs based on representative hydrometric stations for each study area are presented at the end of the appendix for reference (Figure D-8 to Figure D-11).

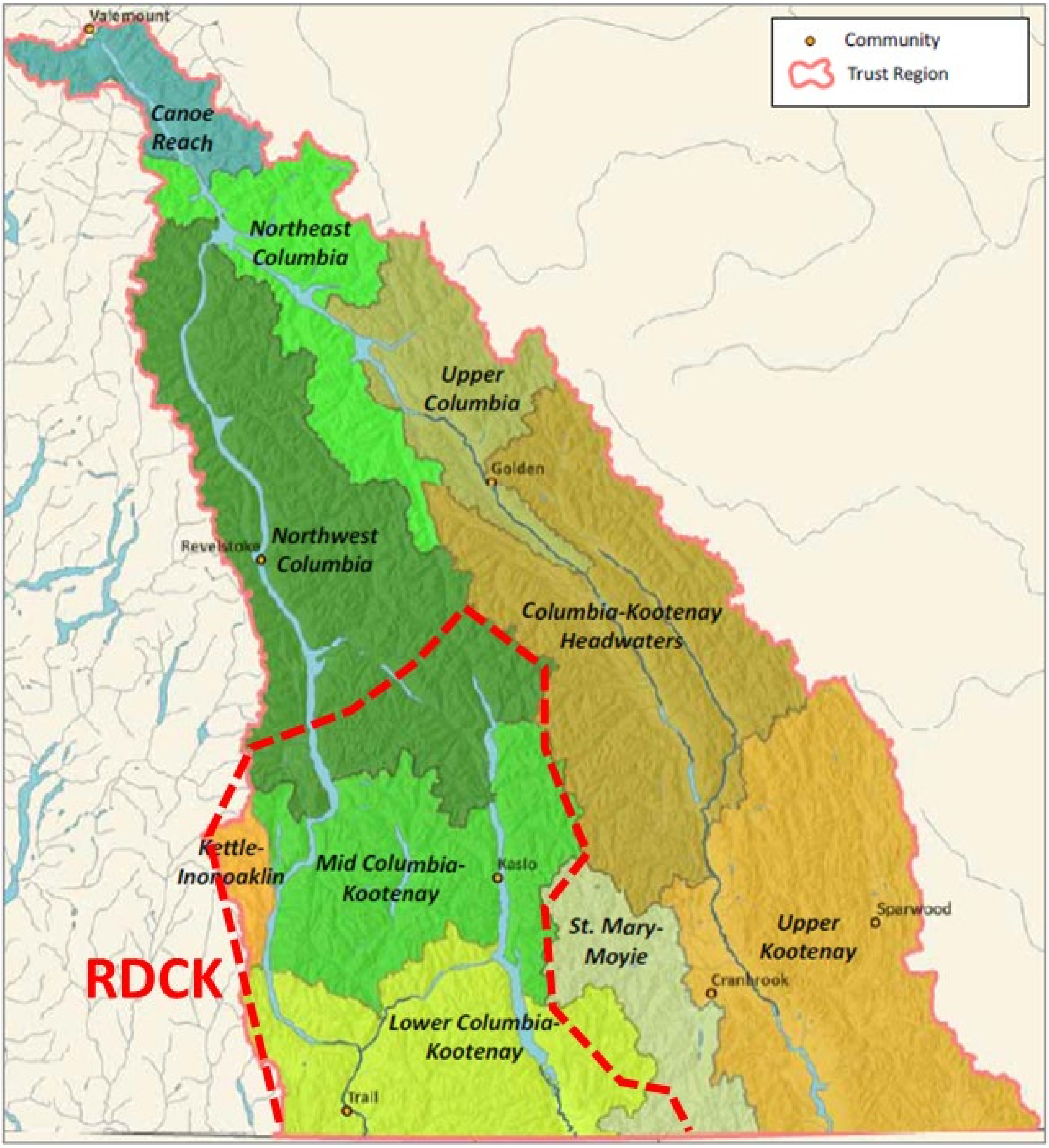

Figure D-3. Regions of the Columbia Basin as defined by patterns of climate and surface runoff. The RDCK contains 5 of these regions, 2 of which cover the clear-water watersheds (CBT, 2017).

Table D-2. Regions of the Columbia Basin covering the RDCK and their current relative snowpack depth (CBT, 2017).

Region	Existing Relative Snowpack Depth	Study Area	Representative Hydrometric Station	Clear-water Flood Watersheds	Elevation Range (m)
Lower Columbia-Kootenay	Moderate snowpack at higher elevations	Goat River	08NH004	Goat River	532 to 2622
		Salmo River	08NE074	Erie Creek Upstream End	712 to 2287
Mid Columbia-Kootenay	Moderate to deep snowpack	Crawford Creek	ungauged watershed	Crawford Creek	530 to 2627
		Kaslo Creek	08NH005	Keen Creek	704 to 2797
				Upper Kaslo Creek	699 to 2670
				Kalso Creek at Kootenay Lake	549 to 2785
		Burton Creek	Ungauged watershed	Snow Creek	465 to 2731
				Burton at Arrow Lake	439 to 2785
				Caribou Creek	1117 to 2630
		Slocan River	08NJ013	Lemon Creek	538 to 2604
				Little Slocan River	498 to 2803
				Slocan River	450 to 2973

D.4. CLIMATE CHANGE IMPACT ASSESSMENT

Assessments of climate change impacts for all clear-water watersheds were performed to quantify the anticipated changes in the annual maximum streamflow by 2050 under the RCP 8.5 emission scenario. Four different approaches were used which can be classified into statistically-based and process-based assessments.

D.4.1. Statistically-based Assessment

Two statistically-based methods were developed to assess the effect of climate change on flood quantiles. The first method was based on an examination of the historical annual maximum flood series data to identify statistically significant trends (positive or negative). The second method was based on the index-flood model developed as part of the Regional Flood Frequency Analysis (Regional FFA) (see Appendix C) to estimate the climate-adjusted index flood using climate-adjusted variables derived from downscaled global circulation model (GCM) predictions (Wang et al., 2016). The two methods are described in more detail and results are presented in the following sections.

D.4.1.1. Streamflow Trend Analysis

Statistical streamflow trend analysis on the annual maximum series (AMS)[1] was performed on suitable gauges (e.g., sufficient period of record, not regulated) located within the watersheds of clear-water study areas and within the hydrological regions formed as part of the Regional FFA.

The presence of a trend (positive or negative) in the AMS was inferred to be caused, at least in part, by climate change. The Mann-Kendall (M-K) statistical test was used to conduct the trend analyses. The M-K test was preferred over alternative statistical tests because it is non-parametric, and therefore does not assume a functional relationship between time and streamflow magnitude. The M-K test detects consistently increasing or decreasing trends in time series. The M-K test examines for an absence of trend in the time series (the null hypothesis) and returns the probability that the null hypothesis (that there is no monotonic trend in the series) is true. Failing the null hypothesis would in turn suggest that there is a statistically significant temporal trend in the time series. The M-K test was applied only to hydrometric stations with periods of records which spanned the year 2000 to ensure the time series included the most current climate.

Although it was assumed that statistically significant trends were at least in part caused by climate change, changes to the watershed's land cover (e.g., wildfire, insect infestations, changes in land use) were considered as possible causes to trends in peak discharges. Furthermore, the peak flow records often capture a small window of the flood history at a given location. The limited record lengths make it difficult to differentiate between a long-term trend cause by climate change and the intrinsic climate variability captured in the time series. Consequently, the presence of a statistically significant trend in the peak flow time series could not be solely attributed to climate change.

D.4.1.1.1 Assessment of Streamflow Gauges within Study Areas

One or more suitable streamflow gauges were identified on the Slocan, Kaslo and Salmo Rivers for trend analysis. A streamflow gauge with historical streamflow data is available on the Goat River (*Goat River Near Erickson* (08NH004)); however, this gauge cannot be used for assessment of trends as the Goat River is regulated. Of the six streamflow gauges assessed for the three rivers, none were found to show strong or even weak evidence of a trend in the AMS.

---

[1] The Annual Maximum Series (AMS) is a time series of the largest peak discharge for each year.

Table D-3. Trend results for streamflow gauges within the clear-water flood study areas (where suitable hydrometric station exist).

Hydrometric Station	Name	Start Year	End Year	p-value	Trend Direction	Sen's Slope[1]
	Slocan River					
08NJ013	Slocan River Near Crescent Valley	1914	2018	0.18	-	0.48
08NJ160	Lemon Creek Above South Lemon Creek	1973	2017	0.23	-	0.17
Kaslo River						
08NH005	Kaslo River Below Kemp Creek	1972	2017	0.32	-	-0.21
08NH132	Keen Creek Below Kyawats Creek	1974	2016	0.79	-	0.04
Salmo River						
08NE074	Salmo River Near Salmo	1949	2018	0.47	-	-0.29
08NE114	Hidden Creek Near the Mouth	1973	2016	0.73	-	0.02

Notes:

The Sen's slope is a robust estimate of the magnitude of a trend and commonly used to identify the slope of a trend line in hydrological time series (Yue et al. 2002). It is considered robust because it is sensitive to outliers.

D.4.1.1.2 Assessment of Streamflow Trends within Homogenous Regions

Each clear-water flood watershed was assigned to a homogeneous region as part of the Regional FFA formed using cluster analysis. (see Section 4.5 in Appendix C). A trend analysis was performed on the annual peak streamflow time series recorded at the hydrometric stations located within the homogeneous region assigned to the clear-water flood watersheds.

D.4.1.1.2.1 1 West – for Watersheds < 500 km^2

Within the "1 West – for watersheds less than 500 km^2" hydrological region, one hydrometric station out of 15 reported a statistically significant trend ($p < 0.05$ - less than a 5% chance of rejecting the null hypothesis) in the flood series: *Kuskanax near Nakusp* (08NE006). The trend in the magnitude of the flood series for that station was in the decreasing direction (Table D-4).

Table D-4. Trend results for the hydrometric stations in the 1 West – for watersheds < 500 km^2 hydrologic region.

Hydrometric Station Code	Start Year	End Year	p-value	Trend Direction	Sen's Slope[1]
08LB038	1985	2016	0.246	-	0.33
08NP004	1995	2017	0.239	-	0.13
08NH131	1973	2004	0.444	-	0.19
08KA001	1969	2013	0.738	-	0.06
08NJ168	1983	2014	0.475	-	0.04
08NB014	1973	2017	0.431	-	-0.25
08NH132	1974	2016	0.795	-	0.04
08ND019	1973	2005	0.650	-	0.13
08NE006	1968	2011	0.006	Decreasing*	-1.33
08NK022	1977	2015	0.143	-	-0.19
08NG076	1973	2017	0.314	-	0.07
08KA009	1967	2018	0.881	-	-0.04
08KB006	1978	2015	0.386	-	0.20
08LE086	1997	2016	1.000	-	0.00
08KA010	1908	2015	0.118	-	-0.25

Notes:

1. The Sen's slope is a robust estimate of the magnitude of a trend and commonly used to identify the slope of a trend line in hydrological time series (Yue et al. 2002). It is considered robust because it is sensitive to outliers.

* Strong evidence of trend (p < 5%) – less than 5% chance that the null hypothesis – that there is no trend – is true.

** Weak evidence of trend (p < 10%)– less than 10% chance that the null hypothesis – that there is no trend – is true.

D.4.1.1.2.2 1 West – for Watersheds > 500 km^2

Within the "1 West – for watersheds greater than 500 km^2" hydrological region, one out of 15 hydrometric stations reporting a statistically significant trend in the flood series (*Fraser River at Red Pass*, 08KA007) with a trend in the decreasing direction (Table D-5).

Table D-5. Trend results for the hydrometric stations in the 1 West – for watersheds > 500 km^2 hydrologic region.

Hydrometric Station Code	Start Year	End Year	p-value	Trend Direction	Sen's Slope[1]
08NB019	1985	2018	0.836	-	0.20
08NB012	1970	2017	0.818	-	0.11
08LE024	1973	2017	0.143	-	-1.07
08NP001	1929	2017	0.845	-	-0.06
08NK018	1973	2015	0.530	-	-0.23
08KA007	1955	2016	0.016	Decreasing*	-0.81
08NH130	1973	2012	0.990	-	0.00
08ND012	1964	2018	0.670	-	-0.11
08ND013	1964	2017	0.228	-	0.72
08NA006	1912	2017	0.317	-	-0.61
12358500	1940	2017	0.623	-	-0.45
08KA013	1998	2017	0.576	-	3.25
12355500	1911	2017	0.857	-	-0.11
08LE027	1915	2017	0.598	-	0.15
08NA011	1949	2018	0.319	-	-0.36

Notes:

1. The Sen's slope is a robust estimate of the magnitude of a trend and commonly used to identify the slope of a trend line in hydrological time series (Yue et al. 2002). It is considered robust because it is sensitive to outliers.

* Strong evidence of trend ($p < 5\%$) – less than 5% chance that the null hypothesis – that there is no trend – is true.

** Weak evidence of trend ($p < 10\%$)– less than 10% chance that the null hypothesis – that there is no trend – is true.

D.4.1.1.2.3 4 East – for Watersheds < 500 km^2

Within the "4 East – for watersheds less than 500 km^2" hydrological region, 19 hydrometric stations were analysed for presence of a trend (Table D-6). The M-K test identified two stations as having statistically significant trends in their time series with the first showing an increasing trend (*Boundary Creek near Porthill Idaho,* 12321500) and the second showing a decreasing trend (*Arrow Creek near Erickson*, 08NH084). Two other stations, *Redfish Creek near Harrop* (08NJ061) and *Outlet Creek near Metaline Falls* (12397100), were found to have marginally statistically significant decreasing trends ($p < 0.1$ - less than a 10% chance of rejecting the null hypothesis), while *St-Mary River below Morris Creek* (08NG077) was found to have a marginally statistically significant increasing trend ($p < 0.1$).

Table D-6. Trend results for the hydrometric stations in the 4 East – for Watersheds > 500 km^2 hydrologic region.

Hydrometric Station Code	Start Year	End Year	p-value	Trend Direction	Sen's Slope[1]
08NK026	1986	2018	0.332	-	-0.01
08NJ130	1945	2017	0.177	-	0.01
12321500	1929	2017	0.002	Increasing**	0.23
08NH084	1980	2015	0.009	Decreasing**	-0.30
08NH005	1972	2017	0.322	-	-0.21
08NE110	1971	2015	0.567	-	0.14
08NJ061	1968	2017	0.052	Decreasing**	-0.06
08NG077	1973	2017	0.083	Increasing*	0.50
08NN023	1974	2015	0.555	-	-0.12
08NE087	2001	2017	0.964	-	-0.01
08NH016	1947	2017	0.504	-	-0.02
08NJ160	1973	2017	0.229	-	0.17
12313000	1928	2002	0.386	-	1.58
08NJ026	1995	2017	0.239	-	0.13
12397100	1959	2015	0.065	Decreasing*	-0.07
08NE114	1973	2016	0.727	-	0.02
08NE039	1930	2017	0.507	-	-0.06
12304040	1990	2000	0.533	-	0.43
08NH115	1964	2017	0.303	-	0.00

Notes:

1 The Sen's slope is a robust estimate of the magnitude of a trend and commonly used to identify the slope of a trend line in hydrological time series (Yue et al. 2002). It is considered robust because it is sensitive to outliers.

* Strong evidence of trend (p < 5%) – less than 5% chance that the null hypothesis – that there is no trend – is true.

** Weak evidence of trend (p < 10%)– less than 10% chance that the null hypothesis – that there is no trend – is true.

D.4.1.1.2.4 7 – for Watersheds > 500 km^2

Within the "7 – for watersheds greater than 500 km^2" hydrological region, 17 hydrometric stations were analysed for presence of a trend (Table D-7). The M-K test identified three USGS stations as having statistically significant decreasing trends in their time series: *Thompson River near Thompson Falls MT* (12389500), *Yaak River near Troy MT* (12304500), and *Yakima River at Umtanum, WA* (12484500). One other station, *Colville River at Kettle Falls, WA* (12409000), was found to have a marginally statistically significant increasing trend (p < 0.1).

Table D-7. Trend results for the hydrometric stations in the 7 – for Watersheds > 500 km^2 hydrologic region.

Hydrometric Station Code	Start Year	End Year	p-value	Trend Direction	Sen's Slope[1]
13339500	1980	2017	0.237	-	0.61
12414900	1966	2017	0.185	-	0.67
12433890	1972	2012	0.553	-	0.43
12354000	1911	2017	0.129	-	-0.98
12388200	1990	2010	0.124	-	0.77
12301300	1948	2016	0.189	-	-0.15
12365000	1931	2006	0.528	-	-0.08
12306500	1930	2017	0.983	-	0.00
12389500	1948	2017	0.044	Decreasing*	-0.55
12370000	1922	2017	0.290	-	-0.15
12304500	1948	2017	0.006	Decreasing*	-1.37
12302055	1948	2017	0.408	-	-0.35
12413000	1912	2017	0.542	-	0.75
12409000	1923	2017	0.076	Increasing**	0.13
12414500	1911	2017	0.935	-	0.00
12413500	1911	2017	0.125	-	1.67
12484500	1906	2017	0.021	Decreasing*	-0.70

Notes:

1 The Sen's slope is a robust estimate of the magnitude of a trend and commonly used to identify the slope of a trend line in hydrological time series (Yue et al. 2002). It is considered robust because it is sensitive to outliers.

* Strong evidence of trend (p < 5%) – less than 5% chance that the null hypothesis – that there is no trend – is true.

** Weak evidence of trend (p < 10%)– less than 10% chance that the null hypothesis – that there is no trend – is true.

D.4.1.2. Statistical Flood Frequency Modelling

A statistical approach to estimating flood quantiles for the clear-water flood watersheds was performed using the Regional FFA model. The multivariate regression model to estimate the index-flood (mean annual peak flow) included three climatic variables as predictors: MAP, MAT, and PAS. This regression model was calibrated using historical values of climatic variables, thus representing current conditions.

To estimate the climate-adjusted index flood for 2050, projected values of the climatic variables were input to the regression model. These projected values were estimated from model ensemble results for the RCP 8.5 emissions scenario using the ClimateNA v5.10 software package, available at http://tinyurl.com/ClimateNA, and based on the methodology described by Wang et al. (2016). The historical and climate-adjusted MAP, MAT, and PAS for the clear-water flood watersheds in the RDCK region are presented in Table D-8.

Table D-8. Climate variables used in the index flood quantile regression model with historical and climate-adjusted values for the clear-water flood watersheds in the RDCK.

Study Area	Watershed	MAP (mm)		MAT (°C)		PAS (Snow Water Equivalent, mm)	
		Historical Value	Climate-adjusted	Historical Value	Climate-adjusted	Historical Value	Climate-adjusted
Crawford Creek	Crawford Creek	1116	1175	3.0	6.4	590	384
Kaslo Creek	Keen Creek	1390	1472	1.3	4.9	857	618
	Upper Kaslo Creek	1244	1316	2.7	6.3	668	437
	Kalso Creek at Kootenay Lake	1312	1389	2.1	5.7	756	523
Burton Creek	Burton at Arrow Lake	1242	1315	2.4	5.9	704	483
	Caribou Creek	1259	1334	2.4	6.0	709	484
	Snow Creek	1227	1299	2.3	5.8	700	483
Slocan River	Little Slocan River	1161	1230	2.8	6.3	643	428
	Lemon Creek	1322	1404	2.7	6.3	754	503
	Slocan River	1224	1297	3.0	6.6	666	446
Goat River	Goat River	857	897	3.2	6.7	433	282
Salmo River	Erie Creek Upstream End	1265	1334	3.8	7.4	617	371

Note:

1. The ensemble model projections are averages across 15 CMIP5 models (CanESM2, ACCESS1.0, IPSL-CM5A-MR, MIROC5, MPI-ESM-LR, CCSM4, HadGEM2-ES, CNRM-CM5, CSIRO Mk 3.6, GFDL-CM3, INM-CM4, MRI-CGCM3, MIROC-ESM, CESM1-CAM5, GISS-E2R).

Climate-adjusted flood quantiles were calculated using the climate-adjusted index flood and the regional growth curves. The regional growth curves are assumed to be stationary. The ratio between the magnitude of the index-flood and the other flood quantiles was assumed to be the same in a climate-adjusted context. The regional growth curves are presented in the Regional FFA (Appendix C). Historical and climate-adjusted flood quantiles are summarized in Table D-9. Results show a small decrease in magnitude between the historical and climate-adjusted flood quantiles. Examination of the regression model for the index flood revealed that both the MAP and PAS were dominant predictors. The increase in the MAP was found to offset the decrease in the PAS resulting in little change in the estimate of the climate-adjusted index flood.

Table D-9. Historical and climate-adjusted flood quantiles for clear-water flood watersheds in the RDCK.

Study Area	Clearwater Watershed	Index-flood		2-year return period (0.5 AEP)		20-year return period (0.05 AEP)		200-year return period (0.005 AEP)	
		Historical (m^3/s)	Climate-adjusted (m^3/s)	Historical (m^3/s)	Climate-adjusted (m^3/s)	Historical (m^3/s)	Climate-adjusted (m^3/s)	Historical (m^3/s)	Climate-adjusted (m^3/s)
Crawford Creek	Crawford Creek	27	27	25	24	50	49	78	76
Kaslo Creek	Keen Creek	45	45	42	41	75	74	115	114
	Upper Kaslo Creek	38	37	34	34	70	68	109	106
	Kalso Creek at Kootenay Lake	81	80	74	73	150	148	234	230
Burton Creek	Burton at Arrow Lake	81	79	73	71	149	145	232	227
	Caribou Creek	42	41	38	37	78	76	121	119
	Snow Creek	45	44	41	40	83	81	129	126
Slocan River	Little Slocan River	103	100	94	91	191	186	297	289
	Lemon Creek	39	38	35	34	72	69	111	108
	Slocan River	347	339	315	308	642	627	1000	977
Goat River	Goat River	110	109	100	98	172	170	317	312
Salmo River	Erie Creek Upstream End	35	34	32	31	65	63	102	97

Note:

1. Final flood quantiles for Upper Kaslo Creek, Kaslo Creek at Kootenay Lake, Lemon Creek, Little Slocan River, Slocan River, Salmo River, and Goat River were estimated using a pro-rated calculation because they are gauged by a hydrometric station. The flood quantiles reported in this table were not used for subsequent analysis.

D.4.2. Process-based Assessment

To complement the statistical assessment, results from process-based modelling were examined. Process-based models involve the direct application of the downscaled GCM model forecasts into hydrological models. Process-based assessments are better suited for situations where a threshold change in process is likely e.g., a transition from nival (snowmelt dominated) runoff regime to pluvial-hybrid (snow influenced) runoff regime streamflow.

D.4.2.1. Climate-adjusted Streamflow

PCIC provides simulated daily streamflow time series for over 120 sites located in the Peace, upper Columbia, Fraser, and Campbell River watersheds. The time series are simulated at Water Survey of Canada (WSC) hydrometric stations and BC Hydro project sites. The simulated time series represent naturalized flow conditions (i.e., with effects of upstream regulation removed) for those sites affected by storage regulation. The hydrologic projections were forced with GCM data downscaled to a 1/16-degree resolution using Bias-Correction Spatial Disaggregation (BCSD) (Wood et al., 2004) following Werner (2011). Application of the Variable Infiltration Capacity (VIC) model and the generation of hydrologic projections for the Peace, Fraser, upper Columbia, and Campbell River watersheds are described in Shrestha et al. (2012) and Schnorbus et al. (2011, 2014).

An ensemble of 8 models forecasting daily streamflow time series for locations near the study area was accessed from PCIC’s website. This included forecasted time series on the Slocan and Salmo Rivers, specifically:

- Slocan River Near Crescent Valley (08NJ013)
- Salmo River Near Salmo (08NE074).

The RCP 8.5 emissions scenario was not available for this dataset so the IPCC A2 Emission Scenario (business as usual) was selected as the most similar. The 200-year flood quantile was assessed for three periods between 2009-2038, 2039-2068 and 2069-2098 and compared to the 200-year flood quantile based on the historical modelling (1955-2009). Maps showing the trend in the 200-year flood for the PCIC assessed sites and the location of the clear-water flood watersheds in the study for the three periods are shown in Figures D-4 to D-6 for the three periods assessed.

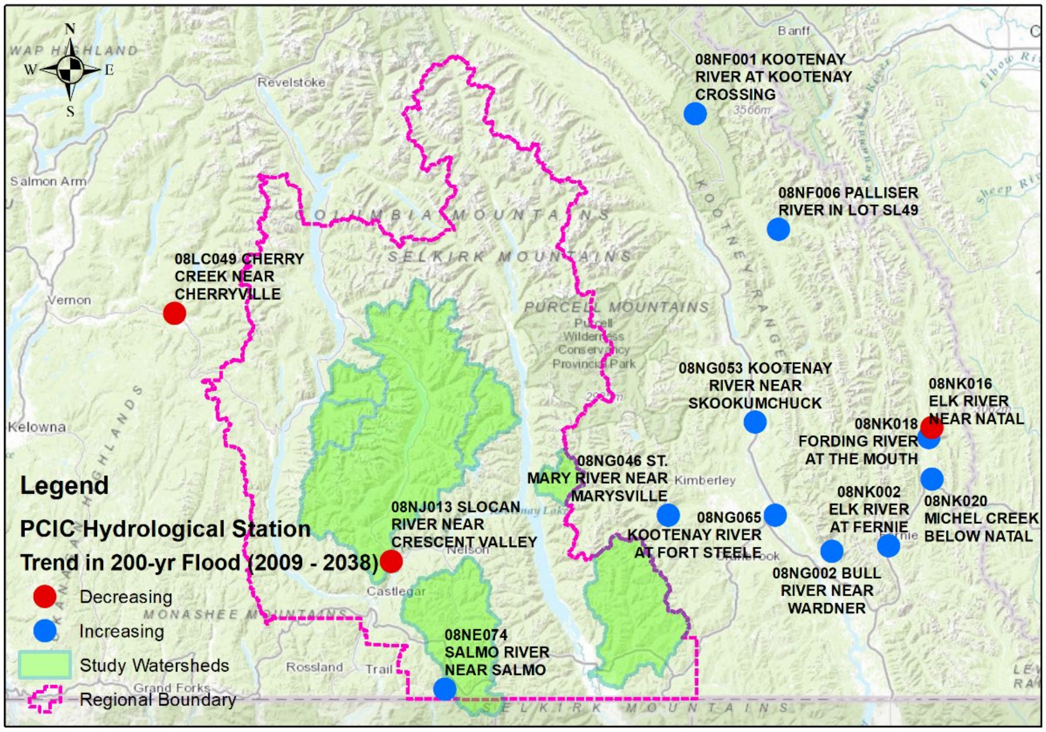

Figure D-4. Map showing nearby the PCIC hydrometric stations examined and their trend in the 200-year flood (period between 2009-2038).

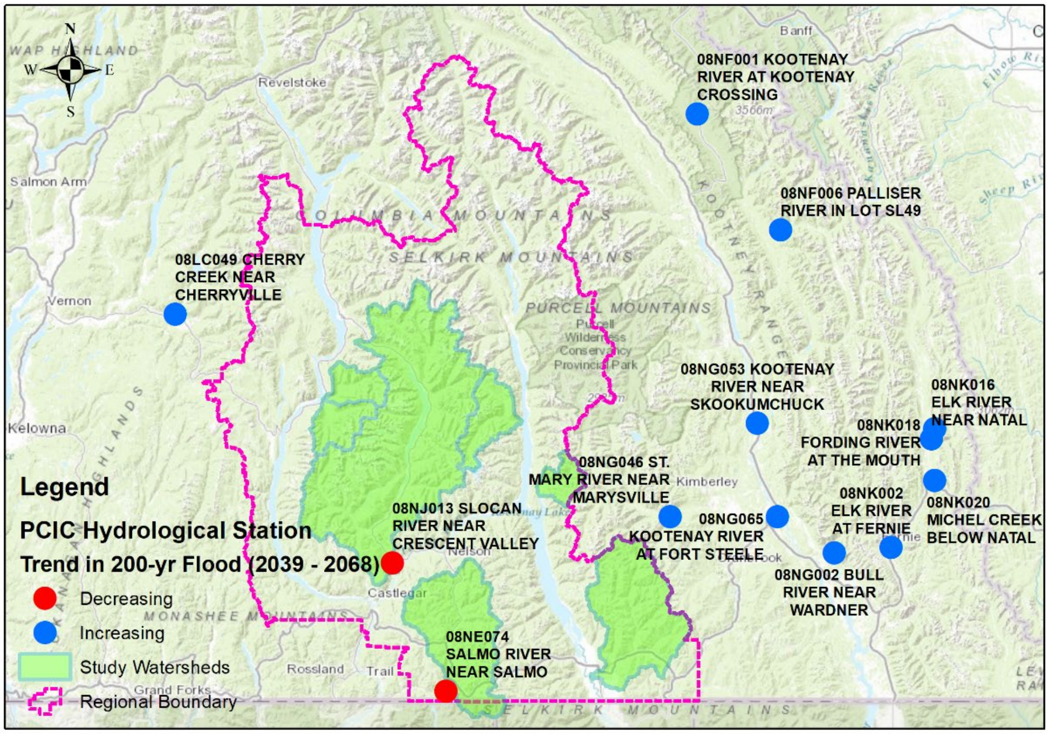

Figure D-5. Map showing nearby the PCIC hydrometric stations examined and their trend in the 200-year flood (period between 2039-2068).

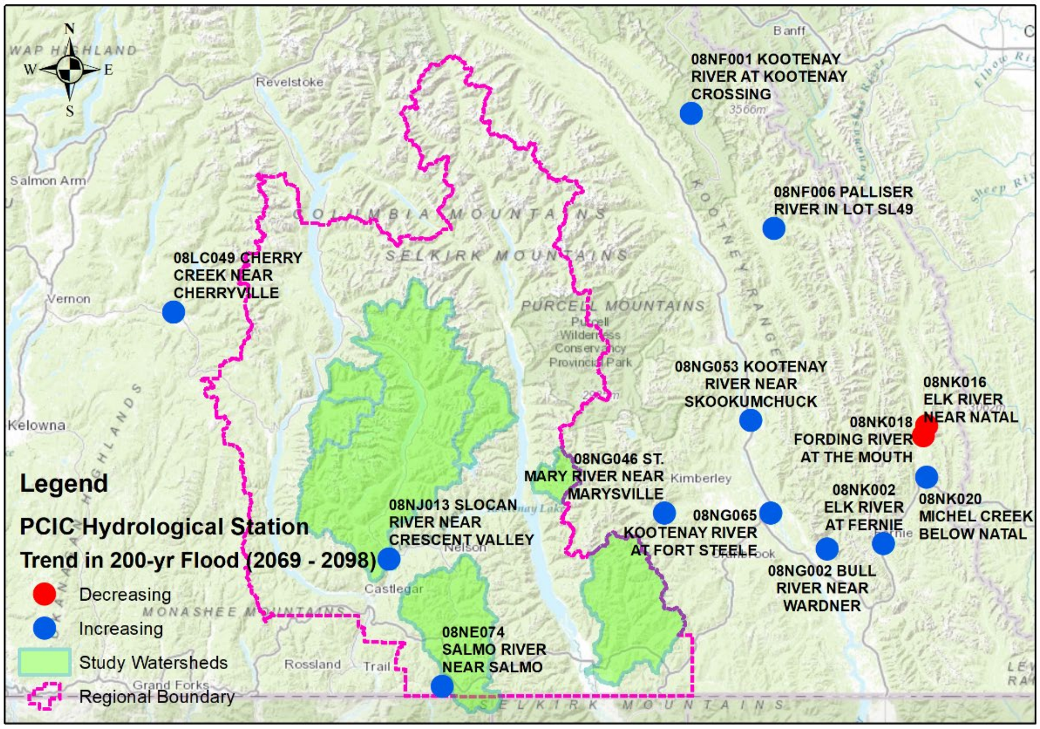

Figure D-6. **Map showing nearby the PCIC hydrometric stations examined and their trend in the 200-year flood (period between 2069-2098).**

The maps show that, in general, most of the thirteen stations examined show an increase in the magnitude of the 200-year flood over time with some exceptions based on an assessment of the mean of the eight models. A bar chart of the results for the individual hydrometric stations is shown in Figure D-7. The expected change in 200-year flood for the 2039-2068 period varies between -9% and +28% from the 1955-2009 period. For the 2069-2098 period, the range in the change of the 200-year flood magnitude increases from -7% and +60% from the 1955-2009 period. The mean of the predicted changes in the 200-year flood for Slocan River Near Crescent Valley (08NJ013) show virtually no change for the 2009-2038 period (-0.1%) followed by a small decrease and small increase for the 2039-2068 (-5%) and 2069-2098 (+16%) periods respectively. The mean of the predicted changes in the 200-year flood for Salmo River Near Salmo (08NE074) show a small increase for the 2009-2038 period (+8%) followed by small decrease for the 2039-2068 period (-97%) followed by a large increase for the 2069-2098 period (+60%).

Boxplots of the results for the three periods for the eight model runs are provided in Figure D- 12a and Figure D-12b. The boxplots provide a sense of the uncertainty in the analysis by the considerable range in the estimated 200-year flood quantile. Of note, the PCIC hydrologic model output was found by BGC to poorly predict historical flood quantiles.

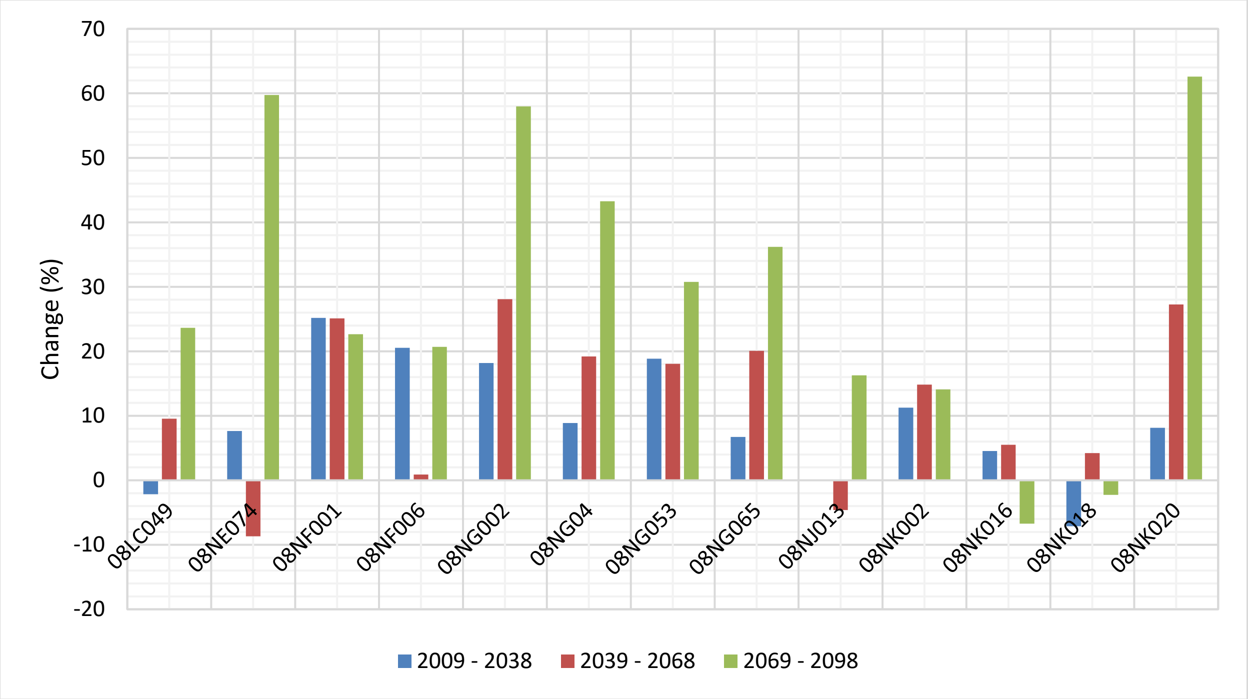

Figure D-7. **Bar-graph of the PCIC hydrometric stations and their change in the magnitude of the 200-year flood for the three periods examined compared to the 1955-2009 historical period.** ***Note that Station 08NJ013 and 08NE074 are stations located on the Slocan and Salmo Rivers respectively*.**

D.4.3. Legislated Guidelines

The Engineers and Geoscientists British Columbia (EGBC, 2018) guidelines state that when a historical trend is not detectable, a 10% adjustment can be applied to the design flood to account for likely future change in water input from precipitation. In cases where the information of future local conditions is inadequate to make an informed decision on the impacts of climate on hydrology, the EGBC guidelines suggest “adjusting expected flood magnitude and frequency according to the projected change in runoff during the life of the project, or by 20% in small watersheds (<50 km^2) for which information of future local conditions is inadequate to provide reliable guidance.” These guidelines also include consideration of potential effects of land use change.

D.5. SUMMARY

The impacts of climate change on flood quantile estimates were assessed using statistical and processed-based methods. The statistical methods included a trend assessment on historical flood events using the Mann-Kendall test as well as the application of climate-adjusted variables (mean annual precipitation, mean annual temperature, and precipitation as snow) to the Regional FFA model. The process-based methods included a trend analysis for climate-adjusted flood and precipitation data offered by PCIC.

The results of the statistical and process-based methods were found to be inconsistent across the RDCK. The results of the statistical flood frequency modelling generally show a small decrease in the flood magnitude, while the results of the process-based modelling generally show an increase with a wide range in magnitude. Although general trends for the region are predicted by GCMs and downscaled models, there is a wide range of predictions and estimation of future local conditions. The wide range in magnitude can be a function of many variables including watershed characteristics (e.g., proportion of watershed elevation above a given threshold) which were not explicitly addressed in this assessment.

D.6. CONCLUSION

The guidance offered by the climate changes impact assessment results is considered unreliable for estimating climate-adjusted flood quantiles on a site-specific basis. As a result, flood quantile estimates were adjusted by 20% for all catchments to account for the uncertainty in the impacts of climate change as per the EGBC (2018) guidelines.

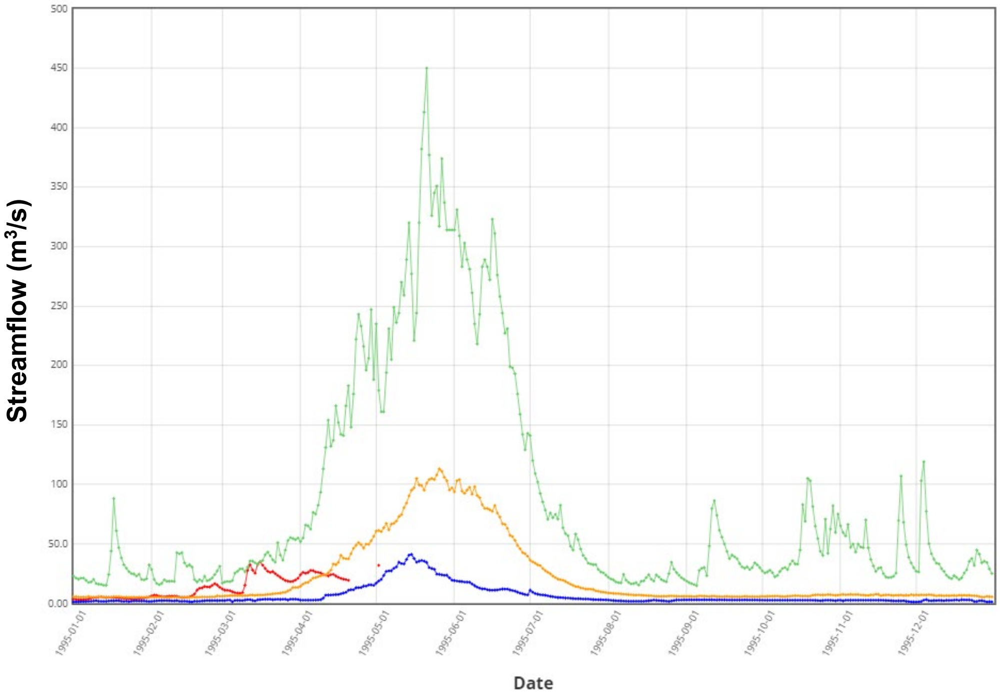

Figure D-8. Example freshet-driven hydrologic regime for Goat River near Erickson (08NH004). Green line is the maximum streamflow, the blue line is the minimum streamflow, the orange line is the median, and the red line is the 1995 streamflow.

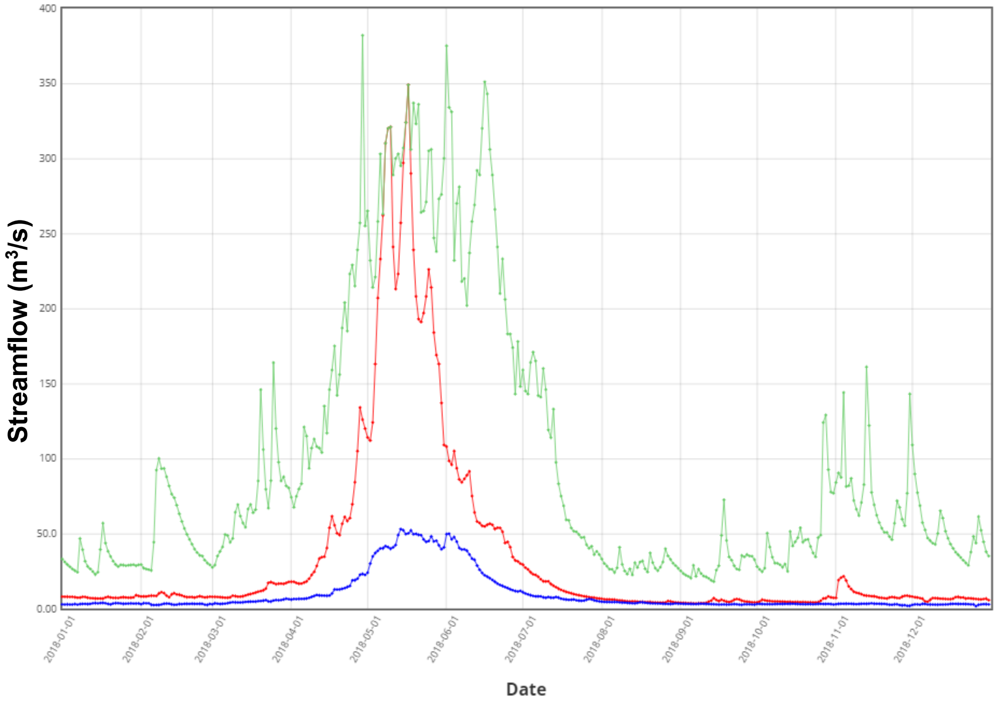

Figure D-9. Example freshet-driven hydrologic regime for Salmo River near Salmo (08NE074). Green line is the maximum streamflow, the blue line is the minimum streamflow, and the red line is the 2018 streamflow.

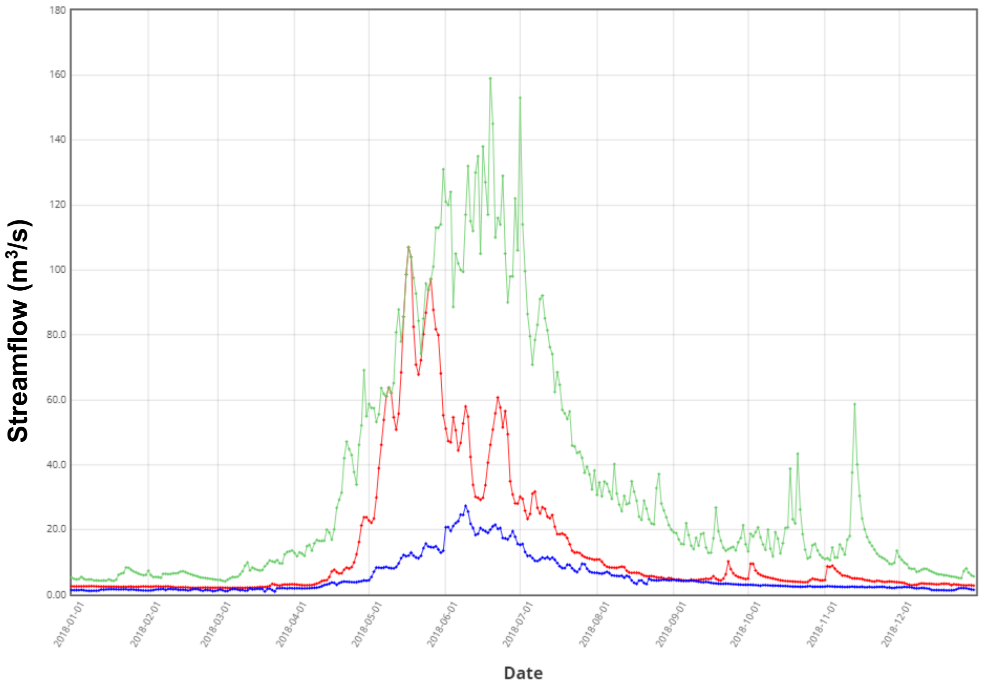

Figure D-10. Example freshet-driven hydrologic regime for Kaslo below Kemp Creek (08NH005). Green line is the maximum streamflow, the blue line is the minimum streamflow, and the red line is the 2018 streamflow.

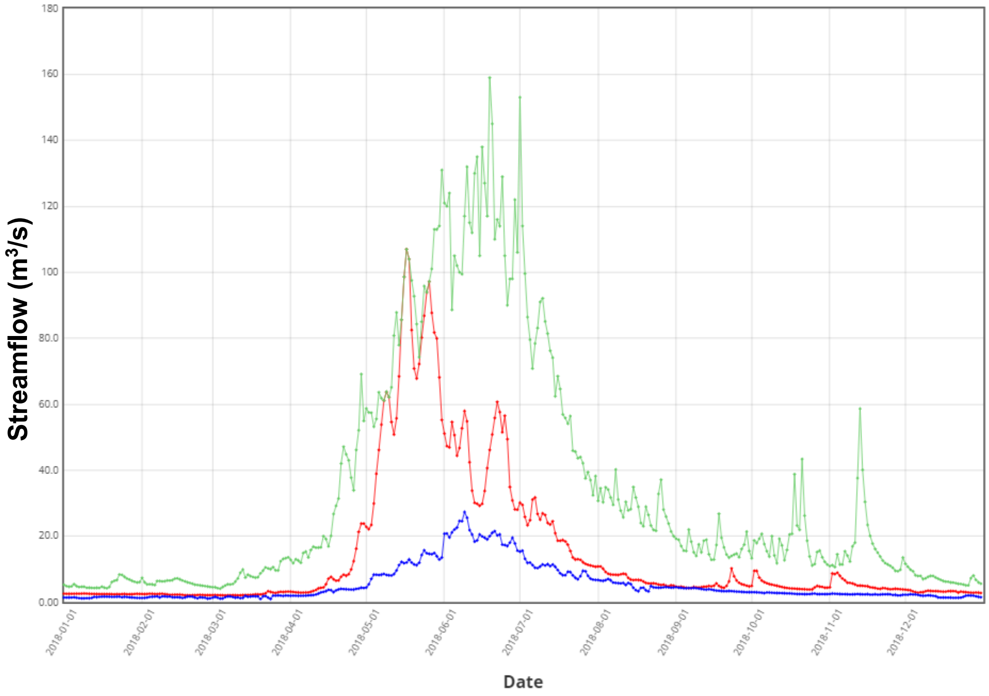

Figure D-11. Example freshet-driven hydrologic regime for Slocan River near Crescent Valley (08NJ013). Green line is the maximum streamflow, the blue line is the minimum streamflow, and the red line is the 2018 streamflow.

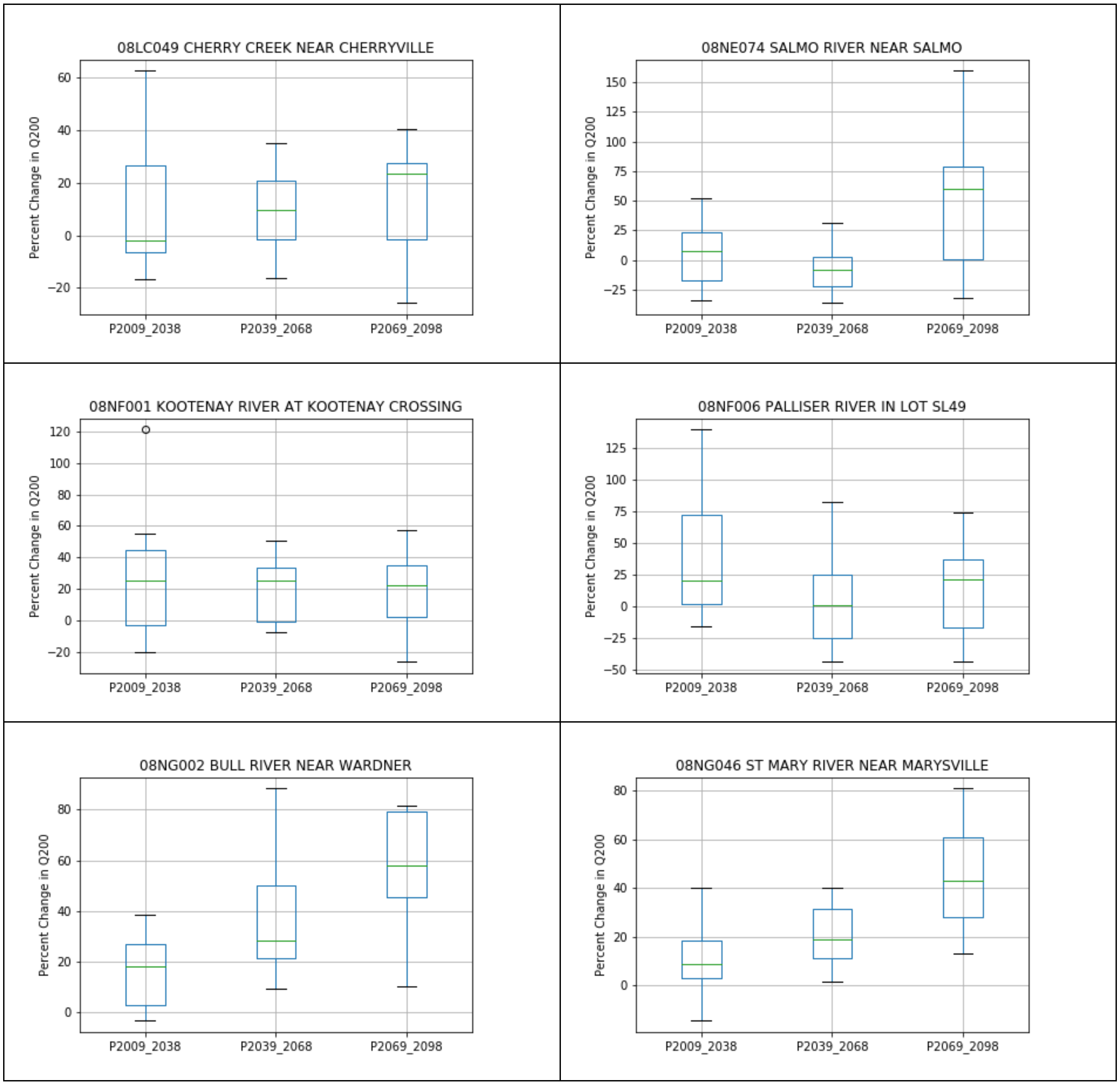

Figure D-12a. Boxplots of the PCIC Hydrological Stations and their change in the magnitude of the 200-year flood for the three periods examined compared to the 1955-2009 historical period. Boxplots represent the interquartile range from the ensemble of 8 GCM models.

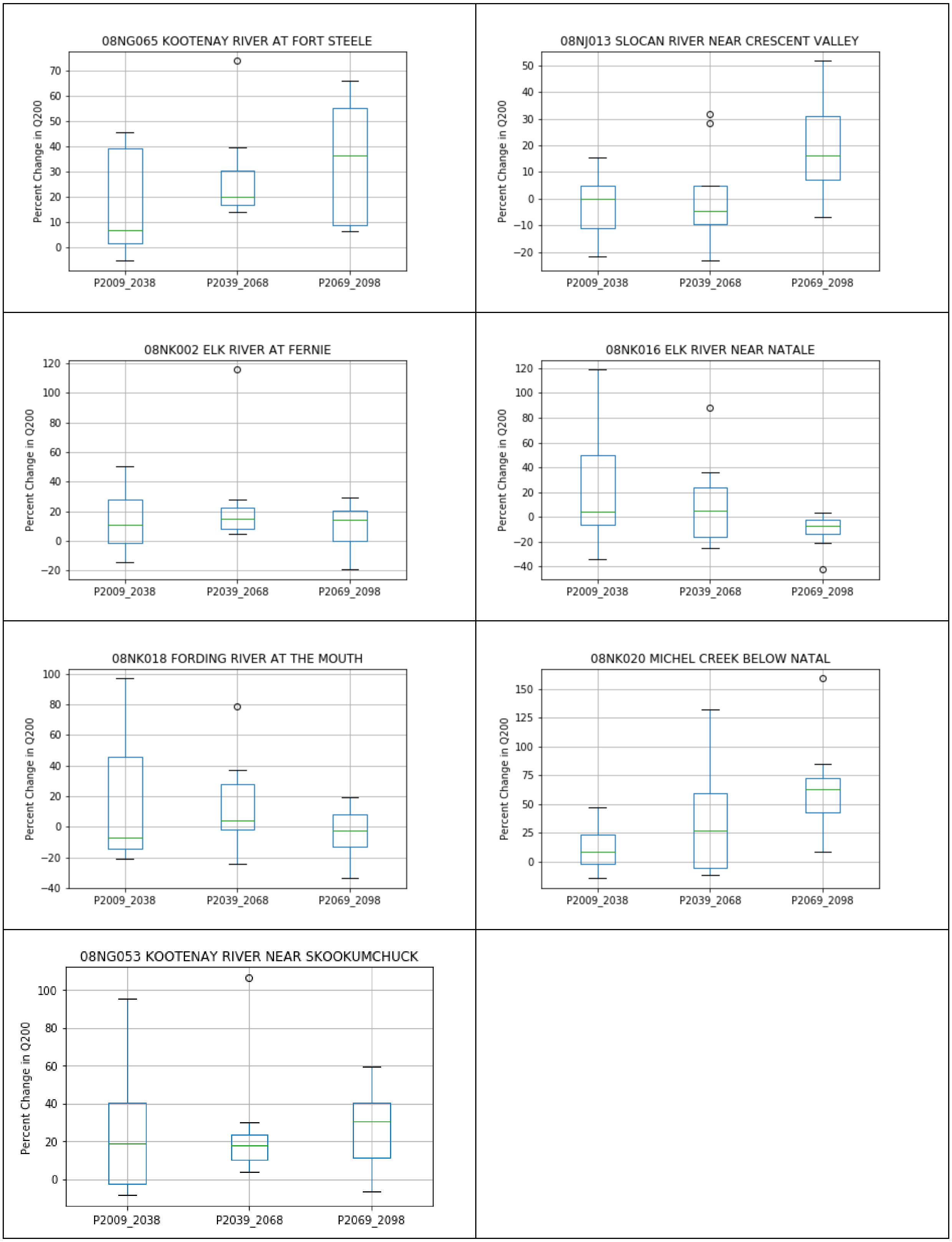

Figure D-12b. Boxplots of the PCIC Hydrological Stations and their change in the magnitude of the 200-year flood (continued).

REFERENCES

Barnett, T. P., Pierce, D. W., Hidalgo, H. G., Bonfils, C., Santer, B. D., Das, T., Mirin, A. A. (2008). Human-induced changes in the hydrology of the western United States. *Science, 319*(5866), 1080–1083.

Columbia Basin Trust (CBT). (2017). *Water Monitoring and Climate Change in the Upper Columbia Basin – Summary of Current Status and Opportunities*.

Déry, S. J., Stahl, K., Moore, R., Whitfield, P., Menounos, B., & Burford, J. E. (2009). Detection of runoff timing changes in pluvial, nival, and glacial rivers of western Canada. *Water Resources Research, 45*, W04426. https://doi.org/10.1029/2008WR006975

Eaton, B. & Moore, R. (2010) Regional hydrology. In R. Pike, T. Redding, R. Moore, R. Winkler, K. Bladon (Eds), *Compendium of Forest Hydrology and Geomorphology in British Columbia, Land Management Handbook 66, Vol 1, BC* (Chap 4). Ministry of Forests and Range, Forest Science Program and FORREX Forum for Research and Extension in Natural Resources: Victoria, BC and Kamloops, BC, URL htto://www.for.gov.bc.ca/Lmh/Lmh66.htm

Engineers and Geoscientists BC (EGBC). (2018). *Professional Practice Guidelines – Legislated Flood Assessments in a Changing Climate in BC*. Version 2.1.

Farjad, B., Gupta, A., & Marceau, D.J. (2016). Annual and seasonal variations of hydrological processes under climate change scenarios in two sub-catchments of a complex watershed. *Water Resources Management, 30*(8), 2851-2865. https://doi.org/10.1007/s11269-016-1329-3

Harder, P., Pomeroy, J.W., & Westbrook, C.J. (2015). Hydrological resilience of a Canadian Rockies headwaters basin subject to changing climate, extreme weather, and forest management. *Hydrological Processes, 29*, 3905-3924. https://doi.org/10.1002/hyp.10596

Kang, D.H., Shi, X., Gao, H., & Déry, S. J. (2014). On the changing contribution of snow to the hydrology of the Fraser River basin, Canada. *Journal of Hydrometeorology, 15*(4), 1344–1365.

Knutti, R., Massin, D., & Gettelman, A. (2013). Climate model genealogy: Generation CMIP5 and how we got there. *Geophysical Research Letters, 40*(6), 1194-1199. https://doi.org/10.1002/grl.50256

Loukas, A. & Quick, M.C. (1999). The effect of climate change on floods in British Columbia. *Nordic Hydrology, 30*(3), 231-256. https://doi.org/10.2166/nh.1999.0013

Pacific Climate Impacts Consortium (PCIC). (2011). Hydrologic *Impacts of Climate Change in the Peace, Campbell and Columbia Watersheds, British Columbia, Canada: Hydrologic Modeling Project Final Report (Part II)*.

Pacific Climate Impacts Consortium (PCIC). (2012). Plan2Adapt. Retrieved from https://www.pacificclimate.org/analysis-tools/plan2adapt.

Pacific Climate Impacts Consortium (PCIC). (2013). Climate Summary for: Kootenay / Boundary Region. Retrieved from https://www.pacificclimate.org/sites/default/files/publications/Climate_Summary-Kootenay-Boundary.pdf

Pacific Climate Impacts Consortium (PCIC). (2014). Station Hydrologic Model Output. Downloaded from https://data.pacificclimate.org/portal/hydro_stn/map/ on November 2019.

Pacific Climate Impacts Consortium (PCIC). (2019). Statistically Downscaled Climate Scenarios. Downloaded from https://data.pacificclimate.org/portal/downscaled_gcms/map/ on November 2019. Method: BCCAQ v2.

Prein, A.F., Rasmussen, R.M., Ikeda, K., Liu, C., Clark, M.P, & Holland, G.J. (2017). The future intensification of hourly precipitation extremes. *Nature Climate Change, 7*, 48-52. http://dx.doi.org/10.1038/nclimate3168

Schnorbus, M.A., Bennett, K.E., Werner, A.T., & Berland, A.J. (2011). *Hydrologic Impacts of Climate Change in the Peace, Campbell and Columbia Watersheds, British Columbia, Canada*. Pacific Climate Impacts Consortium, University of Victoria, Victoria, BC, 157 p.

Schnorbus, M., Werner, A., & Bennett, K. (2014). Impacts of climate change in three hydrologic regimes in British Columbia, Canada. *Hydrological Processes, 28*, 1170-1189. https://doi.org/10.1002/hyp.9661

Shrestha, R.R., Schnorbus, M.A., Werner, A.T., & Berland, A.J. (2012). Modelling spatial and temporal variability of hydrologic impacts of climate change in the Fraser River basin, British Columbia, Canada. *Hydrological Processes, 26*, 1840–1860. https://doi.org/10.1002/hyp.9283.

Wang, T., Hamann, A. Spittlehouse, D.L., & Carroll, C. (2016). Locally downscaled and spatially customizable climate data for historical and future periods for North America. *PLoS One 11*, e0156720. https://doi.org/10.1371/journal.pone.0156720

Werner, A. T. (2011). BCSD downscaled transient climate projections for eight select GCMs over British Columbia, Canada. Pacific Climate Impacts Consortium, University of Victoria, Victoria, BC, 63 p.

Whitfield, P.H., Cannon, A.J., & Reynolds, C.J. (2002). Modelling streamflow in present and future climates: examples from the Georgia Basin, British Columbia. *Canadian Water Resources Journal, 27*(4), 427–456. https://doi.org/10.4296/cwrj2704427

Wood, A.W., Leung, L.R., Sridhar, V., & Lettenmaier, D.P. (2004). Hydrologic implications of dynamical and statistical approaches to downscaling climate model outputs. *Climate Change*, 62, 189–216. https://doi.org/10.1023/B:CLIM.0000013685.99609.9e.

APPENDIX E
HYDRAULIC ASSESSMENT METHODS

E.1. INTRODUCTION

This appendix describes the approach used to develop a hydraulic model to estimate flood inundation extents for 20-, 50-, 200- and 500-year return period floods in the Salmo River study area. The following sections describe the methods used to develop the hydraulic model including model selection, model domain, scenarios and sensitivity analyses.

E.2. MODELLING SOFTWARE

Modelling results, including water surfaces profiles, water depths and flow velocities, were estimated using HEC-RAS version 5.0.7 hydraulic model. HEC-RAS is a public domain hydraulic modelling program developed and supported by the United States Army Corps of Engineers (Brunner & CEIWR-HEC, 2016). This version of HEC-RAS supports both one-dimensional (1-D) and two-dimensional (2-D) hydraulic modelling.

For this study, a 2-D hydraulic model was selected. The 2-D model is suited for the Salmo River study area which includes complex flow pathways across the floodplain near the confluence between the Salmo River and Erie Creek in the Village of Salmo. The 2-D model also provides more detailed information on the flow depths and velocities than a 1-D model. A 2-D model also removes some of the subjective modelling techniques, which are involved in the development of 1-D models, such as defining ineffective flow areas, levee markers, and cross-section orientation.

A limitation of 2-D models in HEC-RAS is with the modelling of bridges. The 2-D model cannot model high-flows (e.g., when the water surface elevation is greater than the low cord of the bridge). Incorporation of bridge piers can be accomplished within the 2-D model but at significant computational cost. To address this, 1-D models were created and used to check the water surface elevations at bridges against the 2-D models.

E.3. MODEL DOMAIN AND BOUNDARY CONDITIONS

E.3.1. Model Domain

The model domain covers a 32 km section of the Salmo River and a 7 km section of Erie Creek (Figure E-1). The upstream boundary on the Salmo River is located 1.4 km above of the Town of Ymir. The downstream boundary on the Salmo River is 700 m below the confluence with the South Salmo River. The upstream boundary on Erie Creek is located approximately 1.5 km north of Erie Lake.

Figure E-1. Salmo River study area. Satellite imagery from Bing.

E.3.2. Boundary Conditions

The upstream boundaries on the Salmo River and Erie Creek were modelled as inflow boundaries. The upstream boundaries were defined as steady-state inflow hydrographs for the flood quantiles of interest. Discharge along Erie Creek and the Salmo River was increased incrementally by accounting for discrete contributions from tributaries. Seven tributaries along the Salmo River, including Erie Creek, and one tributary along Erie Creek (Erie Lake) were included as inflow boundaries (Figure E-2). Locally pro-rated results of a flood frequency analysis (FFA) were used to estimate peak discharge for the gauged Salmo River and infer discharge contributions from tributaries in a procedure detailed in Section 4.3.1. Erie Creek is ungauged; therefore, regional FFA was used to estimate peak discharge (Appendix C).

The normal depth boundary condition was used at the downstream boundary below the South Salmo River. This assumes that the friction slope (approximately equal to the water slope) is equal to the channel slope. For the Salmo River model, the friction slope at the downstream boundary was set equal to the local surveyed channel slope (0.007 m/m, or 0.7%). The normal depth assumption can cause errors in model results at the downstream boundary. Therefore, the downstream boundary was set approximately 500 m downstream of the downstream end of the study area so that the uncertainty of the friction slope propagating upstream would not affect modelling results within the study area.

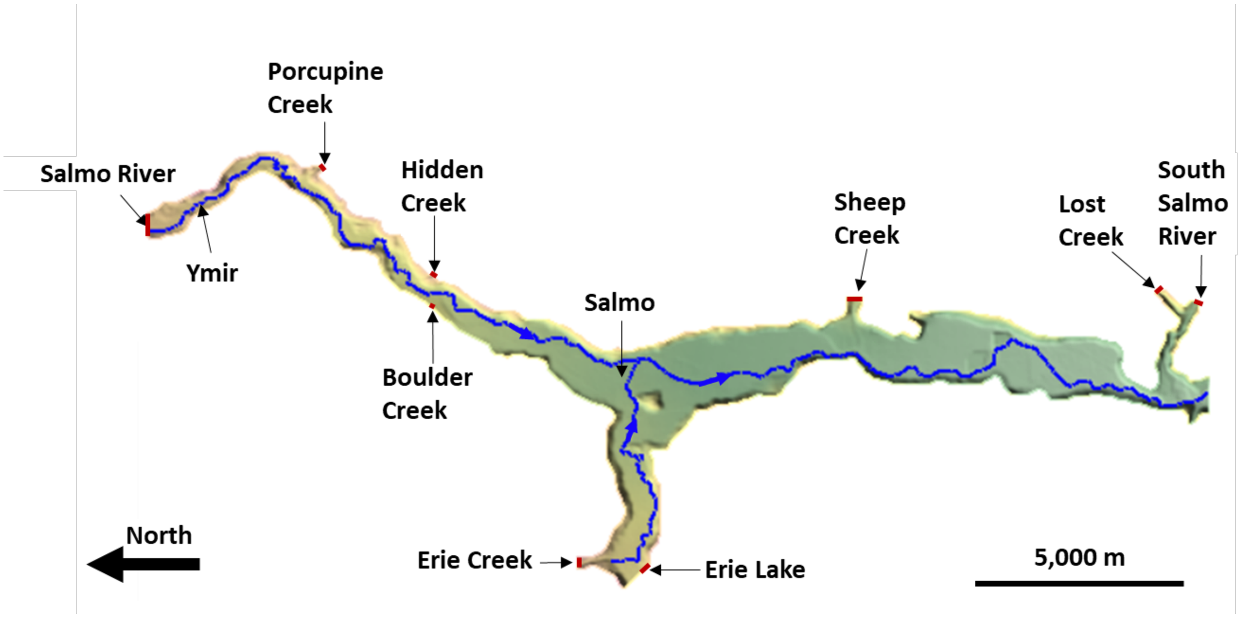

Figure E-2. Salmo River study area modelling domain and location of tributaries modelled as upstream boundaries.

E.4. CHANNEL AND FLOODPLAIN HYDRAULIC ROUGHNESSES

As common with many hydraulic models, HEC-RAS 2-D uses the Manning's roughness coefficient (Manning's n) to parameterize friction losses in the channel and floodplain. Measured discharge and water depth data for flood events were not available for the Salmo River and Erie Creek, and therefore the model is uncalibrated.

In-channel Manning's n values were estimated using Jarrett's equation (1984):

$$n = 0.39S^{0.38}R^{-0.16}$$

where S is the energy slope assumed equal to the channel slope, and R is the hydraulic radius of the stream, in feet.

The reach-averaged channel slope along the Salmo River ranged between 0.0052 m/m (0.52%) upstream of the confluence with Erie Creek, and 0.0030 m/m (0.30%) downstream of the confluence with Erie Creek. The reach-averaged channel slope along Erie Creek was 0.0097 m/m (0.97%). Jarrett's equation is based on 75 observations of streams in Colorado, for which bed material ranged from cobbles to small boulders, and energy slopes ranged from 0.2 % to 9%. Therefore, Jarrett's equation was considered to be suitable for the Salmo River study area.

Preliminary estimates of in-channel Manning's n values using Jarrett's equation ranged between 0.030 and 0.039 along the Salmo River and the lower reaches of Erie Creek, depending on local channel slope and flow depth. A single, median value of 0.035 was adopted for the in-channel portion of the Salmo River and most of Erie Creek. A Manning's n value of 0.045 was assigned to the upstream-most 850 m of Erie Creek's in-channel domain to reflect the above-average channel slope (approximately 0.011 m/m, or 1.1%). A sensitivity on the model results to the in-channel Manning's n is provided in Section E.8.

The Manning's n values on the floodplain were selected with guidance from the literature and using empirical equations. Manning's n values for floodplain areas were based on land cover types (Figure E-3) with Manning's n values for each land cover type from Chow (1959). The spatial land cover distributions were imported from digital land cover maps from the North American Land Change Monitoring System (NRCan, 2019).

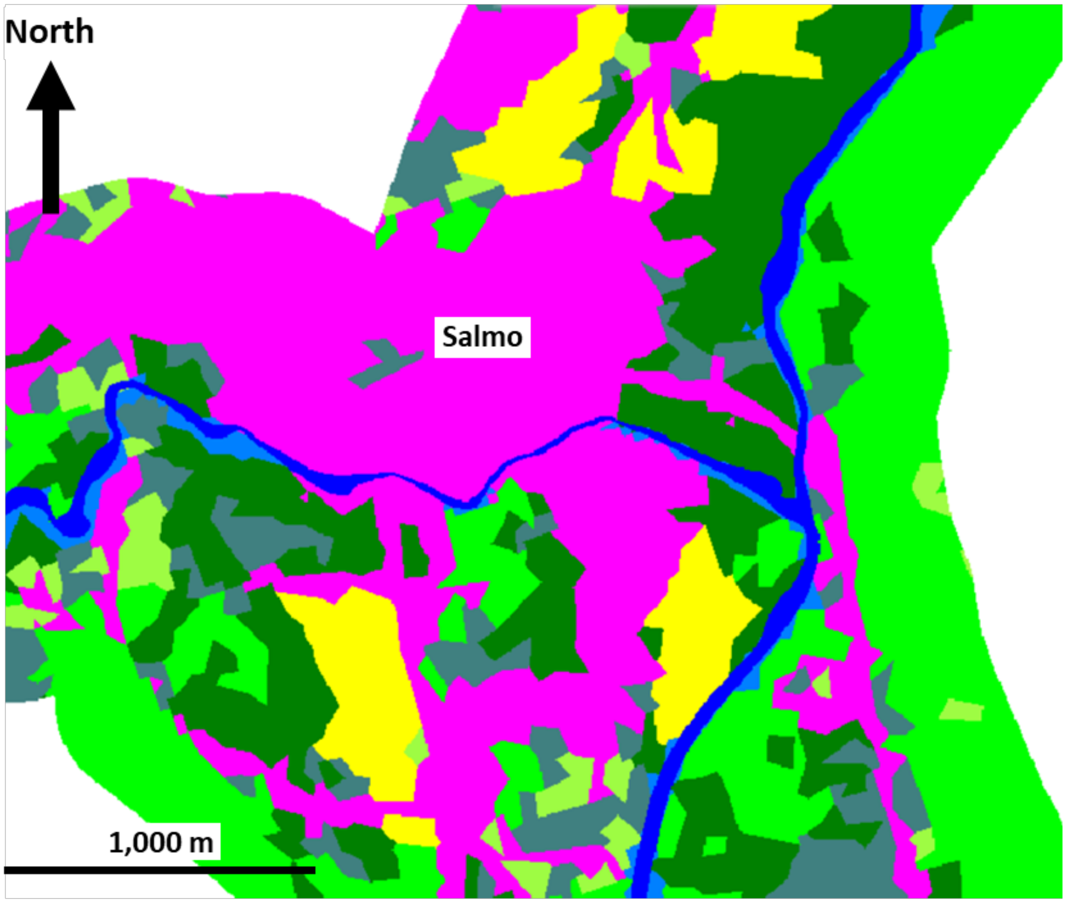

Land Class	Manning's n Value	Color
In-channel domain	0.035	🟦
Wetland	0.03	🟦
Barren Lands	0.044	🟧
Cropland	0.035	🟨
Mixed Forest	0.1	🟩
Temperate or Sub-Polar Grassland	0.035	🟩
Temperate or Sub-Polar Needleleaf Forest	0.1	🟩
Temperate or Sub-Polar Shrubland	0.07	⬛
Urban Built-up	0.025	🟪
Water	0.044	🟦

Figure E-3. Manning's n roughness layer defined for the model.

E.5. MODEL MESHING

The HEC-RAS software for 2-D modelling uses an irregular mesh to simulate the flow of water over the terrain. Irregular meshes are useful for development of numerically efficient 2-D models to allow refinement of the model in locations where the flow is changing rapidly and/or where increased resolution is desired. With 2-D models, the objective is to define a model with sufficient accuracy and resolution that minimizes model runtime.

The default cell geometries created by HEC-RAS are rectangular, but other cell geometries with up to eight faces can be selected to suit the problem under consideration. Within HEC-RAS, a 2-D mesh is generated based on the following inputs:

- The model perimeter (the model domain or extent of the model)
- Refinement areas which are user-defined sub-domains where the mesh properties (e.g., mesh resolution) are adjusted
- Breaklines, which are linear features created to align the mesh with terrain features which influence the flow such as dikes, ditches, terraces, and embankments. HEC-RAS allows for mesh resolution adjustments near breaklines.

From these inputs, HEC-RAS generates the mesh consisting of computational points, typically located at the cell centroids, and cell faces, for which hydraulic properties are computed prior to simulation runs.

E.5.1. Initial Mesh Development

For the Salmo River study area, a base model resolution of 20 m was selected. A refinement region was created within the in-channel domains of the Salmo River and Erie Creek with a resolution of 3 m. Breaklines were placed along the channel bank crests, and the top of dykes and road embankments. Near these breaklines, the mesh resolution was refined to 5 m.

E.5.2. Mesh Refinement

Based on the results of preliminary simulation runs, additional breaklines were introduced in areas where ‘leakage’ was noted between cells. Leakage is a result of the cell faces not aligning with terrain features and/or cells that are too large and hydraulically connects areas separated by a physical barrier to flow (e.g., a local ridge in the underlying terrain). A total of 82 breaklines were used to represent terrain features and guide the mesh generation algorithm. An additional 44 channel and floodplain cross sections located at key locations (e.g., high building density, bridge crossing) were also input as breaklines to locally orient the mesh and compute cross-sectional properties (e.g., total discharge through a cross section). The final mesh consisted of approximately 450,000 computational cells with an average cell area of 72 m^2. An example of the mesh developed is given in Figure E-4.

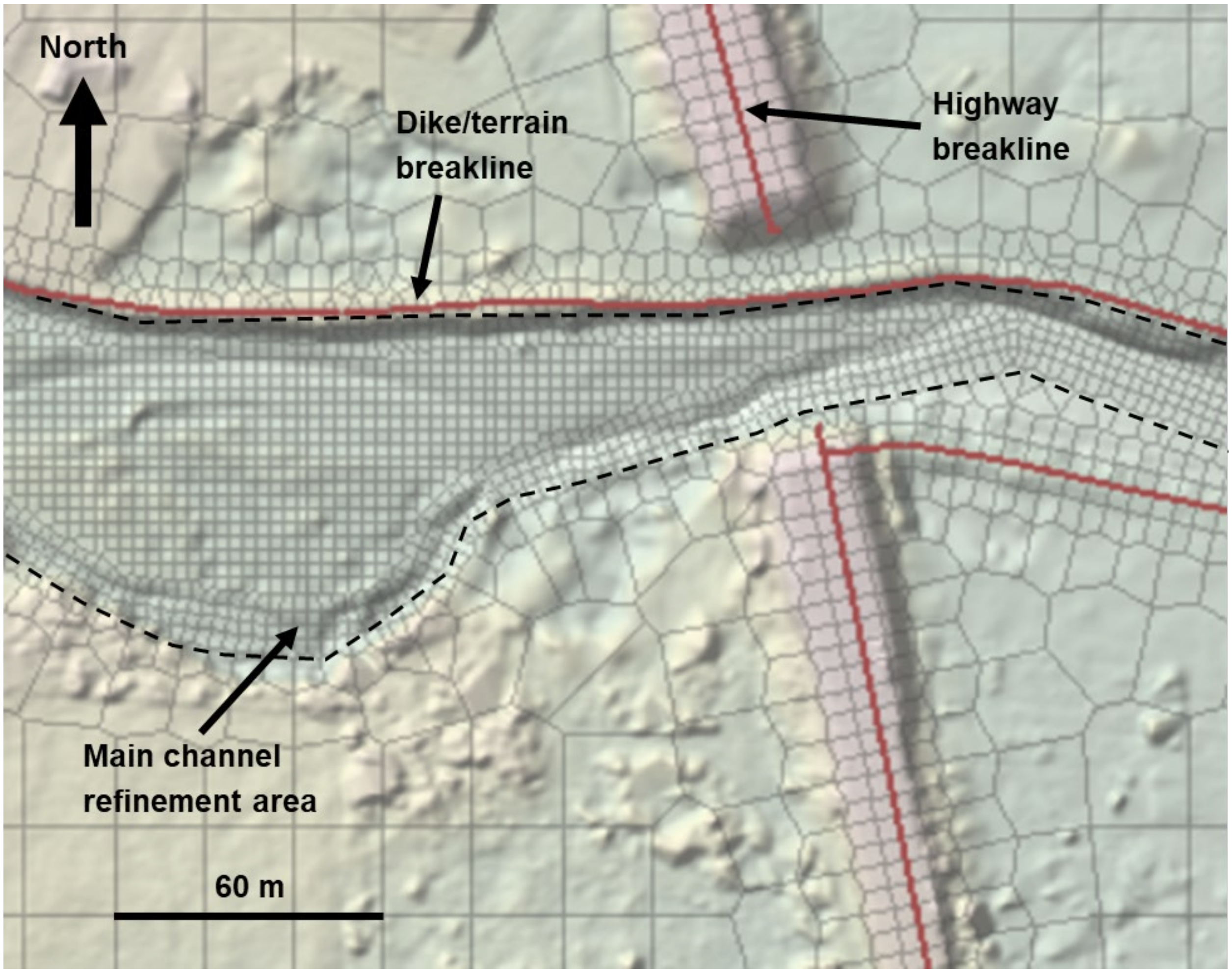

Figure E-4. Example of the mesh used for the model showing the breaklines and refinement areas.

E.5.3. Hydraulic Structures

E.5.3.1. Bridge Crossings

As indicated in Section E.2, bridge crossings cannot be readily modelled with HEC-RAS 2-D v5.0.7. Bridge decks were removed from the terrain model for 2-D simulations and separate HEC-RAS 1-D models of the bridge crossings were developed. A total of 13 bridge crossings of the Salmo River and Erie Creek were identified within the study area (Figure E-5). Bridges were surveyed by Midwest Surveys in July – September 2019 to capture bridge and pier dimensions, as well as low chord (bottom-of-deck) and top-of-deck elevations (Figure E-6). Additional bridge data were received from the BC Ministry of Transportation and Infrastructure (BC MOTI) in January 2020. A brief description of these bridges is provided below, followed by a table summarizing key bridge dimensions and characteristics, modelling approach, and results of the 1-D models (Table E-1).

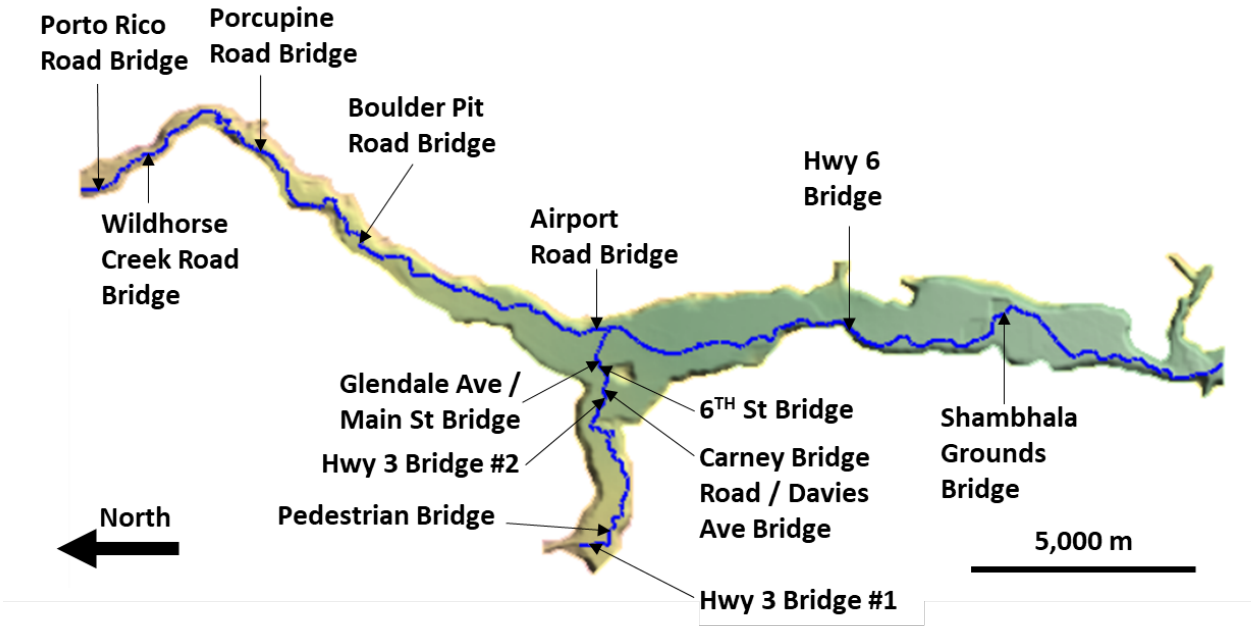

Figure E-5. Bridge crossings along the Salmo River and Erie Creek within the study area.

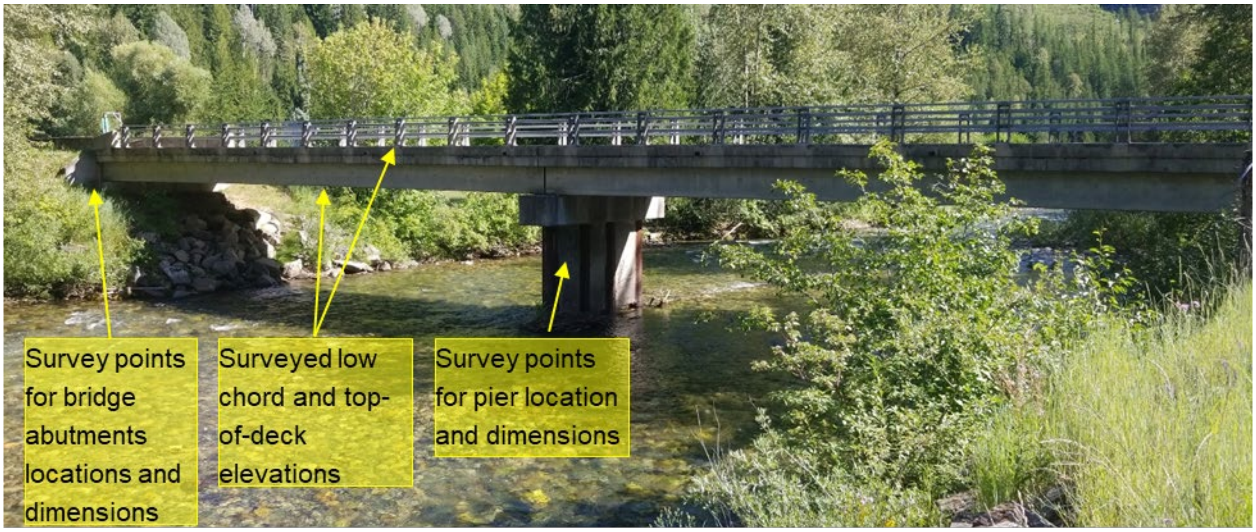

Figure E-6. Example of surveyed bridge structure features.

Salmo River – Porto Rico Road Bridge

The Porto Rico Road bridge was constructed in 1965 and is 31 m long and 8 m wide (Figure E-7). The bridge deck is skewed 60° to the main flow direction and is supported mid-channel by a 0.4 m wide elongated central pier. The upstream end of the pier is protected by a triangular fender plate to deflect incoming flows and debris. Bridge abutments are sloped and armoured with riprap.

Figure E-7. **Porto Rico Road bridge over the Salmo River looking downstream (south). Photo: Midwest Survey July 28, 2019.**

Salmo River – Wildhorse Creek Road Bridge

The Wildhorse Creek Road bridge was constructed in 1975 and is 28 m long and 7 m wide (Figure E-8). The single span bridge deck is skewed 65^{o} to the main flow direction and rests on vertical concrete abutments.

Figure E-8. **Wildhorse Creek Road bridge over the Salmo River looking downstream (south). Photo: Midwest Survey July 28, 2019.**

Salmo River – Porcupine Road Bridge

The Porcupine Road bridge was constructed in 1990 and is a 45 m long and 5 m wide (Figure E-9). The bridge deck is oriented perpendicular (90°) to the main flow direction and is supported mid-channel by an elongated central pier comprising four 0.45 m diameter piles. Bridge abutments are sloped and armoured with riprap.

Figure E-9. Porcupine Road bridge over the Salmo River looking downstream (southeast). Photo: Midwest Survey July 28, 2019.

Salmo River – Boulder Pit Road Bridge

The Boulder Pit Road bridge is 32 m long and 5 m wide (Figure E-10). The single span bridge deck is oriented perpendicular to the main flow direction.

Figure E-10. Boulder Pit Road bridge over the Salmo River looking upstream (east). Photo: Midwest Survey July 29, 2019.

Salmo River – Airport Road Bridge

The Airport Road bridge was constructed in 1956 and is 40 m long and 10 m wide. The single span bridge deck is skewed 45° to the main flow direction, and rests on piles founded in the banks of the river. The bridge abutments are sloped and armoured with riprap (Figure E-11).

Figure E-11. Airport Road bridge over the Salmo River looking across (east) from the right bank. Photo: BGC Engineering July 31, 2019.

Salmo River – Highway 6 Bridge

The Highway 6 bridge was constructed in 1980 and is 78 m long and 12 m wide (Figure E-12). The bridge deck is skewed 45° to the main flow direction and is supported by two 1.7 m diameter concrete piles, located approximately 36 m apart. Bridge abutments are sloped and armoured with riprap.

Figure E-12. Highway 6 bridge over the Salmo River looking across (east) from the right bank. Photo: Midwest Survey July 29, 2019.

Salmo River – Shambhala[1] Grounds Bridge

The Shambhala Grounds bridge was constructed in 2018 and is 46 m long and 5 m wide. The single span bridge deck is oriented perpendicular to the main flow direction and rests on piles founded in the banks of the river (Figure E-13). The bridge abutments are sloped and armoured with riprap.

Figure E-13. Shambhala Grounds bridge over the Salmo River looking upstream (northeast) from the right bank. Photo: Midwest Survey July 29, 2019.

Erie Creek – Highway 3 Bridge (upstream)

The Highway 3 bridge (upstream) was constructed in 1952 and is 19 m long and 9 m wide. The single span bridge deck is oriented perpendicular to the main flow direction, and rests on near-vertical concrete abutments (Figure E-14).

Figure E-14. Highway 3 bridge (upstream) over Erie Creek looking upstream (north). Photo: Midwest Survey August 7, 2019.

---

[1] The bridge owner is Shambhala Music Festival. The name of the bridge is unknown.

Erie Creek – Pedestrian Bridge

The pedestrian bridge is 46 m long and 6 m wide. The single span bridge deck is skewed 50° to the main flow direction and rests on concrete piles founded in the banks of the creek (Figure E-15).

Figure E-15. Pedestrian bridge over Erie Creek looking upstream (northwest) from the right bank. Photo: Midwest Survey August 8, 2019.

Erie Creek – Highway 3 Bridge (downstream)

The Highway 3 bridge (downstream) was constructed in 1980 and is 49 m long and 11 m wide (Figure E-16). The single span bridge deck is oriented perpendicular to the main flow direction. Each bridge abutment comprises 12 piles founded in the bank of the river. The bridge abutments are armoured with riprap.

Figure E-16. Highway 3 bridge (downstream) over Erie Creek looking downstream (east) from the left bank. Photo: Midwest Survey August 8, 2019.

Erie Creek – Carney Bridge Road / Davies Avenue Bridge

The Carney Bridge Road / Davies Avenue bridge was constructed in 2010 and is 22 m long and 6 m wide (Figure E-17). The single span bridge deck is oriented perpendicular to the main flow direction and is supported by two arches anchored to concrete abutments and armoured with riprap.

Figure E-17. Carney Bridge Road / Davies Avenue bridge over Erie Creek looking downstream (east). Photo: Midwest Survey August 8, 2019.

Erie Creek – 6th Street Bridge

The 6th Street pedestrian bridge was constructed in 2017 and is 33 m long. The single span bridge deck is oriented perpendicular to the main flow direction. The bridge abutments are sloped and armoured with riprap (Figure E-18).

Figure E-18. 6th Street bridge over Erie Creek looking downstream (northeast). Photo: Midwest Survey August 7, 2019.

Erie Creek – Glendale Avenue / Main Street Bridge

The Glendale Avenue / Main Street bridge is approximately 30 m long and 11 m wide. The single span bridge deck is oriented perpendicular to the main flow direction and rests on concrete piles founded in the banks of the river and armoured with riprap (Figure E-19).

Figure E-19. Glendale Avenue / Main Street bridge over Erie Creek looking upstream (west) from the left bank. Photo: Midwest Survey August 6, 2019.

Table E-1. Bridge crossings along the Salmo River and Erie Creek within the study area.

Bridge Crossing	Latitude (°)	Longitude (°)	Length (m)	Width (m)	Deck orientation to flow direction (°)	Low chord elevation (m)	Number of in-channel piers	2-D hydraulic model 200-year flood water surface elevation (m)	Freeboard (m)	1-D hydraulic model		Impact of the bridge on flood extent
										(Yes/No)	Rationale	
Erie Creek												
Highway 3 Bridge #1	49.1922	-117.3326	19	9	90	717.1	0	716.1	1.0	No	Bridge deck is free spanning with no piers.	No measurable impact expected
Pedestrian Bridge	49.1885	-117.3278	46	6	30	708.9	0	707.6	1.3	No	Bridge deck is free spanning with no piers.	No measurable impact expected
Highway 3 Bridge #2	49.1898	-117.2847	49	11	90	669.06	0	666.7	2.4	No	Bridge deck is free spanning with no piers.	No measurable impact expected
Carney Bridge Road / Davies Avenue Bridge	49.1895	-117.2829	22	6	90	667.4	0	665.8	1.6	No	Bridge deck is free spanning with no piers.	No measurable impact expected
6th Street Bridge	49.1905	-117.2772	33	3	90	663.9	0	662.7	1.2	Yes	Included in the bridge model for the Glendale Avenue / Main Street Bridge given proximity	No measurable impact expected
Glendale Avenue / Main Street Bridge	49.1913	-117.2751	30	11	90	663.3	2	661.6	1.7	Yes	In-channel obstructions (2 piers) expected to reduce flow conveyance.	No measurable impact expected
Salmo River												
Porto Rico Road Bridge	49.2913	-117.2227	31	8	60	737.1	1	736.6	0.5	Yes	In-channel obstruction (one pier) expected to reduce flow conveyance.	No measurable impact predicted
Wildhorse Creek Road Bridge	49.2818	-117.2125	28	7	65	728.4	0	727.5	0.9	No	Bridge deck is free spanning with no piers.	No measurable impact expected
Porcupine Road Bridge	49.2606	-117.2108	45	5	90	708.6	1	707.3	1.3	Yes	In-channel obstruction (one pier) expected to reduce flow conveyance.	No measurable impact predicted
Boulder Pit Road Bridge	49.2390	-117.2386	32	5	90	691.35	0	691.4	-0.05	Yes	2-D simulations suggested that the 200-year flood flows would interact with the bridge deck.	Increased water surface elevation over a distance of approximately 200 m upstream of the bridge was predicted.
Airport Road Bridge	49.1907	-117.2659	40	10	50	660.1	0	658.2	1.9	No	Bridge deck is free spanning with no piers.	No measurable impact predicted
Highway 6 Bridge	49.1411	-117.2640	78	12	45	644	2	641.9	2.1	Yes	In-channel obstruction (two piers) expected to reduce flow conveyance.	No measurable impact predicted
Shambahla Grounds Bridge	49.1094	-117.2609	46	5	90	623.1	0	623.5	-0.4	Yes	2-D simulations suggested that the 200-year flood flows would interact with the bridge deck.	Increased water surface elevation over a distance of approximately 150 m upstream of the bridge was predicted.

Note: Bridge crossings are listed in a downstream direction.

E.5.3.2. Dikes

Approximately 1,000 m of dike have been constructed on the left (north) bank of Erie Creek, which are managed by the Village of Salmo and regulated under the Dike Maintenance Act (Figure E-20). Historical records indicate that in the mid-1960s the Ministry of Transportation and Highways constructed approximately 12,000 feet (3,650 m) of diking along the left (east) bank of the Salmo River downstream of the confluence with Erie Creek (BC MoE, 1981). Dike construction initially used streambed sediments dredged from the channel to increase flow conveyance. The dikes were upgraded in the following decades, including local placement of a riprap armour, typically following flood events in response to bank erosion that threatened dike integrity. Currently the dikes south of the confluence with Erie Creek are considered an orphan flood protection structure that is not being maintained by an owner or diking authority (Boyer, 2009).

Figure E-20. Regulated dikes along the left (north) bank of Erie Creek. Satellite imagery from Bing.

E.6. SIMULATION SETTINGS

The hydraulic model described above was run using a Courant-controlled time step. Reducing the Courant number threshold to a value closer to 1 mechanically reduces the computational time step; however, this also improves numerical convergence, thus reducing overall runtime. Optimized runtimes resulted in an initial time step varying between 0.3 and 1 second, and a maximum Courant number varying between 1.7 and 2, depending on the modelled scenario (see Section E.7). The various models were run for 24 hours to reach a steady state using the full momentum equations. The full momentum equations provide accurate representation of flow dynamics, especially where sharp contraction, expansions or changes in flow direction are observed.

E.7. MODELLING SCENARIOS

Scenarios were run for the 20-, 50-, 200-, and 500-year flood events. A summary of the modelled events is provided in Table E-2. The sensitivity analysis to the in-channel Manning's n values on the results of the 200-year peak discharge resulted in two additional scenarios, as detailed in Section E.8.

Table E-2. Modelled scenarios.

Scenario	Discharge at Downstream Boundary (m^3/s)		Dike Breach
	Salmo River	Erie Creek	
20-year flow	475	85	No
50-year flow	530	100	No
200-year flow	605	130	No
200-year (+10% Manning's n)	605	130	No
200-year flow (-10% Manning's n)	605	130	No
500-year flow	650	150	No

E.8. SENSITIVITY ANALYSIS

A sensitivity analysis to Manning's n was performed to address the limitations of an uncalibrated model. For the 200-year flood event, two additional scenarios were run: one where a 10% increase was applied to the in-channel's Manning's n value (n=0.039), and a second where the in-channel's Manning's n value was decreased by 10% (n=0.032).

When the value of Manning's n was increased by 10% the water surface elevation (WSE) was found to increase by 0 to 23 cm along the Salmo River, and 0 to 17 cm along Erie Creek. Similarly, a decrease in the value of Manning's n by 10% resulted in a decrease in WSE of 0 to 23 cm along the Salmo River, and 1 to 14 cm along Erie Creek. The change in the WSE along the channel thalwegs of the Salmo River and Erie Creek are shown in Figure E-21 and Figure E-22, respectively.

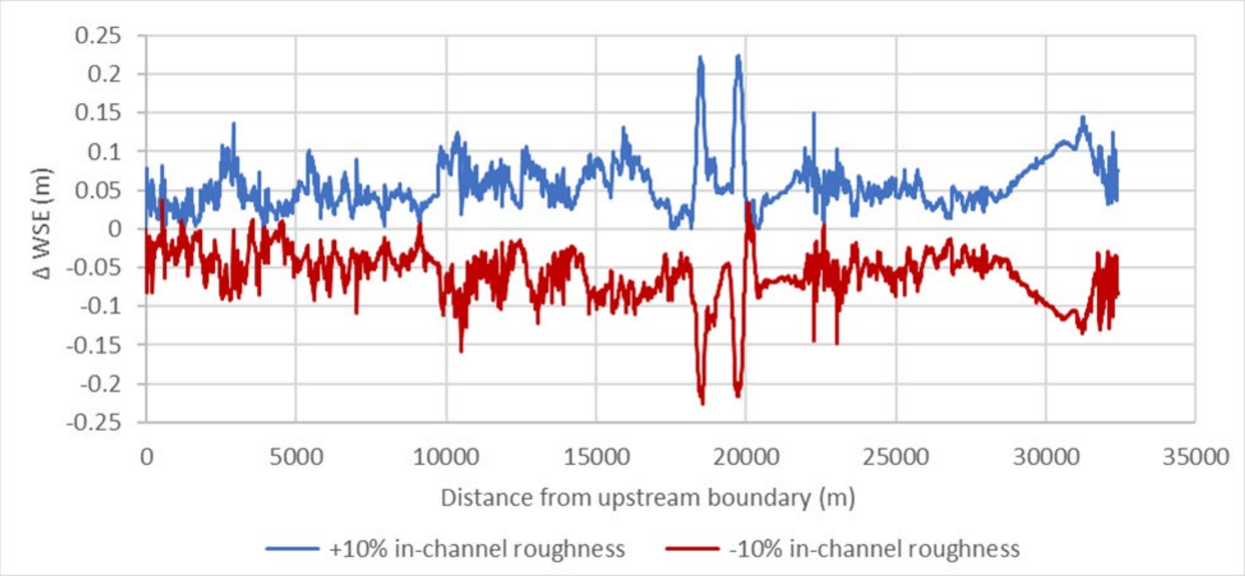

Figure E-21. Change in water surface elevation (WSE) along the channel thalweg of the Salmo River.

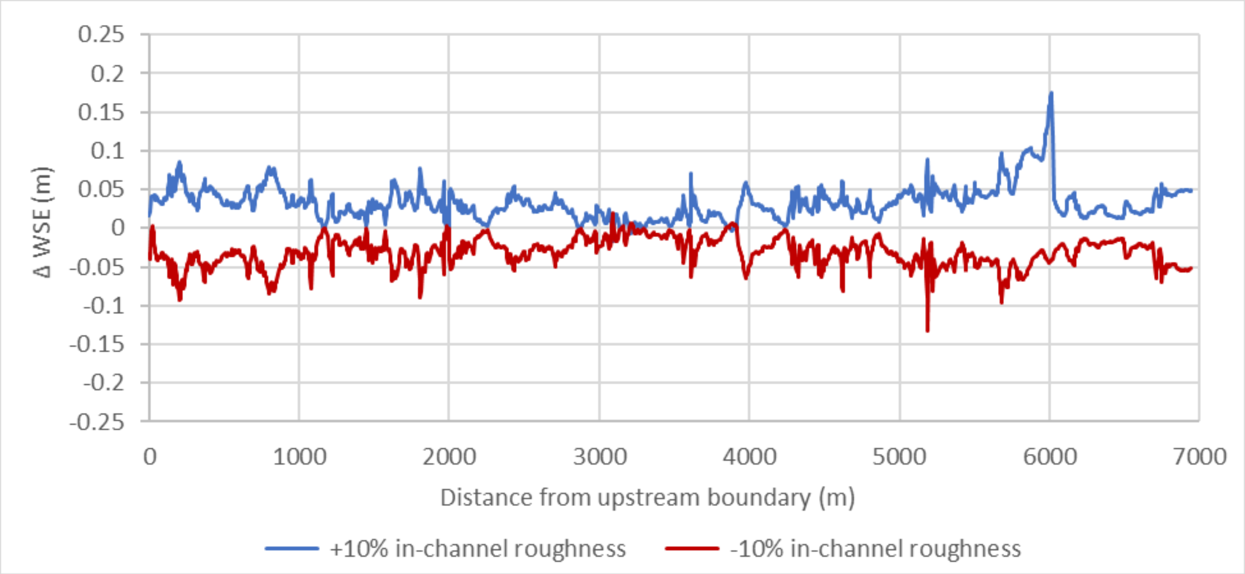

Figure E-22. Change in water surface elevation (WSE) along the channel thalweg of Erie Creek.

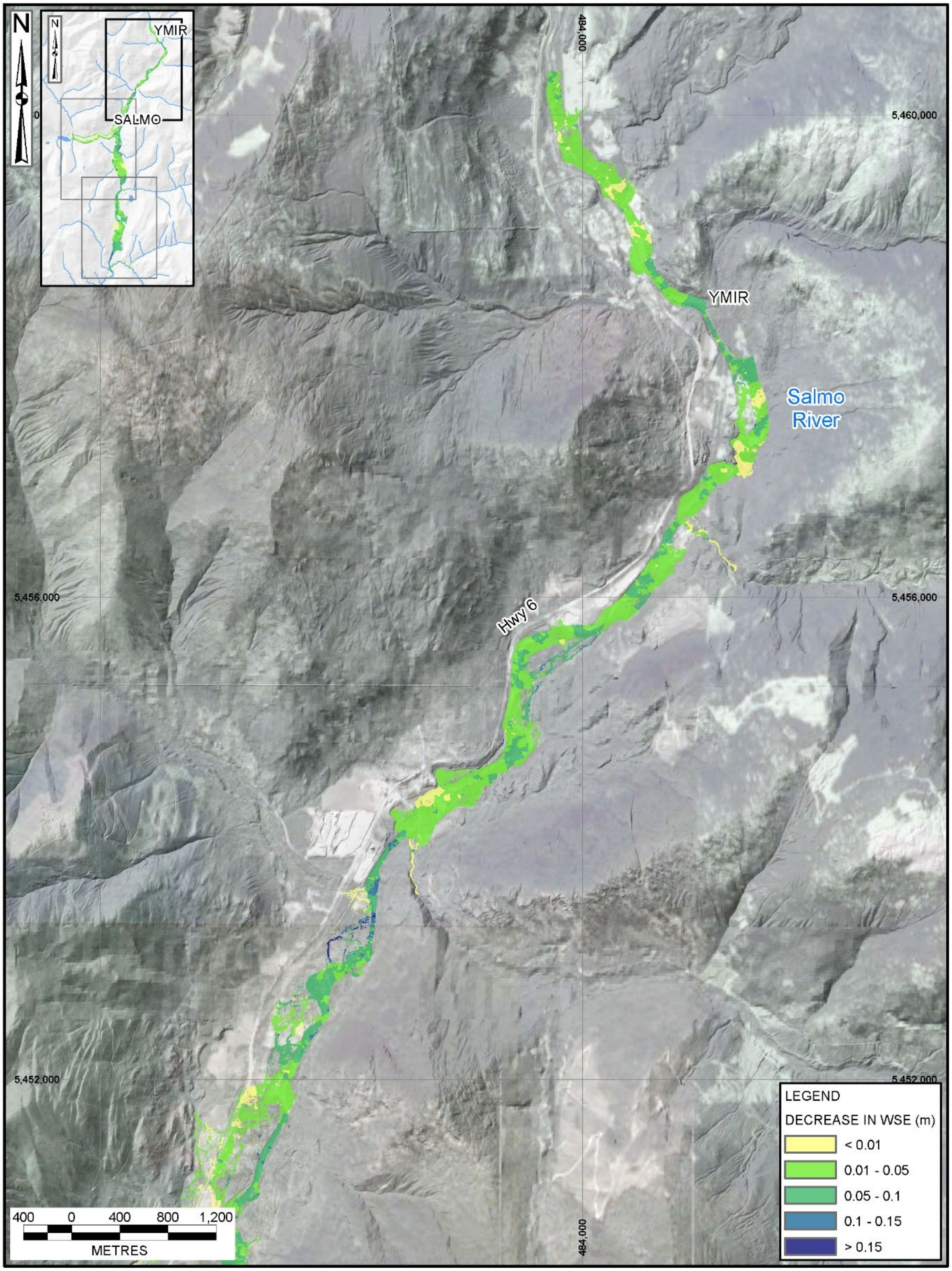

Figure E-23. Change in WSE cause by a 10% decrease in in-channel roughness (Sheet 1 of 3). Coordinate system is NAD83 UTM Zone 11N. Background imagery is a combination of RDCK orthophotos and World Imagery basemap.

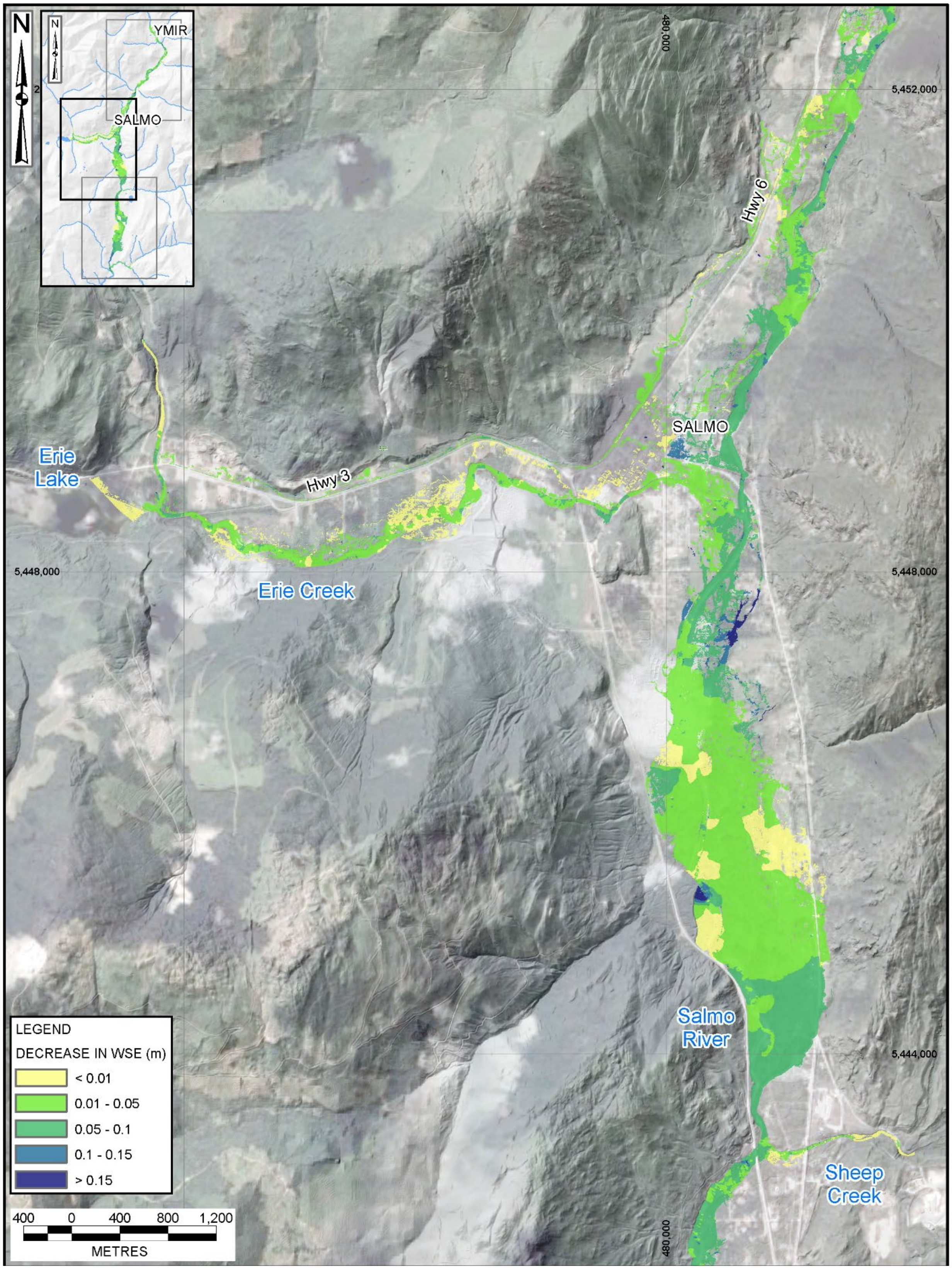

Figure E-24. Change in WSE cause by a 10% decrease in in-channel roughness (Sheet 2 of 3).

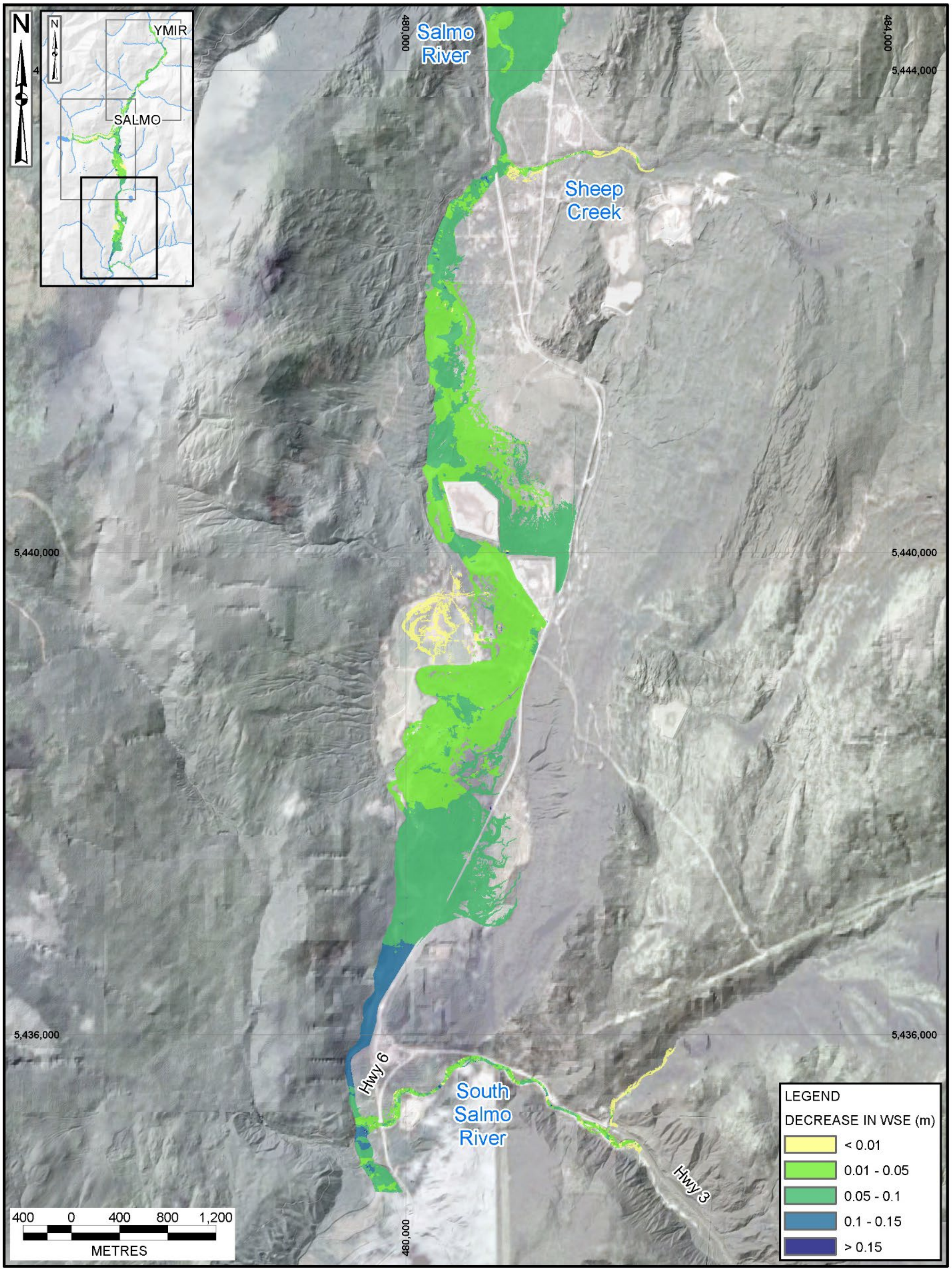

Figure E-25. Change in WSE cause by a 10% decrease in in-channel roughness (Sheet 3 of 3).

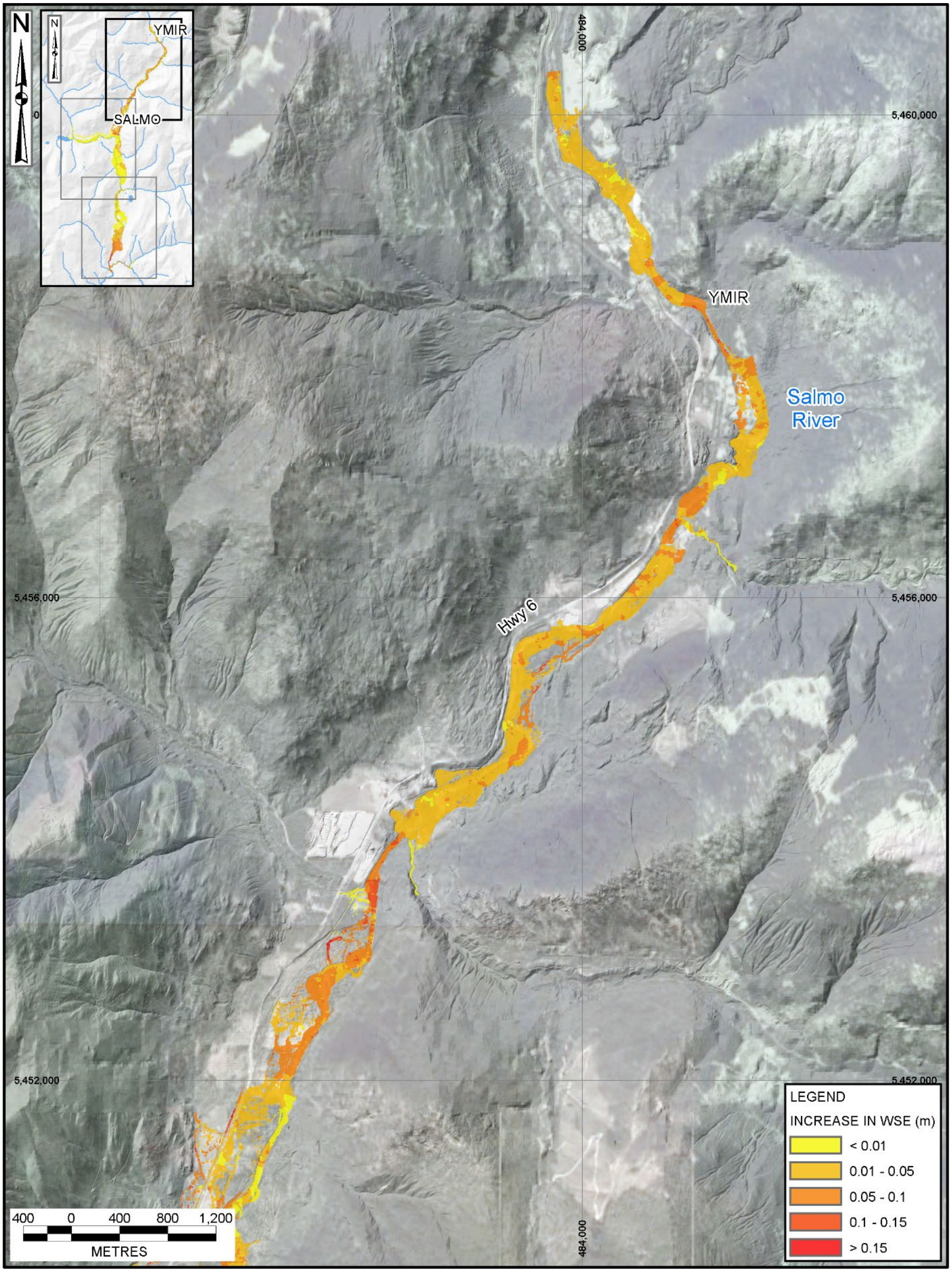

Figure E-26. Change in WSE cause by a 10% increase in in-channel roughness (Sheet 1 of 3).

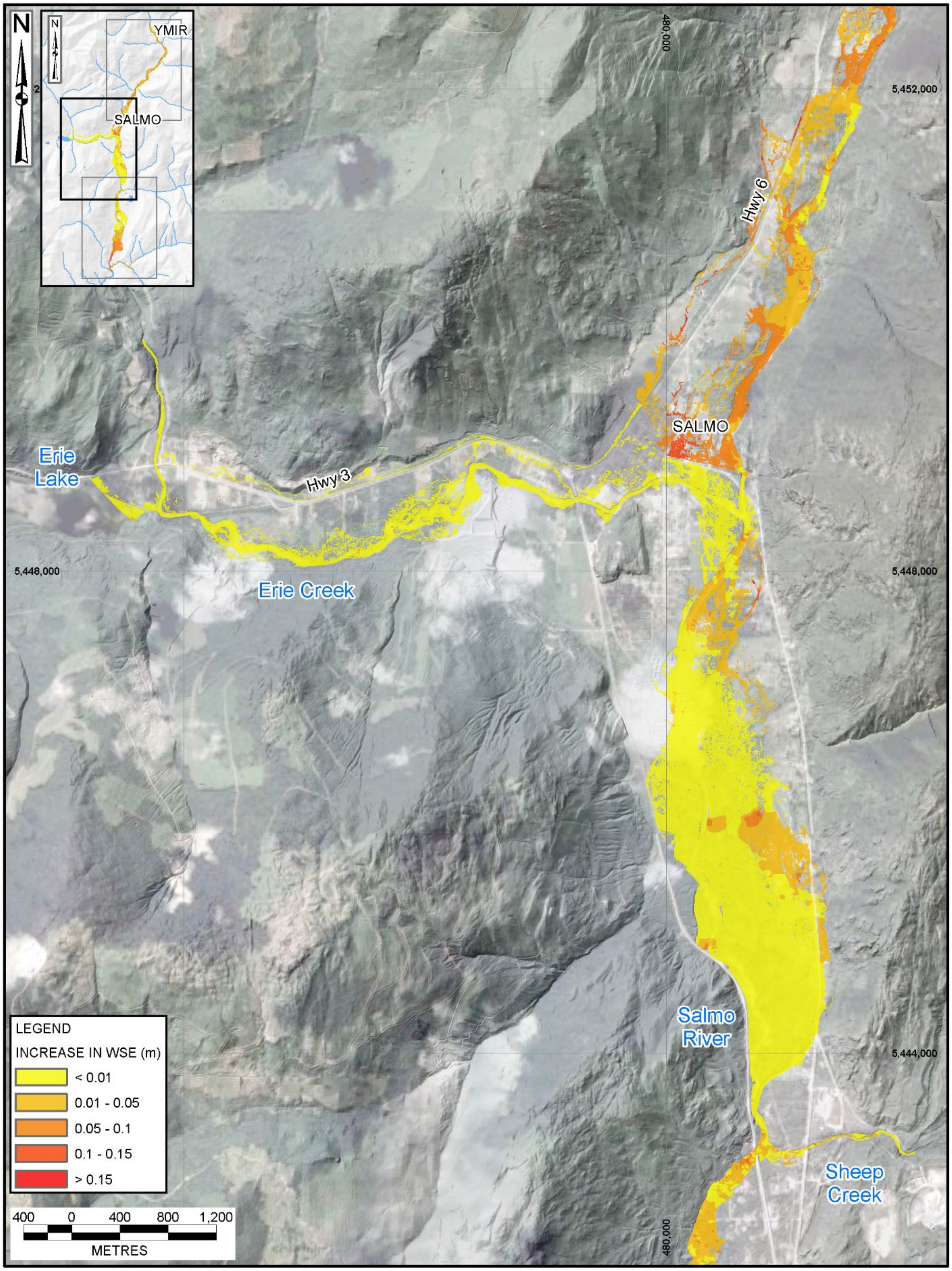

Figure E-27. Change in WSE cause by a 10% increase in in-channel roughness (Sheet 2 of 3).

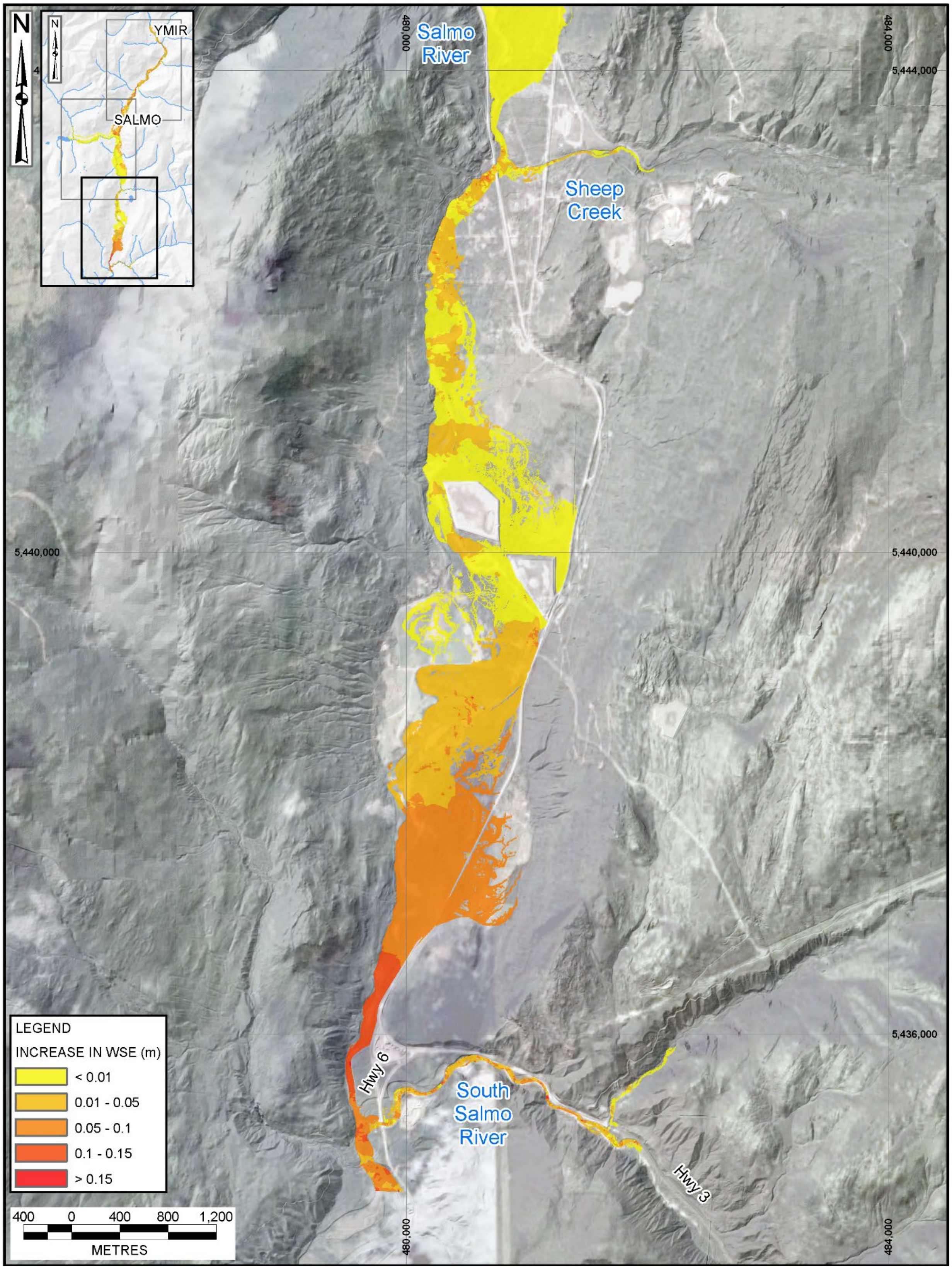

Figure E-28. Change in WSE cause by a 10% increase in in-channel roughness (Sheet 3 of 3).

REFERENCES

Boyer, D. (2009). *Orphan Flood Protection Works*. Letter addressed to Ramona Mattix, Manager of Development Services RDCK. March 24, 2009.

British Columbia Ministry of Environment (BC MoE), Water Management Branch. (1981, May). *Salmo River - Flood Protection*.

Brunner, G.W. & CEIWR-HEC. (2016). *HEC-RAS River Analysis System 2D Modeling User's Manual*. Retrieved from www.hec.usace.army.mil

Chow, V.T. (1959). *Open-channel hydraulics.* New York, McGraw-Hill, 680 p.

Jarrett, R.D. (1984). Hydraulics of high-gradient streams. *American Society of Civil Engineers, Journal of Hydraulic Engineering, 110*(HY11), 1519-1539.

Natural *Resources Canada (NRCan). (2019,* November 28). 2015 land cover of Canada – Landsat-8 [Data]. Resolution 30-metre. Retrieved from https://www.nrcan.gc.ca/science-and-data/science-and-research/earth-sciences/geography/topographic-information/whats-new/2015-land-cover-canada-landsat-8-30-metre-resolution-now-available/22427.

DRAWINGS

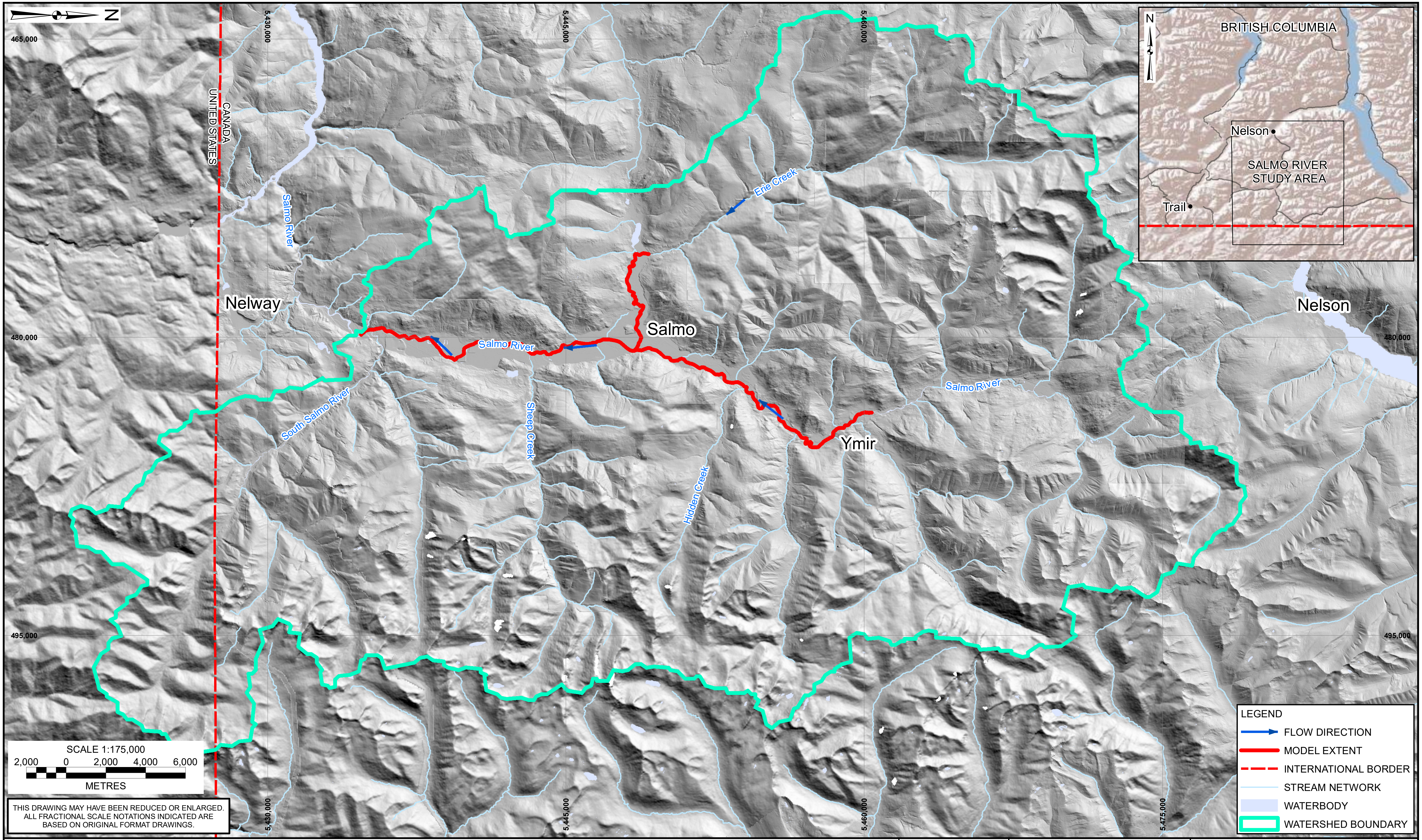

LEGEND
- FLOW DIRECTION
- MODEL EXTENT
- INTERNATIONAL BORDER
- STREAM NETWORK
- WATERBODY
- WATERSHED BOUNDARY

THIS DRAWING MAY HAVE BEEN REDUCED OR ENLARGED. ALL FRACTIONAL SCALE NOTATIONS INDICATED ARE BASED ON ORIGINAL FORMAT DRAWINGS.

NOTES:
1. ALL DIMENSIONS ARE IN METRES UNLESS OTHERWISE NOTED.
2. THIS DRAWING MUST BE READ IN CONJUNCTION WITH BGC'S REPORT TITLED "RDCK FLOODPLAIN AND STEEP CREEK STUDY - SALMO RIVER ", AND DATED MARCH 2020.
3. WHERE AVAILABLE, BASE TOPOGRAPHIC DATA BASED ON LIDAR PROVIDED BY REGIONAL DISTRICT OF CENTRAL KOOTENAY, DATED 2018 AND DISPLAYED AS A HILLSHADE. IF LIDAR WAS NOT AVAILABLE, BASE TOPOGRAPHIC DATA BASED ON SRTM DATA FROM 2018.
4. COORDINATE SYSTEM IS NAD83 CSRS UTM zone 11N.
5. UNLESS BGC AGREES OTHERWISE IN WRITING, THIS DRAWING SHALL NOT BE MODIFIED OR USED FOR ANY PURPOSE OTHER THAN THE PURPOSE FOR WHICH BGC GENERATED IT.
BGC SHALL HAVE NO LIABILITY FOR ANY DAMAGES OR LOSS ARISING IN ANY WAY FROM ANY USE OR MODIFICATION OF THIS DOCUMENT NOT AUTHORIZED BY BGC.
ANY USE OF OR RELIANCE UPON THIS DOCUMENT OR ITS CONTENT BY THIRD PARTIES SHALL BE AT SUCH THIRD PARTIES' SOLE RISK.

SCALE: 1:175,000
DATE: MAR 2020
DRAWN: MW
CHECKED: PS
APPROVED: RM

BGC ENGINEERING INC.
AN APPLIED EARTH SCIENCES COMPANY

CLIENT: REGIONAL DISTRICT CENTRAL KOOTENAY

PROJECT: RDCK FLOODPLAIN AND STEEP CREEK STUDY
SALMO RIVER

TITLE: SITE LOCATION MAP

PROJECT No.: 0268-007
DWG No.: 01

X:\Projects\0268\007_RDCK_NDMP_Stream_2_Support\GIS\Production\Report\20191030_RDCK_Floodplain_And_SC_Study_CLEARWATER\SalmoRiver\FINAL_COPIES\01_SalmoRiverSiteLocationMap.mxd Date: April 20, 2020 Time: 10:40 AM

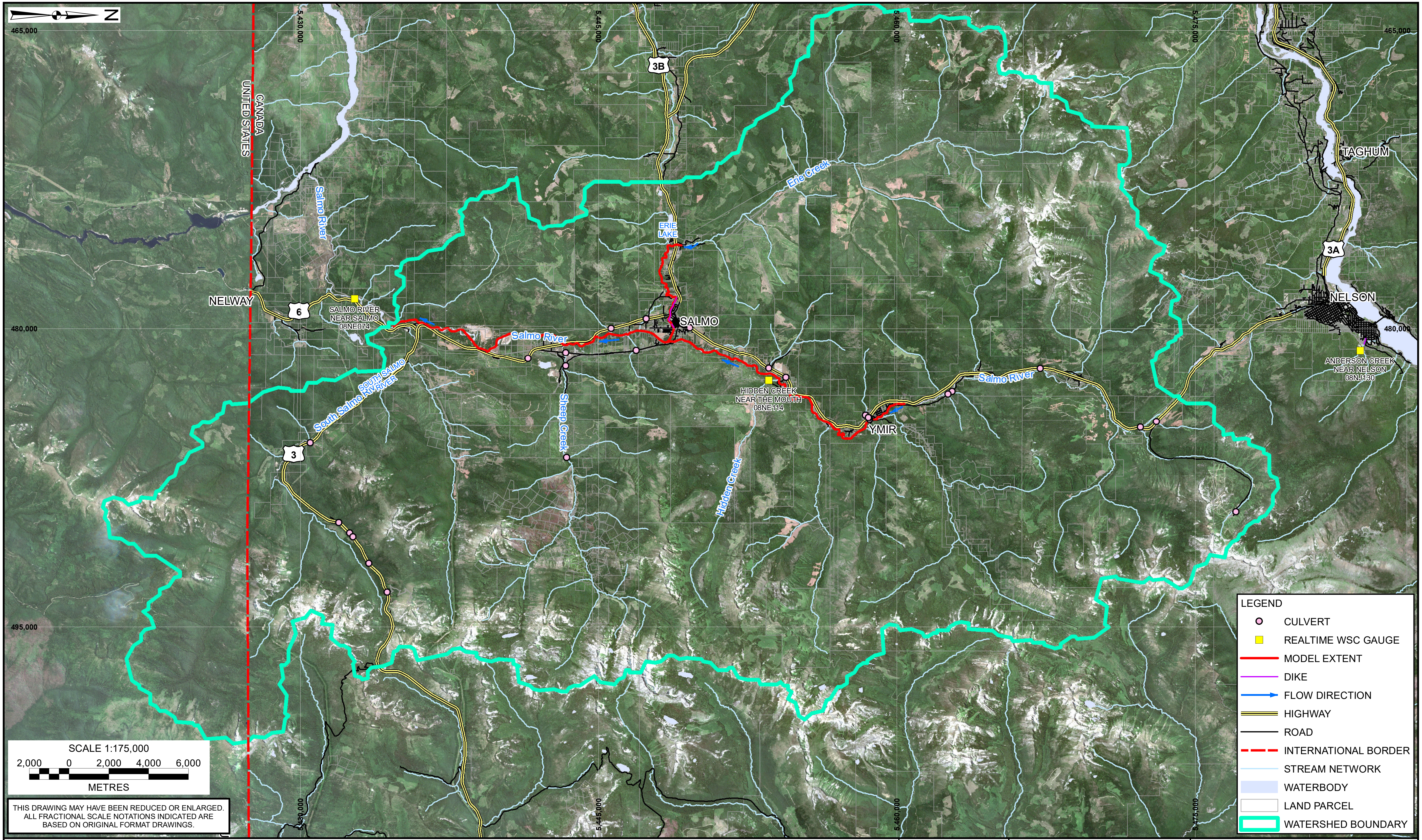

THIS DRAWING MAY HAVE BEEN REDUCED OR ENLARGED.
ALL FRACTIONAL SCALE NOTATIONS INDICATED ARE
BASED ON ORIGINAL FORMAT DRAWINGS.

NOTES:
1. ALL DIMENSIONS ARE IN METRES UNLESS OTHERWISE NOTED.
2. THIS DRAWING MUST BE READ IN CONJUNCTION WITH BGC'S REPORT TITLED "RDCK FLOODPLAIN AND STEEP CREEK STUDY - SALMO RIVER ", AND DATED MARCH 2020.
3. BASE IMAGERY SOURCED FROM SENTINEL 2 MISSION, DATED AUGUST 2019.
4. COORDINATE SYSTEM IS NAD83 CSRS UTM zone 11N.
5. DIKE LOCATIONS FROM FLOOD AND PROTECTION WORKS: STRUCTURAL WORKS DATASET PROVIDED BY BC MFLNRO (2017).
6. UNLESS BGC AGREES OTHERWISE IN WRITING, THIS DRAWING SHALL NOT BE MODIFIED OR USED FOR ANY PURPOSE
OTHER THAN THE PURPOSE FOR WHICH BGC GENERATED IT. BGC SHALL HAVE NO LIABILITY FOR ANY DAMAGES OR LOSS
ARISING IN ANY WAY FROM ANY USE OR MODIFICATION OF THIS DOCUMENT NOT AUTHORIZED BY BGC. ANY USE OF OR
RELIANCE UPON THIS DOCUMENT OR ITS CONTENT BY THIRD PARTIES SHALL BE AT SUCH THIRD PARTIES' SOLE RISK.

SCALE:	1:175,000
DATE:	MAR 2020
DRAWN:	MW
CHECKED:	PS
APPROVED:	RM

BGC ENGINEERING INC.
AN APPLIED EARTH SCIENCES COMPANY

CLIENT:

PROJECT: RDCK FLOODPLAIN AND STEEP CREEK STUDY
SALMO RIVER

TITLE:
STUDY OVERVIEW MAP

PROJECT No.:	DWG No:
0268-007	02

X:\Projects\0268\007_RDCK_NDMP_Stream_2_Support\GIS\Production\Report\20191030_RDCK_Floodplain_And_SC_Study_CLEARWATER\SalmoRiver\FINAL_COPIES\02_SalmoRiverSiteWatershedMap.mxd Date: April 20, 2020 Time: 10:40 AM

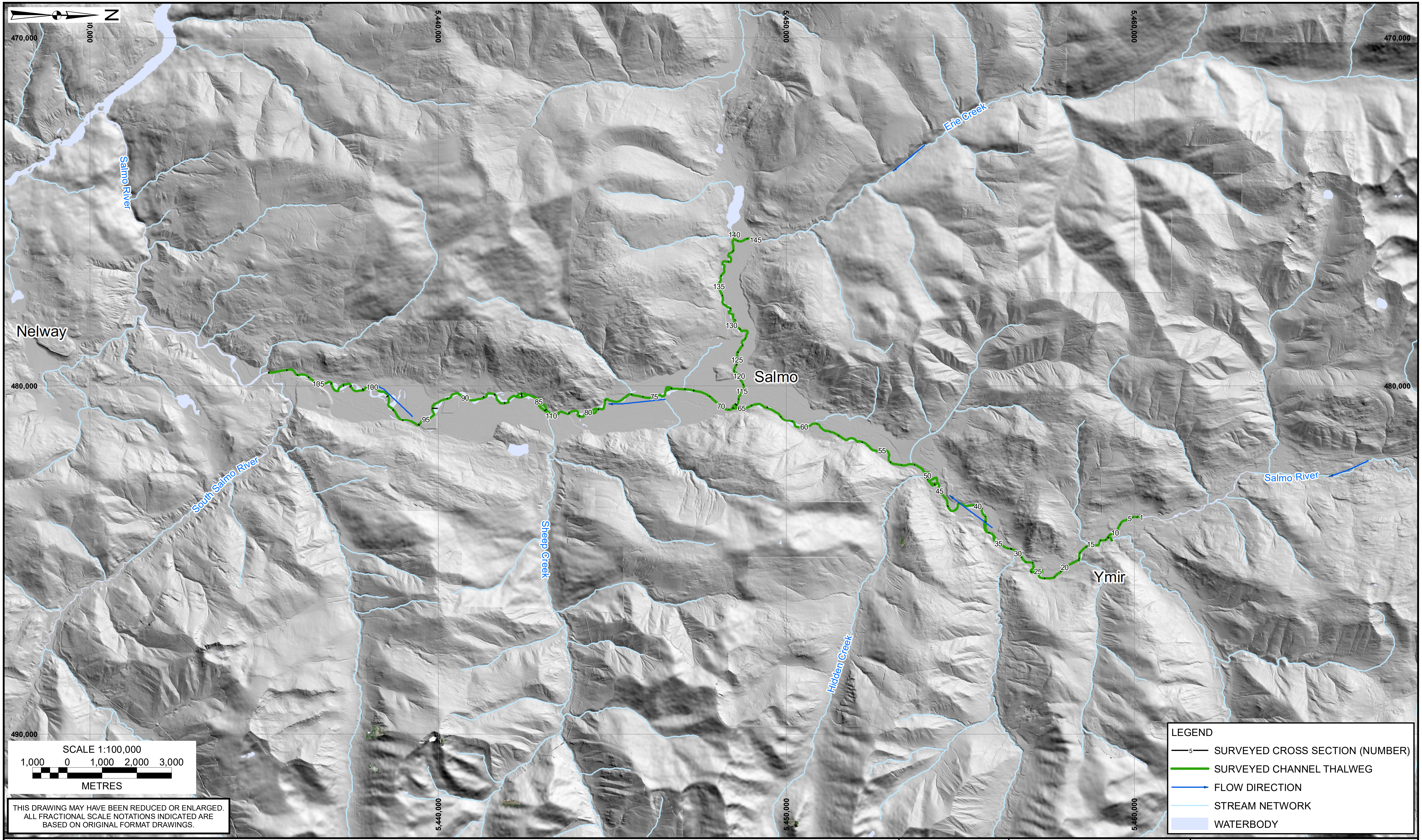

THIS DRAWING MAY HAVE BEEN REDUCED OR ENLARGED.
ALL FRACTIONAL SCALE NOTATIONS INDICATED ARE
BASED ON ORIGINAL FORMAT DRAWINGS.

LEGEND

—5—	SURVEYED CROSS SECTION (NUMBER)
🟩	SURVEYED CHANNEL THALWEG
→	FLOW DIRECTION
—	STREAM NETWORK
▨	WATERBODY

NOTES:
1. ALL DIMENSIONS ARE IN METRES UNLESS OTHERWISE NOTED.
2. THIS DRAWING MUST BE READ IN CONJUNCTION WITH BGC'S REPORT TITLED "RDCK FLOODPLAIN AND STEEP CREEK STUDY - SALMO RIVER ", AND DATED MARCH 2020.
3. WHERE AVAILABLE, BASE TOPOGRAPHIC DATA BASED ON LIDAR PROVIDED BY REGIONAL DISTRICT OF CENTRAL KOOTENAY, DATED 2018 AND DISPLAYED AS A HILLSHADE. IF LIDAR WAS NOT AVAILABLE, BASE TOPOGRAPHIC DATA BASED ON SRTM DATA FROM 2018.
4. COORDINATE SYSTEM IS NAD 1983 CSRS UTM Zone 11N.
5. UNLESS BGC AGREES OTHERWISE IN WRITING, THIS DRAWING SHALL NOT BE MODIFIED OR USED FOR ANY PURPOSE OTHER THAN THE PURPOSE FOR WHICH BGC GENERATED IT.
BGC SHALL HAVE NO LIABILITY FOR ANY DAMAGES OR LOSS ARISING IN ANY WAY FROM ANY USE OR MODIFICATION OF THIS DOCUMENT NOT AUTHORIZED BY BGC.
ANY USE OF OR RELIANCE UPON THIS DOCUMENT OR ITS CONTENT BY THIRD PARTIES SHALL BE AT SUCH THIRD PARTIES' SOLE RISK.

SCALE: 1:100,000
DATE: MAR 2020
DRAWN: MW
CHECKED: PS
APPROVED: RM

BGC ENGINEERING INC.
AN APPLIED EARTH SCIENCES COMPANY

CLIENT: REGIONAL DISTRICT CENTRAL KOOTENAY

PROJECT: RDCK FLOODPLAIN AND STEEP CREEK STUDY
SALMO RIVER

TITLE: SURVEY LOCATION MAP

PROJECT No.: 0268-007
DWG No: 03

X:\Projects\0268\007_RDCK_NDMP_Stream_2_Support\GIS\Production\Report\20191030_RDCK_Floodplain_And_SC_Study_CLEARWATER\SalmoRiver\FINAL_COPIES\03_SalmoRiverSurveyLocations.mxd Date: April 20, 2020 Time: 10:44 AM

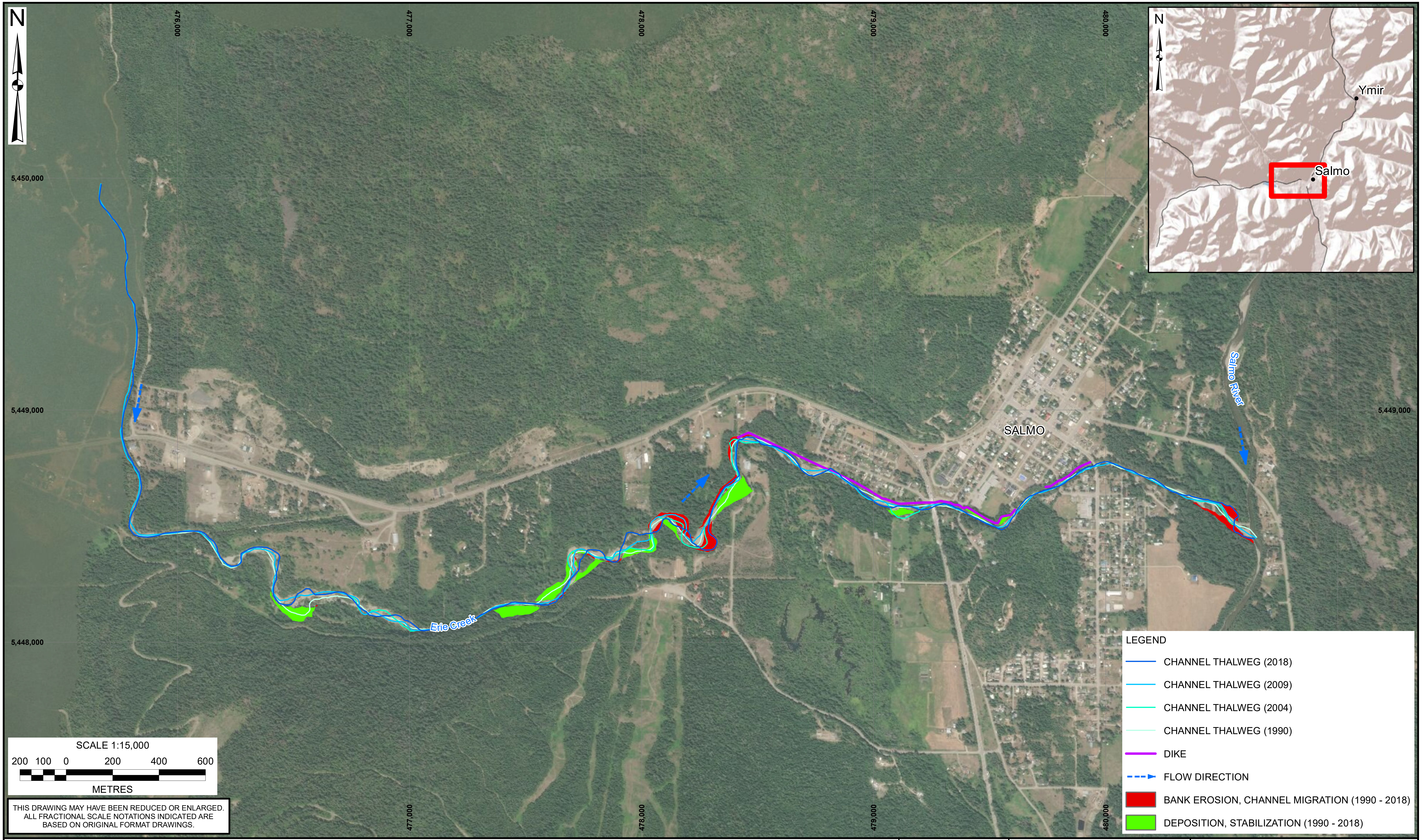

THIS DRAWING MAY HAVE BEEN REDUCED OR ENLARGED.
ALL FRACTIONAL SCALE NOTATIONS INDICATED ARE
BASED ON ORIGINAL FORMAT DRAWINGS.

NOTES:
1. ALL DIMENSIONS ARE IN METRES UNLESS OTHERWISE NOTED.
2. THIS DRAWING MUST BE READ IN CONJUNCTION WITH BGC'S REPORT TITLED "RDCK FLOODPLAIN AND STEEP CREEK STUDY - SALMO RIVER", AND DATED MARCH 2020.
3. BASE IMAGERY SOURCE REFERENCED IN TABLE 4-2 OF REPORT.
4. COORDINATE SYSTEM IS NAD 1983 CSRS UTM ZONE 11N.
5. CHANGE DETECTION CRITERIA DESCRIBED IN TABLE 4-5 OF REPORT. HISTORICAL THALWEGS INTERPRETED FROM PHOTOGRAPHS AND MANUALLY DIGITIZED.
6. UNLESS BGC AGREES OTHERWISE IN WRITING, THIS DRAWING SHALL NOT BE MODIFIED OR USED FOR ANY PURPOSE OTHER THAN THE PURPOSE FOR WHICH BGC GENERATED IT. BGC SHALL HAVE NO LIABILITY FOR ANY DAMAGES OR LOSS ARISING IN ANY WAY FROM ANY USE OR MODIFICATION OF THIS DOCUMENT NOT AUTHORIZED BY BGC. ANY USE OF OR RELIANCE UPON THIS DOCUMENT OR ITS CONTENT BY THIRD PARTIES SHALL BE AT SUCH THIRD PARTIES' SOLE RISK.

SCALE:	1:15,000
DATE:	MAR 2020
DRAWN:	MW
CHECKED:	ES/VC
APPROVED:	PS

BGC ENGINEERING INC.
AN APPLIED EARTH SCIENCES COMPANY

CLIENT:
REGIONAL DISTRICT CENTRAL KOOTENAY

PROJECT: RDCK FLOODPLAIN AND STEEP CREEK STUDY
SALMO RIVER

TITLE: HISTORICAL CHANNEL CHANGE
ERIE CREEK

PROJECT No.: 0268-007

DWG No: 04

X:\Projects\0268\007_RDCK_NDMP_Stream_2_Support\GIS\Production\Report\20191030_RDCK_Floodplain_And_SC_Study_CLEARWATER\SalmoRiver\FINAL_COPIES\04_ErieCreekHistoricalChannelChange.mxd Date: April 20, 2020 Time: 11:47 AM

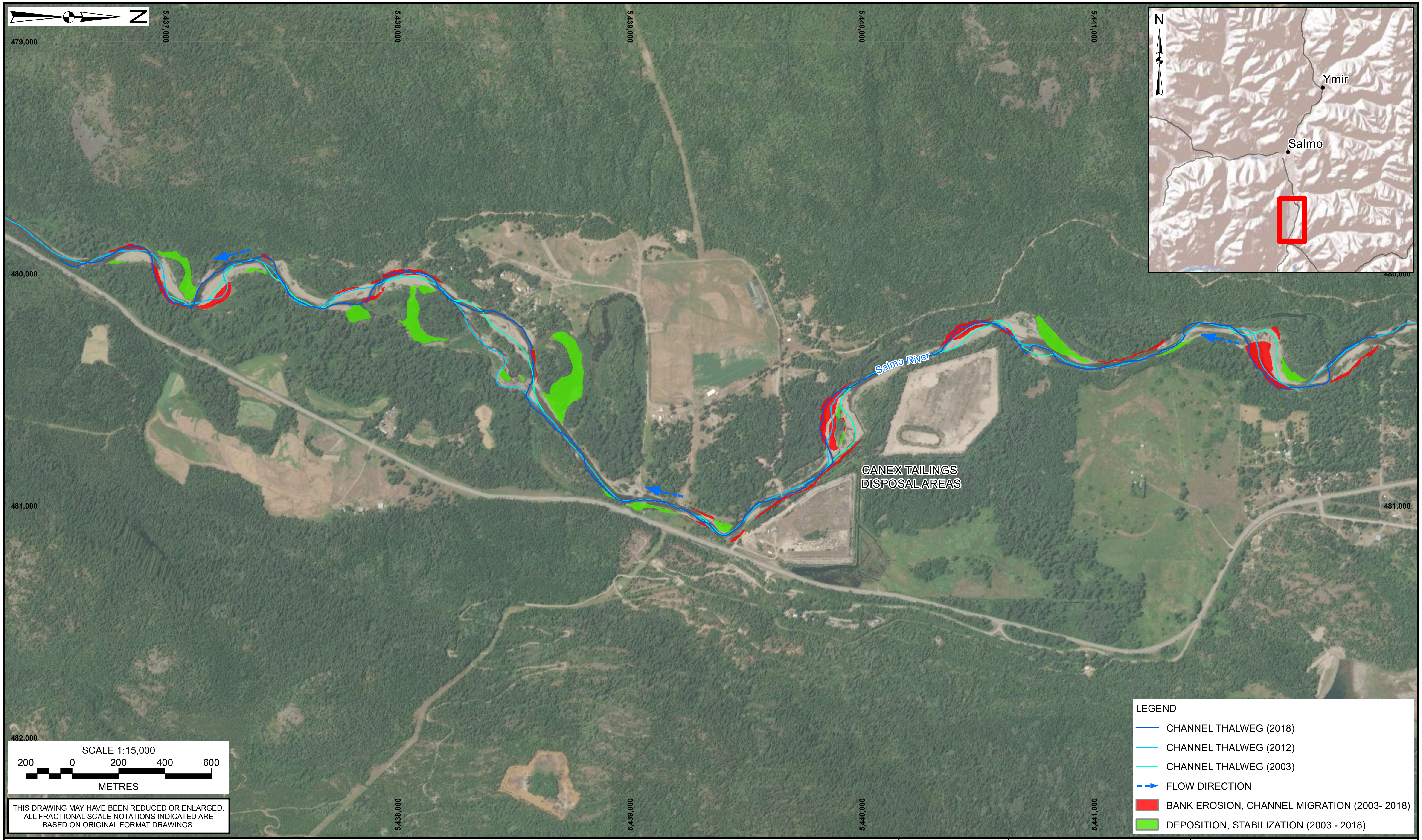

THIS DRAWING MAY HAVE BEEN REDUCED OR ENLARGED.
ALL FRACTIONAL SCALE NOTATIONS INDICATED ARE
BASED ON ORIGINAL FORMAT DRAWINGS.

NOTES:
1. ALL DIMENSIONS ARE IN METRES UNLESS OTHERWISE NOTED.
2. THIS DRAWING MUST BE READ IN CONJUNCTION WITH BGC'S REPORT TITLED "RDCK FLOODPLAIN AND STEEP CREEK STUDY - SALMO RIVER", AND DATED MARCH 2020.
3. BASE IMAGERY SOURCE REFERENCED IN TABLE 4-2 OF REPORT.
4. COORDINATE SYSTEM IS NAD 1983 CSRS UTM Zone 11N.
5. CHANGE DETECTION CRITERIA DESCRIBED IN TABLE 4-5 OF REPORT. HISTORICAL THALWEGS INTERPRETED FROM PHOTOGRAPHS AND MANUALLY DIGITIZED.
6. UNLESS BGC AGREES OTHERWISE IN WRITING, THIS DRAWING SHALL NOT BE MODIFIED OR USED FOR ANY PURPOSE OTHER THAN THE PURPOSE FOR WHICH BGC GENERATED IT. BGC SHALL HAVE NO LIABILITY FOR ANY DAMAGES OR LOSS ARISING IN ANY WAY FROM ANY USE OR MODIFICATION OF THIS DOCUMENT NOT AUTHORIZED BY BGC. ANY USE OF OR RELIANCE UPON THIS DOCUMENT OR ITS CONTENT BY THIRD PARTIES SHALL BE AT SUCH THIRD PARTIES' SOLE RISK.

SCALE:	1:15,000
DATE:	MAR 2020
DRAWN:	MW
CHECKED:	ES/VC
APPROVED:	PS

BGC ENGINEERING INC.
AN APPLIED EARTH SCIENCES COMPANY

CLIENT:
REGIONAL DISTRICT CENTRAL KOOTENAY

PROJECT:
RDCK FLOODPLAIN AND STEEP CREEK STUDY
SALMO RIVER

TITLE:
HISTORICAL CHANNEL CHANGE
SALMO RIVER SOUTH SECTION

PROJECT No.: 0268-007
DWG No.: 05

X:\Projects\0268\007_RDCK_NDMP_Stream_2_Support\GIS\Production\Report\20191030_RDCK_Floodplain_And_SC_Study_CLEARWATER\SalmoRiver\FINAL_COPIES\05_SouthSalmoRiverHistoricalChannelChange.mxd Date: April 20, 2020 Time: 11:49 AM

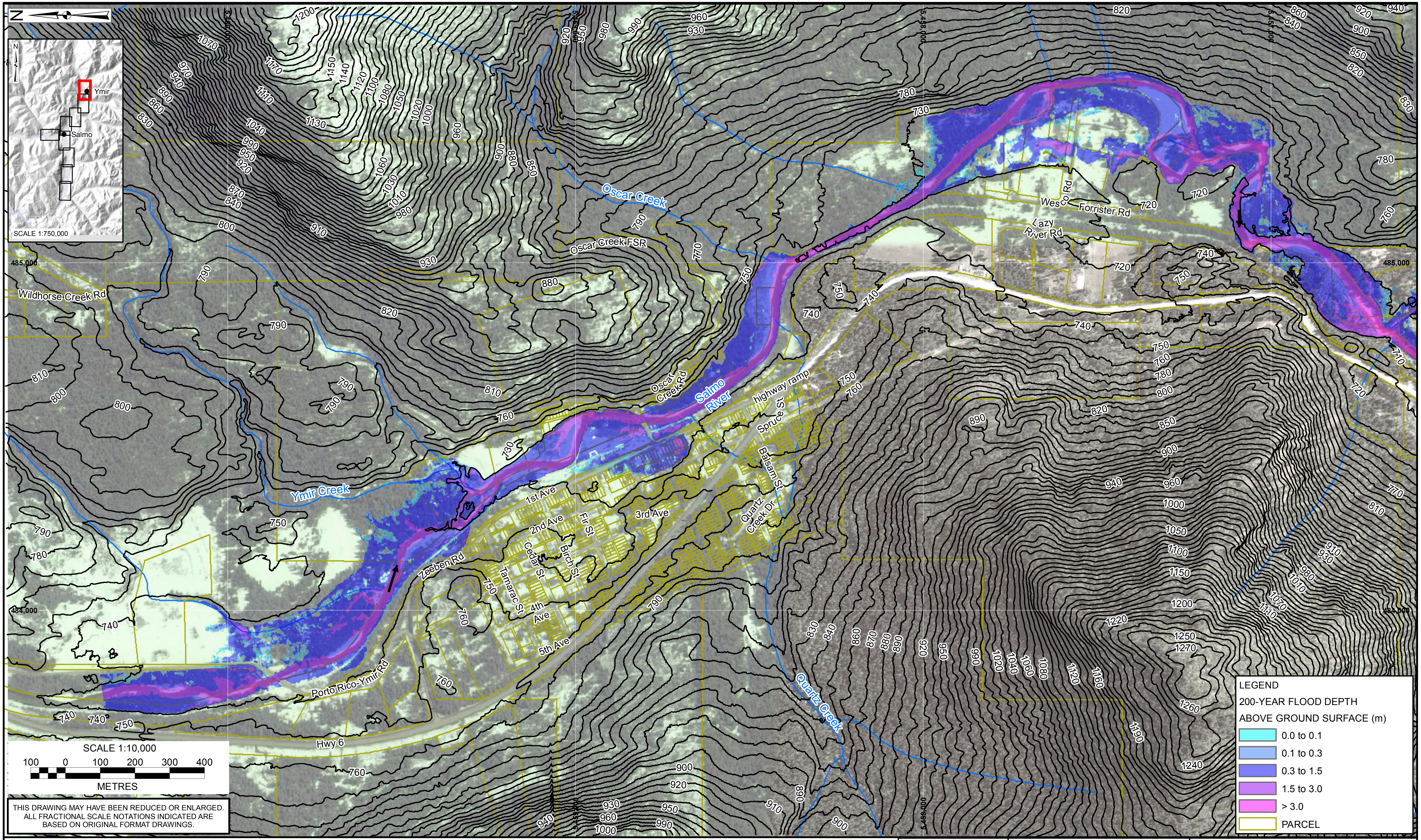

THIS DRAWING MAY HAVE BEEN REDUCED OR ENLARGED. ALL FRACTIONAL SCALE NOTATIONS INDICATED ARE BASED ON ORIGINAL FORMAT DRAWINGS.

NOTES:
1. ALL DIMENSIONS ARE IN METRES UNLESS OTHERWISE NOTED.
2. THIS DRAWING MUST BE READ IN CONJUNCTION WITH BGC'S REPORT TITLED "RDCK FLOODPLAIN AND STEEP CREEK STUDY SALMO RIVER", AND DATED MARCH 2020.
3. BASE TOPOGRAPHIC DATA BASED ON LIDAR PROVIDED BY RDCK DATED 2017 AND 2018. CONTOUR INTERVAL IS 10 m. IMAGERY FROM GOOGLE EARTH.PARCEL DATA FROM PARCELMAP BC. DIKE DATA FROM DATA BC. FLOOD DEPTH BASED ON THE 200-YEAR FLOOD USING THE INSTANTANEOUS PEAK DISCHARGE ADJUSTED FOR CLIMATE CHANGE
4. PROJECTION IS NAD 1983 UTM ZONE 11N. VERTICAL DATUM IS CGVD2013.
5. UNLESS BGC AGREES OTHERWISE IN WRITING, THIS DRAWING SHALL NOT BE MODIFIED OR USED FOR ANY PURPOSE OTHER THAN THE PURPOSE FOR WHICH BGC GENERATED IT. BGC SHALL HAVE NO LIABILITY FOR ANY DAMAGES OR LOSS ARISING IN ANY WAY FROM ANY USE OR MODIFICATION OF THIS DOCUMENT NOT AUTHORIZED BY BGC. ANY USE OF OR RELIANCE UPON THIS DOCUMENT OR ITS CONTENT BY THIRD PARTIES SHALL BE AT SUCH THIRD PARTIES' SOLE RISK.

SCALE:	1:10,000
DATE:	MAR 2020
DRAWN:	LL
CHECKED:	PG, PS
APPROVED:	RM

BGC ENGINEERING INC.
AN APPLIED EARTH SCIENCES COMPANY

CLIENT:
REGIONAL DISTRICT OF CENTRAL KOOTENAY

PROJECT:
RDCK FLOODPLAIN AND STEEP CREEK STUDY
SALMO RIVER

TITLE:
200-YEAR FLOOD HAZARD
(SHEET 01 OF 9)

PROJECT No.:	DWG No:
0268 007	06

X:\Projects\0268007_RDCK_NDMP_Stream_2_Support\GIS\Production\Report\20191218_RDCK_Clearwater_FCL\200-Year Flood_Hazard_DDP.mxd

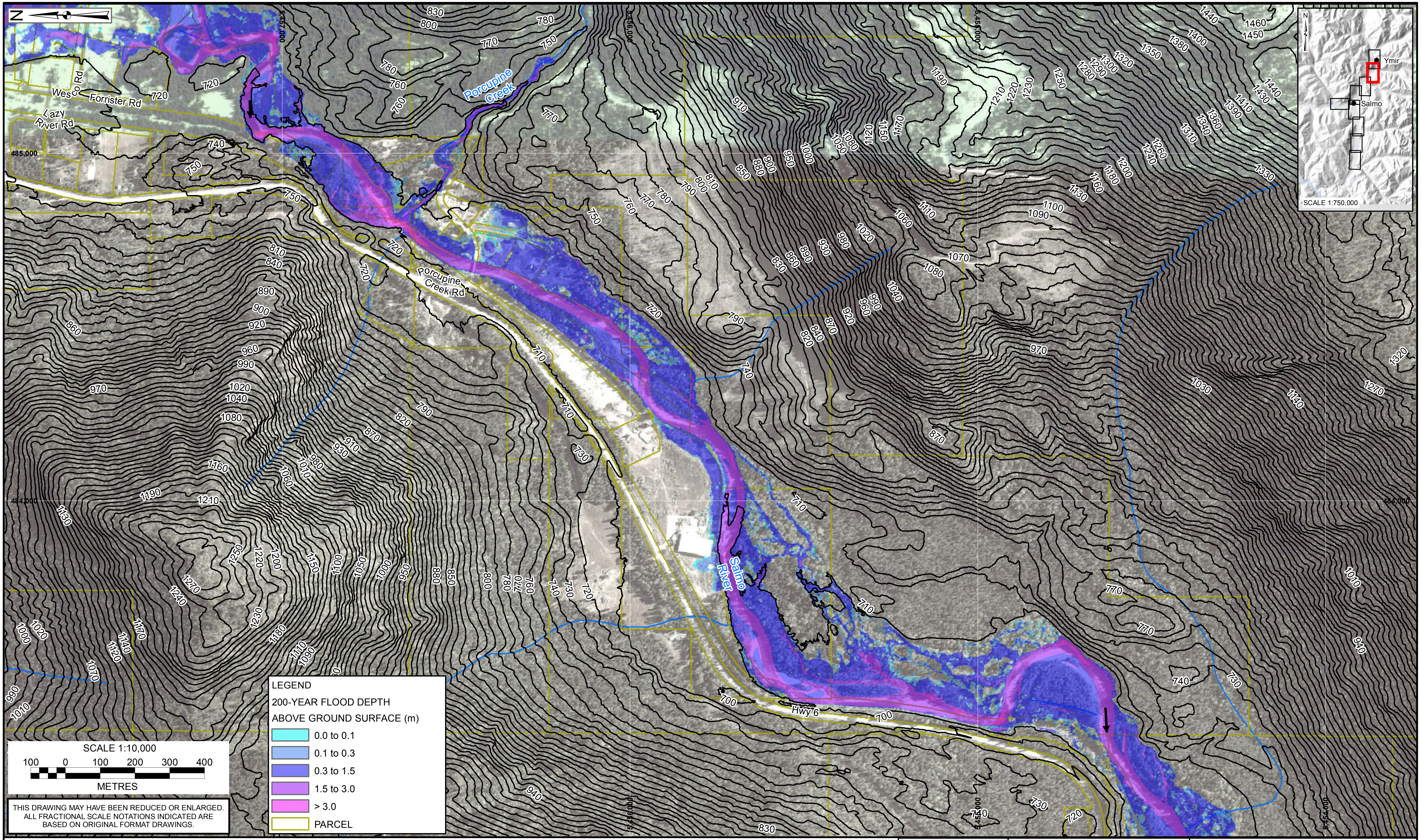

LEGEND

200-YEAR FLOOD DEPTH
ABOVE GROUND SURFACE (m)

🟦	0.0 to 0.1
🟦	0.1 to 0.3
🟦	0.3 to 1.5
🟪	1.5 to 3.0
🟪	> 3.0
☐	PARCEL

THIS DRAWING MAY HAVE BEEN REDUCED OR ENLARGED.
ALL FRACTIONAL SCALE NOTATIONS INDICATED ARE
BASED ON ORIGINAL FORMAT DRAWINGS.

NOTES:
1. ALL DIMENSIONS ARE IN METRES UNLESS OTHERWISE NOTED.
2. THIS DRAWING MUST BE READ IN CONJUNCTION WITH BGC'S REPORT TITLED "RDCK FLOODPLAIN AND STEEP CREEK STUDY SALMO RIVER", AND DATED MARCH 2020.
3. BASE TOPOGRAPHIC DATA BASED ON LIDAR PROVIDED BY RDCK DATED 2017 AND 2018. CONTOUR INTERVAL IS 10 m. IMAGERY FROM GOOGLE EARTH.PARCEL DATA FROM PARCELMAP BC.
DIKE DATA FROM DATA BC. FLOOD DEPTH BASED ON THE 200-YEAR FLOOD USING THE INSTANTANEOUS PEAK DISCHARGE ADJUSTED FOR CLIMATE CHANGE
4. PROJECTION IS NAD 1983 UTM ZONE 11N. VERTICAL DATUM IS CGVD2013.
5. UNLESS BGC AGREES OTHERWISE IN WRITING, THIS DRAWING SHALL NOT BE MODIFIED OR USED FOR ANY PURPOSE OTHER THAN THE PURPOSE FOR WHICH BGC GENERATED IT. BGC SHALL HAVE NO LIABILITY FOR ANY DAMAGES OR LOSS ARISING IN ANY WAY FROM ANY USE OR MODIFICATION OF THIS DOCUMENT NOT AUTHORIZED BY BGC. ANY USE OF OR RELIANCE UPON THIS DOCUMENT OR ITS CONTENT BY THIRD PARTIES SHALL BE AT SUCH THIRD PARTIES' SOLE RISK.

SCALE: 1:10,000
DATE: MAR 2020
DRAWN: LL
CHECKED: PG, PS
APPROVED: RM

BGC ENGINEERING INC.
AN APPLIED EARTH SCIENCES COMPANY

CLIENT:
REGIONAL DISTRICT
CENTRAL KOOTENAY

PROJECT:
RDCK FLOODPLAIN AND STEEP CREEK STUDY
SALMO RIVER

TITLE:
200-YEAR FLOOD HAZARD
(SHEET 02 OF 9)

PROJECT No.: 0268 007
DWG No: 06

X:\Projects\0268\007_RDCK_NDMP_Stream_2_Support\GIS\Production\Report\20191218_RDCK_Clearwater_FCL\200-Year Flood_Hazard_DDP.mxd

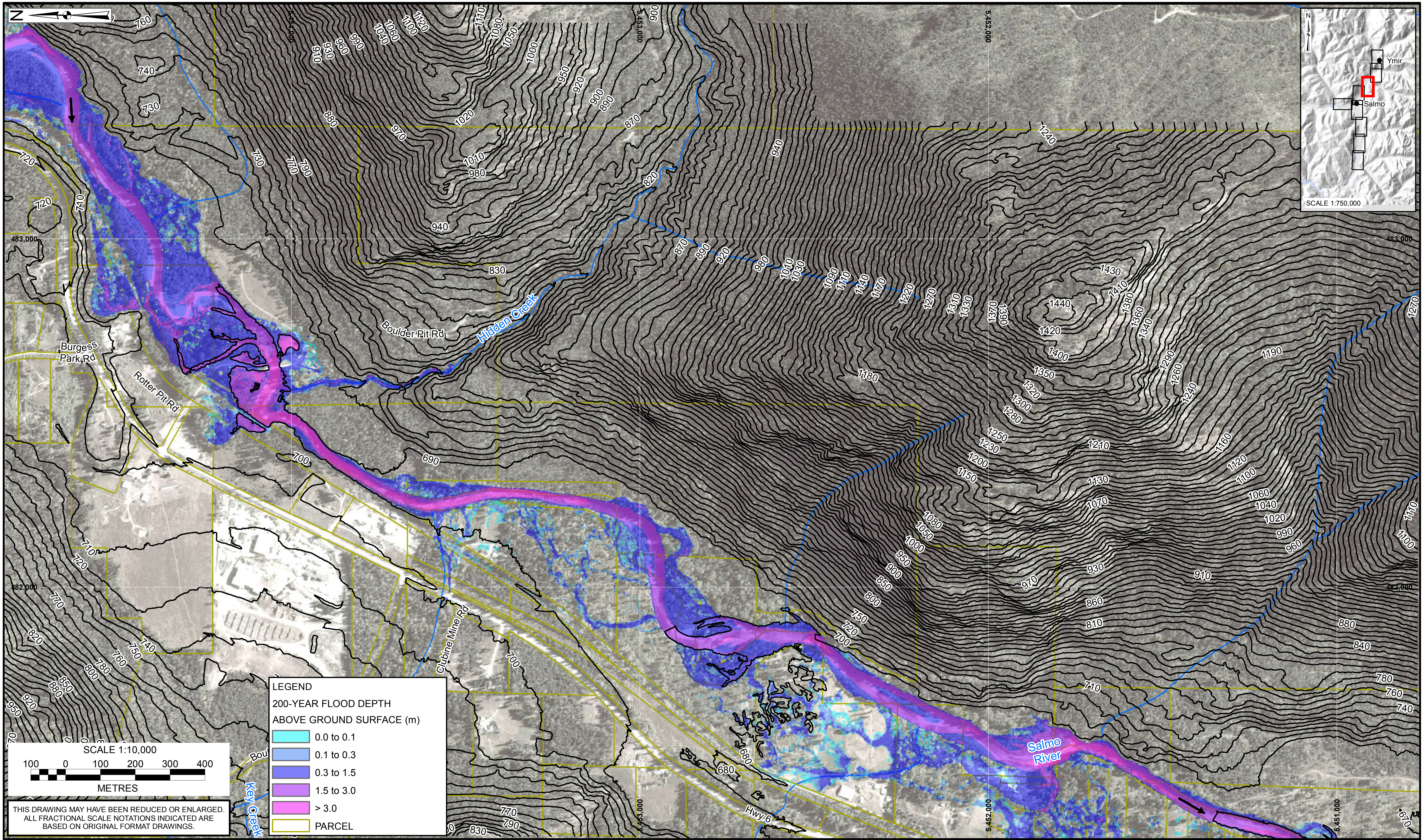

THIS DRAWING MAY HAVE BEEN REDUCED OR ENLARGED. ALL FRACTIONAL SCALE NOTATIONS INDICATED ARE BASED ON ORIGINAL FORMAT DRAWINGS.

NOTES:
1. ALL DIMENSIONS ARE IN METRES UNLESS OTHERWISE NOTED.
2. THIS DRAWING MUST BE READ IN CONJUNCTION WITH BGC'S REPORT TITLED "RDCK FLOODPLAIN AND STEEP CREEK STUDY SALMO RIVER", AND DATED MARCH 2020.
3. BASE TOPOGRAPHIC DATA BASED ON LIDAR PROVIDED BY RDCK DATED 2017 AND 2018. CONTOUR INTERVAL IS 10 m. IMAGERY FROM GOOGLE EARTH.PARCEL DATA FROM PARCELMAP BC. DIKE DATA FROM DATA BC. FLOOD DEPTH BASED ON THE 200-YEAR FLOOD USING THE INSTANTANEOUS PEAK DISCHARGE ADJUSTED FOR CLIMATE CHANGE
4. PROJECTION IS NAD 1983 UTM ZONE 11N. VERTICAL DATUM IS CGVD2013.
5. UNLESS BGC AGREES OTHERWISE IN WRITING, THIS DRAWING SHALL NOT BE MODIFIED OR USED FOR ANY PURPOSE OTHER THAN THE PURPOSE FOR WHICH BGC GENERATED IT. BGC SHALL HAVE NO LIABILITY FOR ANY DAMAGES OR LOSS ARISING IN ANY WAY FROM ANY USE OR MODIFICATION OF THIS DOCUMENT NOT AUTHORIZED BY BGC. ANY USE OF OR RELIANCE UPON THIS DOCUMENT OR ITS CONTENT BY THIRD PARTIES SHALL BE AT SUCH THIRD PARTIES' SOLE RISK.

SCALE:	1:10,000
DATE:	MAR 2020
DRAWN:	LL
CHECKED:	PG, PS
APPROVED:	RM

BGC ENGINEERING INC.
AN APPLIED EARTH SCIENCES COMPANY

CLIENT:

PROJECT:
RDCK FLOODPLAIN AND STEEP CREEK STUDY
SALMO RIVER

TITLE:
200-YEAR FLOOD HAZARD
(SHEET 03 OF 9)

PROJECT No.:	DWG No:
0268 007	06

X:\Projects\0268007_RDCK_NDMP_Stream_2_Support\GIS\Production\Report\20191218_RDCK_Clearwater_FCL\200-Year Flood_Hazard_DDP.mxd

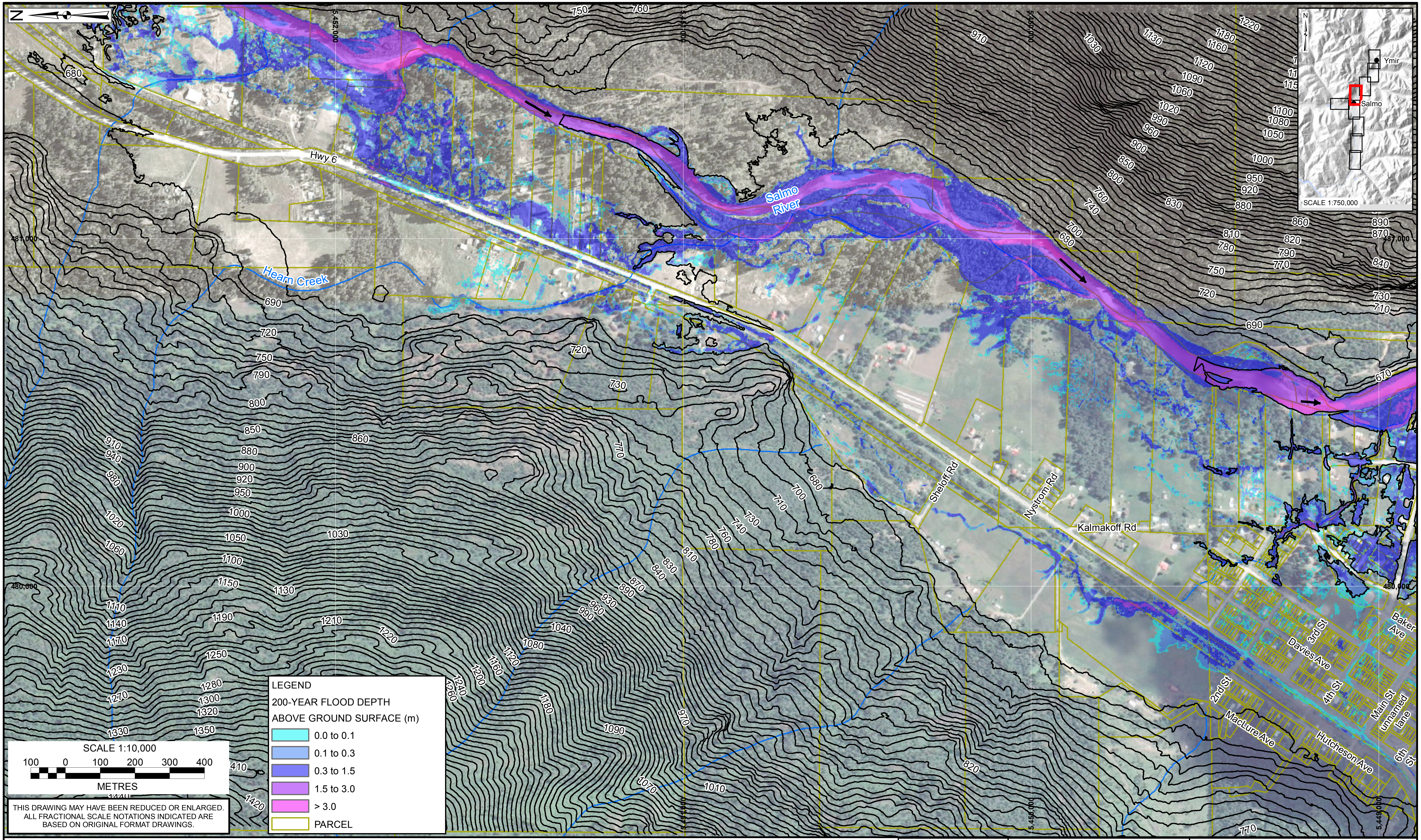

THIS DRAWING MAY HAVE BEEN REDUCED OR ENLARGED. ALL FRACTIONAL SCALE NOTATIONS INDICATED ARE BASED ON ORIGINAL FORMAT DRAWINGS.

X:\Projects\0268007_RDCK_NDMP_Stream_2_Support\GIS\Production\Report\20191218_RDCK_Clearwater_FCL\200-Year Flood_Hazard_DDP.mxd

NOTES:
1. ALL DIMENSIONS ARE IN METRES UNLESS OTHERWISE NOTED.
2. THIS DRAWING MUST BE READ IN CONJUNCTION WITH BGC'S REPORT TITLED "RDCK FLOODPLAIN AND STEEP CREEK STUDY SALMO RIVER", AND DATED MARCH 2020.
3. BASE TOPOGRAPHIC DATA BASED ON LIDAR PROVIDED BY RDCK DATED 2017 AND 2018. CONTOUR INTERVAL IS 10 m. IMAGERY FROM GOOGLE EARTH.PARCEL DATA FROM PARCELMAP BC. DIKE DATA FROM DATA BC. FLOOD DEPTH BASED ON THE 200-YEAR FLOOD USING THE INSTANTANEOUS PEAK DISCHARGE ADJUSTED FOR CLIMATE CHANGE
4. PROJECTION IS NAD 1983 UTM ZONE 11N. VERTICAL DATUM IS CGVD2013.
5. UNLESS BGC AGREES OTHERWISE IN WRITING, THIS DRAWING SHALL NOT BE MODIFIED OR USED FOR ANY PURPOSE OTHER THAN THE PURPOSE FOR WHICH BGC GENERATED IT. BGC SHALL HAVE NO LIABILITY FOR ANY DAMAGES OR LOSS ARISING IN ANY WAY FROM ANY USE OR MODIFICATION OF THIS DOCUMENT NOT AUTHORIZED BY BGC. ANY USE OF OR RELIANCE UPON THIS DOCUMENT OR ITS CONTENT BY THIRD PARTIES SHALL BE AT SUCH THIRD PARTIES' SOLE RISK.

SCALE:	1:10,000
DATE:	MAR 2020
DRAWN:	LL
CHECKED:	PG, PS
APPROVED:	RM

BGC ENGINEERING INC.
AN APPLIED EARTH SCIENCES COMPANY

CLIENT:

PROJECT:
RDCK FLOODPLAIN AND STEEP CREEK STUDY
SALMO RIVER

TITLE:
200-YEAR FLOOD HAZARD
(SHEET 04 OF 9)

PROJECT No.:	DWG No:
0268 007	06

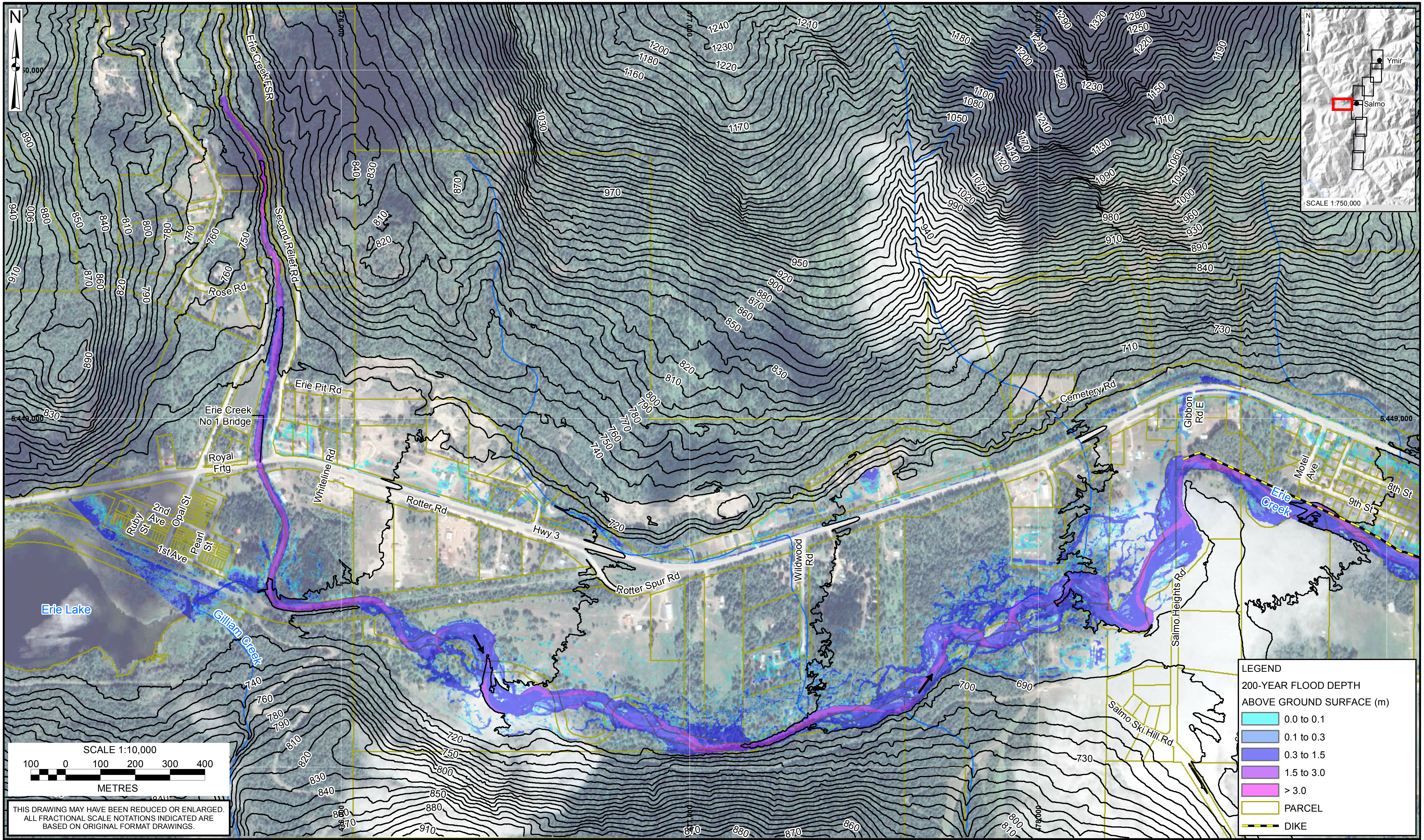

THIS DRAWING MAY HAVE BEEN REDUCED OR ENLARGED.
ALL FRACTIONAL SCALE NOTATIONS INDICATED ARE
BASED ON ORIGINAL FORMAT DRAWINGS.

NOTES:
1. ALL DIMENSIONS ARE IN METRES UNLESS OTHERWISE NOTED.
2. THIS DRAWING MUST BE READ IN CONJUNCTION WITH BGC'S REPORT TITLED "RDCK FLOODPLAIN AND STEEP CREEK STUDY SALMO RIVER", AND DATED MARCH 2020.
3. BASE TOPOGRAPHIC DATA BASED ON LIDAR PROVIDED BY RDCK DATED 2017 AND 2018. CONTOUR INTERVAL IS 10 m. IMAGERY FROM GOOGLE EARTH.PARCEL DATA FROM PARCELMAP BC. DIKE DATA FROM DATA BC. FLOOD DEPTH BASED ON THE 200-YEAR FLOOD USING THE INSTANTANEOUS PEAK DISCHARGE ADJUSTED FOR CLIMATE CHANGE
4. PROJECTION IS NAD 1983 UTM ZONE 11N. VERTICAL DATUM IS CGVD2013.
5. UNLESS BGC AGREES OTHERWISE IN WRITING, THIS DRAWING SHALL NOT BE MODIFIED OR USED FOR ANY PURPOSE OTHER THAN THE PURPOSE FOR WHICH BGC GENERATED IT. BGC SHALL HAVE NO LIABILITY FOR ANY DAMAGES OR LOSS ARISING IN ANY WAY FROM ANY USE OR MODIFICATION OF THIS DOCUMENT NOT AUTHORIZED BY BGC. ANY USE OF OR RELIANCE UPON THIS DOCUMENT OR ITS CONTENT BY THIRD PARTIES SHALL BE AT SUCH THIRD PARTIES' SOLE RISK.

SCALE: 1:10,000
DATE: MAR 2020
DRAWN: LL
CHECKED: PG, PS
APPROVED: RM

BGC ENGINEERING INC.
AN APPLIED EARTH SCIENCES COMPANY

CLIENT:

REGIONAL DISTRICT OF CENTRAL KOOTENAY

PROJECT:
RDCK FLOODPLAIN AND STEEP CREEK STUDY
SALMO RIVER

TITLE:
200-YEAR FLOOD HAZARD
(SHEET 05 OF 9)

PROJECT No.: 0268 007
DWG No: 06

X:\Projects\0268007_RDCK_NDMP_Stream_2_Support\GIS\Production\Report\20191218_RDCK_Clearwater_FCL\200-Year Flood_Hazard_DDP.mxd

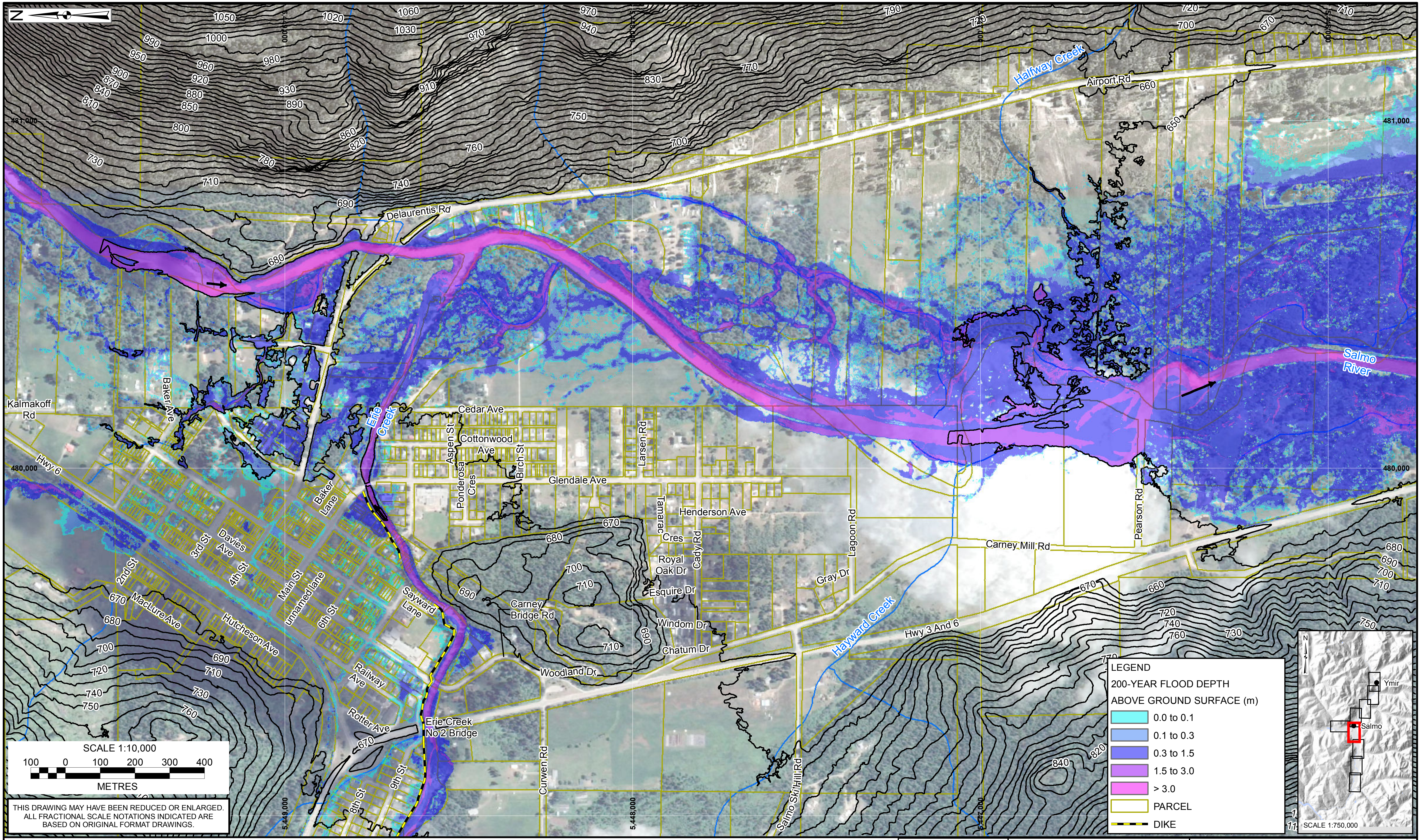

THIS DRAWING MAY HAVE BEEN REDUCED OR ENLARGED.
ALL FRACTIONAL SCALE NOTATIONS INDICATED ARE
BASED ON ORIGINAL FORMAT DRAWINGS.

X:\Projects\0268007_RDCK_NDMP_Stream_2_Support\GIS\Production\Report\20191218_RDCK_Clearwater_FCL\200-Year Flood_Hazard_DDP.mxd

NOTES:
1. ALL DIMENSIONS ARE IN METRES UNLESS OTHERWISE NOTED.
2. THIS DRAWING MUST BE READ IN CONJUNCTION WITH BGC'S REPORT TITLED "RDCK FLOODPLAIN AND STEEP CREEK STUDY SALMO RIVER", AND DATED MARCH 2020.
3. BASE TOPOGRAPHIC DATA BASED ON LIDAR PROVIDED BY RDCK DATED 2017 AND 2018. CONTOUR INTERVAL IS 10 m. IMAGERY FROM GOOGLE EARTH.PARCEL DATA FROM PARCELMAP BC. DIKE DATA FROM DATA BC. FLOOD DEPTH BASED ON THE 200-YEAR FLOOD USING THE INSTANTANEOUS PEAK DISCHARGE ADJUSTED FOR CLIMATE CHANGE
4. PROJECTION IS NAD 1983 UTM ZONE 11N. VERTICAL DATUM IS CGVD2013.
5. UNLESS BGC AGREES OTHERWISE IN WRITING, THIS DRAWING SHALL NOT BE MODIFIED OR USED FOR ANY PURPOSE OTHER THAN THE PURPOSE FOR WHICH BGC GENERATED IT. BGC SHALL HAVE NO LIABILITY FOR ANY DAMAGES OR LOSS ARISING IN ANY WAY FROM ANY USE OR MODIFICATION OF THIS DOCUMENT NOT AUTHORIZED BY BGC. ANY USE OF OR RELIANCE UPON THIS DOCUMENT OR ITS CONTENT BY THIRD PARTIES SHALL BE AT SUCH THIRD PARTIES' SOLE RISK.

SCALE: 1:10,000
DATE: MAR 2020
DRAWN: LL
CHECKED: PG, PS
APPROVED: RM

BGC ENGINEERING INC.
AN APPLIED EARTH SCIENCES COMPANY

CLIENT:
REGIONAL DISTRICT CENTRAL KOOTENAY

PROJECT:
RDCK FLOODPLAIN AND STEEP CREEK STUDY
SALMO RIVER

TITLE:
200-YEAR FLOOD HAZARD
(SHEET 06 OF 9)

PROJECT No.: 0268 007
DWG No: 06

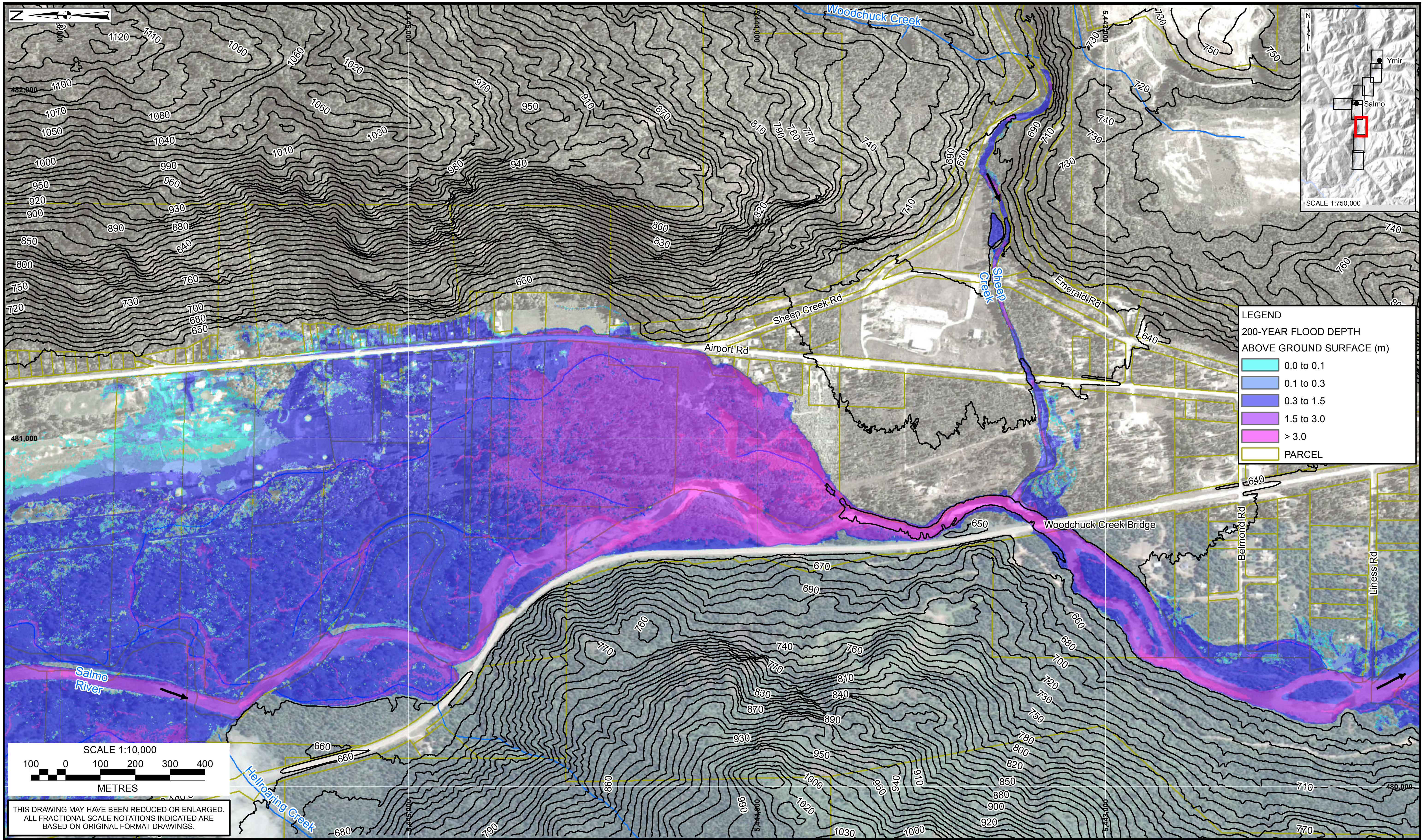

LEGEND

200-YEAR FLOOD DEPTH

ABOVE GROUND SURFACE (m)

🟦 0.0 to 0.1

🟦 0.1 to 0.3

🟦 0.3 to 1.5

🟪 1.5 to 3.0

🟪 > 3.0

☐ PARCEL

SCALE 1:10,000

100 0 100 200 300 400

METRES

THIS DRAWING MAY HAVE BEEN REDUCED OR ENLARGED.
ALL FRACTIONAL SCALE NOTATIONS INDICATED ARE
BASED ON ORIGINAL FORMAT DRAWINGS.

X:\Projects\0268\007_RDCK_NDMP_Stream_2_Support\GIS\Production\Report\20191218_RDCK_Clearwater_FCL\200-Year Flood_Hazard_DDP.mxd

NOTES:
1. ALL DIMENSIONS ARE IN METRES UNLESS OTHERWISE NOTED.
2. THIS DRAWING MUST BE READ IN CONJUNCTION WITH BGC'S REPORT TITLED "RDCK FLOODPLAIN AND STEEP CREEK STUDY SALMO RIVER", AND DATED MARCH 2020.
3. BASE TOPOGRAPHIC DATA BASED ON LIDAR PROVIDED BY RDCK DATED 2017 AND 2018. CONTOUR INTERVAL IS 10 m. IMAGERY FROM GOOGLE EARTH.PARCEL DATA FROM PARCELMAP BC.
DIKE DATA FROM DATA BC. FLOOD DEPTH BASED ON THE 200-YEAR FLOOD USING THE INSTANTANEOUS PEAK DISCHARGE ADJUSTED FOR CLIMATE CHANGE
4. PROJECTION IS NAD 1983 UTM ZONE 11N. VERTICAL DATUM IS CGVD2013.
5. UNLESS BGC AGREES OTHERWISE IN WRITING, THIS DRAWING SHALL NOT BE MODIFIED OR USED FOR ANY PURPOSE OTHER THAN THE PURPOSE FOR WHICH BGC GENERATED IT. BGC SHALL HAVE NO LIABILITY FOR ANY DAMAGES OR LOSS ARISING IN ANY WAY FROM ANY USE OR MODIFICATION OF THIS DOCUMENT NOT AUTHORIZED BY BGC. ANY USE OF OR RELIANCE UPON THIS DOCUMENT OR ITS CONTENT BY THIRD PARTIES SHALL BE AT SUCH THIRD PARTIES' SOLE RISK.

SCALE:	1:10,000
DATE:	MAR 2020
DRAWN:	LL
CHECKED:	PG, PS
APPROVED:	RM

BGC ENGINEERING INC.
AN APPLIED EARTH SCIENCES COMPANY

CLIENT:
REGIONAL DISTRICT CENTRAL KOOTENAY

PROJECT:
RDCK FLOODPLAIN AND STEEP CREEK STUDY
SALMO RIVER

TITLE:
200-YEAR FLOOD HAZARD
(SHEET 07 OF 9)

PROJECT No.:	DWG No:
0268 007	06

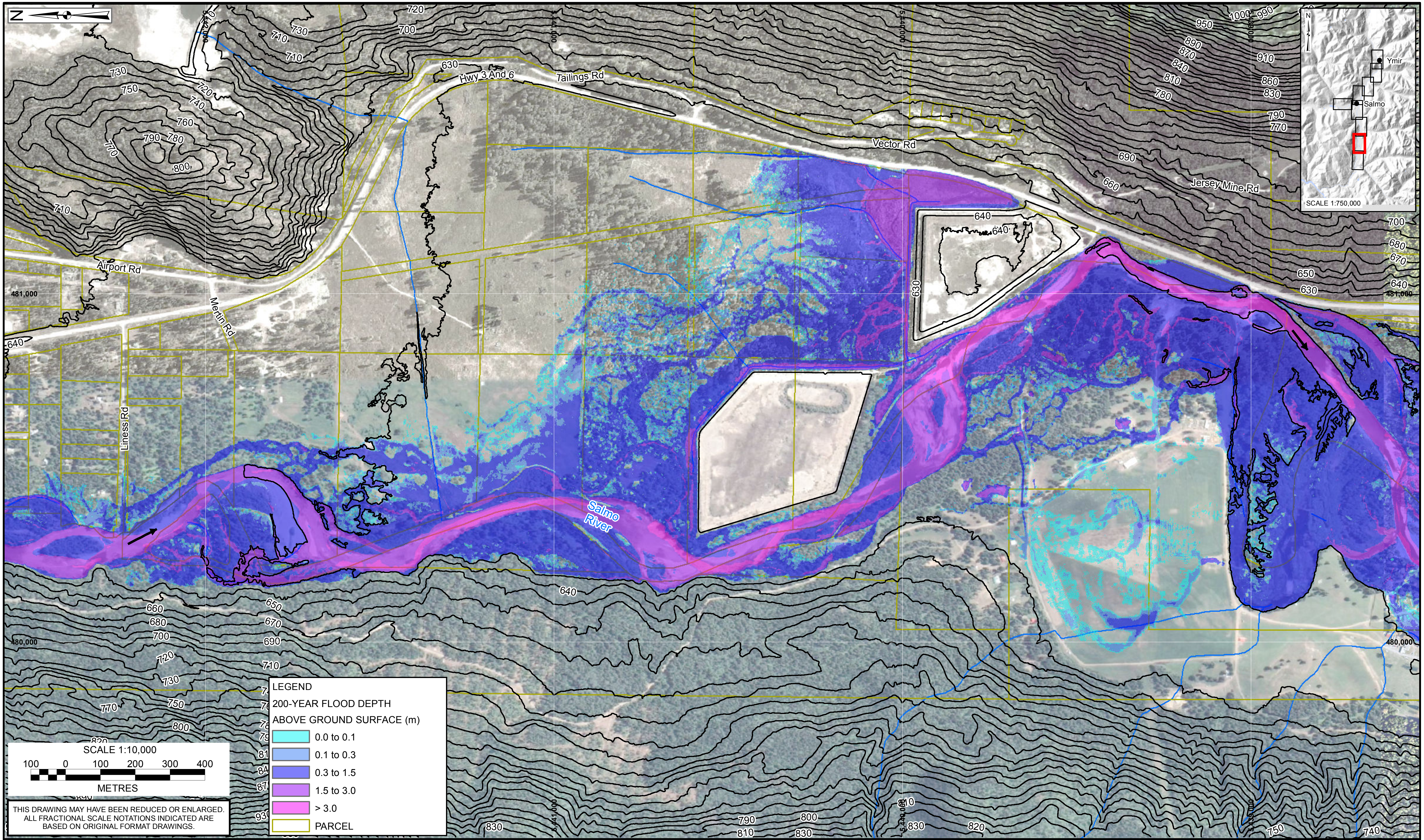

LEGEND

200-YEAR FLOOD DEPTH

ABOVE GROUND SURFACE (m)

🟦	0.0 to 0.1
🟦	0.1 to 0.3
🟦	0.3 to 1.5
🟪	1.5 to 3.0
🟪	> 3.0
☐	PARCEL

SCALE 1:10,000

100 0 100 200 300 400

METRES

THIS DRAWING MAY HAVE BEEN REDUCED OR ENLARGED. ALL FRACTIONAL SCALE NOTATIONS INDICATED ARE BASED ON ORIGINAL FORMAT DRAWINGS.

NOTES:
1. ALL DIMENSIONS ARE IN METRES UNLESS OTHERWISE NOTED.
2. THIS DRAWING MUST BE READ IN CONJUNCTION WITH BGC'S REPORT TITLED "RDCK FLOODPLAIN AND STEEP CREEK STUDY SALMO RIVER", AND DATED MARCH 2020.
3. BASE TOPOGRAPHIC DATA BASED ON LIDAR PROVIDED BY RDCK DATED 2017 AND 2018. CONTOUR INTERVAL IS 10 m. IMAGERY FROM GOOGLE EARTH.PARCEL DATA FROM PARCELMAP BC. DIKE DATA FROM DATA BC. FLOOD DEPTH BASED ON THE 200-YEAR FLOOD USING THE INSTANTANEOUS PEAK DISCHARGE ADJUSTED FOR CLIMATE CHANGE
4. PROJECTION IS NAD 1983 UTM ZONE 11N. VERTICAL DATUM IS CGVD2013.
5. UNLESS BGC AGREES OTHERWISE IN WRITING, THIS DRAWING SHALL NOT BE MODIFIED OR USED FOR ANY PURPOSE OTHER THAN THE PURPOSE FOR WHICH BGC GENERATED IT. BGC SHALL HAVE NO LIABILITY FOR ANY DAMAGES OR LOSS ARISING IN ANY WAY FROM ANY USE OR MODIFICATION OF THIS DOCUMENT NOT AUTHORIZED BY BGC. ANY USE OF OR RELIANCE UPON THIS DOCUMENT OR ITS CONTENT BY THIRD PARTIES SHALL BE AT SUCH THIRD PARTIES' SOLE RISK.

SCALE:	1:10,000
DATE:	MAR 2020
DRAWN:	LL
CHECKED:	PG, PS
APPROVED:	RM

BGC ENGINEERING INC.
AN APPLIED EARTH SCIENCES COMPANY

CLIENT:

PROJECT:
RDCK FLOODPLAIN AND STEEP CREEK STUDY
SALMO RIVER

TITLE:
200-YEAR FLOOD HAZARD
(SHEET 08 OF 9)

PROJECT No.: 0268 007

DWG No: 06

X:\Projects\0268\007_RDCK_NDMP_Stream_2_Support\GIS\Production\Report\20191218_RDCK_Clearwater_FCL\200-Year Flood_Hazard_DDP.mxd

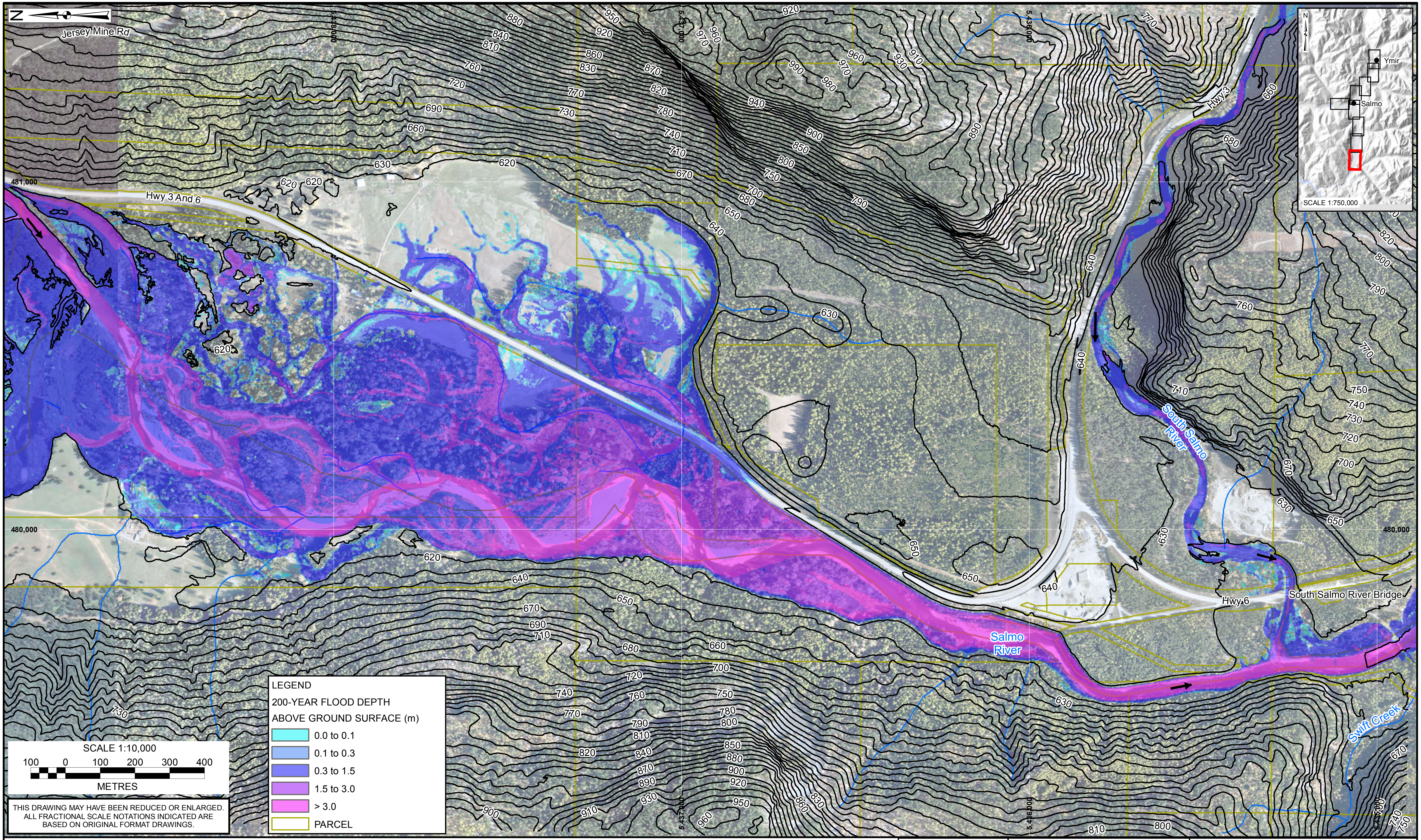

LEGEND

200-YEAR FLOOD DEPTH

ABOVE GROUND SURFACE (m)

🟦	0.0 to 0.1
🟦	0.1 to 0.3
🟦	0.3 to 1.5
🟪	1.5 to 3.0
🟪	> 3.0
☐	PARCEL

THIS DRAWING MAY HAVE BEEN REDUCED OR ENLARGED.
ALL FRACTIONAL SCALE NOTATIONS INDICATED ARE
BASED ON ORIGINAL FORMAT DRAWINGS.

NOTES:
1. ALL DIMENSIONS ARE IN METRES UNLESS OTHERWISE NOTED.
2. THIS DRAWING MUST BE READ IN CONJUNCTION WITH BGC'S REPORT TITLED "RDCK FLOODPLAIN AND STEEP CREEK STUDY SALMO RIVER", AND DATED MARCH 2020.
3. BASE TOPOGRAPHIC DATA BASED ON LIDAR PROVIDED BY RDCK DATED 2017 AND 2018. CONTOUR INTERVAL IS 10 m. IMAGERY FROM GOOGLE EARTH.PARCEL DATA FROM PARCELMAP BC. DIKE DATA FROM DATA BC. FLOOD DEPTH BASED ON THE 200-YEAR FLOOD USING THE INSTANTANEOUS PEAK DISCHARGE ADJUSTED FOR CLIMATE CHANGE
4. PROJECTION IS NAD 1983 UTM ZONE 11N. VERTICAL DATUM IS CGVD2013.
5. UNLESS BGC AGREES OTHERWISE IN WRITING, THIS DRAWING SHALL NOT BE MODIFIED OR USED FOR ANY PURPOSE OTHER THAN THE PURPOSE FOR WHICH BGC GENERATED IT. BGC SHALL HAVE NO LIABILITY FOR ANY DAMAGES OR LOSS ARISING IN ANY WAY FROM ANY USE OR MODIFICATION OF THIS DOCUMENT NOT AUTHORIZED BY BGC. ANY USE OF OR RELIANCE UPON THIS DOCUMENT OR ITS CONTENT BY THIRD PARTIES SHALL BE AT SUCH THIRD PARTIES' SOLE RISK.

SCALE:	1:10,000
DATE:	MAR 2020
DRAWN:	LL
CHECKED:	PG, PS
APPROVED:	RM

BGC ENGINEERING INC.
AN APPLIED EARTH SCIENCES COMPANY

CLIENT:
REGIONAL DISTRICT CENTRAL KOOTENAY

PROJECT:
RDCK FLOODPLAIN AND STEEP CREEK STUDY
SALMO RIVER

TITLE:
200-YEAR FLOOD HAZARD
(SHEET 09 OF 9)

PROJECT No.: 0268 007

DWG No: 06

X:\Projects\0268\007_RDCK_NDMP_Stream_2_Support\GIS\Production\Report\20191218_RDCK_Clearwater_FCL\200-Year Flood_Hazard_DDP.mxd

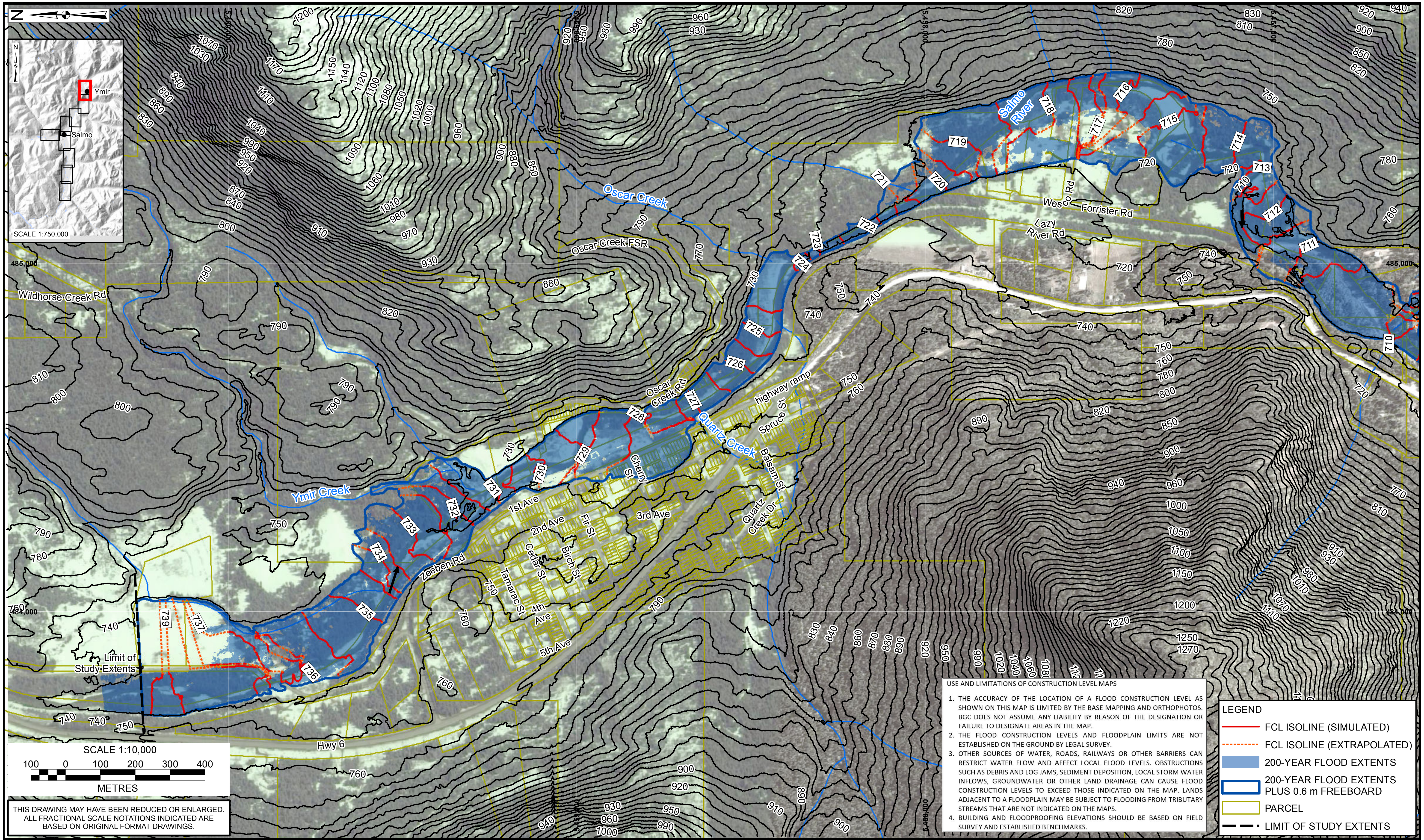

SCALE 1:10,000

100 0 100 200 300 400

METRES

THIS DRAWING MAY HAVE BEEN REDUCED OR ENLARGED. ALL FRACTIONAL SCALE NOTATIONS INDICATED ARE BASED ON ORIGINAL FORMAT DRAWINGS.

USE AND LIMITATIONS OF CONSTRUCTION LEVEL MAPS

1. THE ACCURACY OF THE LOCATION OF A FLOOD CONSTRUCTION LEVEL AS SHOWN ON THIS MAP IS LIMITED BY THE BASE MAPPING AND ORTHOPHOTOS. BGC DOES NOT ASSUME ANY LIABILITY BY REASON OF THE DESIGNATION OR FAILURE TO DESIGNATE AREAS IN THE MAP.
2. THE FLOOD CONSTRUCTION LEVELS AND FLOODPLAIN LIMITS ARE NOT ESTABLISHED ON THE GROUND BY LEGAL SURVEY.
3. OTHER SOURCES OF WATER, ROADS, RAILWAYS OR OTHER BARRIERS CAN RESTRICT WATER FLOW AND AFFECT LOCAL FLOOD LEVELS. OBSTRUCTIONS SUCH AS DEBRIS AND LOG JAMS, SEDIMENT DEPOSITION, LOCAL STORM WATER INFLOWS, GROUNDWATER OR OTHER LAND DRAINAGE CAN CAUSE FLOOD CONSTRUCTION LEVELS TO EXCEED THOSE INDICATED ON THE MAP. LANDS ADJACENT TO A FLOODPLAIN MAY BE SUBJECT TO FLOODING FROM TRIBUTARY STREAMS THAT ARE NOT INDICATED ON THE MAPS.
4. BUILDING AND FLOODPROOFING ELEVATIONS SHOULD BE BASED ON FIELD SURVEY AND ESTABLISHED BENCHMARKS.

LEGEND

— FCL ISOLINE (SIMULATED)
- - - FCL ISOLINE (EXTRAPOLATED)
▇ 200-YEAR FLOOD EXTENTS
☐ 200-YEAR FLOOD EXTENTS PLUS 0.6 m FREEBOARD
☐ PARCEL
— — · LIMIT OF STUDY EXTENTS

NOTES:
1. ALL DIMENSIONS ARE IN METRES UNLESS OTHERWISE NOTED.
2. THIS DRAWING MUST BE READ IN CONJUNCTION WITH BGC'S REPORT TITLED "RDCK FLOODPLAIN AND STEEP CREEK STUDY SALMO RIVER", AND DATED APRIL 2020.
3. BASE TOPOGRAPHIC DATA BASED ON LIDAR PROVIDED BY RDCK DATED 2017 AND 2018. CONTOUR INTERVAL IS 10 m. IMAGERY FROM GOOGLE EARTH.
PARCEL DATA FROM PARCELMAP BC. DIKE DATA FROM DATA BC. FLOOD CONSTRUCTION LEVEL BASED ON THE WATER SURFACE ELEVATION FROM THE 200-YEAR FLOOD USING THE INSTANTANEOUS PEAK DISCHARGE ADJUSTED FOR CLIMATE CHANGE PLUS 0.6 m FREEBOARD
4. PROJECTION IS NAD 1983 UTM ZONE 11N. VERTICAL DATUM IS CGVD2013.
5. UNLESS BGC AGREES OTHERWISE IN WRITING, THIS DRAWING SHALL NOT BE MODIFIED OR USED FOR ANY PURPOSE OTHER THAN THE PURPOSE FOR WHICH BGC GENERATED IT. BGC SHALL HAVE NO LIABILITY FOR ANY DAMAGES OR LOSS ARISING IN ANY WAY FROM ANY USE OR MODIFICATION OF THIS DOCUMENT NOT AUTHORIZED BY BGC. ANY USE OF OR RELIANCE UPON THIS DOCUMENT OR ITS CONTENT BY THIRD PARTIES SHALL BE AT SUCH THIRD PARTIES' SOLE RISK.

SCALE: 1:10,000
DATE: MAR 2020
DRAWN: LL
CHECKED: PG, PS
APPROVED: RM

BGC ENGINEERING INC.
AN APPLIED EARTH SCIENCES COMPANY

CLIENT: REGIONAL DISTRICT CENTRAL KOOTENAY

PROJECT:
RDCK FLOODPLAIN AND STEEP CREEK STUDY
SALMO RIVER

TITLE:
200-YEAR FLOOD CONSTRUCTION LEVEL
(SHEET 01 OF 9)

PROJECT No.: 0268 007
DWG No: 07

X:\Projects\0268007_RDCK_NDMP_Stream_2_Support\GIS\Production\Report\20191218_RDCK_Clearwater_FCL\200-Year Flood Construction Limits_DDP.mxd

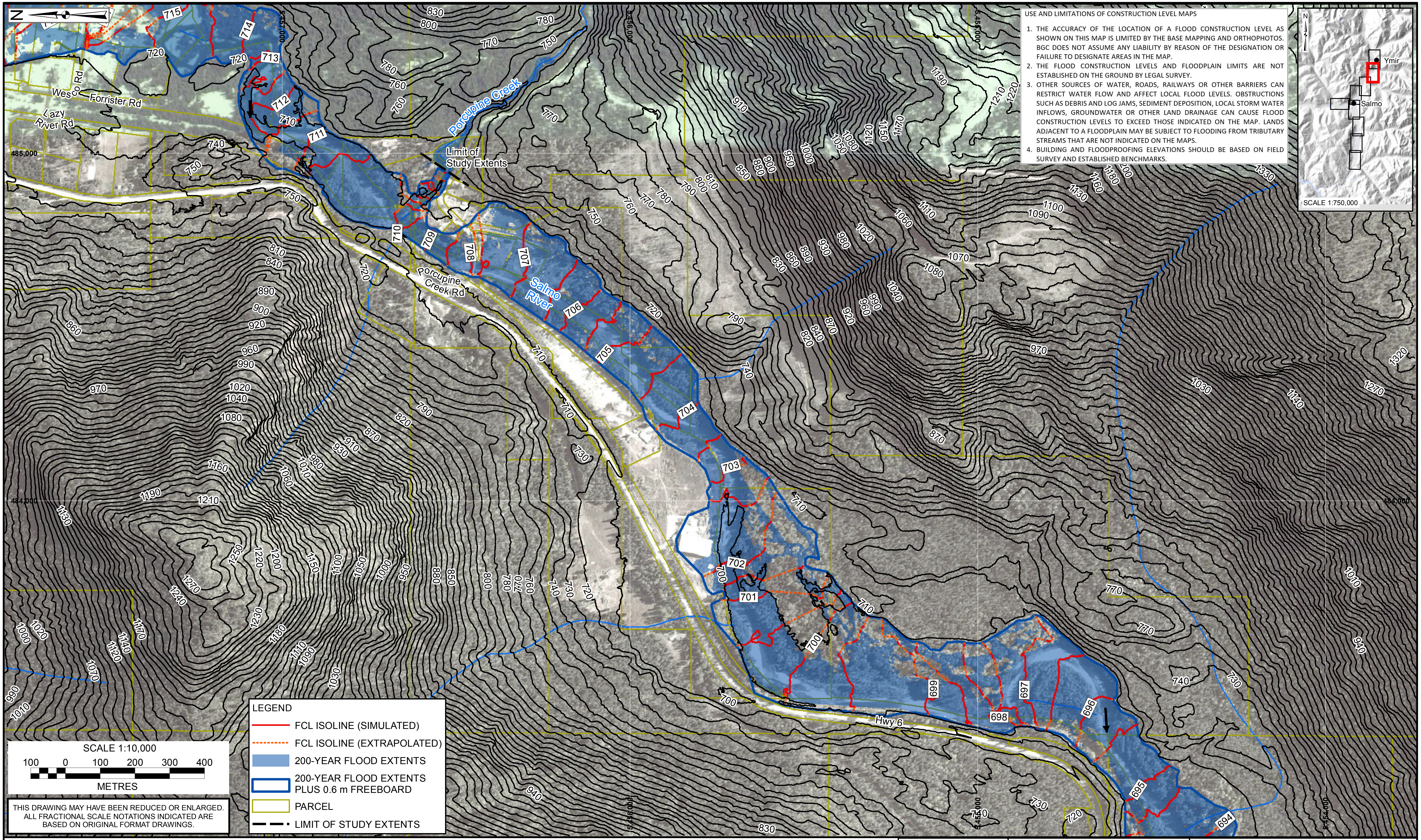

USE AND LIMITATIONS OF CONSTRUCTION LEVEL MAPS

1. THE ACCURACY OF THE LOCATION OF A FLOOD CONSTRUCTION LEVEL AS SHOWN ON THIS MAP IS LIMITED BY THE BASE MAPPING AND ORTHOPHOTOS. BGC DOES NOT ASSUME ANY LIABILITY BY REASON OF THE DESIGNATION OR FAILURE TO DESIGNATE AREAS IN THE MAP.
2. THE FLOOD CONSTRUCTION LEVELS AND FLOODPLAIN LIMITS ARE NOT ESTABLISHED ON THE GROUND BY LEGAL SURVEY.
3. OTHER SOURCES OF WATER, ROADS, RAILWAYS OR OTHER BARRIERS CAN RESTRICT WATER FLOW AND AFFECT LOCAL FLOOD LEVELS. OBSTRUCTIONS SUCH AS DEBRIS AND LOG JAMS, SEDIMENT DEPOSITION, LOCAL STORM WATER INFLOWS, GROUNDWATER OR OTHER LAND DRAINAGE CAN CAUSE FLOOD CONSTRUCTION LEVELS TO EXCEED THOSE INDICATED ON THE MAP. LANDS ADJACENT TO A FLOODPLAIN MAY BE SUBJECT TO FLOODING FROM TRIBUTARY STREAMS THAT ARE NOT INDICATED ON THE MAPS.
4. BUILDING AND FLOODPROOFING ELEVATIONS SHOULD BE BASED ON FIELD SURVEY AND ESTABLISHED BENCHMARKS.

LEGEND

🟥	FCL ISOLINE (SIMULATED)
- - -	FCL ISOLINE (EXTRAPOLATED)
🟦	200-YEAR FLOOD EXTENTS
▭	200-YEAR FLOOD EXTENTS PLUS 0.6 m FREEBOARD
▭	PARCEL
— —	LIMIT OF STUDY EXTENTS

SCALE 1:10,000

100 0 100 200 300 400

METRES

THIS DRAWING MAY HAVE BEEN REDUCED OR ENLARGED. ALL FRACTIONAL SCALE NOTATIONS INDICATED ARE BASED ON ORIGINAL FORMAT DRAWINGS.

X:\Projects\0268007_RDCK_NDMP_Stream_2_Support\GIS\Production\Report\20191218_RDCK_Clearwater_FCL\200-Year Flood Construction Limits_DDP.mxd

NOTES:
1. ALL DIMENSIONS ARE IN METRES UNLESS OTHERWISE NOTED.
2. THIS DRAWING MUST BE READ IN CONJUNCTION WITH BGC'S REPORT TITLED "RDCK FLOODPLAIN AND STEEP CREEK STUDY SALMO RIVER", AND DATED APRIL 2020.
3. BASE TOPOGRAPHIC DATA BASED ON LIDAR PROVIDED BY RDCK DATED 2017 AND 2018. CONTOUR INTERVAL IS 10 m. IMAGERY FROM GOOGLE EARTH. PARCEL DATA FROM PARCELMAP BC. DIKE DATA FROM DATA BC. FLOOD CONSTRUCTION LEVEL BASED ON THE WATER SURFACE ELEVATION FROM THE 200-YEAR FLOOD USING THE INSTANTANEOUS PEAK DISCHARGE ADJUSTED FOR CLIMATE CHANGE PLUS 0.6 m FREEBOARD
4. PROJECTION IS NAD 1983 UTM ZONE 11N. VERTICAL DATUM IS CGVD2013.
5. UNLESS BGC AGREES OTHERWISE IN WRITING, THIS DRAWING SHALL NOT BE MODIFIED OR USED FOR ANY PURPOSE OTHER THAN THE PURPOSE FOR WHICH BGC GENERATED IT. BGC SHALL HAVE NO LIABILITY FOR ANY DAMAGES OR LOSS ARISING IN ANY WAY FROM ANY USE OR MODIFICATION OF THIS DOCUMENT NOT AUTHORIZED BY BGC. ANY USE OF OR RELIANCE UPON THIS DOCUMENT OR ITS CONTENT BY THIRD PARTIES SHALL BE AT SUCH THIRD PARTIES' SOLE RISK.

SCALE:	1:10,000
DATE:	MAR 2020
DRAWN:	LL
CHECKED:	PG, PS
APPROVED:	RM

BGC ENGINEERING INC.
AN APPLIED EARTH SCIENCES COMPANY

CLIENT:

REGIONAL DISTRICT OF CENTRAL KOOTENAY

PROJECT:
RDCK FLOODPLAIN AND STEEP CREEK STUDY
SALMO RIVER

TITLE:
200-YEAR FLOOD CONSTRUCTION LEVEL
(SHEET 02 OF 9)

PROJECT No.:	DWG No:
0268 007	07

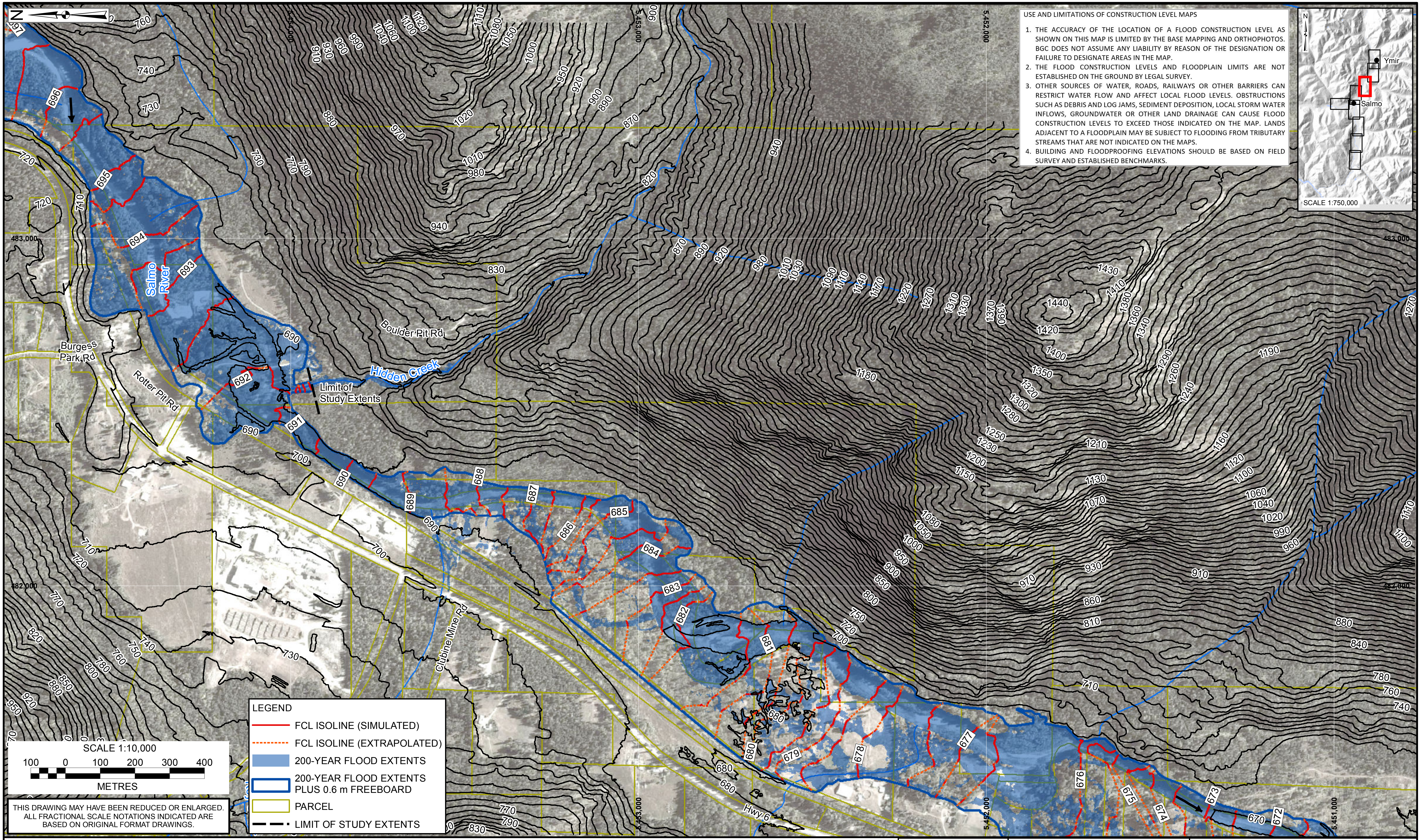

USE AND LIMITATIONS OF CONSTRUCTION LEVEL MAPS

1. THE ACCURACY OF THE LOCATION OF A FLOOD CONSTRUCTION LEVEL AS SHOWN ON THIS MAP IS LIMITED BY THE BASE MAPPING AND ORTHOPHOTOS. BGC DOES NOT ASSUME ANY LIABILITY BY REASON OF THE DESIGNATION OR FAILURE TO DESIGNATE AREAS IN THE MAP.
2. THE FLOOD CONSTRUCTION LEVELS AND FLOODPLAIN LIMITS ARE NOT ESTABLISHED ON THE GROUND BY LEGAL SURVEY.
3. OTHER SOURCES OF WATER, ROADS, RAILWAYS OR OTHER BARRIERS CAN RESTRICT WATER FLOW AND AFFECT LOCAL FLOOD LEVELS. OBSTRUCTIONS SUCH AS DEBRIS AND LOG JAMS, SEDIMENT DEPOSITION, LOCAL STORM WATER INFLOWS, GROUNDWATER OR OTHER LAND DRAINAGE CAN CAUSE FLOOD CONSTRUCTION LEVELS TO EXCEED THOSE INDICATED ON THE MAP. LANDS ADJACENT TO A FLOODPLAIN MAY BE SUBJECT TO FLOODING FROM TRIBUTARY STREAMS THAT ARE NOT INDICATED ON THE MAPS.
4. BUILDING AND FLOODPROOFING ELEVATIONS SHOULD BE BASED ON FIELD SURVEY AND ESTABLISHED BENCHMARKS.

LEGEND

🟥	FCL ISOLINE (SIMULATED)
🟧	FCL ISOLINE (EXTRAPOLATED)
🟦	200-YEAR FLOOD EXTENTS
☐	200-YEAR FLOOD EXTENTS PLUS 0.6 m FREEBOARD
☐	PARCEL
— —	LIMIT OF STUDY EXTENTS

THIS DRAWING MAY HAVE BEEN REDUCED OR ENLARGED. ALL FRACTIONAL SCALE NOTATIONS INDICATED ARE BASED ON ORIGINAL FORMAT DRAWINGS.

NOTES:
1. ALL DIMENSIONS ARE IN METRES UNLESS OTHERWISE NOTED.
2. THIS DRAWING MUST BE READ IN CONJUNCTION WITH BGC'S REPORT TITLED "RDCK FLOODPLAIN AND STEEP CREEK STUDY SALMO RIVER", AND DATED APRIL 2020.
3. BASE TOPOGRAPHIC DATA BASED ON LIDAR PROVIDED BY RDCK DATED 2017 AND 2018. CONTOUR INTERVAL IS 10 m. IMAGERY FROM GOOGLE EARTH. PARCEL DATA FROM PARCELMAP BC. DIKE DATA FROM DATA BC. FLOOD CONSTRUCTION LEVEL BASED ON THE WATER SURFACE ELEVATION FROM THE 200-YEAR FLOOD USING THE INSTANTANEOUS PEAK DISCHARGE ADJUSTED FOR CLIMATE CHANGE PLUS 0.6 m FREEBOARD
4. PROJECTION IS NAD 1983 UTM ZONE 11N. VERTICAL DATUM IS CGVD2013.
5. UNLESS BGC AGREES OTHERWISE IN WRITING, THIS DRAWING SHALL NOT BE MODIFIED OR USED FOR ANY PURPOSE OTHER THAN THE PURPOSE FOR WHICH BGC GENERATED IT. BGC SHALL HAVE NO LIABILITY FOR ANY DAMAGES OR LOSS ARISING IN ANY WAY FROM ANY USE OF OR RELIANCE UPON THIS DOCUMENT NOT AUTHORIZED BY BGC. ANY USE OF OR RELIANCE UPON THIS DOCUMENT OR ITS CONTENT BY THIRD PARTIES SHALL BE AT SUCH THIRD PARTIES' SOLE RISK.

SCALE:	1:10,000
DATE:	MAR 2020
DRAWN:	LL
CHECKED:	PG, PS
APPROVED:	RM

BGC ENGINEERING INC.
AN APPLIED EARTH SCIENCES COMPANY

CLIENT:
REGIONAL DISTRICT CENTRAL KOOTENAY

PROJECT:
RDCK FLOODPLAIN AND STEEP CREEK STUDY
SALMO RIVER

TITLE:
200-YEAR FLOOD CONSTRUCTION LEVEL
(SHEET 03 OF 9)

PROJECT No.: 0268 007

DWG No: 07

X:\Projects\0268\007_RDCK_NDMP_Stream_2_Support\GIS\Production\Report\20191218_RDCK_Clearwater_FCL\200-Year Flood Construction Limits_DDP.mxd

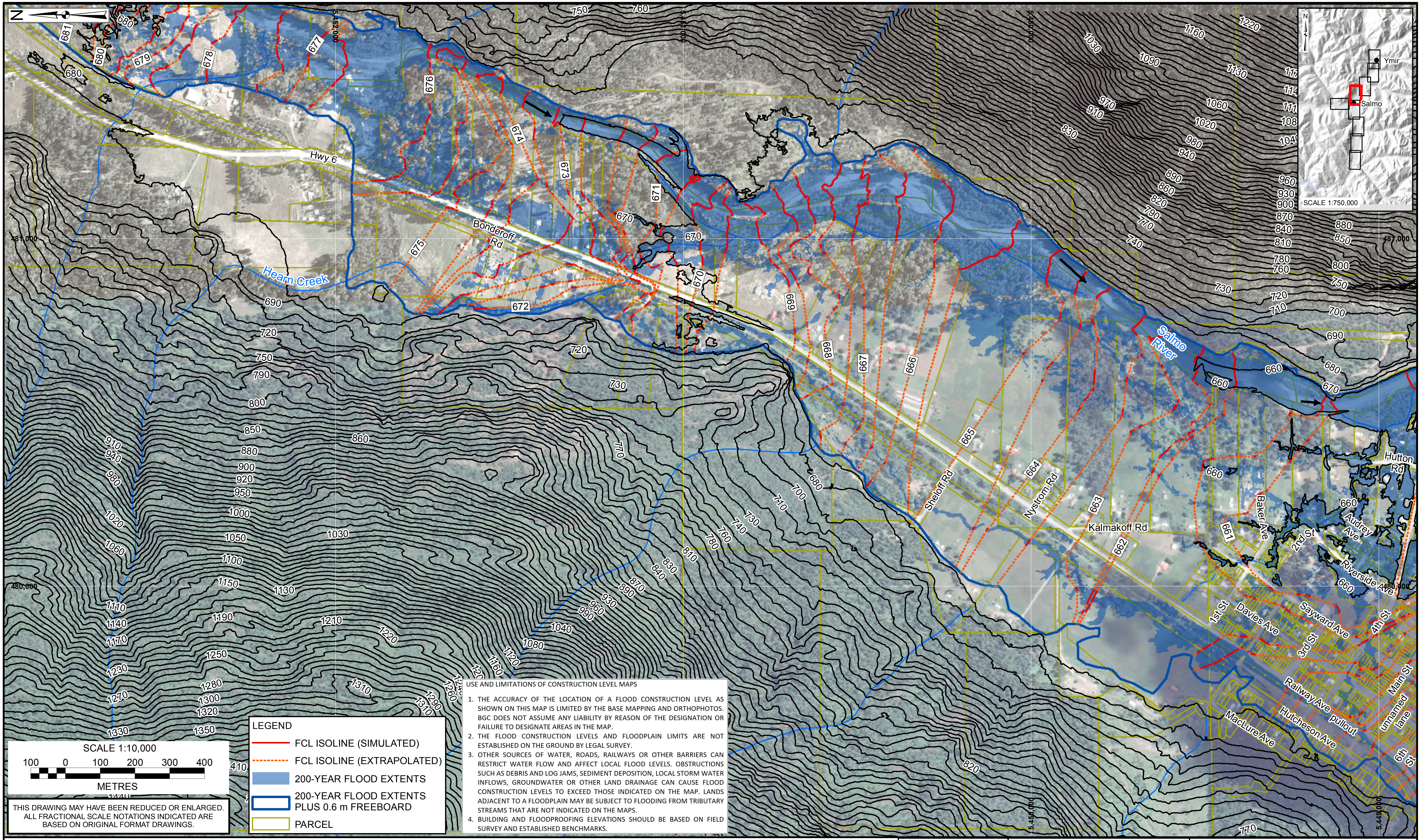

THIS DRAWING MAY HAVE BEEN REDUCED OR ENLARGED.
ALL FRACTIONAL SCALE NOTATIONS INDICATED ARE
BASED ON ORIGINAL FORMAT DRAWINGS.

USE AND LIMITATIONS OF CONSTRUCTION LEVEL MAPS

1. THE ACCURACY OF THE LOCATION OF A FLOOD CONSTRUCTION LEVEL AS SHOWN ON THIS MAP IS LIMITED BY THE BASE MAPPING AND ORTHOPHOTOS. BGC DOES NOT ASSUME ANY LIABILITY BY REASON OF THE DESIGNATION OR FAILURE TO DESIGNATE AREAS IN THE MAP.
2. THE FLOOD CONSTRUCTION LEVELS AND FLOODPLAIN LIMITS ARE NOT ESTABLISHED ON THE GROUND BY LEGAL SURVEY.
3. OTHER SOURCES OF WATER, ROADS, RAILWAYS OR OTHER BARRIERS CAN RESTRICT WATER FLOW AND AFFECT LOCAL FLOOD LEVELS. OBSTRUCTIONS SUCH AS DEBRIS AND LOG JAMS, SEDIMENT DEPOSITION, LOCAL STORM WATER INFLOWS, GROUNDWATER OR OTHER LAND DRAINAGE CAN CAUSE FLOOD CONSTRUCTION LEVELS TO EXCEED THOSE INDICATED ON THE MAP. LANDS ADJACENT TO A FLOODPLAIN MAY BE SUBJECT TO FLOODING FROM TRIBUTARY STREAMS THAT ARE NOT INDICATED ON THE MAPS.
4. BUILDING AND FLOODPROOFING ELEVATIONS SHOULD BE BASED ON FIELD SURVEY AND ESTABLISHED BENCHMARKS.

NOTES:
1. ALL DIMENSIONS ARE IN METRES UNLESS OTHERWISE NOTED.
2. THIS DRAWING MUST BE READ IN CONJUNCTION WITH BGC'S REPORT TITLED "RDCK FLOODPLAIN AND STEEP CREEK STUDY SALMO RIVER", AND DATED APRIL 2020.
3. BASE TOPOGRAPHIC DATA BASED ON LIDAR PROVIDED BY RDCK DATED 2017 AND 2018. CONTOUR INTERVAL IS 10 m. IMAGERY FROM GOOGLE EARTH. PARCEL DATA FROM PARCELMAP BC. DIKE DATA FROM DATA BC. FLOOD CONSTRUCTION LEVEL BASED ON THE WATER SURFACE ELEVATION FROM THE 200-YEAR FLOOD USING THE INSTANTANEOUS PEAK DISCHARGE ADJUSTED FOR CLIMATE CHANGE PLUS 0.6 m FREEBOARD
4. PROJECTION IS NAD 1983 UTM ZONE 11N. VERTICAL DATUM IS CGVD2013.
5. UNLESS BGC AGREES OTHERWISE IN WRITING, THIS DRAWING SHALL NOT BE MODIFIED OR USED FOR ANY PURPOSE OTHER THAN THE PURPOSE FOR WHICH BGC GENERATED IT. BGC SHALL HAVE NO LIABILITY FOR ANY DAMAGES OR LOSS ARISING IN ANY WAY FROM ANY USE OR MODIFICATION OF THIS DOCUMENT NOT AUTHORIZED BY BGC. ANY USE OF OR RELIANCE UPON THIS DOCUMENT OR ITS CONTENT BY THIRD PARTIES SHALL BE AT SUCH THIRD PARTIES' SOLE RISK.

X:\Projects\0268\007_RDCK_NDMP_Stream_2_Support\GIS\Production\Report\20191218_RDCK_Clearwater_FCL\200-Year Flood Construction Limits_DDP.mxd

SCALE: 1:10,000
DATE: MAR 2020
DRAWN: LL
CHECKED: PG, PS
APPROVED: RM

BGC ENGINEERING INC.
AN APPLIED EARTH SCIENCES COMPANY

CLIENT:

PROJECT:
RDCK FLOODPLAIN AND STEEP CREEK STUDY
SALMO RIVER

TITLE:
200-YEAR FLOOD CONSTRUCTION LEVEL
(SHEET 04 OF 9)

PROJECT No.: 0268 007
DWG No: 07

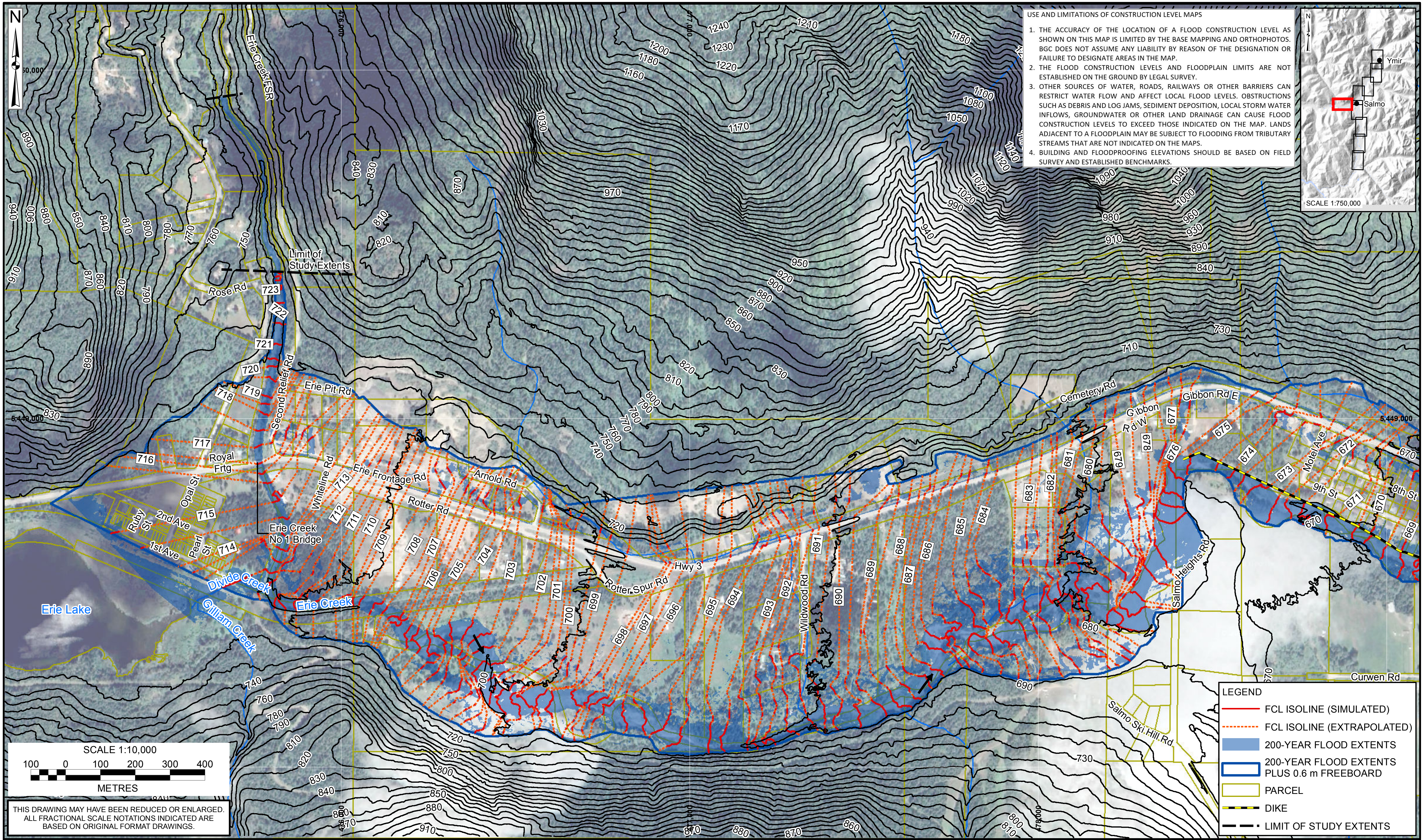

USE AND LIMITATIONS OF CONSTRUCTION LEVEL MAPS

1. THE ACCURACY OF THE LOCATION OF A FLOOD CONSTRUCTION LEVEL AS SHOWN ON THIS MAP IS LIMITED BY THE BASE MAPPING AND ORTHOPHOTOS. BGC DOES NOT ASSUME ANY LIABILITY BY REASON OF THE DESIGNATION OR FAILURE TO DESIGNATE AREAS IN THE MAP.
2. THE FLOOD CONSTRUCTION LEVELS AND FLOODPLAIN LIMITS ARE NOT ESTABLISHED ON THE GROUND BY LEGAL SURVEY.
3. OTHER SOURCES OF WATER, ROADS, RAILWAYS OR OTHER BARRIERS CAN RESTRICT WATER FLOW AND AFFECT LOCAL FLOOD LEVELS. OBSTRUCTIONS SUCH AS DEBRIS AND LOG JAMS, SEDIMENT DEPOSITION, LOCAL STORM WATER INFLOWS, GROUNDWATER OR OTHER LAND DRAINAGE CAN CAUSE FLOOD CONSTRUCTION LEVELS TO EXCEED THOSE INDICATED ON THE MAP. LANDS ADJACENT TO A FLOODPLAIN MAY BE SUBJECT TO FLOODING FROM TRIBUTARY STREAMS THAT ARE NOT INDICATED ON THE MAPS.
4. BUILDING AND FLOODPROOFING ELEVATIONS SHOULD BE BASED ON FIELD SURVEY AND ESTABLISHED BENCHMARKS.

THIS DRAWING MAY HAVE BEEN REDUCED OR ENLARGED. ALL FRACTIONAL SCALE NOTATIONS INDICATED ARE BASED ON ORIGINAL FORMAT DRAWINGS.

NOTES:
1. ALL DIMENSIONS ARE IN METRES UNLESS OTHERWISE NOTED.
2. THIS DRAWING MUST BE READ IN CONJUNCTION WITH BGC'S REPORT TITLED "RDCK FLOODPLAIN AND STEEP CREEK STUDY SALMO RIVER", AND DATED APRIL 2020.
3. BASE TOPOGRAPHIC DATA BASED ON LIDAR PROVIDED BY RDCK DATED 2017 AND 2018. CONTOUR INTERVAL IS 10 m. IMAGERY FROM GOOGLE EARTH. PARCEL DATA FROM PARCELMAP BC. DIKE DATA FROM DATA BC. FLOOD CONSTRUCTION LEVEL BASED ON THE WATER SURFACE ELEVATION FROM THE 200-YEAR FLOOD USING THE INSTANTANEOUS PEAK DISCHARGE ADJUSTED FOR CLIMATE CHANGE PLUS 0.6 m FREEBOARD
4. PROJECTION IS NAD 1983 UTM ZONE 11N. VERTICAL DATUM IS CGVD2013.
5. UNLESS BGC AGREES OTHERWISE IN WRITING, THIS DRAWING SHALL NOT BE MODIFIED OR USED FOR ANY PURPOSE OTHER THAN THE PURPOSE FOR WHICH BGC GENERATED IT. BGC SHALL HAVE NO LIABILITY FOR ANY DAMAGES OR LOSS ARISING IN ANY WAY FROM ANY USE OF MODIFICATION OF THIS DOCUMENT NOT AUTHORIZED BY BGC. ANY USE OF OR RELIANCE UPON THIS DOCUMENT OR ITS CONTENT BY THIRD PARTIES SHALL BE AT SUCH THIRD PARTIES' SOLE RISK.

SCALE:	1:10,000
DATE:	MAR 2020
DRAWN:	LL
CHECKED:	PG, PS
APPROVED:	RM

BGC ENGINEERING INC.
AN APPLIED EARTH SCIENCES COMPANY

CLIENT:

PROJECT:
RDCK FLOODPLAIN AND STEEP CREEK STUDY
SALMO RIVER

TITLE:
200-YEAR FLOOD CONSTRUCTION LEVEL
(SHEET 05 OF 9)

PROJECT No.: 0268 007
DWG No: 07

X:\Projects\0268007_RDCK_NDMP_Stream_2_Support\GIS\Production\Report\20191218_RDCK_Clearwater_FCL\200-Year Flood Construction Limits_DDP.mxd

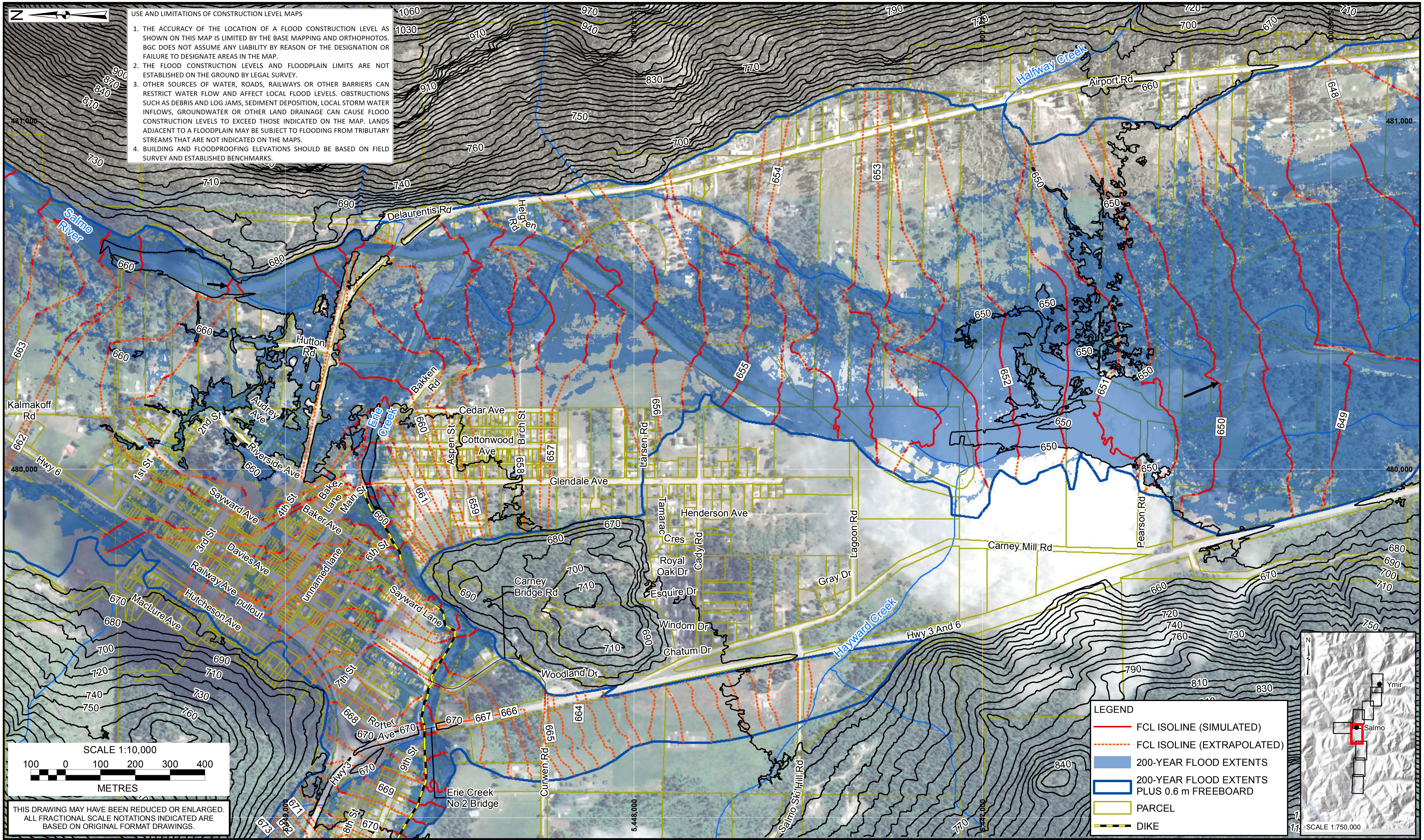

USE AND LIMITATIONS OF CONSTRUCTION LEVEL MAPS

1. THE ACCURACY OF THE LOCATION OF A FLOOD CONSTRUCTION LEVEL AS SHOWN ON THIS MAP IS LIMITED BY THE BASE MAPPING AND ORTHOPHOTOS. BGC DOES NOT ASSUME ANY LIABILITY BY REASON OF THE DESIGNATION OR FAILURE TO DESIGNATE AREAS IN THE MAP.
2. THE FLOOD CONSTRUCTION LEVELS AND FLOODPLAIN LIMITS ARE NOT ESTABLISHED ON THE GROUND BY LEGAL SURVEY.
3. OTHER SOURCES OF WATER, ROADS, RAILWAYS OR OTHER BARRIERS CAN RESTRICT WATER FLOW AND AFFECT LOCAL FLOOD LEVELS. OBSTRUCTIONS SUCH AS DEBRIS AND LOG JAMS, SEDIMENT DEPOSITION, LOCAL STORM WATER INFLOWS, GROUNDWATER OR OTHER LAND DRAINAGE CAN CAUSE FLOOD CONSTRUCTION LEVELS TO EXCEED THOSE INDICATED ON THE MAP. LANDS ADJACENT TO A FLOODPLAIN MAY BE SUBJECT TO FLOODING FROM TRIBUTARY STREAMS THAT ARE NOT INDICATED ON THE MAPS.
4. BUILDING AND FLOODPROOFING ELEVATIONS SHOULD BE BASED ON FIELD SURVEY AND ESTABLISHED BENCHMARKS.

LEGEND
- FCL ISOLINE (SIMULATED)
- FCL ISOLINE (EXTRAPOLATED)
- 200-YEAR FLOOD EXTENTS
- 200-YEAR FLOOD EXTENTS PLUS 0.6 m FREEBOARD
- PARCEL
- DIKE

SCALE 1:10,000
100 0 100 200 300 400
METRES

THIS DRAWING MAY HAVE BEEN REDUCED OR ENLARGED. ALL FRACTIONAL SCALE NOTATIONS INDICATED ARE BASED ON ORIGINAL FORMAT DRAWINGS.

X:\Projects\0268\007_RDCK_NDMP_Stream_2_Support\GIS\Production\Report\20191218_RDCK_Clearwater_FCL\200-Year Flood Construction Limits_DDP.mxd

NOTES:
1. ALL DIMENSIONS ARE IN METRES UNLESS OTHERWISE NOTED.
2. THIS DRAWING MUST BE READ IN CONJUNCTION WITH BGC'S REPORT TITLED "RDCK FLOODPLAIN AND STEEP CREEK STUDY SALMO RIVER", AND DATED APRIL 2020.
3. BASE TOPOGRAPHIC DATA BASED ON LIDAR PROVIDED BY RDCK DATED 2017 AND 2018. CONTOUR INTERVAL IS 10 m. IMAGERY FROM GOOGLE EARTH. PARCEL DATA FROM PARCELMAP BC. DIKE DATA FROM DATA BC. FLOOD CONSTRUCTION LEVEL BASED ON THE WATER SURFACE ELEVATION FROM THE 200-YEAR FLOOD USING THE INSTANTANEOUS PEAK DISCHARGE ADJUSTED FOR CLIMATE CHANGE PLUS 0.6 m FREEBOARD
4. PROJECTION IS NAD 1983 UTM ZONE 11N. VERTICAL DATUM IS CGVD2013.
5. UNLESS BGC AGREES OTHERWISE IN WRITING, THIS DRAWING SHALL NOT BE MODIFIED OR USED FOR ANY PURPOSE OTHER THAN THE PURPOSE FOR WHICH BGC GENERATED IT. BGC SHALL HAVE NO LIABILITY FOR ANY DAMAGES OR LOSS ARISING IN ANY WAY FROM ANY USE OR MODIFICATION OF THIS DOCUMENT NOT AUTHORIZED BY BGC. ANY USE OF OR RELIANCE UPON THIS DOCUMENT OR ITS CONTENT BY THIRD PARTIES SHALL BE AT SUCH THIRD PARTIES' SOLE RISK.

SCALE: 1:10,000
DATE: MAR 2020
DRAWN: LL
CHECKED: PG, PS
APPROVED: RM

BGC ENGINEERING INC.
AN APPLIED EARTH SCIENCES COMPANY

CLIENT: REGIONAL DISTRICT CENTRAL KOOTENAY

PROJECT: RDCK FLOODPLAIN AND STEEP CREEK STUDY
SALMO RIVER

TITLE: 200-YEAR FLOOD CONSTRUCTION LEVEL
(SHEET 06 OF 9)

PROJECT No.: 0268 007
DWG No: 07

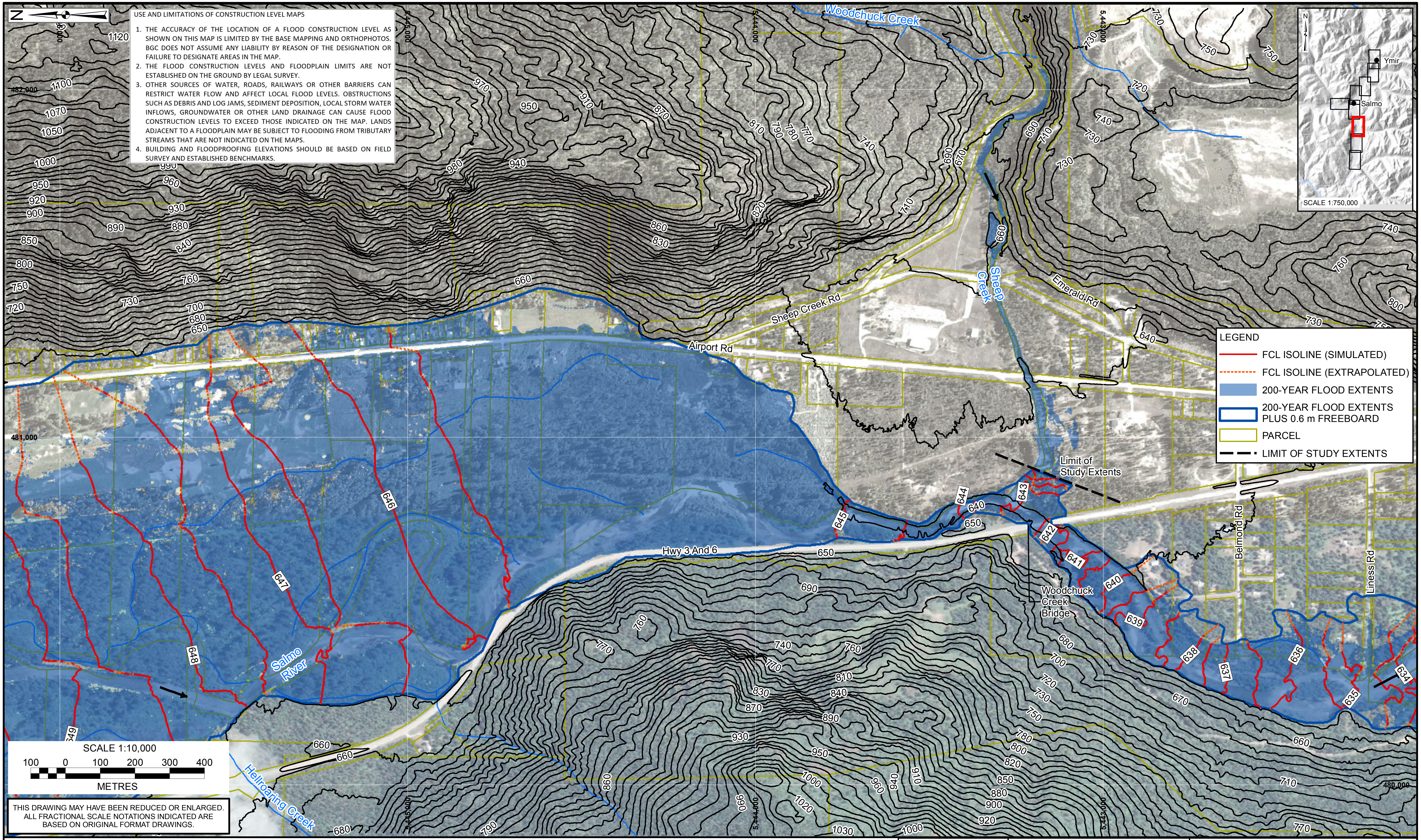

USE AND LIMITATIONS OF CONSTRUCTION LEVEL MAPS

1. THE ACCURACY OF THE LOCATION OF A FLOOD CONSTRUCTION LEVEL AS SHOWN ON THIS MAP IS LIMITED BY THE BASE MAPPING AND ORTHOPHOTOS. BGC DOES NOT ASSUME ANY LIABILITY BY REASON OF THE DESIGNATION OR FAILURE TO DESIGNATE AREAS IN THE MAP.
2. THE FLOOD CONSTRUCTION LEVELS AND FLOODPLAIN LIMITS ARE NOT ESTABLISHED ON THE GROUND BY LEGAL SURVEY.
3. OTHER SOURCES OF WATER, ROADS, RAILWAYS OR OTHER BARRIERS CAN RESTRICT WATER FLOW AND AFFECT LOCAL FLOOD LEVELS. OBSTRUCTIONS SUCH AS DEBRIS AND LOG JAMS, SEDIMENT DEPOSITION, LOCAL STORM WATER INFLOWS, GROUNDWATER OR OTHER LAND DRAINAGE CAN CAUSE FLOOD CONSTRUCTION LEVELS TO EXCEED THOSE INDICATED ON THE MAP. LANDS ADJACENT TO A FLOODPLAIN MAY BE SUBJECT TO FLOODING FROM TRIBUTARY STREAMS THAT ARE NOT INDICATED ON THE MAPS.
4. BUILDING AND FLOODPROOFING ELEVATIONS SHOULD BE BASED ON FIELD SURVEY AND ESTABLISHED BENCHMARKS.

LEGEND

—	FCL ISOLINE (SIMULATED)
-----	FCL ISOLINE (EXTRAPOLATED)
▬	200-YEAR FLOOD EXTENTS
▭	200-YEAR FLOOD EXTENTS PLUS 0.6 m FREEBOARD
▭	PARCEL
— —	LIMIT OF STUDY EXTENTS

THIS DRAWING MAY HAVE BEEN REDUCED OR ENLARGED. ALL FRACTIONAL SCALE NOTATIONS INDICATED ARE BASED ON ORIGINAL FORMAT DRAWINGS.

NOTES:
1. ALL DIMENSIONS ARE IN METRES UNLESS OTHERWISE NOTED.
2. THIS DRAWING MUST BE READ IN CONJUNCTION WITH BGC'S REPORT TITLED "RDCK FLOODPLAIN AND STEEP CREEK STUDY SALMO RIVER", AND DATED APRIL 2020.
3. BASE TOPOGRAPHIC DATA BASED ON LIDAR PROVIDED BY RDCK DATED 2017 AND 2018. CONTOUR INTERVAL IS 10 m. IMAGERY FROM GOOGLE EARTH. PARCEL DATA FROM PARCELMAP BC. DIKE DATA FROM DATA BC. FLOOD CONSTRUCTION LEVEL BASED ON THE WATER SURFACE ELEVATION FROM THE 200-YEAR FLOOD USING THE INSTANTANEOUS PEAK DISCHARGE ADJUSTED FOR CLIMATE CHANGE PLUS 0.6 m FREEBOARD
4. PROJECTION IS NAD 1983 UTM ZONE 11N. VERTICAL DATUM IS CGVD2013.
5. UNLESS BGC AGREES OTHERWISE IN WRITING, THIS DRAWING SHALL NOT BE MODIFIED OR USED FOR ANY PURPOSE OTHER THAN THE PURPOSE FOR WHICH BGC GENERATED IT. BGC SHALL HAVE NO LIABILITY FOR ANY DAMAGES OR LOSS ARISING IN ANY WAY FROM ANY USE OR MODIFICATION OF THIS DOCUMENT NOT AUTHORIZED BY BGC. ANY USE OF OR RELIANCE UPON THIS DOCUMENT OR ITS CONTENT BY THIRD PARTIES SHALL BE AT SUCH THIRD PARTIES' SOLE RISK.

SCALE:	1:10,000
DATE:	MAR 2020
DRAWN:	LL
CHECKED:	PG, PS
APPROVED:	RM

BGC ENGINEERING INC.
AN APPLIED EARTH SCIENCES COMPANY

CLIENT:

PROJECT:
RDCK FLOODPLAIN AND STEEP CREEK STUDY
SALMO RIVER

TITLE:
200-YEAR FLOOD CONSTRUCTION LEVEL
(SHEET 07 OF 9)

PROJECT No.:	DWG No:
0268 007	07

X:\Projects\0268007_RDCK_NDMP_Stream_2_Support\GIS\Production\Report\20191218_RDCK_Clearwater_FCL\200-Year Flood Construction Limits_DDP.mxd

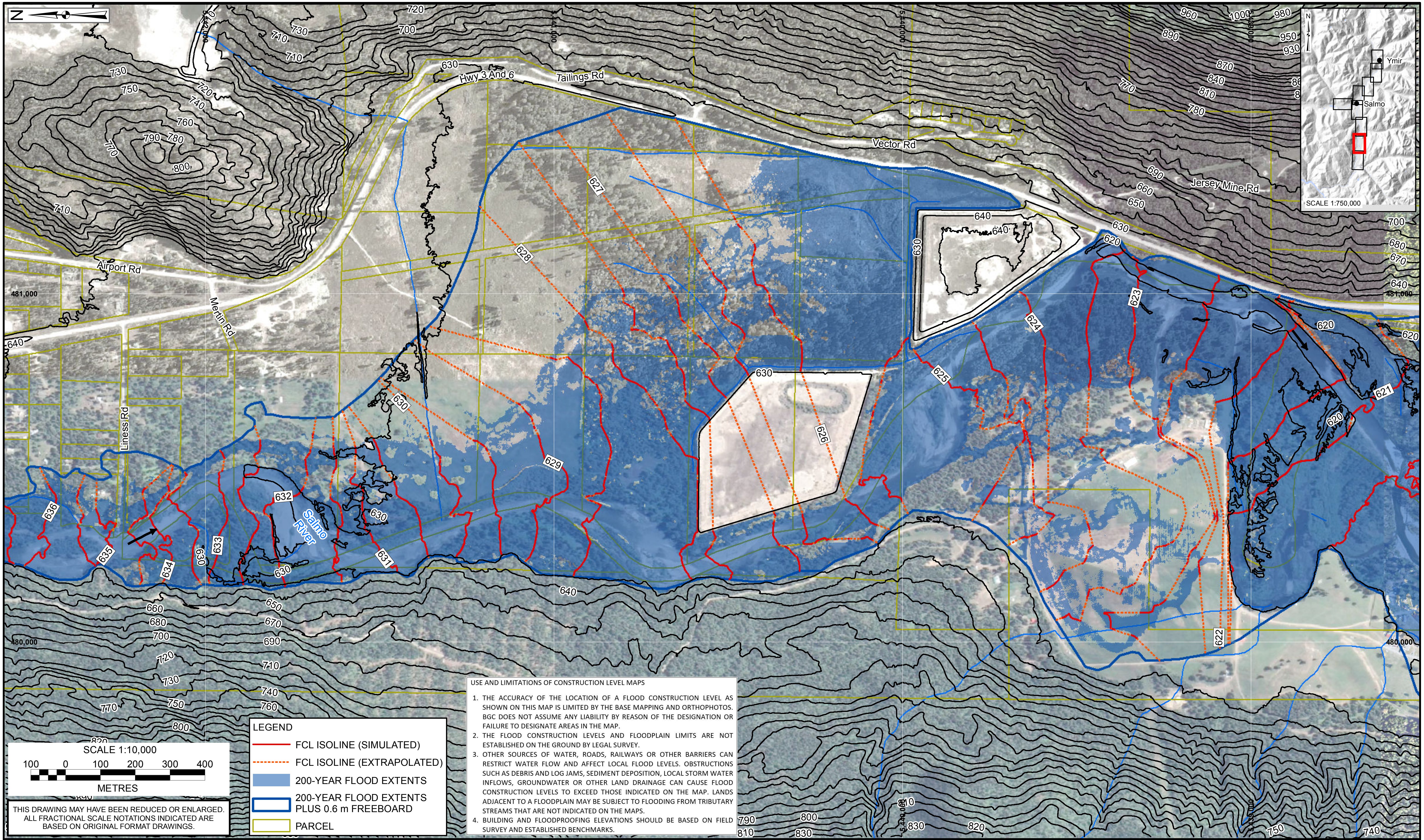

LEGEND

🟥	FCL ISOLINE (SIMULATED)
┅	FCL ISOLINE (EXTRAPOLATED)
🟦	200-YEAR FLOOD EXTENTS
▭	200-YEAR FLOOD EXTENTS PLUS 0.6 m FREEBOARD
▭	PARCEL

SCALE 1:10,000

100 0 100 200 300 400

METRES

THIS DRAWING MAY HAVE BEEN REDUCED OR ENLARGED. ALL FRACTIONAL SCALE NOTATIONS INDICATED ARE BASED ON ORIGINAL FORMAT DRAWINGS.

USE AND LIMITATIONS OF CONSTRUCTION LEVEL MAPS

1. THE ACCURACY OF THE LOCATION OF A FLOOD CONSTRUCTION LEVEL AS SHOWN ON THIS MAP IS LIMITED BY THE BASE MAPPING AND ORTHOPHOTOS. BGC DOES NOT ASSUME ANY LIABILITY BY REASON OF THE DESIGNATION OR FAILURE TO DESIGNATE AREAS IN THE MAP.
2. THE FLOOD CONSTRUCTION LEVELS AND FLOODPLAIN LIMITS ARE NOT ESTABLISHED ON THE GROUND BY LEGAL SURVEY.
3. OTHER SOURCES OF WATER, ROADS, RAILWAYS OR OTHER BARRIERS CAN RESTRICT WATER FLOW AND AFFECT LOCAL FLOOD LEVELS. OBSTRUCTIONS SUCH AS DEBRIS AND LOG JAMS, SEDIMENT DEPOSITION, LOCAL STORM WATER INFLOWS, GROUNDWATER OR OTHER LAND DRAINAGE CAN CAUSE FLOOD CONSTRUCTION LEVELS TO EXCEED THOSE INDICATED ON THE MAP. LANDS ADJACENT TO A FLOODPLAIN MAY BE SUBJECT TO FLOODING FROM TRIBUTARY STREAMS THAT ARE NOT INDICATED ON THE MAPS.
4. BUILDING AND FLOODPROOFING ELEVATIONS SHOULD BE BASED ON FIELD SURVEY AND ESTABLISHED BENCHMARKS.

NOTES:
1. ALL DIMENSIONS ARE IN METRES UNLESS OTHERWISE NOTED.
2. THIS DRAWING MUST BE READ IN CONJUNCTION WITH BGC'S REPORT TITLED "RDCK FLOODPLAIN AND STEEP CREEK STUDY SALMO RIVER", AND DATED APRIL 2020.
3. BASE TOPOGRAPHIC DATA BASED ON LIDAR PROVIDED BY RDCK DATED 2017 AND 2018. CONTOUR INTERVAL IS 10 m. IMAGERY FROM GOOGLE EARTH.
   PARCEL DATA FROM PARCELMAP BC. DIKE DATA FROM DATA BC. FLOOD CONSTRUCTION LEVEL BASED ON THE WATER SURFACE ELEVATION FROM THE 200-YEAR FLOOD USING THE INSTANTANEOUS PEAK DISCHARGE ADJUSTED FOR CLIMATE CHANGE PLUS 0.6 m FREEBOARD
4. PROJECTION IS NAD 1983 UTM ZONE 11N. VERTICAL DATUM IS CGVD2013.
5. UNLESS BGC AGREES OTHERWISE IN WRITING, THIS DRAWING SHALL NOT BE MODIFIED OR USED FOR ANY PURPOSE OTHER THAN THE PURPOSE FOR WHICH BGC GENERATED IT. BGC SHALL HAVE NO LIABILITY FOR ANY DAMAGES OR LOSS ARISING IN ANY WAY FROM ANY USE OF OR RELIANCE UPON THIS DOCUMENT OR ITS CONTENT BY THIRD PARTIES SHALL BE AT SUCH THIRD PARTIES' SOLE RISK.

SCALE:	1:10,000
DATE:	MAR 2020
DRAWN:	LL
CHECKED:	PG, PS
APPROVED:	RM

BGC ENGINEERING INC.
AN APPLIED EARTH SCIENCES COMPANY

CLIENT:

PROJECT:
RDCK FLOODPLAIN AND STEEP CREEK STUDY
SALMO RIVER

TITLE:
200-YEAR FLOOD CONSTRUCTION LEVEL
(SHEET 08 OF 9)

PROJECT No.:	DWG No:
0268 007	07

X:\Projects\0268\007_RDCK_NDMP_Stream_2_Support\GIS\Production\Report\20191218_RDCK_Clearwater_FCL\200-Year Flood Construction Limits_DDP.mxd

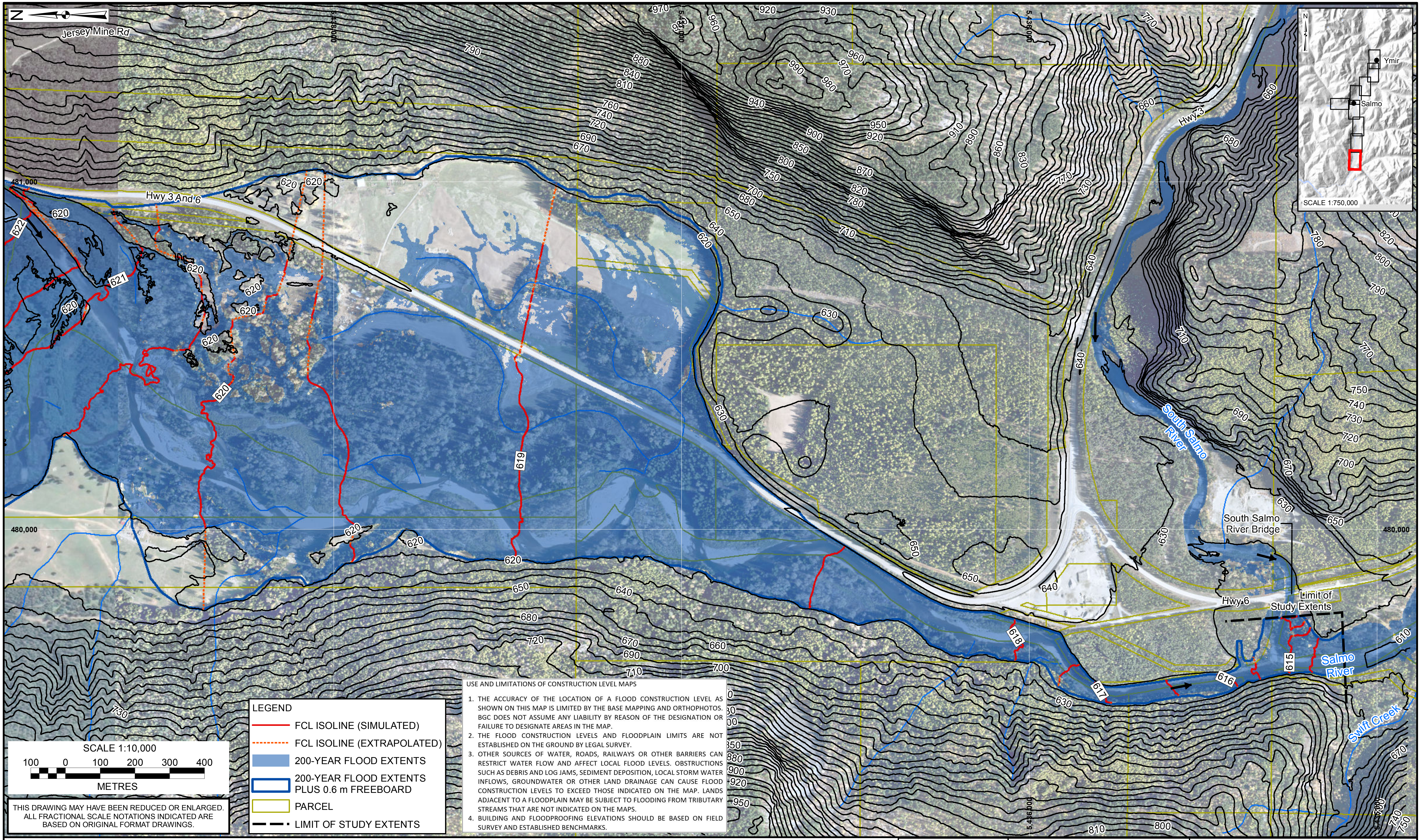

LEGEND

🟥	FCL ISOLINE (SIMULATED)
┅	FCL ISOLINE (EXTRAPOLATED)
🟦	200-YEAR FLOOD EXTENTS
▢	200-YEAR FLOOD EXTENTS PLUS 0.6 m FREEBOARD
▢	PARCEL
━ ━	LIMIT OF STUDY EXTENTS

SCALE 1:10,000

100 0 100 200 300 400

METRES

THIS DRAWING MAY HAVE BEEN REDUCED OR ENLARGED.
ALL FRACTIONAL SCALE NOTATIONS INDICATED ARE
BASED ON ORIGINAL FORMAT DRAWINGS.

USE AND LIMITATIONS OF CONSTRUCTION LEVEL MAPS

1. THE ACCURACY OF THE LOCATION OF A FLOOD CONSTRUCTION LEVEL AS SHOWN ON THIS MAP IS LIMITED BY THE BASE MAPPING AND ORTHOPHOTOS. BGC DOES NOT ASSUME ANY LIABILITY BY REASON OF THE DESIGNATION OR FAILURE TO DESIGNATE AREAS IN THE MAP.
2. THE FLOOD CONSTRUCTION LEVELS AND FLOODPLAIN LIMITS ARE NOT ESTABLISHED ON THE GROUND BY LEGAL SURVEY.
3. OTHER SOURCES OF WATER, ROADS, RAILWAYS OR OTHER BARRIERS CAN RESTRICT WATER FLOW AND AFFECT LOCAL FLOOD LEVELS. OBSTRUCTIONS SUCH AS DEBRIS AND LOG JAMS, SEDIMENT DEPOSITION, LOCAL STORM WATER INFLOWS, GROUNDWATER OR OTHER LAND DRAINAGE CAN CAUSE FLOOD CONSTRUCTION LEVELS TO EXCEED THOSE INDICATED ON THE MAP. LANDS ADJACENT TO A FLOODPLAIN MAY BE SUBJECT TO FLOODING FROM TRIBUTARY STREAMS THAT ARE NOT INDICATED ON THE MAPS.
4. BUILDING AND FLOODPROOFING ELEVATIONS SHOULD BE BASED ON FIELD SURVEY AND ESTABLISHED BENCHMARKS.

NOTES:
1. ALL DIMENSIONS ARE IN METRES UNLESS OTHERWISE NOTED.
2. THIS DRAWING MUST BE READ IN CONJUNCTION WITH BGC'S REPORT TITLED "RDCK FLOODPLAIN AND STEEP CREEK STUDY SALMO RIVER", AND DATED APRIL 2020.
3. BASE TOPOGRAPHIC DATA BASED ON LIDAR PROVIDED BY RDCK DATED 2017 AND 2018. CONTOUR INTERVAL IS 10 m. IMAGERY FROM GOOGLE EARTH.
PARCEL DATA FROM PARCELMAP BC. DIKE DATA FROM DATA BC. FLOOD CONSTRUCTION LEVEL BASED ON THE WATER SURFACE ELEVATION FROM THE 200-YEAR FLOOD USING THE INSTANTANEOUS PEAK DISCHARGE ADJUSTED FOR CLIMATE CHANGE PLUS 0.6 m FREEBOARD
4. PROJECTION IS NAD 1983 UTM ZONE 11N. VERTICAL DATUM IS CGVD2013.
5. UNLESS BGC AGREES OTHERWISE IN WRITING, THIS DRAWING SHALL NOT BE MODIFIED OR USED FOR ANY PURPOSE OTHER THAN THE PURPOSE FOR WHICH BGC GENERATED IT. BGC SHALL HAVE NO LIABILITY FOR ANY DAMAGES OR LOSS ARISING IN ANY WAY FROM ANY USE OR MODIFICATION OF THIS DOCUMENT NOT AUTHORIZED BY BGC. ANY USE OF OR RELIANCE UPON THIS DOCUMENT OR ITS CONTENT BY THIRD PARTIES SHALL BE AT SUCH THIRD PARTIES' SOLE RISK.

SCALE:	1:10,000
DATE:	MAR 2020
DRAWN:	LL
CHECKED:	PG, PS
APPROVED:	RM

BGC ENGINEERING INC.
AN APPLIED EARTH SCIENCES COMPANY

CLIENT:

REGIONAL DISTRICT OF CENTRAL KOOTENAY

PROJECT:
RDCK FLOODPLAIN AND STEEP CREEK STUDY
SALMO RIVER

TITLE:
200-YEAR FLOOD CONSTRUCTION LEVEL
(SHEET 09 OF 9)

PROJECT No.:	DWG No:
0268 007	07

X:\Projects\0268007_RDCK_NDMP_Stream_2_Support\GIS\Production\Report\20191218_RDCK_Clearwater_FCL\200-Year Flood Construction Limits_DDP.mxd